

Departamento de Física  
Universidade do Minho

Ph.D. Thesis

# Thin films for gas sensors

José Miguel Alves Correia Pires\*

27/11/2003

\*Financial support from the *Fundação para a Ciência e a Tecnologia* (Contract ref. *PRAXIS 4/4.1/BD/4563* under project *PRAXIS/2/2.1/TPAR/2044/95*) is gratefully acknowledged



Ad Deum qui lætificat iuventutem



# Resumo

Nos últimos anos tem-se assistido a um aumento dos investimentos na investigação de novos materiais para aplicação em sensores. Apesar de já existir um bom número de dispositivos explorados comercialmente, muitas vezes, quer devido aos elevados custos de produção, quer devido a uma crescente exigência do ponto de vista das características de funcionamento, continua a ser necessário procurar novos materiais ou novas formas de produção que permitam baixar os custos e melhorar o desempenho dos dispositivos. No campo dos sensores de gases têm-se verificado contínuos avanços nos últimos anos. Continua todavia a ser necessário conhecer melhor, tanto os processos de produção dos materiais, como os mecanismos que regulam a sensibilidade dos dispositivos aos gases, de modo a orientar adequadamente a investigação dos novos materiais, nomeadamente no que se refere à optimização dos parâmetros que não satisfazem ainda os requisitos do mercado.

Um dos materiais que tem mostrado melhores qualidades para aplicação em sensores de gases de tipo resistivo é o dióxido de estanho. Este material tem sido produzido sob diversas formas e usando diferentes técnicas, como sejam: sol-gel [1], pulverização catódica (*sputtering*) por magnetron [2–4], sinterização de pós [5, 6], ablação laser [7] ou RGTO [8]. Os resultados obtidos revelam que as características dos dispositivos são muito dependentes das técnicas usadas na sua produção. A deposição usando *sputtering* reactivo por magnetron é uma técnica que permite obter filmes finos de óxido de estanho com diferentes características, quer do ponto de vista da estrutura, quer da composição, e por isso, também, com diferentes sensibilidades aos gases.

No âmbito deste trabalho, foram produzidos filmes de SnO<sub>2</sub> usando *sputtering* DC reactivo com diferentes condições de deposição. Os substratos usados foram lâminas de vidro e o alvo foi estanho com 99.9 % de pureza. Foi estudada a influência da atmosfera de deposição, da pressão parcial do O<sub>2</sub>, da temperatura do substrato e da potência da descarga na estrutura do material depositado. Durante a deposição, além dos parâmetros já referidos, foram também registados a pressão de base antes da entrada dos gases de *sputtering*, os fluxos de oxigénio e argon durante a deposição, a distância alvo-substrato, o tempo de deposição, a corrente e a tensão aplicadas ao magnetron. Foram feitas algumas experiências usando uma fonte RF, para comparação.

Para caracterizar os filmes produzidos, foi medida a massa de todas as amostras e determinada a transmitância para radiação de comprimento de onda entre 200 nm e 2500 nm. Alguns filmes foram estudados usando as técnicas de: microscopia electrónica de varrimento (SEM), microscopia de força atómica (AFM), Microanálise por raios-X (EDX), espectroscopia de fotoelectrões de raios-X (XPS) e difracção de raios-X (XRD).

As análises EDX efectuadas não permitiram identificar outros elementos na composição dos filmes produzidos, além do estanho e do oxigénio. Por outro lado, as análises da composição da superfície efectuadas por XPS, mostravam nas amostras mais antigas e nas de menor espessura, para além do carbono, algumas impurezas de sódio, que deverão ter difundido a partir do substrato de vidro. Esta hipótese foi confirmada fazendo algumas deposições em substratos de aço e de latão. A energia de ligação correspondente ao pico 3d<sub>5/2</sub> do estanho estava de acordo com o valor esperado para uma ligação Sn–O em SnO<sub>2</sub>. Os picos 1s do oxigénio apresentam, antes de uma limpeza rápida com um feixe iónico, uma assimetria que indica a presença de diferentes

espécies de oxigénio na superfície do material.

Todas as análises XRD das películas que apresentavam um aspecto transparente, revelaram uma estrutura tetragonal típica do dióxido de estanho. Contudo, nem todos os filmes produzidos eram transparentes. Os filmes de aspecto negro e opaco, apresentavam uma estrutura amorfa, correspondendo a amostras produzidas com baixa pressão parcial de oxigénio. Verificou-se que após o recozimento das amostras opacas em atmosfera com oxigénio, o material adquiria uma estrutura policristalina semelhante à dos filmes transparentes. Verificou-se também que os microcristais apresentavam uma orientação preferencial que varia com as condições de deposição, nomeadamente a pressão total de deposição.

As imagens obtidas por SEM, de cortes das amostras, revelaram na maior parte dos casos uma estrutura densa, de grãos alongados na direcção perpendicular à superfície. Esta estrutura evoluía para uma estrutura colunar e mais porosa, quando a pressão de deposição era aumentada. Dado que a maioria dos filmes apresentava uma orientação preferencial dos cristais e nalguns casos deformações na estrutura cristalina, não foi possível determinar o tamanho dos nanocristais a partir da fórmula de Scherrer. Estimativas do diâmetro dos grãos foram obtidas a partir da morfologia das superfícies e da estrutura dos cortes observados no microscópio electrónico. A variação da temperatura do substrato durante a deposição permitiu produzir amostras com diferente micro-estrutura; observando-se grãos de maior diâmetro nas amostras produzidas à temperatura de 400° C.

Verificou-se que a temperatura do substrato durante a deposição, o tempo de deposição (e consequentemente a espessura) e a pressão total de deposição das películas, introduzem alterações na rugosidade da superfície das amostras. As imagens, obtidas por AFM, de três amostras produzidas usando diferentes atmosferas de deposição, permitiram observar que o aumento da pressão de deposição, mantendo constante a razão entre o oxigénio e o argon, dá origem a um aumento de rugosidade. Também se verifica um aumento da rugosidade das amostras, quando se aumenta a temperatura dos substratos ou se aumenta o tempo de deposição.

No âmbito deste trabalho desenvolveu-se também um sistema automatizado que permite medir variações da resistência de filmes finos em atmosfera controlada. O sistema é constituído por uma câmara com 160 cm<sup>3</sup> de volume, contendo duas pontas de prova metálicas que fazem o contacto eléctrico no filme. Para fazer o aquecimento das amostras durante os ensaios usa-se uma resistência e um termopar colocados no suporte da amostra e ligados a um controlador, que determina a temperatura medida pelo termopar e controla a potência fornecida à resistência, de modo a atingir e manter uma temperatura previamente determinada. Tanto a temperatura do suporte, como a resistência do filme são registadas por um computador, com uma frequência definida pelo utilizador. A temperatura de trabalho do filme e os tempos de exposição ao gás cuja sensibilidade se pretende avaliar são também definidos pelo utilizador. Diferentes concentrações do gás que se pretende detectar podem ser definidas regulando simultaneamente os fluxos deste e da mistura gasosa usada como referência. Foi usada como atmosfera de referência ar sintético seco. As linhas de gás estão ligadas a uma bomba rotativa que permite evacuar o sistema até uma pressão de  $3 \times 10^2$  Pa. Deste modo assegura-se a remoção dos gases que entram na câmara quando esta é aberta para substituição das amostras. A entrada e saída de gases na câmara é controlada por um sistema de válvulas electromagnéticas, também controladas pelo computador.

As análises feitas até ao momento da sensibilidade dos filmes ao monóxido de carbono mostraram uma baixa repetibilidade dos valores medidos. Supõe-se que este facto resulta de uma instabilidade na estrutura dos filmes, causada principalmente pela mobilidade dos defeitos à temperatura a que foram efectuadas as medições. Para se comprovar esta hipótese seria necessário usar substratos muito puros, para evitar a introdução de impurezas no filme e simultaneamente testar tratamentos térmicos até temperaturas próximas da fusão do SnO<sub>2</sub>, que permitissem equilibrar a estrutura de defeitos do material.

Verificou-se, contudo, que as películas produzidas apresentam uma sensibilidade não desprezável a concentrações de monóxido de carbono superiores a 200 ppm. Nos casos em que a resistência medida da amostra era superior a 100 MΩ não foi possível determinar a existência dessa sensibilidade. Os tempos de resposta do material ao CO variaram entre 2 e 5 minutos. Não foi possível medir o tempo de recuperação devido à deriva observada nos valores da resistência e à dificuldade em garantir a total remoção do CO presente na câmara, mantendo a pressão constante. Para determinar o tempo de remoção do CO está a ser estudada a hipótese de medir a concentração produzida dentro da câmara usando um sensor comercial. Este esquema obriga contudo a algumas alterações à estrutura do equipamento.

Está a ser iniciada uma colaboração com outros grupos de investigação que trabalham nesta área, nomeadamente no que diz respeito à produção de substratos mais adequados para o estudo da sensibilidade aos gases e à obtenção de resultados de sensibilidade complementares aos obtidos com o sistema desenvolvido na Universidade do Minho.





# Agradecimentos

De todas as secções, parece-me ser esta a mais difícil de escrever. Não posso apresentar uma lista de nomes, pois não seria capaz de me lembrar de todas as pessoas que me ajudaram... Ao longo dos anos em que trabalhei neste projecto, tive o apoio de muitas pessoas. Mais ainda, não é possível realizar um projecto desta natureza sem contar com os conhecimentos transmitidos por todos aqueles que se debruçaram sobre este tema antes de mim!

Começando pelos meus orientadores (estes vou ter de pôr os nomes...), não posso deixar de mencionar o Professor Doutor Borges de Almeida que foi quem em primeiro lugar me propôs este desafio e me foi apoiando em todos estes anos, e o Prof. Doutor Vasco Teixeira que me foi empurrando para congressos e reuniões internacionais onde tive a oportunidade de contactar com os especialistas mundiais desta área e que me continua a animar a prosseguir com este trabalho.

Será também necessário agradecer à Fundação para a Ciência e a Tecnologia, o apoio concedido através da bolsa de referência PRAXIS 4/4.1/BD/4563 integrada no projecto PRAXIS/2/2.1/TPAR/2044/95, que me permitiu uma dedicação plena a este projecto. Agradeço também à Fundação Gulbenkian o apoio para a participação no 8th International Meeting on Chemical Sensors em Basileia e à Fundação Luso-Americana para o Desenvolvimento o apoio para participar na 9th International Meeting on Chemical Sensors em Boston, onde pude contactar com os melhores especialistas desta área.

Depois vem a minha família, os meus amigos, todos os meus colegas do Departamento de Física, dos quais seria difícil fazer uma recordação exaustiva, e também os funcionários da Universidade: desde a oficina de electrónica à de mecânica, passando pela secretaria, a segurança e até as funcionárias da limpeza, que encontrava quando tinha de ir ao laboratório fora de horas.

Quantos aos fornecedores do mais variado material que foi necessário para as experiências, num primeiro impulso não me apetecia agradecer a todos. Algumas vezes foi preciso insistir repetidamente até conseguir que me enviassem o que tinha pedido... Apesar de tudo julgo que tenho de agradecer a todos: a uns pelo exemplo de competência, pela amabilidade, pela diligência com que atenderam às minhas solicitações; aos outros, porque pelas dificuldades que criaram me foram mostrando materialmente, a importância das virtudes que encontrava nos anteriores.

Por último, agora que termino este trabalho e volto a Lisboa, queria agradecer a todos os que encontrei no Minho, em especial aos que participam nas actividades do Centro Cultural Montemuro, onde passava grande parte dos meus tempos livres. Aí encontrei grandes amigos e também a eles devo uma boa parte deste trabalho.



# Contents

<b>1. Introduction</b>	<b>1</b>
<b>2. Gas sensors' state of the art</b>	<b>5</b>
2.1. What is a sensor? . . . . .	5
2.1.1. Sensor definitions . . . . .	5
2.1.2. Classification approaches . . . . .	5
2.1.3. Sensor characteristics . . . . .	7
2.2. Chemical sensors . . . . .	10
2.2.1. Classification . . . . .	10
2.2.2. Manufacturing processes . . . . .	11
2.2.3. Characterization . . . . .	13
2.3. Thin film resistive gas sensors . . . . .	18
2.3.1. Metal oxide based gas sensors . . . . .	20
2.3.2. Sputtered tin dioxide layers for CO sensors . . . . .	22
<b>3. Characterization of tin dioxide thin films</b>	<b>25</b>
3.1. Composition . . . . .	25
3.1.1. Bulk composition . . . . .	25
3.1.2. Surface composition . . . . .	26
3.2. Bulk characterization . . . . .	30
3.2.1. Crystalline structure . . . . .	30
3.2.2. Grain structure . . . . .	32
3.2.3. Optical properties . . . . .	33
3.3. Surface morphology . . . . .	36
3.4. Film thickness . . . . .	36
3.4.1. Dependence of film characteristics on thickness . . . . .	40
<b>4. Reactive magnetron sputtering deposition</b>	<b>41</b>
4.1. Plasma processes . . . . .	41
4.2. Magnetron sputtering . . . . .	42
4.3. Thin film growth . . . . .	42
4.4. The DC sputtering chamber . . . . .	44
4.5. Pressure gauges . . . . .	46
4.6. Deposition parameters . . . . .	47
4.6.1. Sputtering atmosphere . . . . .	48
4.6.2. Temperature . . . . .	51
4.6.3. Oxygen partial pressure . . . . .	52
4.6.4. Applied power . . . . .	52
4.7. Repeatability . . . . .	54
4.8. Other parameters . . . . .	54

<b>5. A chamber for gas sensor response testing</b>	<b>57</b>
5.1. Controlling atmosphere composition . . . . .	57
5.1.1. Gas flow in the testing chamber . . . . .	58
5.2. Controlling the surface temperature . . . . .	60
5.3. Electrical measurements . . . . .	61
5.4. Data acquisition system . . . . .	63
5.5. Sensitivity . . . . .	63
5.6. Studying sensor performance . . . . .	64
5.6.1. Resistance response ratio . . . . .	64
5.6.2. Response and recovery times . . . . .	65
5.6.3. Short and long-term stability . . . . .	66
<b>6. Tin dioxide response to carbon monoxide</b>	<b>67</b>
6.1. The sensor output . . . . .	67
6.2. The layer structure . . . . .	70
6.3. Surface interactions . . . . .	73
6.3.1. Adsorption and desorption . . . . .	74
6.3.2. Reactions . . . . .	76
6.3.3. Catalysts and catalysis . . . . .	76
6.3.4. Equilibrium and non-equilibrium . . . . .	79
6.4. Microscopic models . . . . .	79
6.5. Experimental and theoretical work . . . . .	81
6.6. Optimization of tin oxide layers . . . . .	82
6.6.1. Sample preparation . . . . .	82
6.6.2. Limits and yields . . . . .	83
<b>7. Conclusions</b>	<b>85</b>
7.1. Overview of future work . . . . .	86
<b>A. Temperature control</b>	<b>91</b>
A.1. PID Proportional Controllers . . . . .	91
A.2. Device connections . . . . .	91
A.3. Communication interface . . . . .	93
A.4. Communication protocol . . . . .	98
A.5. Routines . . . . .	101
A.6. User interface . . . . .	105
<b>B. Power source control</b>	<b>111</b>
B.1. Communication interface . . . . .	111
B.2. Communication protocol . . . . .	112
B.3. Routines . . . . .	114
B.4. User interface and data acquisition . . . . .	118
<b>C. Electric valves control</b>	<b>133</b>
C.1. The parallel port . . . . .	134
C.2. Commands and routines . . . . .	135
<b>D. Multimeter data acquisition</b>	<b>137</b>
D.1. Communication interface . . . . .	137
D.2. Communication language . . . . .	139

<b>E. Gas sensor testing procedure</b>	<b>143</b>
E.1. User interface . . . . .	143
E.2. The program . . . . .	159
<b>F. Optical parameters computation</b>	<b>169</b>
F.1. The input files . . . . .	169
F.2. The program . . . . .	170
<b>G. Sample labelling</b>	<b>197</b>
<b>Bibliography</b>	<b>199</b>
<b>List of Figures</b>	<b>209</b>
<b>List of Tables</b>	<b>211</b>
<b>List of Routines</b>	<b>213</b>
<b>Glossary</b>	<b>215</b>



# 1. Introduction

What then shall I liken the sperm whale to for fragrance, considering his magnitude?

HERMAN MELVILLE, in *Moby Dick*

Gases are materials constituted by atoms or molecules in continuous motion with random orientation. The average distance between particles in gas phase is much wider than the typical interatomic distances inside a molecule, so that the interactions with each other are much reduced. In an ideal gas, these interactions are perfectly elastic collisions. The pressure,  $P$ , the number of particles,  $N$ , the temperature,  $T$ , and the volume,  $V$ , of an ideal gas are related by a simple formula, the ideal gas equation:  $PV = NkT$ , where  $k$  is the Boltzmann constant. In nature, however, a perfect or ideal gas can hardly be found. Real gases show deviations from this law, due mainly to the non-elastic character of the interactions.

Air, for instance, is a mixture of several gases whose main components are nitrogen and oxygen. Other components of air usually showing small concentrations are argon, other inert gases, carbon dioxide and hydrogen. The composition of air is constantly varying due to the interchange of atoms and molecules between air and the surrounding bodies and also, because of the diffusion and interaction of the particles in the gas phase. This makes atmosphere a fully open system, spatially in-homogeneous and with rich internal dynamics. One of the compounds whose concentration shows a higher variation in air is water vapour. Other substances usually detected in varying concentrations are ozone, carbon monoxide, sulphur or nitrogen oxides and several organic volatile compounds. Also important is noting that very small solid (smoke, dust) or liquid particles (the clouds, the fog) can be carried in suspension by air.

Since air acts as a source of substances for biological processes, the absence of some of its components or the presence of unusual compounds can severely disturb the processes that depend upon it. That is the case when concentration of oxygen has been highly reduced locally in a combustion process or when a toxic compound is carried in air. Since oxygen is odourless, its shortage in atmosphere can only be perceived by the side effects on the respiratory processes. Other gaseous compounds can sometimes be perceived by smell, but in many cases they are also odourless.

The human olfactory system is able to recognize many odours that can be classified into, at least, ten primary qualities [9]. These primary qualities correspond to classes of receptor cells that show identical responses to identical gaseous compounds or groups of compounds. In man the receptor cells are located in a modified form of the respiratory epithelium called olfactory epithelium [10]. Some of the gaseous molecules that are captured by the receptor cells, interact with the receptor molecules and generate a potential that is transmitted, by the cell axon, to the secondary neurons, in the glomerula of the olfactory bulb [9]. Different molecules can be distinguished by the olfaction if they generate different potential signals in the different types of receptor cells. The response of each kind of receptor cell to a given molecule defines thus a characteristic pattern that makes possible its identification by the olfaction. The information transmitted by the olfactory cells is processed in the brain, that generates the odour sense. In man, the olfactory epithelium is restricted to an area of about  $2.5 \text{ cm}^2$  in each nasal mucosa [11]. The olfactory sensing system is highly sensitive, selective and fault-tolerant in healthy conditions, with

## 1. Introduction

a detection threshold that can be as high as one part of an odorant substance in  $10^{12}$  parts [12].

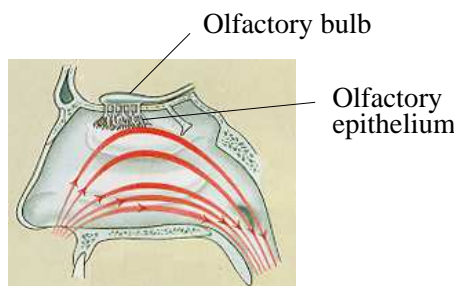


Figure 1.1.: Picture showing the position of the olfactory epithelium and air flow during normal breathing

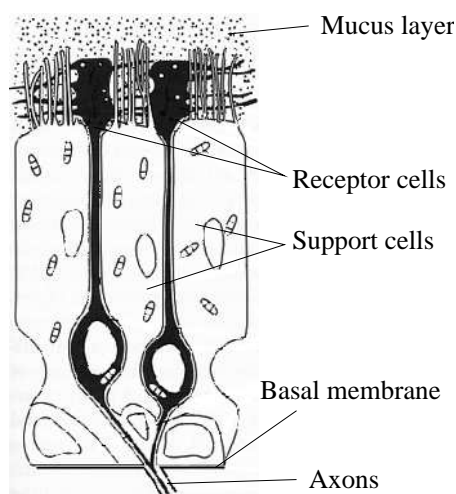


Figure 1.2.: Detail of the olfactory epithelium showing the receptor cells' structure

Natural odours are usually composed by complex mixtures of small organic molecules with relative molecular masses in the range of 18 u to 300 u [13], that are carried by air along with many other chemical compounds. The odour properties, including perceived intensity, of a molecule depend on the shape, the size and the characteristics of the polar group, so that a low volatility species can be sensed intensely, while another present in high concentration can have only a low intensity smell. Olfaction may recognize a harmful substance, but more frequently it will be sensitive to natural and harmless compounds that result from biological processes. Given the good properties of the olfaction sense for distinguishing the odour of food, beverages, perfumes or tobaccos, the sensory qualities of this kind of products are usually evaluated by trained panels of people, who smell the products on a routine basis to maintain process and product control. However, olfaction is subject to variation with health, diet or age, so that the quality control of those products would profit if there was an unequivocal process to identify the different odours.

Gas composition analysis is nowadays performed using well established analytical methods, such as gas chromatography combined with mass spectrometry. Also widely used are flame-ionization, photo-ionization and electron-capture gas chromatography detectors. The first commercial gas chromatograph appeared fifty years ago. Since then gas chromatography developed rapidly and soon became the prominent method used for separating and analysing mixtures of volatile components. Although effective in identification of specific molecules in a mixture, gas



chromatography results, and more generally other current analytical chemistry techniques, show a very limited time and space resolution. Portable gas-chromatographs have been available for many years and the emergence of on-site direct-inlet mass spectrometers, Fourier infrared spectrophotometers, portable ion-mobility spectrometers and tunable atomic-line molecular spectrometers are very useful for identification of contaminants in field, however the improved analytical capabilities of these instruments are partially offset by their complexity and high cost [14]. The same does not hold for gas sensor systems. The latter are usually devices with lower detection range and versatility but which show better characteristics for routine analysis, given their lower production costs, simple user procedures and high time and spatial resolution on the detection of specific chemicals or odours.

Gas sensor systems, sometimes called electronic noses, are devices that are able to capture and process signals generated by specific and reproducible interaction processes with gas molecules, in one or more built-in sensitive layers. The development of this kind of devices has only been possible by the systematic production and characterization of new sensing materials, the availability of fast and sensitive electronic measuring systems and the fast growing knowledge in information theory to analyse multidimensional complex data. When the sensing layer and the electronic circuitry are integrated in the same chip the device can be made very small and the production cost significantly lowered. There are already commercial gas sensor devices used for identification of specific contaminants or common mixtures. However much has yet to be done in order to improve sensitivity, selectivity and production cost of these devices.

The critical part of the sensor systems are the sensor elements, since a sensor array cannot produce better information than that contained in the sensors' responses. In order to make sensor systems portable, cheaper or usable for monitoring of air quality, sensor elements: should require low power for operation; should be compatible with a simple sampling system or even have no need for one; should have no need for external carrier or reactant gases; should be made small and if possible compatible with microelectronic technologies; should have reversible and reproducible responses; should have adequate sensitivity and should have response times lower than one minute and long term stability if used in continuous operation or response times of a few seconds and short warm-up time if used for single gas analysis. It would also be useful to have sensors insensitive to ambient temperature and to the most common variable compounds of air, especially water vapour; with reproducible production characteristics; without hysteresis or drifts; with linear responses, fast recovery times and long lifetimes. Using modern pattern recognition techniques, like artificial neural network techniques, it is possible to work with non-linear or noisy data and make up for non-selectivity, long or short-term instabilities and ageing of the sensor elements.

The main purpose of this work is to study and develop new materials for gas sensing elements starting from the knowledge in thin film production using magnetron sputtering, available in the Physics department at University of Minho. The structure of this report is summarised below. Some concepts used on sensor development and specifically on gas sensors' research are described in chapter 2. It is also explained the reason to start studying tin dioxide response to CO. In the following chapter are presented the characteristics of tin dioxide thin films produced by DC reactive magnetron sputtering. Chapter 4 describes the sputtering process and discusses the correlation between deposition parameters and the thin film's characteristics observed. On Chapter 5 is described the setup built in our laboratory for gas sensing characterization. The results of the gas sensing characterization of the produced tin dioxide films and some of the main models used to explain the sensing mechanism observed on solid-state resistive gas sensors are discussed on Chapter 6. And finally, chapter 7 summarises the main conclusions of this work and also points some directions for future research, that may be carried out in our laboratory at the University of Minho.

## 1. *Introduction*

## 2. Gas sensors' state of the art

### 2.1. What is a sensor?

#### 2.1.1. Sensor definitions

There is no commonly accepted definition for sensor. However, in order to make clear what is designated here by sensor, it will be adopted one of the commonly accepted definitions. For this purpose, it was chosen a definition given by Jacob Fraden in the *Handbook of modern sensors* [15], which states that “a sensor is a device that receives a signal or stimulus and responds with an electrical signal”. The reason for the output of a sensor to be limited to electrical signals is related to the present development of signal processing, that is almost exclusively performed using electronic devices. Given this definition a sensor should be a device that receives a physical, chemical or biological signal and converts it into an electric signal, that should be compatible with electronic circuits. This definition may also be supported from the etymological origin of the word sensor. Sensor seems to come from the word *sense* given that usually sensor devices try to mimic or reproduce human senses' characteristics. In the biological senses the output is also an electrical signal that is transmitted to the nervous system.

Another term with a meaning similar to sensor is transducer. Sometimes transducer is used as a synonym for sensor, as is the case in a series on sensors edited by Göpel *et al.* [16–19]. Nevertheless, transducer will be distinguished from sensor throughout this report. Transducer will be used to designate any device which converts a stimulus into any other form, whether electric or not. In this sense a sensor is only the transducer that produces an electric output. A sensor may be composed by a series of transducers responding in the end with an electrical output, in which case, given the above definition, the last transducer in the series could also be termed a sensor. A transducer may also be called sensor element, when it is part of a sensor.

Usually sensors are part of larger complex systems, made by many other transducers, signal conditioners, signal processors, memory devices and actuators. However complex, the components of a sensor system may be grouped in three different units. The first is the sensor unit, the second is the modifier or signal processor and the third is the output transducer. The second class of components receives the electrical output of the sensors and transforms it into a more suitable form, e. g., amplifying, converting to digital form or linearizing the signal. The third class, termed the output transducer, converts again the electrical signal into a non-electrical parameter. When this last parameter can be perceived by the human senses the output transducer is called a display and the whole system may be called a measuring system. If the output transducer is used to cause some action it is called an actuator and the whole system is a control system.

Both control and measuring systems may be included in a larger group of the information processing systems. These are systems that gather data from a variety of sources and process it in order to produce usable information.

#### 2.1.2. Classification approaches

Classification of sensors is another difficult task. Some common classification schemes group the sensors by the applications, the input stimuli, the conversion mechanisms, the materials used,

## 2. Gas sensors' state of the art

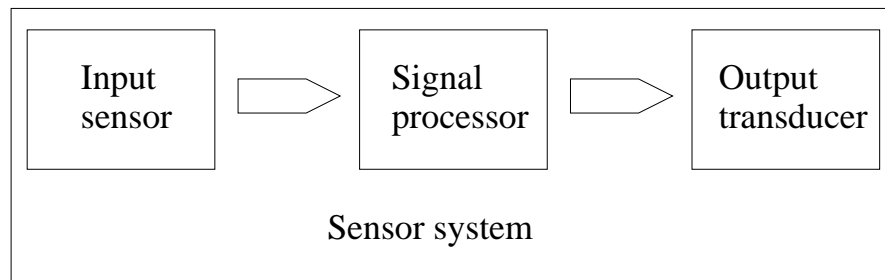


Figure 2.1.: Typical structure of a sensor system

the production technologies or the sensors characteristics such as cost, accuracy or range. Each of these approaches may be helpful in different sensor development stages.

Table 2.1.: Classification scheme based on the sensor' input stimulus

Class	Detected Properties
Mechanical	length, acceleration, flow, force, pressure, etc.
Thermal	temperature, specific heat, heat flow, etc.
Electrical	charge, current, voltage, resistance, inductance, etc.
Magnetic	magnetic flux density, magnetic moment, etc.
Optical	light intensity, wavelength, polarization, etc.
Radiation	type, number or energy of radiation particles; light properties far from the visible spectrum; etc.
Chemical	composition, concentration, pH, etc.

Possibly the best way to start is grouping the sensors by their input stimuli, i.e., looking at what they measure. According to the form of energy that originates the stimulus, the sensors can be divided into seven classes: mechanical, thermal, electrical, magnetic, optical, radiation or chemical. There are some ambiguities in this kind of grouping that will not be argued, since the purpose of introducing this classification is giving an overview of the different branches of sensor research. Mechanical sensors may be used to measure length, acceleration, flow, force, pressure or acoustic wave amplitude, for instance. Thermal sensors are used to measure temperature, specific heat, heat flow or entropy. Electrical sensors are used, for example, to measure charge, current, voltage, resistance, inductance or capacitance. Magnetic sensors are used to measure magnetic field intensity, magnetic flux density, magnetic moment or magnetic permeability. Optical sensors, sometimes also called radiant sensors, may be used to measure light properties, such as, intensity, phase, wavelength or polarization; or optical properties of a material, such as, emissivity or reflectivity. When the wavelength of the detected electromagnetic radiation is far from the visible spectrum, either above or below this region, the devices are called radiation sensors. These may also be used to determine the type of radiation particles, or to count or measure the energy of atomic particles. Finally, chemical sensors are the ones used to determine chemical properties of substances, such as the composition of a mixture, the concentration of a substance, the pH or the rate of a chemical reaction. Gas sensors are obviously included in the chemical sensors' class. In Section 2.2 this type of sensors will be analysed with more detail.

Another way to group the sensors is looking at the conversion mechanisms. This approach is mainly used when studying a conversion mechanism by itself. It is worth noticing that using this classification scheme the same sensor can be included in several classes inasmuch as each sensor usually uses more than one conversion mechanism. To give an example it is clear that the way to

measure a chemical quantity may involve first a conversion to a thermal quantity and only then the conversion to the electrical signal. This is the case in some common calorimetric gas sensors used to detect flammable gases by the temperature change caused by the oxidation of the gas in a surface containing a proper catalyst. The gas first reacts producing heat and the consequent rise of the temperature is converted to an electrical signal using, e.g., a platinum resistor. A common classification is one that divides the conversion mechanisms into self-generating or modulating. Self-generating mechanisms or principles are the ones that do not need an auxiliary energy source, such as, the photoelectric effect. Modulating mechanisms are the ones where an energy flow other than the one supplied by the input stimulus is modulated by the measurand, as observed in resistive gas sensors. Some authors use the words active and passive to refer to these two classes. However these terms will not be used in this work since there is no agreement as to which should be called active and which should be called passive mechanisms.

The sensor's characteristics may also be used to classify the sensors. This approach is frequently observed in catalogues or data sheets and is very useful when looking for sensors that meet specific demands. Having in mind the sensors' applications it may be noticed that sensors for outdoor use need to be less influenced by environmental conditions than those used indoors, where environmental factors usually change little. Sensors used for continuous monitoring should have long term stability but may have lower resolution than a sensor used for accurate, but timely spaced measurements. Sensors intended for domestic applications should be much cheaper than the ones used for military or scientific purposes. These factors should not be overlooked in the development of new sensors. The fact that a sensor being developed shows lower sensitivity than previously studied ones, does not mean that it is not worthwhile to continue the research, since it might show characteristics other than sensitivity that may be advantageous in some application where a high sensitivity is not fundamental.

Finally, one must consider the materials and the technologies used to produce the sensors. These two classifications are important for development engineers and research centres, since the knowledge on materials' production technology is a key issue in sensor development. At the Functional Coatings Group in the University of Minho Physics Department, there is a long experience on magnetron sputtering thin film production of several inorganic materials. Some of them, such as tin dioxide, have good properties to build devices for gas sensing. However, there is a myriad of different materials and technologies used in sensor manufacturing. Each sensor is usually built using several of these materials and techniques. To avoid extending too much this overview, specific examples of materials and technologies will only be discussed in Section 2.2, when manufacturing of chemical sensors is reported.

### 2.1.3. Sensor characteristics

Some sensor's characteristics have already been referred previously. Now these and other characteristics, that may be useful to evaluate sensor performance in a specific application, will be explained. Since there is no standard procedure to estimate quantitatively sensors' characteristics and in order to keep this introduction as general as possible, it will not be proposed a method to evaluate quantitatively each characteristic; this will be done later, when needed.

Sensors' characteristics can be grouped into static or dynamic parameters, environmental conditions and structural related characteristics. Static parameters are the ones that describe the transfer function of a sensor, i.e., the relation between the input and the output of a sensor, when the input does not vary significantly with time. On the other hand, dynamic characteristics try to describe the performance of the sensor taking account of the variation of the stimulus with time. Environmental conditions are all those factors that interfere with the sensor mechanisms and thus change its response to the input stimulus. Finally, structural related characteristics are those that result from the specific design and components of the sensor. In these last characteristics

## 2. Gas sensors' state of the art

could be included: cost, weight, power consumption, lifetime and compatibility with silicon based manufacturing technologies.

Two important characteristics referred earlier are accuracy and resolution. Accuracy is an estimate of how close the measured value is to the true value. It should not be confused with precision, that evaluates how exactly and in repeated measurements the input stimulus is measured. A measure that is precise but not accurate shows a deviation from the true value that is called *error*. A measurement procedure that is not precise produces an *uncertainty* in the output value. In the latter case the output of the sensor does not permit the determination of a definite value of the measurand but rather an interval within which the true value should be. In the case of discrete unknowns, such as the number of  $\beta$  particles reaching a Geiger-Mueller detector, it could be argued there is the possibility to obtain values without uncertainty.

Resolution is the smallest increment in the input stimulus that results in a detectable increment in the output. This parameter is obviously limited by the precision, but also by noise, sensitivity and repeatability. The smallest increment of the measurand from a zero value that causes a detectable output is often called the detection threshold and the span of the input stimulus that produces a meaningful output is called range or span.

Although sensitivity has no standard definition, in gas sensors' research it is a widely used parameter. In the majority of the publications dealing with gas sensors, sensitivity is estimated using the ratio of the output response of the device to the output in a reference atmosphere, and is a dimensionless value. However, in many other fields of research, sensitivity is defined as the ratio of the measurand variation to the variation of the output. Since this last definition is more general than the former, it is preferred and will be used in the following. The former estimate will be called the response ratio. Given the absence of a common definition one has to be very careful when comparing the sensitivities reported for different devices.

Noise is a random fluctuation in the sensor output that might be caused by random fluctuations in the measurand or by external interferences in the conversion mechanisms. Repeatability is the difference in the output of the sensor when the input value is consecutively reached using identical procedures. This is a very limiting factor, since a low repeatability can lead to very high uncertainty in the output value. A difference in the output of a sensor, for a given input value, can otherwise be caused by hysteresis. This is the difference in the output of a sensor, when the input value is reached from opposite directions. If a sensor shows hysteresis, the output value depends on the history of the sensor, i.e., if the previous input stimulus was lower than the present one the output may be different from the one observed when the previous value was higher. Nevertheless this does not change the uncertainty. The error, though, can increase if this factor is not counterbalanced by the signal processing.

In order to simplify processing of the output signal it would be desirable to have a linear transfer function. Usually this is not the case, and so a useful parameter is the linearity of a sensor, which measures the closeness of the transfer function to a linear function. Sometimes, although not linear in the whole range, the transfer function can be approximated by a linear function at certain input intervals. Related to this parameter, although more general, there is distortion, which is a measure of the deviation from an expected output. When the transfer function is not linear, one can try to approximate it using another function, like a sinusoidal waveform or an exponential, for example. The deviation of the transfer function from this model equation is then the distortion.

Finally, there are some parameters much relevant to the coupling with the electronic interface, that should also be included in the static characteristics. These are the form of the electrical output, the form of the modulating signal (when needed), the output impedance, the leakage current and the grounding. These characteristics do not generally alter the performance of the sensor if the electronic circuit is properly designed, nevertheless they can change its operation

or production cost.

Dynamic characteristics are more difficult to evaluate than static ones. One way to perform this evaluation could be to observe response of a sensor using input sinusoidal signals of every possible frequency and amplitude. However, in most cases those signals cannot be easily produced experimentally. When it is possible to produce input sinusoidal signals of different frequency, the change of amplitude and phase of the output signal can be determined as a function of an input unit signal, producing a function that is called the frequency response. From this response a lower and upper cutoff frequency, a phase shift and a resonant frequency can be determined. If the sensor response followed the input stimulus with perfect fidelity, there would be no phase shift and the frequency response would be a constant. When there is a lower cutoff frequency the sensor is unable to measure constant input signals. The upper cutoff frequency is usually related to the sensor' response speed. This speed may be characterized by the time required by the sensor to reach a given percentage of the steady-state or the maximum level, after exposure to a step input signal. Another way to study the frequency response of the sensor is to observe the behaviour of the output when the sensor is excited with an impulse signal. If we could produce an ideal impulse,  $\delta(t)$ , the Fourier transform of the response would be the frequency response of the sensor [20].

There are two important characteristics that are neither strictly static nor dynamic. These are warm-up time and reliability. Warm-up time is the time needed for the sensor to operate within the specified accuracy, after applying the modulating signal or the power needed to establish the operating conditions<sup>1</sup>. Reliability is the ability of a device to operate under specified conditions, with the specified characteristics and for the specified period. To evaluate the reliability of a sensor it is necessary to find out the most frequent failure mechanisms and the best operating conditions. Then it is also important the have means to estimate ageing of the device.

As mentioned before the performance of a sensor may depend on the environmental conditions. Under this group of parameters can be included temperature, pressure, contact with reactive compounds, electromagnetic noise and vibration. These parameters should always be determined carefully, but specially if the sensor is to work under highly variable environmental conditions. In the latter case proper isolation of the device should be provided in order to prevent degradation of the response due to the environment. Many other characteristics could be mentioned in here. Below some that frequently arise in the chemical sensor field will be presented.

In the gas sensor field there is one important environmental parameter that is called selectivity, that estimates the sensitivity of a device to substances other than the one whose measurement is required. This parameter is particularly important if the device is sensitive to the most frequent components of the analysed atmosphere. In sensor arrays a deviation of the output signal due to the operation of neighbour devices can happen, this is usually termed crosstalk. In gas sensors, crosstalk can happen when the interaction of a gas in the sensor surface results in a new compound that induces a response in one of the neighbouring sensors. Most of the drifts and instabilities observed in sensor devices are caused by environmental parameters or the device structure. Short and long-term drifts should be distinguished. Short-term drifts can be observed during warm-up, while the device has not yet reached the normal operating conditions and normally do not constitute a problem, while long-term drifts are frequently related with ageing of the sensors, and can seriously degrade device performance.

---

<sup>1</sup>Metal oxide gas sensors, for instance, operate at higher than ambient temperature, and thus need to be heated to function properly.

## 2.2. Chemical sensors

As defined previously, chemical sensors are devices used to ascertain the chemical properties of materials. This is a fast growing field of research where steadily appear new ideas and prototypes. Unlike other sensor fields, though, the number of mass-produced devices do not generally follow the research activity. Many chemical sensor devices have large batch-to-batch irreproducibility, which originates high costs due to the need to calibrate each single device; skilled staff are usually needed for accurate calibration and general troubleshooting and, in many cases, devices are not even suited for mass production [21]. Another problem is the large number of interfering parameters, that make very difficult a complete characterization of chemical sensors. Thus frequently the progress in technology surpasses science and reduces sensor optimization to a trial and error process.

### 2.2.1. Classification

For the purpose of presenting the state-of-the-art of chemical sensor technologies it is necessary to put some order in the available devices. As in the case of general sensors (see Table 2.1 on page 6), considering the detection principles, chemical sensors can be classified into electrical, magnetic, thermal, optical, mechanical or radiation sensors. A classification could also be tried having in mind the materials or the technologies, however, the former is preferable since it can give a broader view of this field of research. Some of the materials and technologies employed in the production of this kind of sensors will be reviewed in the next section.

In the sensors based on electrical properties the output signal is either generated by a reaction involving charge transport or is modulated by that reaction. This implies that there must be an electric current flow through the active sensor material in order to make a measurement, and thus, at least two electrodes. One of the first devices used to sense a chemical quantity was the electrochemical cell. Over the years several modifications have been introduced in the original configuration of the cell in order to widen the measuring scope and optimize the performance of the device. An electrochemical cell is usually built with two or more electronic conductors, called the electrodes, immersed in an electrolyte, which is an ionic conductor. The electrolyte might be a solid, a liquid or a gas. A more recent example is the field effect chemical sensor. This is a solid state device similar in its working principle to the JFET or the MOSFET devices. In these devices a conducting channel exists between the source and the drain electrodes, that is modulated by the potential of a third electrode that is called the gate. In field effect chemical sensors the potential generated at the gate depends on the chemical quantity being measured. This quantity can therefore be determined by observing the current flowing from the source to the drain of the device. In this same class of chemical sensors based on electric properties are included the thin film chemoresistive sensors. These are very promising devices because they can be made very small and cheap and are compatible with silicon technology, which opens the possibility to integrate the sensors in the processing electronic circuit.

Neither the magnetic nor the radiation sensors are usually included in the chemical sensors' field. This kind of sensors, as mentioned before, may be used to detect magnetic or radiation properties of materials. This alone does not justify the inclusion in the chemical sensors class since these are not chemical, but rather physical properties. However, if these properties are used to determine composition they can be included in that class, and thus it is worth to include them here.

Chemical sensors based in thermal properties measurements are also an important class. These are mostly used to detect flammable gases because of the exothermic character of their reaction with oxygen. The most common of these devices have a catalytic layer that promotes the reaction at low temperature, and a temperature sensor that measures the temperature vari-



ation caused by the heat exchange. Both the presence of a substance and its concentration in atmosphere can be determined by this kind of sensors. When there is a temperature difference between the sensor and the surrounding atmosphere, the temperature variation can be related to a change of the thermal conductivity of the atmosphere and therefore also used to monitor its composition. Obviously, not only exothermic but also endothermic reactions can be monitored using such a device.

Optical characteristics provide good fingerprints to distinguish different substances and are widely used in materials characterization. Recent advances in optoelectronics and fibre-optic techniques have brought some promising new ways to use these properties in chemical sensors. A fibre-optic chemical sensing device consists usually in a light source, a fibre coupler to lead the light into the fibre, the light guide, a decoupler where the returning light is separated from the exciting light and a light detection and amplification system. The measured properties may be, for instance: absorbance, reflectance, fluorescence, light scattering or refractive index.

Finally there are two types of devices that may be included in the mechanical sensors class, that are the bulk acoustic wave sensors (BAW) and the surface acoustic wave sensors (SAW). The advantages of SAW technology over BAW include the compatibility with planar silicon technology and the possibility of using higher frequencies and potentially higher sensitivity. Acoustic wave sensors' working principle originates in the mutual dependence of electrical and mechanical properties, in a piezoelectric crystal. Typically, in BAW gas sensors a material that adsorbs a given gas is deposited over the piezoelectric crystal, and the variation of the oscillation frequency of the crystal is related to the adsorbed mass. In order to get an unequivocal relation between the adsorbed mass and the detected substance it is necessary that the sensitive material is highly selective. Since adequate selectivities are more easy to get with organic than with inorganic materials, these sensors are generally built with the former type of materials. The fact that there is no need for a flux of energy to go through the sensitive material is also very convenient if organic materials are employed, inasmuch as they are usually more unstable than inorganic materials. In the case of SAW sensors, the influence of the sensitive overlayer on the propagation of the acoustic wave is higher than in BAW, and thus the phase velocity and amplitude of the acoustic wave have a non negligible dependence on the elastic, piezoelectric, dielectric and conductive properties, as well as the mass of the mentioned overlayer. These properties have also been studied as a step towards achieving better selectivity or sensitivity of the devices.

### 2.2.2. Manufacturing processes

In the previous section different mechanisms employed in the design of chemical sensors were described. These mechanisms, along with the materials used, will obviously guide the selection of techniques employed to produce the devices. Mechanical, electrical, thermal and optical properties of the materials have to be considered when designing a new device. A good database of the available materials and their characteristics is then needed in order to get better and faster results in this research. To give some examples, it may be mentioned among the organic materials: electronic conductors like Pb- and Cu-phthalocyanines or ion conductors like Nafion. Other organic compounds are used for their piezoelectric properties, as polyvinylidene or for the high electrical conductivity and optical transmission, as polypyrrole. Oxides also show different properties: SnO<sub>2</sub> and TiO<sub>2</sub> are electron conductors while ZrO<sub>2</sub> and CeO<sub>2</sub> are ion conductors. LiTaO<sub>3</sub> shows good pyroelectric properties and quartz is a widely used piezoelectric material. Some metals like Pt and Pd may be used because of the catalytic properties and a ceramic material like alumina because of the electrical insulation and thermal conductivity properties.

Different preparation procedures have to be employed when the materials are organic or inorganic; when produced in single crystal form or in polycrystalline form; when in bulk or

## 2. Gas sensors' state of the art

with a thin or thick film structure; whether pure or doped with one or more selected elements. It has also been shown previously that a sensor has usually a complex structure. Accordingly, it is important to have in mind not only the techniques used to prepare the surface where the interactions with the material being sensed take place, but also the techniques to produce and assemble all the other sensor elements that carry, transport or protect the generated signal from environmentally adverse conditions. It is almost impossible to have all the known techniques available in a single laboratory or institution, therefore a close cooperation between different research areas is a must in order to develop a sensor device that satisfies the aimed specifications.

Integrated circuit technology, for instance, involves several processing steps. First it is needed a polished semiconductor wafer, usually Si or GaAs. Then a film is grown on the wafer under ultra-high vacuum or in a carefully controlled atmosphere. After the film formation, the wafer often undergoes diffusion or ion implantation for impurity doping. The final step consists in the formation of a pattern mask on the film surface using a lithographic process, followed by etching of unwanted film or substrate parts specified by the mask. These steps are usually repeated several times, using different masks, to produce a microstructured circuit device.

In the case of optochemical sensors, it is necessary to consider the light source, the optical waveguides, the light detector and the techniques used to couple optical waveguides with each other and with the light source and detector. The most frequently used waveguides are the optical fibres. Silica multimode and single-mode fibres are the standard fibre types in optical fibre sensors, but other exist for special purposes, such as: plastic or polymers for low cost, halide glasses for low loss or rubber for extreme bendability. As to the light sources, nowadays there are generally two kinds of optical fibre sensor sources: the light emitting diode (LED) and the laser diode, both of which are semiconductor devices [22]. Optical detectors in these sensors are also usually limited to semiconductor devices: the avalanche photodiodes.



Figure 2.2.: Picture of a Bosch lambda sensor used in the automotive industry to control the combustion atmosphere inside the motor cylinders. This is one of the most common catalytic type sensors.

As a final example of the possible technologies involved in chemical sensor manufacturing it is worth mentioning the lambda sensor, widely used in the automobile industry to control the air-to-fuel ratio (see Fig. 2.2). This belongs to the class of chemical sensors based on potentiometric measurements and commonly consists of a tube of yttria-stabilized zirconia, covered with platinum electrodes. The platinum electrode, that is in contact with the exhaust gas from the engine, is protected by an overcoat that reduces the penetration of undesirable poisoning components containing lead, sulphur or phosphorus. The fabrication of the zirconia electrolyte ceramics starts by the preparation of the powder, to which are added the stabilizing or sintering aids. In order to get a plastic melt that can be moulded into the desired form, the powder is mixed with organic materials and then submitted, e.g., to axial or isostatic pressing, slip casting

or injection moulding. To remove the organic compounds, the material is heated at moderate temperatures and after this sintered at high temperatures to yield the final ceramic product. This may still be submitted to further annealing to stabilize the properties, before the final shaping and application of the electrodes and the protective coatings. The methods used to produce the powders can substantially condition the properties of the final product. Namely, it is known that a homogeneous distribution of the stabilizing additives in the zirconia matrix can be accomplished using the sol-gel process, but the same result is difficult to get by blending milled powders of zirconia with the stabilizing additive, and calcining the resulting mixture [23].

After presenting a few examples reviewing the manufacturing processes employed in chemical sensor development, there is still some need for a more detailed view of the thin film techniques, since this will be the main scope of this report. The difference between thin and thick film techniques should not be found in the actual thickness of the produced layers but rather in the deposition methods and the subsequent device fabrication processes. One of the most used thick film techniques is screen printing. The processes generally followed in this technique to obtain the coatings start by the selection and preparation of the substrate; then the starting material is prepared in ink or paste form; the ink or paste is screen printed onto the substrate and finally fired at a preset temperature-time profile. Other techniques involving similar procedures are painting and dip coating. Compared to vapour deposited thin films, the formerly mentioned thick film processes do not require very complex equipment, which makes possible lower cost mass production of the coatings. However, these do not permit neither a good dimensional control nor a sufficient miniaturization as required in current silicon microfabrication. Over the years, several modifications have been introduced to the basic thick film techniques, leading to a higher dimensional control but also reducing the process simplicity which is one of its major advantages.

Thin film techniques involve both overlayer growth and surface modification techniques. The process mechanisms of these techniques have the specific characteristic of working at the atomic scale, which explains the better dimensional control usually achieved. The processes used in the deposition of inorganic layers can be divided into three different categories: physical, chemical and hybrid methods. The physical processes include the physical vapour deposition (PVD) processes, such as: thermal evaporation, sputtering deposition and ion plating. Chemical processes include not only chemical vapour deposition (CVD), but also deposition from solutions, such as: cathodic deposition, electroless plating or homogeneous precipitation. Finally, there are the methods that combine both physical and chemical processes, like plasma enhanced CVD or laser activated deposition. Many times it is not easy to classify the technologies into these categories, mainly because the technology has developed faster than the detailed knowledge of the deposition mechanisms involved. As to the processes used to modify the surfaces it may be mentioned, for example: lithographic patterning, chemical etching and plasma oxidation. Most of the times thin and thick film organic overlayers need specific coating procedures, that will not be referred in here.

### 2.2.3. Characterization

A thorough optimization of sensor performances can only be done with a systematic characterization of the materials' properties; a good knowledge of the dependence of those properties on the preparation processes and a proper understanding of the sensing mechanisms. In this section some examples of the most common techniques used to characterize sensor's response, sensing mechanisms and materials' properties will be given. The study and control of the manufacturing techniques will be restricted to the field of magnetron sputtering and therefore presented later.

Usually a single characterization technique produces useful data to the study of more than one of the referred aspects, so that the advances observed in one field also bring significant

## 2. Gas sensors' state of the art

advances to the others. In order to present some of the most frequent characterization procedures in use, the focus will be put on the materials properties either macroscopic such as: resistivity, thermal conductivity, refractive index or hardness, or microscopic such as: composition, crystal structure, point defect density or electron-band structure. It may be noted that the majority of the characterization techniques require the use of complex equipment and need to be operated by experts, so that, again the cooperation between institutions and scientists involved in these research areas is very important to the progress of sensor development.

Given that the output of a sensor is an electrical signal, a detailed understanding of its electrical properties is always necessary to design the output processing unit. Furthermore, knowing that most of the chemical sensing mechanisms involve charge transport, electrical characterization of the sensing materials is also needed to understand those mechanisms. If the material is homogeneous some of its bulk properties, such as: dielectric constant, conductivity, carrier mobilities or work functions, can be found in handbooks and databases. Frequently these values are taken at standard conditions that are not verified in sensors applications, nevertheless, they provide a swift and valuable starting point to the characterization procedure. Having in mind the standard values makes it easier to select the most suitable characterization methods and then determine their dependence on the studied chemical input, both under static or dynamic conditions. A common problem when performing electrical measurements is the selection of the electrode materials and the sampling geometry. This should be solved in the first place, because a wrong choice can introduce serious complications to the charge transport processes and may hinder the study of the sensing mechanism.

Further complications arise when the material is not homogeneous. Examples of heterogeneous materials are polycrystalline layers, multi-phase mixtures, layered structures and living tissues. One can easily imagine, considering the diversity of the homogeneous materials and the difficulties experienced in their characterization, that the investigation of the sensing mechanisms is much more difficult when the materials are not homogeneous. To characterize heterogeneous materials, a detailed knowledge of the structure, as well as the role of each of the homogeneous parts and the influence of the interfaces in the charge transport mechanism through the material, is fundamental to understand the sensing mechanisms. Notwithstanding the dimension of the heterogeneous structures, it will help to start by considering the known models describing charge transport processes at the interface of a two layer or two phase material, to proceed afterwards with the development of a model that fits better the actual structure of the material. In recent years, several new techniques have been developed using microcontacts or microelectrodes to evaluate electrical properties of materials with high spatial resolution. Of considerable interest is the use of atomic force and tunnelling microscopes to measure electrical properties with atomic resolution [24–26].

Many materials' properties are temperature dependent and frequently sensors are used in temperature changing conditions, therefore it is always necessary to evaluate the temperature effect on sensors characteristics. In order to measure temperature, well known temperature dependent phenomena are used, such as: thermal expansion, thermal radiation, resistivity or the Seebeck potential. Then, heat transfer processes between the measured and the measuring device have to be studied carefully to yield reproducible results. Since temperature measuring devices generally measure their own temperature, only when there is thermal equilibrium with the measured material can one be sure that the measured value represents the actual temperature of the material. Unfortunately, temperature measurements can seldom be performed under equilibrium with the sensor material, so that, even when the sensor materials and mechanisms are identical, reported temperature dependencies may not be comparable due to different sensor geometry or measurement procedures used. When measuring the temperature of gas sensing surfaces, wide area contacts should not be used in order to leave the surface free to interact with

the chemical sensed material. Non-contact devices, such as the ones based on thermal radiation could be used in some applications, however care must be taken to evaluate the absorption of the thermal radiation by the mediating material and the interference from nearby radiation sources.

The study of the propagation and interaction of electromagnetic radiation with matter is another important field of materials characterization. The electromagnetic spectrum is theoretically infinite, although in practise the detected wavelengths extend from about  $10^3$  m to 10 pm. To the lower wavelengths, correspond higher photon energies and thus different interaction modes with matter. This explains why different portions of the electromagnetic spectrum are studied by separate branches of physics. Optics, for instance, is usually concerned with the propagation of electromagnetic radiation of wavelength from about  $10^2$  nm to  $10^5$  nm, i.e., from the ultraviolet to the near infrared portions of the spectrum. Among the characterization techniques that use this portions of the spectrum there are: optical microscopy, ellipsometry, luminescence spectroscopy, infrared vibrational absorption and Raman spectroscopy. Of the listed techniques, the first two use only the wave character of light and thus, given the dimensions of the wavelength of the radiation used, are better suited to study macroscopic properties. The last three, inasmuch as they involve non-elastic interactions with the material, will be discussed within the group of techniques used to characterize the microscopic properties.

Optical microscopy is a long established technique mainly used to study surface morphology in the millimetre or micrometre range. Over the years it has experienced several advances. Ellipsometry has a more recent history. It uses change of the polarization state of light upon reflection on a surface to get some of the material's properties. Applied in film growth studies it is frequently used to determine the film optical constants. On the other hand, if the optical constants are known in advance, ellipsometry using a monochromatic light beam may be employed to determine layers' thickness. This technique shows an extremely high surface sensitivity (about  $10^{-1}$  monolayers of an adsorbate) and, by fitting calculated spectra to the experimental data, may also yield useful information concerning the chemical and structural nature of a film and its global electronic structure [27]. Other spectrometry techniques exist to determine absorption, transmittance or reflection of light, in solid or liquid samples, using polarised or non-polarised light, yielding the optical parameters of the samples and their dependence on the radiation wavelength, and from these making possible to determine other structural properties, such as: density, porosity or impurity concentration.

Mechanical properties of materials are frequently ignored in chemical sensor development. In acoustic wave sensors' development, though, these have to be studied if a complete understanding of the propagation mechanisms is required, since the mechanical properties interfere with the wave propagation through the material. In composite materials it might be important to study these properties, because they affect the interfacial adhesion. Cracks and other mechanical effects observed in vacuum-coated films, for instance, are caused by substrate-induced stresses that are transferred across this interface [28]. This problem, however, is generally unimportant in films with sub-micrometre thickness. In device fabrication, the effects of mechanical shock or vibration need to be evaluated to guarantee reliability of the devices under the usual operating conditions.

The study of microscopic properties of materials, down to the atomic scale, requires the use of suitable probes. There are specific problems in the characterization of liquid or biological materials, but the discussion will be centred on the study of solid samples, since the former are out of the scope of this report. The experimental methods used to study the microscopic properties will be presented according to the probed depth. Among the techniques used to study the surface morphology, can be mentioned Scanning Electron Microscopy (SEM), Atomic Force Microscopy (AFM) and Scanning Tunnelling Microscopy (STM). From the point of view of the probed surface area, STM has the best resolution (producing profiles on the atomic scale),

followed by AFM and SEM, in this order. From the point of view of the sample preparation AFM may be used to observe any solid surface without any preparation. Care must be taken however if the roughness is high since it can damage the needle probe; the same holds for STM samples. In the case of SEM if the sample is not electrically conductive it has to be coated with a conductive film in order to be observed. The experimental conditions used in these techniques can be slightly modified to get different properties from the materials. Information about the electronic structure of the surface can be obtained by studying the dependence of the STM signal on the sign and amplitude of the tip-sample voltage. In SEM different detectors sensitive to various energy ranges of the emitted electrons can be used. If the detector is tuned to the energy range corresponding to inelastically backscattered electrons, resulting from interactions where energy losses due to plasmon excitation and interband transitions occurred, an image sensitive to composition can be produced. Another direct imaging technique able to achieve high resolutions up to the atomic scale is Transmission Electron Microscopy (TEM). Given the limited penetration depth of electrons through solid materials, very thin samples have to be prepared in order to be observed in a transmission electron microscope. This method can be used to study thin film dislocations and grain structures, for instance.

Another technique used to probe the topmost surface layer of solid samples is thermal desorption spectroscopy. This technique is used to study the adsorption mechanisms of particles at surfaces. Heating a sample under Ultra High Vacuum (UHV) conditions, gives rise to a temporary pressure increase due to desorption. Measuring the pressure increase as a function of temperature, information about desorption rates and energies can be determined. Desorption can also be excited using different forms of energy or particles, such as: ions, electrons, photons or high electric fields. Ion Impact Desorption (IID) typically uses argon ions with energy around 100 eV accelerated onto the sample to stimulate desorption. Electron Stimulated Desorption (ESD) uses electrons, PhotoDesorption (PD) uses light and Field Desorption (FD) uses electric fields. Both ESD and FD may be used to get a spatial image of desorption geometry.

Depending on the exciting probe and type of the detected signal the probed depth may be higher or lower. Atomic particles such as ions and electrons have very low penetration on the surfaces. Nevertheless, varying the particle energy the penetration can be changed, but above certain limits this implies also changes in the interaction processes. The same happens with light, although photons have higher penetration compared with ions or electrons with similar kinetic energy. The probed depth of the sample is always determined by the maximum depth from which the detected signal is originated, consequently experimental techniques using ions or electrons are generally used to probe the first few atomic layers of a surface while photons are usually employed to probe deeper into the sample.

Among the techniques involving ions can be mentioned Secondary Ion Mass Spectroscopy (SIMS) and Low-Energy Ion Scattering (LEIS). In SIMS a primary ion beam with a typical energy between 1 KeV and 20 KeV is incident on a surface. Due to the transferred impact energy neutral atoms, molecules, ions and clusters are emitted from the surface. These emitted ions (so-called secondary ions) are analysed and detected by a mass spectrometer. The measured mass spectrum then yields information about the chemical composition of the surface. This experimental technique is also called static SIMS. If higher primary beam currents are used, a higher rate of emission of secondary particles results and therefore considerable quantities of material are removed. During this process, SIMS spectra are monitored which gives information about the chemical elements contained in the removed material. This kind of measurement allows a layer by layer analysis of the sample. When coupled with other surface characterization techniques, such as Auger Electron Spectroscopy (AES) or X-ray Photoelectron Spectroscopy (XPS), ion bombardment permits to obtain spectra that depend on the layer depth and are usually termed depth profiles. The ion beam used in LEIS is similar in its characteristics to the ones used

in SIMS. In the former case, however, the analysed particles are the primary backscattered ions and not the ions removed from the sample. This technique is used to get information about the sample composition, like SIMS. More used than LEIS is Rutherford BackScattering (RBS), which employs high energy ions (in the range between 50 KeV to 5 MeV). Given the higher primary beam energy this technique has also higher penetration depth into the sample. If the angle of incidence of the primary beam in RBS is varied, information about the incorporation of impurities, relaxation effects and quality of overlayers in crystals, may be obtained.

There are a good number of techniques employing electrons either to excite the surface or resulting from the excitation process. The most common might be AES and XPS. But there are some more that deserve to be mentioned, such as, Low Energy Electron Diffraction (LEED) and Electron Energy Loss Spectroscopy (EELS). AES is an electron core-level spectroscopy, in which the excitation process is usually induced by a primary electron beam from an electron gun. The Auger process results in secondary electrons of relatively sharply-defined energy, that are directly related to differences in core-level energies. The measurement of this energy can be used to identify a particular atom and therefore determine the surface composition of the sample. Similar results about the surface composition can be obtained from XPS. This technique generally uses a monochromatic X-ray beam instead of electrons to excite electrons from occupied states into empty states, whence they are removed from the atom and detected by an electron-energy analyser. Otherwise ultraviolet radiation can be used to start the photoemission process, in which case the technique is called Ultraviolet Photoelectron Spectroscopy (UPS). This has higher surface sensitivity given the lower energies of the emitted electrons. Both techniques provide also useful information about the surface electronic band structure. Electrons impinging on a solid surface may also undergo elastic or inelastic scattering. LEED, for instance, uses the diffraction pattern that results from the elastic scattering of an electron beam to check the crystallographic quality of a freshly prepared surface or as a means of obtaining new information about atomic surface structure. On the other hand there is EELS, in which inelastic scattering is employed to study excitations on surfaces or in thin solid films. The different solid excitations that can be observed over the energy range starting at 1 KeV and ending at a few meV, require the use of different experimental equipment in order to obtain adequate energy resolutions at very small and very high excitation energies. Electron energy loss may result from the interaction with phonons, plasmons, adsorbate vibrations, interband or core-level electronic transitions. When EELS is performed with high energetic resolution at primary energies below 20 eV, it is called High Resolution EELS (HREELS). HREELS is mainly used to study the vibrations of adsorbed atoms and molecules.

Neutral atoms and molecules have also been used as probes in characterization techniques. Neutral particles with a low energy (typically below 20 eV) impinging on a solid surface, cannot penetrate into the solid. Therefore, scattering experiments with neutral particle beams provide a probe that yields information exclusively about the outermost atomic layer of a surface. Elastic He atom scattering, for instance, can provide information about the structural properties of a surface [27]. In contrast to electron scattering in LEED, where the electrons penetrate several atomic layers into the solid, only the outermost envelope of the electron density about the surface is probed by the He atoms. This makes this technique relatively insensitive to clean, well-ordered, densely packed metal-surfaces. However, deviations from ideality, such as steps, defects or adsorbates, can affect the elastically scattered intensity in reflection direction, making this technique very useful for characterizing the degree of ideality of a clean surface after preparation.

As already mentioned, depending on the exciting beam energy different interaction processes can occur when light is irradiated onto a surface. Elastic scattering has been discussed before, in the scope of optical characterization of materials. However, there is still another important elastic

scattering process widely used to study the crystal structure of solids, which is X-Ray Diffraction (XRD). The interference patterns are observable in this case, because the wavelengths of X-rays are of the same order of magnitude as atoms' spacing inside crystals. The majority of the processes though, result from inelastic scattering.

Among the characterization techniques taking information out of inelastic scattering processes can be mentioned Energy or Wavelength Dispersive X-ray analysis (EDX/WDX), Extended X-ray Absorption Fine Structure (EXAFS), PhotoLuminescence (PL) and Raman excitation spectroscopy. EDX and WDX<sup>2</sup> use characteristic X-rays emitted by excited elements present in a given sample to determine its composition. Excitation may be obtained either using an electron probe or a light beam with suitable energy. EXAFS is used to study the bulk atomic structure, namely, bond length and coordination numbers, taking this information out of the fine structure of the absorption coefficient spectrum, on the high energy side of an absorption edge. The origin of this fine structure is an interference effect of the photoelectron wave function. Photoluminescence detects an optical transition, from an excited electronic state to a lower electronic state, usually the ground state. It is a very sensitive tool for investigating both intrinsic electronic transitions and electronic transitions from impurities and defects in semiconductors and insulators [29]. Instead of a light beam, accelerated electrons or carrier injection could be used to produce the excited electronic states, in which case the technique would be called cathodoluminescence or electroluminescence, respectively. Luminescence spectroscopies are also employed to characterize microstructured materials like quantum wells and superlattices. Finally there is Raman excitation spectroscopy that is based in light scattering produced by phonons.

The presented list of characterization techniques is certainly not meant to be complete. Otherwise it was inserted to give a broad view of the kind of information that they can offer and to provide some insights on their scope and limitations. Many other could be referred having their own advantages and drawbacks in specific applications. In addition, with the extensive use in many laboratories around the world most of the described techniques have been modified in order to get new or more accurate properties from the data or to make possible their application to new materials. A description of the possibilities introduced by these modifications would require a much more detailed knowledge of each technique, that is beyond the purpose of this report.

### 2.3. Thin film resistive gas sensors

Resistive sensors have been used to measure a wide variety of physical and chemical properties and are among the most common and cheap sensors commercially available. There are for example photoresistive sensors, which use materials that change conductivity with light absorption; thermoresistive sensors in which resistivity variation is controlled by the temperature; piezoresistive sensors, that use the change in resistance with mechanical stress; magnetoresistive sensors based on the resistivity change in the presence of an external magnetic field and chemoresistive that measure the resistivity change produced by the interaction of a chemical substance with the sensing material. The materials employed in these sensors are frequently produced in thin film form and in many cases can be produced by magnetron sputtering. Furthermore, materials of the kind employed in these devices have been prepared in the Thin Films Lab at the University of Minho, for other purposes.

In the gas sensor field, the most suitable materials for sensors of the chemoresistive type are metal oxides. Although the effect of the ambient atmosphere upon the electrical conductance of semiconductors was known before [30, 31], it was not until Seiyama and co-workers [32] that

---

<sup>2</sup>EDX and WDX may also be designated EDS and WDS, taken respectively from Energy or Wavelength Dispersive Spectroscopy



this knowledge was applied to gas detection. The first commercial gas sensor was developed by Tagushi<sup>3</sup> not long after the work of Seiyama. Since then many other devices were developed and the number of materials used in gas detection has not stopped growing. Among the materials employed in resistive gas sensors the most used is tin dioxide. Other metal oxide materials successfully employed in gas sensors include  $\text{WO}_3$  [33–35],  $\text{Ga}_2\text{O}_3$  [36–38],  $\text{In}_2\text{O}_3$  [39–41],  $\text{TiO}_2$  [42–44],  $\text{ZnO}$  [45],  $\text{Fe}_2\text{O}_3$  [46],  $\text{HfO}_x$  [47],  $\text{V}_x\text{O}_y$  [48, 49],  $\text{Cr}_2\text{O}_3$  [50],  $\text{CdIn}_2\text{O}_4$  [51],  $\text{SrTiO}_3$  [52] and  $\text{Li}_2\text{SnO}_3$  [53]. Among the organic materials the phthalocyanines are the most used, but other can be found in reports from the field of organic chemistry.

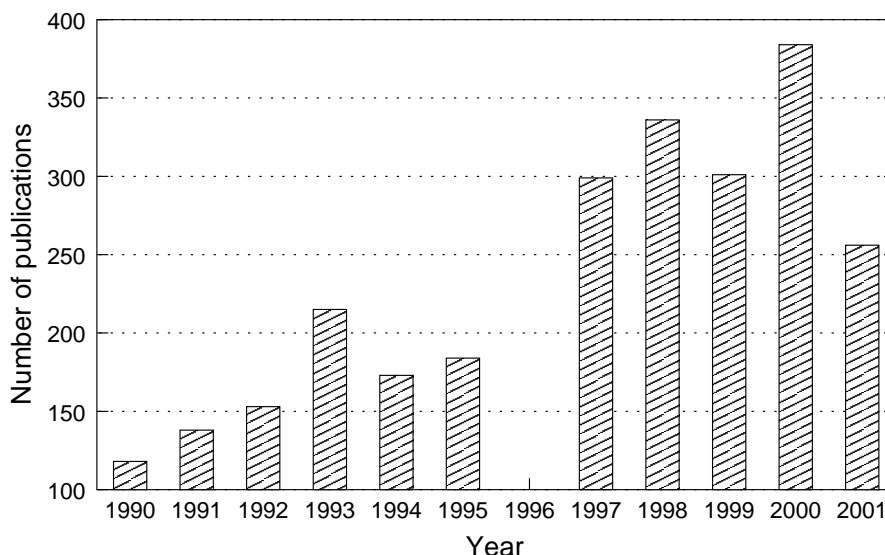


Figure 2.3.: Evolution of the number of papers published from 1990 to 2001 on gas sensors (at the time this search was performed there was no information concerning the year 1996)

The main sources of gas sensor knowledge are international conference proceedings and scientific journals. A number of monographs appeared also in the last decade. A search performed in the Inspec database<sup>4</sup> lists about 1737 reports published on gas sensors since 1995. Fig. 2.3 shows the evolution of the number of publications from 1990 through 2001. A gradual rise can be observed during the stated period. From these 27 % were published on *Sensors and Actuators B (Chemical)*, which makes this journal the leading source of gas sensor knowledge. Almost all the publications listed are written in English, although there are some, about 6 % in other languages. In spite of the growing number of materials successfully employed in gas sensor devices, the fraction of the reports dealing with tin oxide based materials and published from 1995 to 2001 is still 12 %. An attempt was made to estimate the number of publications dedicated to the study of gas sensing materials produced by magnetron sputtering. This search produced only 36 records, which amounts to 2 % of the publications on gas sensors. This number is lower than expected, given the advantages and demonstrated possibilities of this technique. However the true value should be somewhat higher since the search was performed on keywords, title and abstract, and the manufacturing process of the sensing material is not always stated in these sections.

<sup>3</sup>UK patent 1280809 (1970); US patent 3631436 (1970).

<sup>4</sup>Inspec is a database, covering the fields of physics, electrical engineering, electronics, telecommunications, computers, control technology, and information technology; and is maintained by The Institution of Electrical Engineers (IEE).

### **2.3.1. Metal oxide based gas sensors**

Under the influence of ambient gases, metal oxide layers used in gas sensors may undergo either surface or bulk conductance changes. Usually surface conductance changes are associated with electron transport processes, while bulk conductance changes generally imply ion transport. Depending on the type of charge carrier involved in the sensing processes, these devices may be divided into three different groups: electronic conductance sensors, if the charge carriers are electrons or holes; ion conductance sensors, if the charge carriers are exclusively ions and mixed conductance sensors if the charge carriers are electrons and ions. Electrochemical sensors belong to the class of the ion conductance sensors.

The distinction between electronic, ionic and mixed conduction cannot be done exclusively on the basis of the sensing material because the conduction mechanism may change with temperature or applied electric field. Therefore, individual contributions from electronic and ionic conductivities have to be studied under the operating conditions of each device, using proper electron or ion conducting electrodes and measuring procedures that permit an adequate evaluation of local contact influences.

The fabrication of stable three phase boundaries between metals, oxides and the gas phase, is a common problem in gas sensor development. Usually the electric contacts with the sensing material should be ohmic, should not diffuse into the sensing material and should have no interaction with the gas phase. An ohmic contact may be defined as a metal-semiconductor contact that has a negligible contact resistance relative to the bulk resistance of the semiconductor [54]. A satisfactory ohmic contact should not significantly degrade device performance, and should pass the required current with a voltage drop that is small compared with the drop across the active region of the device. Diffusion of electrode material into the sensing layer is a common source of long-term drifts. In order to prevent diffusion a barrier layer may be deposited between the electric contact and the sensing material. Electrode interaction with the gas phase may be used sometimes to improve sensor performance [55], but more frequently it might be a source of uncontrolled interference to the device output.

The interaction mechanisms between the gas phase and the sensing material involve mainly physisorption, chemisorption, surface defects, bulk defects or three phase boundary processes. Physisorption is the weakest form of adsorption to a solid surface and is essentially maintained by van der Waals interactions. Given the unselective character of van der Waals interaction, sensors based on physisorption processes usually exhibit sensitivity to a wide range of gaseous species. Chemisorption, on the other hand, is a stronger interaction, that shows a higher selectivity. In this kind of interactions adsorbates form chemical bonds with the surface atoms and thus the electronic structure of both the adsorbate and the surface are modified. Chemisorption is usually promoted by surface defects.

By a defect one generally means any region where the microscopic arrangement of the particles differ from a perfect crystal. These may be called surface, line or point defects according to whether the imperfect region is bounded on the atomic scale in one, two or three dimensions [56]. However, since this work is mainly concerned with surface processes, the term surface defect will not be used with the meaning stated above, but as opposed to bulk defects, to refer to the defects, whether point or line defects, present in a given surface.

It is known that surface atoms usually arrange themselves, which gives the surface quite different properties from the bulk. Furthermore, the surface on its own and free of defects, given the incomplete coordination, shows an increased reactivity towards the colliding particles and has its own electronic states, different from the bulk. On the surface both line and point defects reveal to be important to gas sensing processes. In the bulk, on the other side, only the point defects will be relevant.

Discrimination between intrinsic and extrinsic defects is also frequent. Meaning by extrinsic

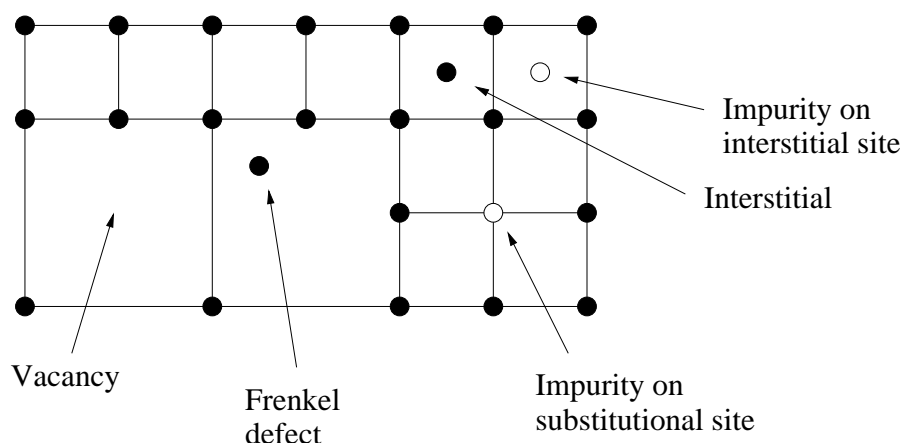


Figure 2.4.: Types of point defects on a simple crystal lattice

defects those that result from the insertion of a foreign particle in the lattice. In this sense, adsorbed atoms may be considered point defects.

The most frequent intrinsic surface defect in n-type semiconducting oxides is a donor-type oxygen vacancy. Other surface defects important in the gas sensing mechanisms are impurities or dopants. Their electronic and geometric influence on sensor properties is usually correlated with catalytic properties [57]. Since many metal oxides are produced in polycrystalline form, surface defects relevant in gas sensor mechanisms include not only the surface contacting the gas, but also the size, shape, structure and contact between the grains.

Mobile point defects make possible ion transport in a material. In many cases, non-stable defects may be a source of drifts, but may also be essential to recover the sensor properties after interaction with the sensed gas. Grain boundaries and crystallite interfere in the charge transport and have been found in some cases to be the key factor that controls the device sensitivity. Finally, instead of impurities at the surface, it is possible to grow a porous catalytic layer over the sensing material to improve sensor performance, which is one of the common possibilities of the three phase boundary processes.

The interaction mechanisms depend not only on the material, but also on the operating conditions of the device. Temperature, for instance, can change adsorption and desorption processes, as well as defect dynamics. At low temperatures, adsorption is favoured, while with increasing temperatures desorption starts to dominate over adsorption. Given the lower binding energies, physisorbed species will desorb before chemisorbed ones. Temperature effect on the defect density depends also on the binding between the atoms that form the crystal structure. Surface reactions may be altered by the temperature, the atmosphere composition or the pressure. Usually the reactions involve several different steps, so that it is necessary to know the reaction paths of the particles that interact with the surface to understand the whole process.

Reactions occurring at the surface of gas sensors mainly fall under the group of heterogeneous catalysis. In a catalysed reaction the equilibrium composition of a system is not disturbed, only the rate at which this equilibrium is attained, is altered [58]. Similarly the sensor surface should not be altered by the reactions taking place on it. Usually the surface just provides a better place for a reaction between gaseous species to occur. Furthermore, all the reaction products should desorb during normal sensor operation. Otherwise the adsorption sites would be blocked and the sensor could no longer be used.

Catalysis is called heterogeneous, when the catalyst and the reactants are in different phases. In the case under consideration the reactants are gases and the catalyst is the solid surface. In order to take place, heterogeneous catalysis requires that at least one of the species adsorbs

on the surface and is modified to a form under which it may readily undergo reaction. There are two main accepted mechanisms for the reaction: the Langmuir-Hinshelwood mechanism, that assumes that the interaction takes place between chemisorbed species, and the Eley-Rideal mechanism, that assumes that the reaction results from the interaction between a gas phase particle and an adsorbed species. Surface defects may behave as active sites for the catalysis, i.e., reaction occurs preferentially at defects [59]. These may be point defects such as impurities or vacancies, line defects such as terrace edges, or grain boundaries, to put some examples.

In order to get high performance gas sensors, it is necessary to have a good control over the sensing material structure. Metal oxides have been produced using several different techniques, either thick-film and ceramic techniques, or thin-film techniques such as thermal evaporation, sputtering or CVD techniques. In general, reports show different response characteristics for gas sensors produced using different techniques. This is to be expected, having in mind that different preparation techniques also supposes different materials' structure.

Usually material development starts by studying the response characteristics of a given oxide material without impurities. Afterwards preparation conditions or procedures might be changed to achieve a different oxide stoichiometry, defect density or crystal structure. A more common procedure, however is to add promoters or a different phase to the structure, in order to change the materials' sensing characteristics. The most affected characteristics are usually response time, sensitivity, selectivity and stability.

Metal oxide semiconductors are mainly used to detect small concentrations of reducing and combustible gases in air. Among these gases there have been found materials with sensitivity to: H<sub>2</sub> [7, 55, 60, 61], CO [62–65], O<sub>3</sub> [41], H<sub>2</sub>S [66–69], NO<sub>x</sub> [70–72], PH<sub>3</sub> [73], NH<sub>3</sub> [74–76], CH<sub>4</sub> [77–79], ethanol [80–84] and LPG [85–87]. In the majority of the devices the detection mechanism of these gases requires oxygen in the atmosphere and is influenced by the presence of water vapour. It may also be observed that with increasing layer temperature, sensitivity reaches a maximum value and then fall towards zero, at higher temperatures [88]. Since the optimum temperature depends on the gas compound, the operating temperature may be used as a means to change the selectivity of the device. As to the response to different concentrations of the sensed analyte, normally these sensors show high resolution at low concentrations, and progressively lower resolution towards higher concentration values. Given that these sensors usually show fast response times, they are very useful to detect lower concentration limits of toxic substances in atmosphere. Other important applications include humidity sensors [53, 89] and oxygen sensors [90].

### 2.3.2. Sputtered tin dioxide layers for CO sensors

Both nitrogen dioxide and carbon monoxide are gases released as a result of combustion processes. Indoor concentrations of NO<sub>2</sub> often exceed outdoor in homes that contain stoves, space heaters or water heaters that are fuelled by gas. The flame temperature in these appliances is sufficiently high to combine some nitrogen and oxygen to form NO, which eventually may be oxidised later to nitrogen dioxide. Carbon monoxide, on the other hand, results from the incomplete combustion of carbon containing fuels such as wood, gasoline or gas, in oxygen deficient atmospheres. High indoor concentrations usually arise from malfunctioning combustion appliances. Average outdoor and indoor CO concentrations usually amount to a few parts per million, though elevated values in the 10 ppm to 20 ppm range are common in parking garages due to the carbon monoxide emitted by motor vehicles [91].

Carbon monoxide toxicity originates in its ability to form a stable compound, called carboxyhemoglobin, with the blood molecule that transports the oxygen to the cells. Carboxyhemoglobin is unable to transport oxygen, thus CO poisoning results in the reduction of the number of active oxygen transporters in blood. Depending on the concentration and duration

of the exposure, poisoning with CO may cause headache, drowsiness, dizziness, excitation, rapid breathing, pallor, cyanosis<sup>5</sup>, excess salivation, nausea, vomiting, hallucinations, confusion, angina<sup>6</sup>, convulsions, and finally unconsciousness. With well established poisoning, the mucosal surface will be bright red (cherry red). Repeated overexposure will cause gradually increasing central nervous system damage, with loss of sensibility in the fingers, poor memory and mental deterioration. Other effects include embryotoxicity, impaired cardiovascular function, pulmonary oedema<sup>7</sup>, pneumonia<sup>8</sup>, gross neuropsychiatric damage, memory impairment, permanent central nervous system damage and cerebral oedema with irreversible brain damage. Chronic exposure may promote development of atherosclerosis<sup>9</sup> [92].

The main characteristics that make carbon monoxide specially dangerous are its odourless and colourless properties. There are nowadays several commercially available CO alarms, which have significantly reduced the risks of carbon monoxide poisoning. However, even now many of these devices either fail to fulfil the new standards or respond to common gases and thus produce unreliable results. Two commonly used types of sensors for the detection of CO are heated semiconductor SnO<sub>2</sub> devices and room-temperature electrochemical sensors. Bârsan et al. [93] compared the performance of some of these devices under short- and long-term operation, concluding that electrochemical sensors have a better analytical sensitivity at higher concentrations, while SnO<sub>2</sub> sensors have a better analytical sensitivity at lower CO concentrations. This result is mainly due to the non-linear dependence of the output signal of the latter devices, which has been referred previously. The same tests showed that the stability of electrochemical sensors is significantly better than the SnO<sub>2</sub> sensors, even excluding an initial 30 minutes stabilisation period after placing the device on the potentiostat. The SnO<sub>2</sub> devices used in these tests were commercially available ceramic sensors from Figaro Engineering Inc. (Osaka, Japan) and thick film Pd and Pt doped devices.

The mechanism responsible for the instability of these sensors is not well established. The same happens with the influence of humidity on the sensitivity of the devices. Studies involving many different characterization techniques, have been growing, but the different characteristics, presented by layers prepared using different methods, have not helped in this task. Given the good properties of SnO<sub>2</sub> layers in CO gas sensing, almost every preparation procedure from ceramic to thin films has been used to produce it. Nevertheless, the possibilities of the different techniques in many cases have not been explored thoroughly. It is worth to remember that sensing behaviour depends not only on the material's characteristics but also on the device configuration and on the working conditions. In order to optimize device performances, it would be interesting to be able to predict in real conditions which factors will dominate and the effect they will produce.

Both RF and DC magnetron sputtering have been used to produce gas sensitive tin oxide layers [94–108]. In this work, exploration of the possibilities of DC magnetron sputtering and characterization of the layers will be performed in order to optimize the sensing characteristics and study the mechanisms that control the sensing properties of SnO<sub>2</sub>.

---

<sup>5</sup>Blue discolouration.

<sup>6</sup>chest pain brought on by exertion, owing to poor blood supply to heart.

<sup>7</sup>excess fluid in body cavities or tissues

<sup>8</sup>inflammation of lungs

<sup>9</sup>formation of deposits in the blood vessels

## 2. *Gas sensors' state of the art*

## 3. Characterization of tin dioxide thin films

### 3.1. Composition

The analysis of the samples' composition was done using EDX and XPS. EDX was used to get information about the bulk composition. It usually permits to identify elements that are present in the sample with a concentration higher than about 0.1 at%. In the case of samples with thickness below 1  $\mu\text{m}$  the elements composing the substrate are sometimes visible in the spectra. Given that the depth resolution depends both on the material structure and on the incident electron beam energy, using a constant beam energy will not alone guarantee a unique depth resolution. On the other hand, if the incident electron beam energy is much reduced, it might fail to ionize the sample elements and thus produce misleading results. Finally, owing to the small lateral resolution that can be made as low as 0.3  $\mu\text{m}$ , EDX may be used to identify the elements composing some of the features with larger size, observed on the samples' surface.

XPS was used to evaluate the surface composition. The sampling depth of this technique is usually lower than 50 Å, so that only the topmost layers are probed. As in the case of EDX, the sampling depth changes with composition and density of the sample. The excitation energy, as already mentioned, is generally provided by an X-ray source, such as the  $K_{\alpha}$  line of magnesium or aluminium and therefore its value cannot be varied. The sampling depth will depend mainly on the energy of the electrons escaping from the surface. Given that there are usually some particles adsorbed on the surface, the sample is often submitted to a cleaning process before the analysis, to guarantee that the sampling volume is closely homogeneous. Similarly again to EDX, XPS can be used to identify elements with atomic number from that of boron to uranium. The detection limit is usually greater than 0.01% of a monolayer. Using both techniques will thus produce complementary information about the analysed samples. The XPS tests were performed in CEMUP, the University of Porto Materials Centre, while the EDX analysis were performed in the scanning electron microscope at the University of Minho.

#### 3.1.1. Bulk composition

Energy dispersive X-ray spectroscopy is a nondestructive instrumental method of qualitative and quantitative analysis of chemical elements based on the measurement of intensities of characteristic X-ray spectra excited by an electron beam. An electron beam of primary energy typically from 2 KeV to 10 KeV, is focused on the sample surface and the energy regulated in order to increase or decrease the sampled depth. In addition to X-ray emission, the interaction of the electron beam with the material results in many different phenomena, such as backscattered, secondary or absorbed electrons and cathodoluminescence. The backscattered electrons have relatively high energy, ranging up to that of the incident electrons, and its fraction is dependent both on the composition and microstructure of the sample. The majority of the secondary electrons comes out with an energy below 50 eV and corresponds to electrons that undergo multiple scattering events on their way to the surface. Their spectral distribution and intensity does not depend on the composition although it depends on the surface morphology. Among secondary electrons, but with energy above 50 eV, some Auger electrons can be identified. These can only

### 3. Characterization of tin dioxide thin films

yield information about the composition of the topmost layers of the sample, since Auger electrons originating further inside undergo inelastic scattering before coming up. Obviously the electrons that lose all the energy inside the sample are absorbed and build a charge in the sample that has to be removed.

X-ray emission from the sample, on the other hand, has higher probe depth since X-ray absorption by matter is weak. Thus, the emitted photons originate from a depth range which is mainly determined by the penetration depth of the high energy primary electrons. In addition to the X-ray photons that result from electronic transitions occurring in the sample, a continuum X-rays spectrum, produced by the deceleration of the incident electrons inside the sample, is present in the emitted radiation. In order to obtain quantitative information about the composition from the emitted X-ray spectrum it is necessary to measure the intensity of the characteristic X-ray peaks and apply corrections taking account of the atomic number of the species, the self-absorption by the sample and the fluorescence. These corrections are usually termed ZAF corrections. The concentration of a given sample is then derived from the ratio of the intensity measured on the sample to the intensity measured on a standard.

Four samples were analysed by EDX: e5a4, e11a2, e16a1 and e99a3. With the exception of sample e16a1, that was intentionally doped with molybdenum, the other three showed no other element apart from tin, oxygen, and silicon from the substrate. No concentration analysis were performed on the obtained spectra.

#### 3.1.2. Surface composition

The XPS spectra were acquired using an ESCALAB 200A (VG Scientific), running under VG5250 software for data acquisition, control and analysis. An unmonochromatized Mg  $K_{\alpha}$  X-ray source was used to excite the samples and the spectrometer was operated in the CAE mode. A wide scan spectra of every sample was obtained in first place with a pass energy of 50 eV, in the range from 0 eV to 1150 eV, to identify the elements existing on the surface. After this scan, detailed spectra of the O 1s and Sn 3d were obtained in order to determine the relative concentration of these elements and the binding states. The pass energy of the detailed spectra was 20 eV. Detailed spectra of the C 1s peaks were also registered in order to evaluate the effect of surface charging on the measured binding energy. Taking into account the kinetic energy of photoelectrons useful for the analysis, the estimated probed depth is within 18 to 24 monolayers. Spectra analysis was performed using peak fitting with a Gaussian-Lorentzian peak shape and a non-linear Shirley type background subtraction, as available on the VG5250 software.

The analysis of samples a14a22, e11a1 and e99a3, showed that apart from oxygen and tin there were also traces of chlorine, sodium and carbon on the surface as can be observed in Fig. 3.1. The film thickness was 6.0  $\mu\text{m}$ , 0.20  $\mu\text{m}$  and 6.9  $\mu\text{m}$  respectively for films: a14a22, e11a1 and e99a3. All the samples were deposited on microscope glass slides. The thicker samples show a small amount of Na, that is lower than the amount observed at the thinner. This supports the hypothesis that these elements reach the surface through diffusion starting at the glass substrates. A sample deposited on steel did not reveal traces of sodium. Sample e99a3 was prepared about one week before the analysis while the other two were prepared about one year before. This, along with thermal cycling that the samples undergo during gas sensing tests, may explain why sample a14a22 shows a higher sodium content than sample e99a3, although both samples have similar thickness.

Between the deposition and the XPS analysis the samples were kept in air and enveloped in aluminium foil to protect them from dust. The carbon detected is probably caused by organic compounds adsorbed after deposition. A depth analysis would permit to verify this hypothesis, but was not available at the time the analysis was performed.

The detailed spectra of the carbon 1s peak revealed a shift of 1.2 eV towards higher binding



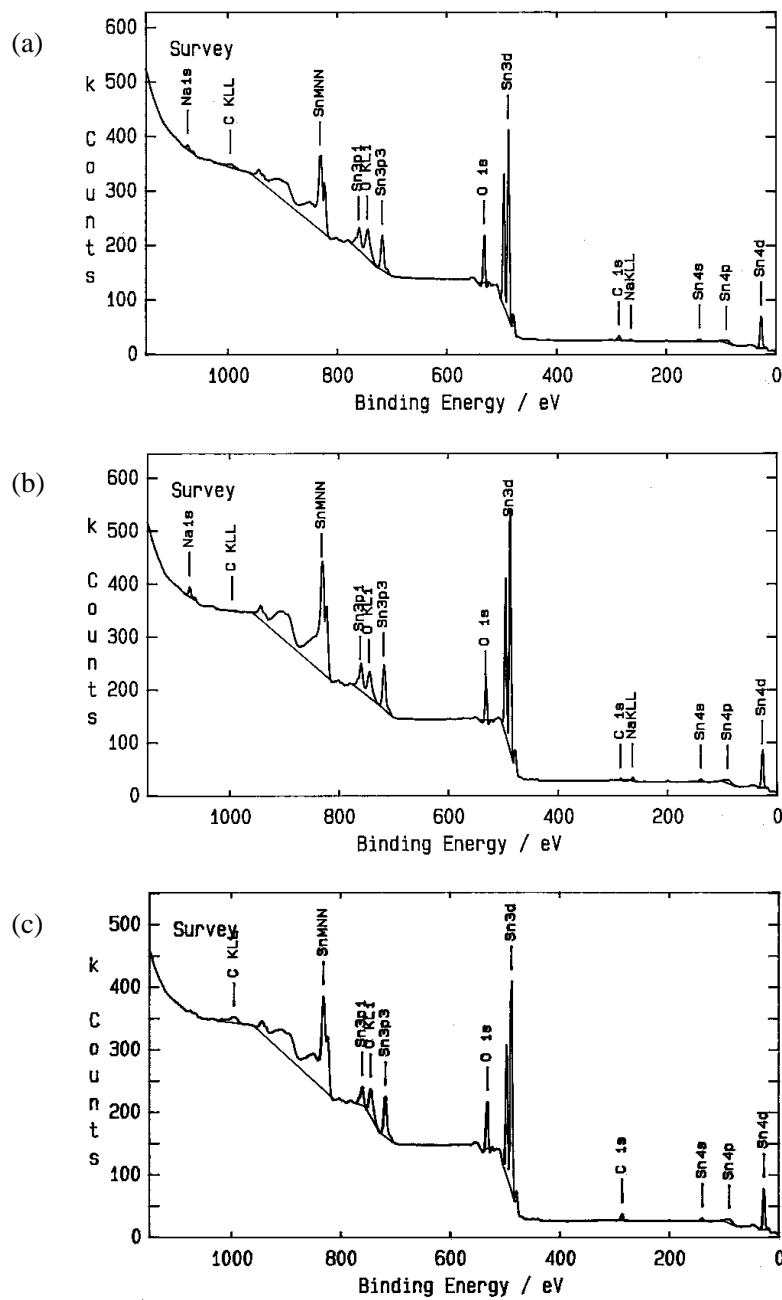


Figure 3.1.: XPS spectra of samples a) a14a22, b) e11a1 and c) e99a3

### 3. Characterization of tin dioxide thin films

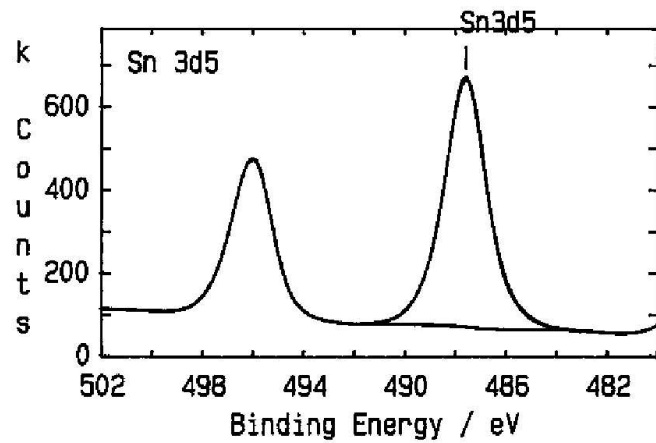
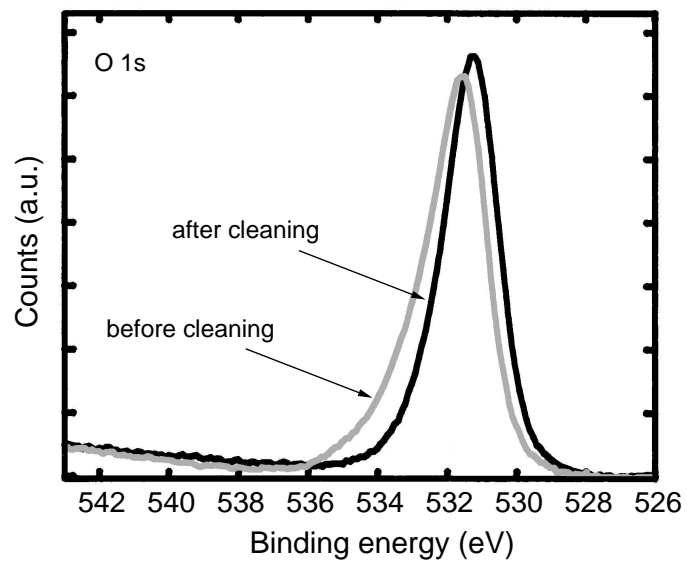


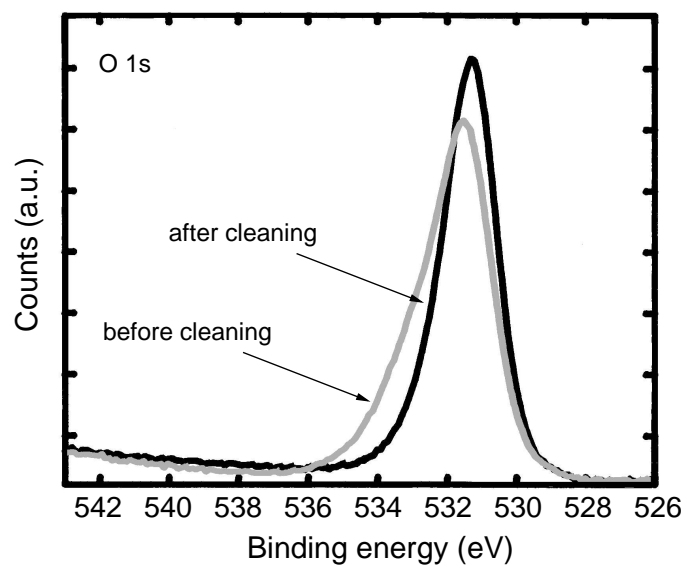
Figure 3.2.: Detail of the XPS Sn 3d<sub>5/2</sub> peak of sample e99a3

energy. Assuming that the carbon peak energy shift is due to the surface charging, the binding energy of the Sn 3d<sub>5/2</sub> peak should be 486.4 eV (see Fig. 3.2), which is very close to the reported value for the binding energy of Sn 3d<sub>5/2</sub> in SnO and SnO<sub>2</sub> samples: 486.8 eV and 486.6 eV, respectively [109]. Observing the peak shape there seems to be only one tin binding state in the sample.

On the other hand, the asymmetric oxygen 1s peak shape observed in Fig. 3.3, leads to suspect of the existence of several different oxygen species on the surface. These may correspond to lattice oxygen, and to one or more adsorbed species on the surface. When the samples undergo a light ion bombardment to remove the usual surface contamination, the oxygen 1s peak approaches a symmetric shape, suggesting that the oxygen species responsible for the asymmetric shape are weakly bound to the surface, as expected in the case of adsorbed species. The electrons corresponding to the removed species show higher binding energy than the others, which may be explained because adsorbed oxygen species are usually ionized. Otherwise, these oxygen species may correspond to organic compounds adsorbed on the surface, given that carbon was also detected.



(a)



(b)

Figure 3.3.: Detail of O 1s peak of XPS spectra of samples a) a14a22 and b) e11a1, before and after a light ion bombardment

## 3.2. Bulk characterization

X-ray diffraction was used to determine the crystalline structure and preferential orientation of the crystallites. SEM was used to observe the morphology of the films' cross section and measure film thickness. Mass measurements were performed before and after film deposition to determine deposited mass. In addition optical transmittance measurements were performed in the range from 200 nm to 2500 nm. The transmittance spectra were then analysed in order to extract information about film thickness and refractive index.

X-ray diffraction spectra were acquired using a Philips diffractometer (model PW1719) in the University of Minho. It was used an X-ray beam (40 KeV, 30 mA) produced by the Cu  $K_{\alpha}$  line. The spectra were scanned in the range  $2\theta_B$ , where  $\theta_B$  is the Bragg diffraction angle, from  $10^{\circ}$  to  $80^{\circ}$ , with step  $0.02^{\circ}$  and step integration time 1.25 s. Before measuring peak intensity and position, the background from the glass substrates was subtracted from the spectrum. Peak position and FWHM were then determined by fitting the resultant peak with two Gaussian functions corresponding to  $K_{\alpha 1}$  and  $K_{\alpha 2}$  radiation, in order to find the true peak position and width. The Scherrer formula [110],

$$D_{gr} = \frac{0.9\lambda}{B \cos(\theta_B)} \quad (3.1)$$

was used to estimate the average crystallite diameter,  $D_{gr}$ . Note that in this formula  $\lambda$  is the X-ray wavelength and  $B$  is the FWHM after correction for the instrument broadening. The orientation of the crystallites was assessed comparing the peak intensities with the values reported by the JCPDS files<sup>1</sup>. The X-ray density was also estimated and compared with the density determined by the mass and volume measurements of the layers.

The SEM images were also obtained in the University of Minho, using a Leica S-360 microscope. In order to observe the layers' cross section the samples were broken and coated with gold before the analysis. The film thickness measured in the electron microscope was subsequently compared with the values obtained by analysis of the transmittance spectra, to compare the accuracy of both methods.

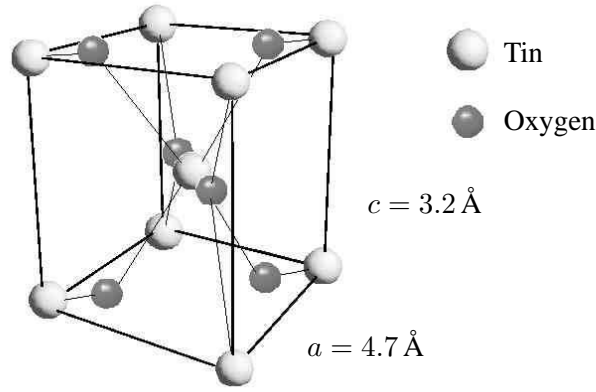
The transmittance spectra were obtained using a Shimadzu UV-3101PC spectrophotometer, in the Physics Department of University of Minho. The spectrophotometer was operated in the spectrum mode with a scanning speed of 700 nm/min. Before each set of experiments the slit width was selected at 0.5 nm and the baseline utility was run without any sample inside the device.

Thin film deposited mass was measured with a Sartorius M5P electronic microbalance by subtracting sample mass after deposition from the mass measured before the deposition. Mass measurements were performed with a precision of at least 0.05 mg.

### 3.2.1. Crystalline structure

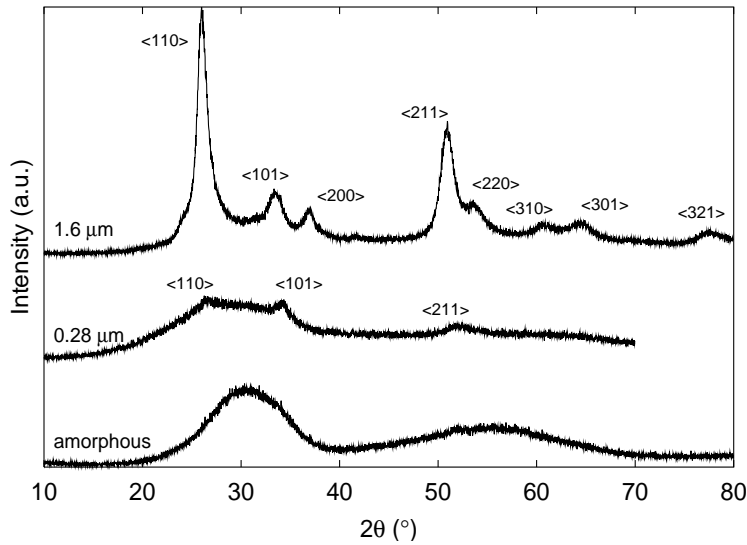
More than thirty samples were analysed by XRD. With the exception of samples a2a2 and a2a3, all the samples showed diffraction peaks corresponding to the SnO<sub>2</sub> tetragonal crystal structure. The referred two samples showed no diffraction peak and had a characteristic dark colour typical of amorphous SnO layers while the other samples were transparent, which is typical of SnO<sub>2</sub> crystalline layers. The cell corresponding to the body centred tetragonal structure of tin oxide is represented in Fig. 3.4. In this system the plane spacing,  $d$ , is given by the equation:

<sup>1</sup>Currently JCPDS has changed the designation to International Centre for Diffraction Data (ICDD), although the Powder Diffraction Files (PDF) are still widely known as JCPDS files

Figure 3.4.: Diagram of a tetragonal SnO<sub>2</sub> unit cell

$$\frac{1}{d^2} = \frac{h^2 + k^2}{a^2} + \frac{l^2}{c^2} \quad (3.2)$$

where  $a$  and  $c$  are the lattice constants and  $h$ ,  $k$  and  $l$  are the Miller indexes of the planes. Using the former equation and the lattice constants reported by the JCPDS files it is possible to compare the plane spacing values of the analysed samples with the ones expected for a tin dioxide single crystal.

Figure 3.5.: XRD spectra of three polycrystalline SnO<sub>2</sub> samples with different thickness

The spectra of samples with thickness lower than  $1 \mu\text{m}$ , show a large background, due to the glass, and low peak intensity which makes more difficult the determination of the peak position and FWHM with good accuracy. This can be observed in Fig. 3.5 where the diffraction spectra of samples a2a2, e5a3 and g11a3 are presented. The thickness of samples a2a2, e5a3 and g11a3 are respectively:  $12.6 \mu\text{m}$ ,  $0.28 \mu\text{m}$  and  $1.6 \mu\text{m}$ . In the spectrum of sample e5a3 can be identified peaks corresponding to directions  $\langle 110 \rangle$ ,  $\langle 101 \rangle$  and  $\langle 211 \rangle$  although the signal to noise ratio does not permit clear identification of neither the peak position nor the FWHM. Spectrum

### 3. Characterization of tin dioxide thin films

from sample a2a2 although very thick shows no diffraction peak. Finally the spectrum of sample g11a3 shows several peaks corresponding all to the tetragonal crystal structure.

Noting in Fig. 3.4 that the cell volume is  $a^2c$ , X-ray density,  $\rho_X$ , of tin oxide crystals is then given by:

$$\rho_X = \frac{2M_{Sn} + 4M_O}{a^2c} \quad (3.3)$$

where  $M_{Sn}$  is the tin atomic mass and  $M_O$  the oxygen atomic mass. Replacing the atomic masses of tin and oxygen in the above expression and using  $a$  and  $c$  in Å, the X-ray density in  $\text{g/cm}^3$  given by:  $\rho_X = 500.455/a^2c$ . Using the values reported in the JCPDS 41-1445 file for the lattice constants of tin oxide tetragonal crystals:  $a = 4.738\text{Å}$  and  $c = 3.187\text{Å}$ , X-ray density becomes  $\rho_X = 6.99\text{g/cm}^3$ , higher than the value determined by mass and volume measurements,  $\rho = 6.95\text{g/cm}^3$  [111] has expected.

#### 3.2.2. Grain structure

All the transparent samples analysed showed a polycrystalline structure, revealed by the XRD spectra and the grain like structures observed in the microscope images. The grain sizes determined using Eq. 3.1 were always lower than the ones observed by electron or atomic force microscopies; frequently one order of magnitude lower. This was expected to some extent since the FWHM measurements neglected the contributions from the non-random orientation of the crystallites and from the film strains. In the analysed samples both dominant orientation and film strains were observed, so that to estimate correctly the grain size from the XRD peak widths, the contributions of the former factors to the FWHM should be accounted for.

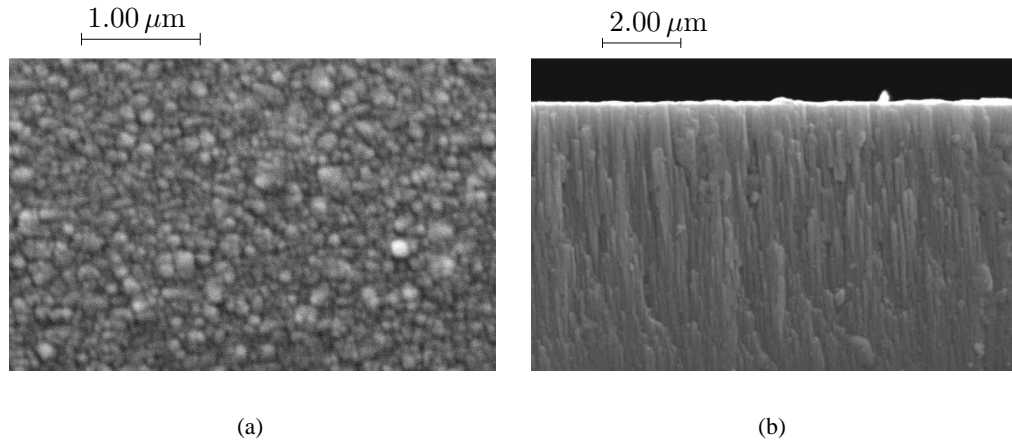


Figure 3.6.: Scanning electron microscope images of a) the surface and b) a cut of sample a14a2

It has already been pointed out in Section 3.2.1 that in films with thickness lower than  $1\ \mu\text{m}$  it was not possible to determine the FWHM of the diffraction peaks with good accuracy, thus the crystallite size was not determined using the Scherrer formula, in these cases. The images of these samples obtained with the scanning electron microscope did not permit to distinguish grain like structures. Thus, the only data that provided some information about the microstructure of the thinner samples was obtained from the observation of the AFM morphology of the surface. Some samples with thickness higher than  $1\ \mu\text{m}$  were observed in the SEM. Fig. 3.6 shows the images of the surface and section of sample a14a2, obtained in the scanning electron microscope. The image of the sectioned film shows clearly a densely packed structure of fibrous grains,

growing perpendicularly to the surface. This structure was detected in most of the analysed samples and is typical of layers corresponding to the zone T of the Thornton diagram [112].

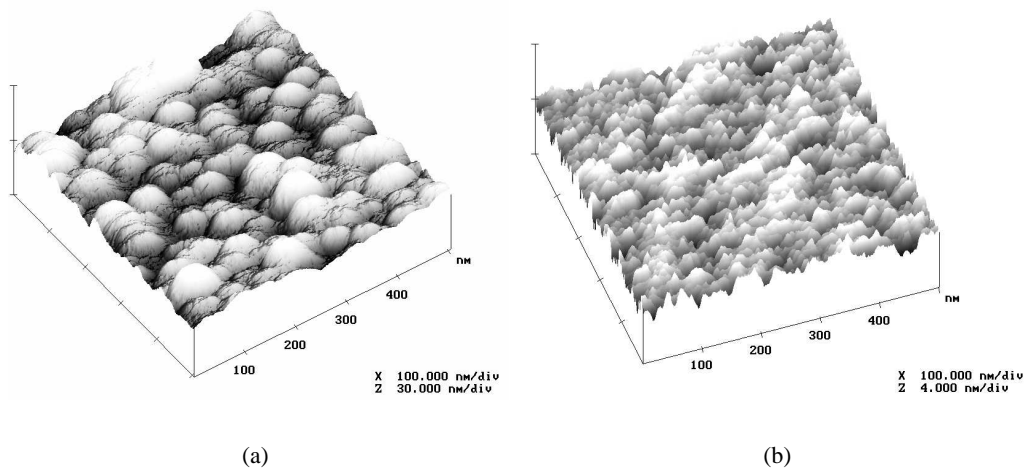


Figure 3.7.: AFM surface plots of samples a) f8a4 and b) h3a4

In the AFM images, significant changes were noticed in the grain like structures observed on the surface. Figs. 3.7(a) and 3.7(b) corresponding respectively to samples f8a4 and h3a4, show a surface where no grain like structure can be detected (that of sample h3a4) and another where these surface structures are well defined (taken from sample f8a4). From the growing structure perceived in the thicker films and observed with SEM, it is expected that diameter of the grains measured in the direction parallel to the layer surface does not change significantly with depth.

### 3.2.3. Optical properties

Tin dioxide films are transparent in the visible region of the spectrum and usually have no colour. When the oxygen content is lowered they become progressively dark and at some point turn completely coal-black. Thick layers of tin dioxide, though transparent, may present a brownish colour. Fig. 3.8 shows two samples where these differences can be appreciated.

The Swanepoel method permitted to determine the layers' refractive index [113]. Fig. 3.9 shows the transmittance spectra obtained for samples with thickness:  $0.20\ \mu\text{m}$ ,  $0.49\ \mu\text{m}$ ,  $1.95\ \mu\text{m}$  and  $6.6\ \mu\text{m}$ . It can be observed that the transmittance is lower than 1% at a wavelength of about  $0.28\ \mu\text{m}$  for all the samples and that the films with higher thickness show more interference

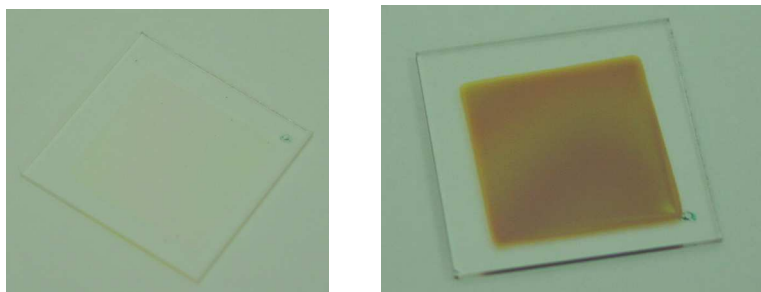


Figure 3.8.: Photograph showing samples with different colour, corresponding to films with different composition and structure

### 3. Characterization of tin dioxide thin films

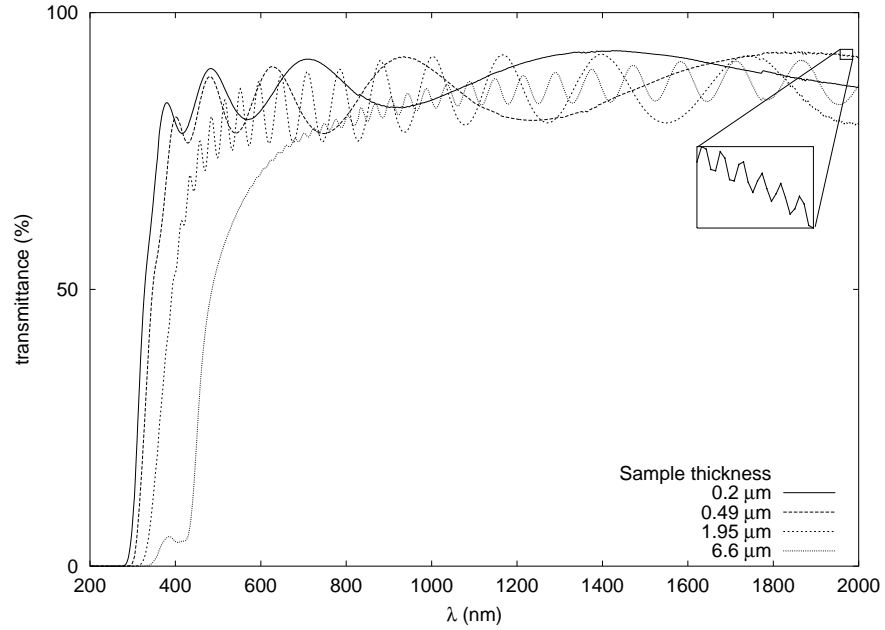


Figure 3.9.: Transmission spectra of SnO<sub>2</sub> layers with different thickness

fringes than thinner ones. This will be important later since the optical parameters will be calculated only at the interference fringe peaks and valleys. In the spectrum of sample with thickness 0.49 μm are also visible, above λ = 1600 nm, the interference fringes due to the substrate. In Fig. 3.9 the detail shows an amplification of this interference fringes, that in the main figure are not distinguishable due to the scale used. This is one of the samples deposited on a glass substrate with .15 mm thickness.

The Swanepoel method assumes that the film has uniform thickness,  $d_f$ , and is deposited on a transparent substrate, with thickness much greater than  $d_f$  and absorption coefficient  $\alpha_s = 0$ . The refractive index of the glass substrates in the weak absorption region,  $n_s$ , was calculated using expression

$$n_s = \frac{1}{T_s} + \left( \frac{1}{T_s^2} - 1 \right)^{1/2} \quad (3.4)$$

and then fitted to a linear function to give  $n_s(\lambda)$ . In the case of thin glass substrates interference fringes were visible in the far infrared range of the spectrum. Since there was no particular need to study the optical properties of the films in those parts of the electromagnetic spectrum, the portions of the transmittance spectra where interference fringes due to the substrate were visible were rejected in order to simplify the analysis.

The film refractive index,  $n_f$ , is determined using expression

$$n_f = [N + (N^2 - n_s^2)^{1/2}]^{1/2} \quad (3.5)$$

where

$$N = 2n_s \frac{T_M - T_m}{T_M T_m} + \frac{n_s^2 + 1}{2}$$

and values  $T_M$  and  $T_m$  are the envelope curves that include, respectively, the maxima and minima of the interference fringes. These curves can be written as



$$T_M = \frac{Ax}{B - Cx + Dx^2} \quad (3.6)$$

$$T_m = \frac{Ax}{B + Cx + Dx^2} \quad (3.7)$$

where

$$A = 16n_f^2 n_s \quad (3.8)$$

$$B = (n_f + 1)^3 (n_f + n_s^2) \quad (3.9)$$

$$C = 2(n_f^2 - 1)(n_f^2 - n_s^2) \quad (3.10)$$

$$D = (n_f - 1)^3 (n_f - n_s^2) \quad (3.11)$$

$$x = \exp^{-\alpha d_f} \quad (3.12)$$

Film thickness,  $d_f$ , is determined using the procedure described in Section 3.4. Maxima and minima of the interference fringes were obtained using the peak pick utility of the spectrometer software while the intermediate values were calculated using a linear interpolation between two consecutive points. Before the interpolation procedure, measured  $T_{MW}$  and  $T_{mW}$  values were corrected for slit width,  $W$ , using expressions

$$T_M = T_{MW} + \left( T_{MW} \frac{W}{w_M} \right)^2 \quad (3.13)$$

$$T_m = T_{mW} + \left( T_{mW} \frac{W}{w_m} \right)^2 \quad (3.14)$$

where

$$w_{M(i)} = \lambda_{m(i-1)} - \lambda_{m(i+1)}$$

$$w_{m(i)} = \lambda_{M(i-1)} - \lambda_{M(i+1)}$$

Peaks corresponding to the region of strong absorption were used in the interpolation, although they were not used in the following calculations. Since thinner samples have less and more widely spaced interference fringes, the refractive index will be determined at fewer wavelength values. Having determined refractive index values it is possible to fit them to a function of the form  $n_f = a/\lambda^2 + b/\lambda + c$ , where  $a$  and  $c$  are constants. This permits to extrapolate the refractive index values for wavelengths different than the measured.

The method makes also possible to determine the extinction coefficient,  $k$ . First it is necessary to calculate absorbance,  $x$ , using Eq. 3.6 or Eq. 3.7. Then using Eq. 3.12 the absorption coefficient,  $\alpha$ , is determined and finally using

$$k = \frac{\alpha d_f}{4\pi} \quad (3.15)$$

the extinction coefficient is obtained. The source code of the program used to determine the optical parameters is presented in appendix F.

### 3.3. Surface morphology

Surface morphology was observed using both scanning electron microscopy and atomic force microscopy. AFM images were obtained with a Digital Instruments NanoScope III operated in the tapping mode. Both the analyses were performed in the University of Minho.

The majority of the samples had very smooth surfaces whose features were hardly observable in the electron microscope. Since the resolving power of the AFM is higher than SEM's, the former technique was preferred. This technique has also the advantage to enable a straightforward analysis of the acquired image in order to extract information about surface roughness.

### 3.4. Film thickness

Film thickness was measured in all the samples using the interference fringes visible in the transmittance spectra. In order to evaluate the accuracy of the former measurement, the section of a few samples was observed and measured in the scanning electron microscope and compared with the values obtained with the Swanepoel method. Since the latter method requires a considerable number of calculations a program was developed in Fortran 77 in order to determine the thickness of the film and the refractive index, using the formulas described in Section 3.2.3.

The transmittance spectra revealed strong inhomogeneities in the film thickness of the samples along some directions. Swanepoel described in 1984 a new method [114] that may be applied to non-uniform films. Some calculations have been done with this new method. A major drawback of the Swanepoel method is the difficulty to obtain thickness values from films with thickness lower than about 300 nm, due to the low number of interference fringes observable in the spectra of those samples.

The peak coordinates calculated by the Shimadzu UV-3101PC spectrophotometer software were saved in a text file. This file may then be loaded by the program that calculates the film thickness. Before the calculus, the program does a selection of the peaks, eliminating the peaks in the region of strong absorption. It was verified that the spectrophotometer *peak pick* utility misses some fringe points in the calculation. In order to detect this situation the peak selection process was altered in order to include a routine that checks the peaks sequence. When needed missing peaks were calculated by fitting a parabolic function to the extremum of the spectrum whose coordinates were required, and then the values added to the file.

The thickness non-uniformity when very high, caused a high reduction of the difference between consecutive maxima and minima of the fringes, as can be observed in Fig. 3.10. Two different procedures were used to deal with this situation. A new routine was introduced in the program that checked the difference between all consecutive extrema and alerted the user in case the values were lower than a predefined limit. The other procedure resulted from the observation that the uniformity was always higher along a given direction, that depended on the substrate placement during deposition. In order to ensure the best results, this direction was marked in all the samples before removing them from the sputtering chamber.

The thickness determination proceeds in the following way. After computing the refractive index values at the extrema of the fringes, using Eq. 3.5, the thickness,  $d_f$ , can be obtained using:

$$d_f = \frac{\lambda_i \lambda_{i+1}}{2(\lambda_i n_{i+1} - \lambda_{i+1} n_i)} \quad (3.16)$$

where  $n_i$  and  $n_{i+1}$  are the refractive indexes at two adjacent maxima (or minima) at  $\lambda_i$  and  $\lambda_{i+1}$ . The thickness values obtained are then used to estimate the interference fringe order,  $m$ , using expression

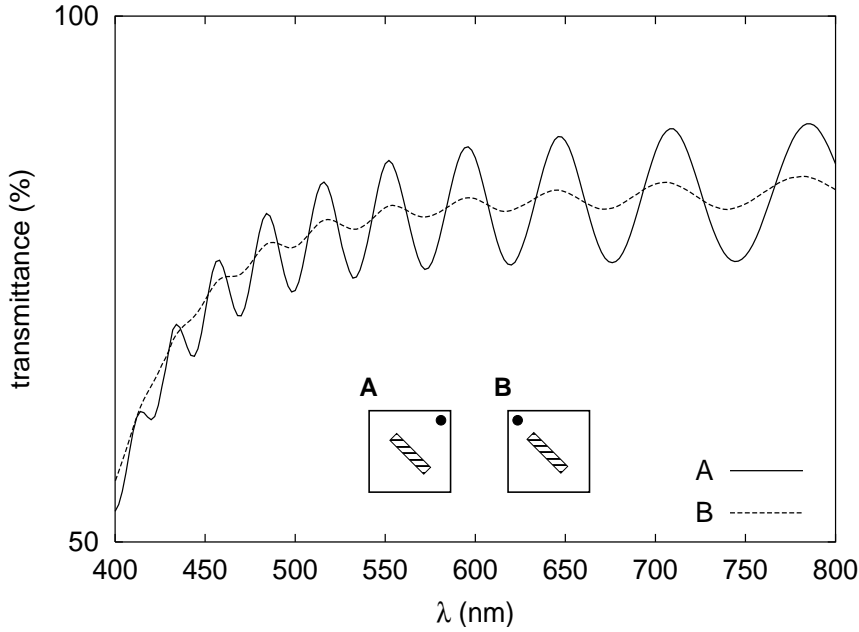


Figure 3.10.: Transmission spectra taken along different directions of one of the thick samples

$$2n_f d_f = m\lambda \quad (3.17)$$

where  $m$  is an integer for the maxima and a half integer for the minima. The calculated values of  $m$  are rounded to the nearest integer in the case of maxima or to the nearest half integer in the case of minima. The deviation from the expected sequence is computed and finally the sequence which matches more values is selected. The thickness is then calculated using Eq. 3.17, with the corrected fringe order. The final thickness is obtained from the mean of the former values. After determining the thickness, the refractive index is again calculated for each wavelength  $\lambda_i$ , using Eq. 3.17 and the former fringe order values.

It is suspected that it was not possible to get the high accuracy predicted by Swanepoel given the non-uniformity of the film thickness. Therefore, a new procedure developed for films with non-uniform thickness was also applied. This new procedure was proposed by Swanepoel in 1984 and may be used for films having a linear variation in  $d_f$  over the illuminated area. It is, however, also valid for the case where several irregularities occur periodically in the form of surface roughness, when there are variations of the refractive index due to non uniformity of the sample and may also account for the effect of finite bandwidth of the spectrometer [114]. In this case the film thickness is expressed as

$$d_f = \bar{d}_f \pm \Delta d \quad (3.18)$$

where  $\bar{d}_f$  is the mean thickness over the illuminated area and  $\Delta d_f$  is the actual variation from the mean value and not the standard deviation<sup>2</sup>. The refractive index and the thickness variation,  $\Delta d_f$ , should now be calculated using the expressions corresponding to the envelopes,  $T_{Md}$  and  $T_{md}$ , around the maxima and minima of the interference fringe patterns in the transparent region ( $\alpha = 0$ )

<sup>2</sup>It should be remembered that the thickness variation is supposed to be linear, so that  $\bar{d}_f + \Delta d_f$  is the maximum thickness and  $\bar{d}_f - \Delta d_f$  is the minimum.

### 3. Characterization of tin dioxide thin films

$$T_{Md} = \frac{\lambda}{2\pi n_f \Delta d_f} \frac{a}{\sqrt{1-b^2}} \arctan \left[ \frac{1+b}{\sqrt{1-b^2}} \tan \left( \frac{2\pi n_f \Delta d_f}{\lambda} \right) \right] \quad (3.19)$$

and

$$T_{md} = \frac{\lambda}{2\pi n_f \Delta d_f} \frac{a}{\sqrt{1-b^2}} \arctan \left[ \frac{1-b}{\sqrt{1-b^2}} \tan \left( \frac{2\pi n_f \Delta d_f}{\lambda} \right) \right] \quad (3.20)$$

where  $a$  and  $b$  are given by expressions

$$a = \frac{A}{B+D} \quad (3.21)$$

$$b = \frac{C}{B+D} \quad (3.22)$$

Constants  $A$ ,  $B$ ,  $C$  and  $D$  are given respectively by Eqs. 3.8, 3.9, 3.10, and 3.11. In order to get  $\Delta d_f$  and  $n_f$ , Eqs. 3.19 and 3.20 have to be solved numerically after the substitution of the experimentally determined values:  $T'_M$  and  $T'_m$ . It should also be noted that the experimental values  $T'_M$  and  $T'_m$  do not correspond to the extrema of the fringes, but should rather be obtained from a fit of an envelope function to the experimental transmission curve, i.e., they should correspond to the points where the envelope functions touch the spectrum. However, the values used in the calculations were the extrema of the fringes, given the small difference between the two.

The calculated  $\Delta d_f$  values depended largely on the transmittance accuracy and varied significantly with the wavelength, which made difficult to find the true values. Given that Eqs. 3.19 and 3.20 were only valid on the transparent region, it was expected that the best value of  $\Delta d_f$  would be found on this region. The spectra, however, showed some irregularities that made difficult to determine unequivocally this region and therefore an accurate determination of  $\Delta d_f$  was not possible. Differently from Swanepoel's results,  $n_f$  values obtained in this process were close to the expected values.

Using the estimated  $\Delta d_f$  value along with the  $T'_M$  and  $T'_m$  determined previously, the following expressions may be used to find out another estimate of the refractive index, and the absorbance,  $x$ .

$$T_{Mx} = \frac{\lambda}{2\pi n_f \Delta d_f} \frac{a_x}{\sqrt{1-b_x^2}} \arctan \left[ \frac{1+b_x}{\sqrt{1-b_x^2}} \tan \left( \frac{2\pi n_f \Delta d_f}{\lambda} \right) \right] \quad (3.23)$$

$$T_{mx} = \frac{\lambda}{2\pi n_f \Delta d_f} \frac{a_x}{\sqrt{1-b_x^2}} \arctan \left[ \frac{1-b_x}{\sqrt{1-b_x^2}} \tan \left( \frac{2\pi n_f \Delta d_f}{\lambda} \right) \right] \quad (3.24)$$

where  $a_x$  and  $b_x$  are defined

$$a_x = \frac{Ax}{B+Dx^2} \quad (3.25)$$

$$b_x = \frac{Cx}{B+Dx^2} \quad (3.26)$$

Again, Eqs. 3.23 and 3.24 have to be solved numerically in order to get  $n_f$  and  $x$ . Once the refractive index values have been calculated, the mean thickness,  $\bar{d}_f$  may be determined using Eq. 3.17. Finally, the absorption coefficient,  $\alpha$ , may be obtained using Eq. 3.12 and using Eq. 3.15, may be obtained the extinction coefficient. Since this method assumes that the radiation used has zero bandwidth, the spectrometer slit width must be reduced to the minimum in order to get the best results.

This method was applied to samples e11a24 and I9a2, whose transmittance spectra are shown in Fig. 3.11. Two different spectra of sample e11a24 were obtained on regions showing different thickness gradients. The spectrum e11a24-A corresponds to an area of the sample where the thickness gradient is higher and thus the interference fringes are smaller as shown in Fig. 3.11. Table 3.1 shows the results of the thickness determination using the scanning electron microscope images (SEM), the Swanepoel method for homogeneous films (Swanepoel homogeneous) and the Swanepoel method for inhomogeneous thin films (Swanepoel inhomogeneous). The spectrum e11a24-A did not permit to determine an accurate value for the parameter  $\Delta d_f$  and thus it was not possible to use the inhomogeneous Swanepoel's method to determine the thickness from this spectrum.

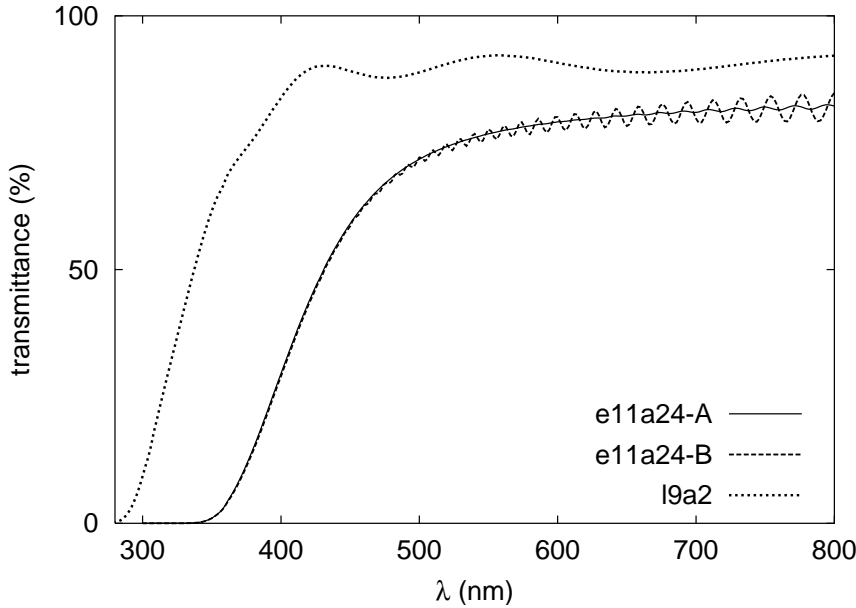


Figure 3.11.: Transmission spectra of samples e11a24 and I9a2. Only the spectrum A of sample e11a24 was successfully used in the determination of the sample's thickness.

Table 3.1.: Thickness values obtained for samples e11a24 and I9a2 using SEM images and transmittance spectra.

Method	Thickness	
	e11a24	I9a2
SEM	6.9 $\mu\text{m}$	0.52 $\mu\text{m}$
Swanepoel homogeneous	7.33 $\mu\text{m}$	0.52 $\mu\text{m}$
Swanepoel inhomogeneous	6.37 $\mu\text{m}$	0.51 $\mu\text{m}$

It may be observed that the results obtained for the thinner sample using the three described methods are similar. As to the thicker sample, the result obtained with the Swanepoel homogeneous' method is clearly higher than the result obtained with the inhomogeneous' method. This was expected, since the fringe modification due to the thickness inhomogeneity results, using the homogeneous method, in a lower estimate of the refraction index. More surprising is the value resulting from the inhomogeneous method, which produces a thickness value that is substantially lower than the one determined by SEM. The main reason for this difference is supposed to be the position where the thickness was measured. Since the thickness gradient is

### 3. Characterization of tin dioxide thin films

very high in this sample, if care is not taken to measure the thickness in exactly the same area, differences greater than  $0.4 \mu\text{m}$  may be observed.

#### 3.4.1. Dependence of film characteristics on thickness

It has been referred already that surface roughness increases considerably with film thickness. This dependence suggests that film growth mechanisms amplify the underlying roughness of previous layers. Similar results have also been observed by other research groups [115].

A noticeable change was also detected in the optical constants of films with different thickness, but grown using similar sputtering conditions. Namely, film thickness was observed to induce a decrease in the optical bandgap and the refractive index.

## 4. Reactive magnetron sputtering deposition

Magnetron sputtering is a thin film deposition technique based on the physical sputtering effects caused by the bombardment of a target material with accelerated ions produced within a glow discharge plasma. A wide variety of thin film materials, from metals to insulators, may be produced using this technique. Usually the thin film composition will be determined exclusively by the elements composing the target, since the only elements occurring in the gas phase are the noble gas ions used to generate the plasma and other particles ejected from the target as the result of the sputtering process. In some cases a reactive element may be introduced in the gas phase that will interact with the deposited elements; this latter case is called reactive sputtering. In order to understand the thin film growth processes and the dependence of its characteristics on the system parameters, it is necessary to know how the particles are removed from the target and how they interact on the substrate surface. Therefore in the following sections ion production, sputtering mechanisms and film growth will be briefly explained, before presenting the system used to produce the tin oxide layers and the correlations found with the deposition parameters.

### 4.1. Plasma processes

Ions used in planar magnetron sputtering systems are generated by glow discharge processes. A glow discharge may be established when a potential is applied between two electrodes in a gas. Once established two or three different regions can be clearly distinguished between the electrodes. Close to the cathode there is a dark region that exists also near the anode although the latter is generally too thin to be observed. Next there is negative glow region and if the separation between the electrodes is higher than a few times the dark space thickness, a positive column develops between the negative glow and the anode. The positive column is the region that more closely resembles a plasma. The plasma does not take a potential between those of the electrodes, but rather acquires a potential slightly higher than that of the anode. Inside the plasma, as expected, the electric field is very low. The main potential difference is therefore observed at the sheaths next to each of the electrodes. The role of the magnetron is forming electron traps that help to sustain the discharge.

Without the magnetron, the electrons emitted from the cathode by ion bombardment are accelerated nearly to the full applied potential in the cathode dark space and enter the negative glow, where they collide with the gas atoms producing the ions required to sustain the discharge. As the electron mean free path increases with gas pressure decrease, at low pressures the ions will be produced far from the cathode where the chances of being captured by the walls are high. At the same time many primary electrons (the ones emitted from the cathode) reach the anode with high energy, inducing secondary electron emission. Therefore, ionization efficiencies are low and self sustained discharges cannot be maintained in planar diodes at pressures below 1.3 Pa [116]. Currents are also limited since voltage increases the primary electron energy and consequently their mean free path. At high pressures the sputtered atom transport is reduced by scattering, which at some point starts to force a decrease in the deposition rate.

#### 4. Reactive magnetron sputtering deposition

On the other hand, with the magnetron system configuration, the primary electron motion is restricted to the vicinity of the cathode and thereby ionization efficiency is increased. This effect is easily obtained imposing a magnetic field parallel to the cathode surface and thus normal to the electric field. In a planar configuration, though, the  $\mathbf{E} \times \mathbf{B}$  motion causes the discharge to be swept to one side. This difficulty can be overcome using cylindrical cathodes, which allow  $\mathbf{E} \times \mathbf{B}$  to close on themselves. Planar magnetrons can be achieved by placing the magnets, directly behind the cathode, in a configuration such that at least one region in front of the cathode surface has a closed path which is perpendicular to the magnetic field lines that are parallel to the surface. Although there are many variations in geometry, all have in common a closed path or region in front of a mostly flat cathode surface, where the magnetic field is normal to the electric field. Bounding this region the magnetic field lines enter the cathode surface. Ideally, at the entry points the field lines are perpendicular to the cathode surface. The ionization region is thus confined to an area adjacent to the cathode surface by one or more endless toroidal electron trapping regions, bounded by a tunnel shaped magnetic field.

### 4.2. Magnetron sputtering

When an ion impinges on the cathode surface several processes may take place: the incident ion will either be implanted or reflected, probably as a neutral and with a large loss of energy; a target atom may be ejected (sputtered); the ion impact and the resulting cascade will cause an amount of structural reordering in the surface layers and secondary electrons may be ejected. Of the mentioned processes the most important for the thin film formation is the sputtering process. The sputtering yield,  $s$ , is defined as the number of atoms ejected from the target per incident particle. Important factors that affect the sputtering yield include surface structure, mass of the bombarding ion and incident energy. The sputtering process is rather insensitive to temperature, and in certain cases, there is even a decrease in  $s$  with increasing target temperature [112].

Near the threshold energy, the sputtering yield rises rapidly with ion energy increase. From about 100 eV upwards, the sputtering yield increases almost linearly with ion energy, where the values begin to be large enough to be useful for film deposition. With further increase in ion energy the sputtering yield reaches a maximum and starts to decrease, mainly due to the larger penetration depth of the ions within the target surface. For light ions, such as hydrogen or helium, the maximum of  $s$  is reached at a few thousand eV, since these particles penetrate rather easily. For heavy ions, such as xenon or mercury, the maximum may not be attained until values near 50 KeV or higher. The sputtering yield dependence on the atomic number of the target atoms for various inert gas ions shows some kind of periodicity. A sputtering yield increase is observed, for instance, when the target material changes from group III-B to group I-B transition metals, but a steep decrease follows from a metal of group I-B to the metal of group III-B of the next period (row of the periodic table). This can be qualitatively understood looking at the electronic structure of transition metals. As the d-orbitals are filled by electrons, collisions among atoms within the solid become more elastic, which results in more efficient energy transfer. On the other hand the bond energies between the atoms become weaker and thus the removal of the atoms is easier. Neutral gas atoms or molecules may also initiate target material sputtering, although in plasma-solid interactions these processes have lesser importance due to the extremely small momentum of the neutral particles.

### 4.3. Thin film growth

In sputtering deposition as in other standard vacuum deposition processes, the material arrives at the substrate mostly in an atomic or molecular form. Using the kinetic theory of gases it is



possible to estimate the frequency with which gas particles impinge on a surface,  $\nu$ , when the gas phase pressure is  $P$ :

$$\nu = \frac{P}{\sqrt{2\pi mkT}} \quad (4.1)$$

In Eq. 4.1,  $m$  is the mass of the gas particles,  $k$  the Boltzmann constant and  $T$  the temperature. Considering that for air the mean particle mass is  $4.8 \times 10^{-23}$  g, collision frequency will be approximately  $3 \times 10^{24} \text{ cm}^{-2}\text{s}^{-1}$  at  $25^\circ \text{C}$  and 1 atm. Given that a perfectly smooth surface of  $1 \text{ cm}^3$  has about  $10^{15}$  atoms, when immersed in a gas at 1 atm pressure, each atom on the surface will be hit about  $10^9$  times each second. At  $5 \times 10^{-3}$  mbar, collision frequency will be reduced to  $1.5 \times 10^{19} \text{ cm}^{-2}\text{s}^{-1}$  which is still a very high frequency. In the case of sputtering the particles that will interest to the film growth will be the ones evaporated from the target and these will have a much lower collision frequency.

The condensed particles may diffuse around the surface, with a motion determined by their binding energy to the substrate, may be incorporated into the lattice or evaporate. Given the high collision frequency of the gas particles inside the deposition chamber these will have a non-negligible influence on the adsorbed particles diffusion. The diffusion process may lead to adsorption, particularly at special site edges or other defects, or the diffusing particle may desorb. During these processes, characteristic activation energies have to be overcome. The corresponding activation energies for adsorption or diffusion depend on the atomic details of each process and will not be considered now. Besides adsorption and surface diffusion, nucleation of more than one adsorbed particle might occur. Interdiffusion of adsorbed particles with the substrate often happens leading to film-substrate interface smoothing. In thermodynamic equilibrium all processes take place in two opposite directions at equal rates. Therefore, in equilibrium no net film growth would be observed, so that layer growth must be a non-equilibrium kinetic process.

The final macroscopic state of the system may not be the most stable one, since it is kinetically determined. In general however, certain parts of the overall process may be kinetically forbidden, whereas others may be in local thermodynamic equilibrium. In this case equilibrium arguments may be applied locally even though the whole growth process is a non-equilibrium one. Given this fact, a global theory of film growth requires a description in terms of rate equations for each of the processes taking place at the surface. Instead of following a more theoretical atomistic approach it is possible to consider the film growth mechanism using a more phenomenological perspective.

Usually, three distinct modes of film growth may be considered: layer by layer growth mode or Frank-Van der Merve mode; island growth mode or Vollmer-Weber mode and layer-plus-island growth mode, that is also called Stransky-Krastanov mode; each named after the investigators associated with their initial description. In layer by layer growth mode the interaction between the substrate and the layer atoms is stronger than between neighbouring atoms. Each new layer starts to grow, only when the last one is completed. If, on the contrary, the interaction between neighbouring atoms is stronger than the overlayer-substrate interaction, the particles will rather form aggregates over the surface, that grow in size and eventually coalesce during film growth. This makes up the island growth mode. The layer-plus-island growth mode is an intermediate case where the film starts to grow layer by layer in a first stage and only afterwards begins the formation of island agglomerates.

In island growth mode, each island is usually a single crystal or contains just a few crystals. On a polycrystalline or amorphous substrate, the orientation of each island will be random and the resultant film will be polycrystalline. On single crystal substrates, the islands orientations may be constrained to a given direction by the substrate structure, so that growth and coalescence leads to the formation of a single crystal film. This case is usually known as epitaxy. If

#### 4. Reactive magnetron sputtering deposition

surface atoms have high mobility, they have greater opportunity of finding low energy positions consistent with crystal growth. Knowing that mobility is increased by surface temperature, it is expected that higher substrate temperature will promote crystal growth. The same effect can be achieved by reducing the deposition rate, which gives more time to the adsorbed species to find an energetically favourable lattice position. Epitaxial growth was also found to be promoted by electron or ion bombardment and increased energy of deposited atoms [117].

The environmental conditions around the substrate during magnetron sputtering deposition deserve also to be mentioned, since they will inevitably affect the film structure obtained. Namely, it was ignored in the above description the effect of the energy of the impinging sputtered atoms, as well as the effect of many other particles that may impact on the surface.

In first place there might be contaminants arriving at the substrate. These may result from an internal source, such as outgassing from a heating substrate, or by an external source such as the sputtering gas. If the contaminant atoms are chemically active, the contamination will be particularly effective and can only be minimized by reducing the contaminant partial pressure. If the contaminant source is outgassing, the system may have to be evacuated to a higher vacuum or the sources of outgassing heated in order to reduce the outgassing rate and guarantee a sufficiently low partial pressure of the contaminant during deposition. On the other hand, if the contaminant comes with the sputtering gas there is no way to reduce its partial pressure without affecting simultaneously the sputtering gas pressure. Thus it is very important to use high purity sputtering gases.

The sputtering gas atoms might also become part of the deposited film. Although the sputtering gas used is usually an inert gas, given its high partial pressure when compared with that of the sputtered atoms it is not surprising that some of these atoms happen to be trapped in the growing film. Inert gas atoms, are only expected to be physisorbed, so if substrate temperature is increased during deposition, they are less likely to be adsorbed and at the same time more likely to be subsequently desorbed. However, there exists an appreciable difference between the interaction of fast gas particles and that of thermal neutrals with the surface. Energetic neutrals may result from the reflection and neutralization of ions that impinge on the target. These neutrals, arriving at the substrate, have much higher probability to be embedded in the growing film than thermal neutrals. In fact, it has been observed that nickel films deposited by sputtering in an argon atmosphere have higher argon content than nickel films produced in a similar atmosphere, but using evaporation [117]. Positive ions may also impact on the substrate due to the sheath voltage drop near its surface.

Negative ions and electrons can only reach the substrate if they have enough energy to cross the space-charge sheath. Once again it is necessary to distinguish fast from slow particles. Fast negative ions and electrons are produced in the target and accelerated in the target sheath. These fast particles can have a major influence on the structure and properties of the growing film and also cause substrate heating. Finally there are also photons arriving at the substrate. Photons can be produced by ion or electron bombardment on any surface or result from relaxation of excited atoms in the glow. In the former case the photons may have high energy, at most as high as the energy of the bombarding particle. Such energies may be, in a sputtering system, of the same order of the accelerating potential at the target, which is usually higher than 200 eV. The main effect of photon bombardment of the substrate will be electron emission, which may also affect the film growth processes occurring at the substrate.

#### 4.4. The DC sputtering chamber

Although this work is mainly concerned with the study of films produced by DC magnetron sputtering, some layers were also deposited using an RF system for comparison. The RF system

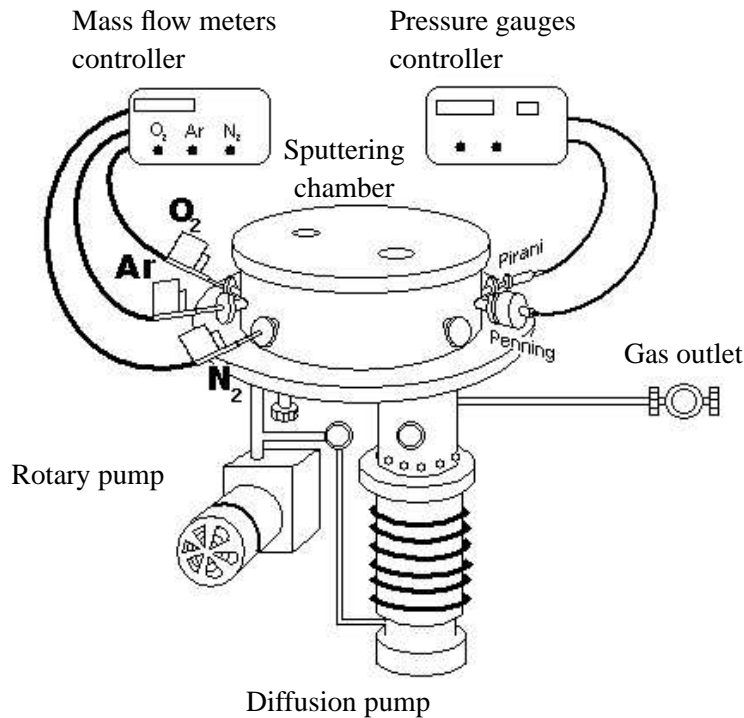


Figure 4.1.: DC sputtering chamber system

used was an Alcatel SCM 650, while the DC is a system built in the Physics Department that is not documented and thus needs a thorough description. The setup of the DC sputtering chamber is outlined in Fig. 4.1.

The chamber is pumped to vacuum using a diffusion pump which is able to reduce the pressure below  $10^{-3}$  Pa. If the chamber is kept open during a long time period it will take longer to reach high vacuum pressures because of outgassing. Heating the chamber walls often accelerates evacuation, by promoting outgassing. The diffusion pump is backed by a rotary pump, that is also used to do primary vacuum inside the chamber before connecting the diffusion pump. In order to change the substrates the chamber has to be open, so that usually the frequency of experiments is dependent on the time required to reach high pressures inside the chamber.

The sputtering gases are fed into the chamber using three Bronkhorst High-Tech F-201C-FA mass flow meters. One is calibrated for argon, other for oxygen and the third for nitrogen. The maximum flow reached by each mass flow meter is 200 sccm for the argon device, 50 sccm for  $O_2$  and 20 sccm for  $N_2$ . The control and measurement is performed using a power supply and readout system, provided by Bronkhorst. This permits to set the flow at a given percentage of the maximum flow, of the mass flow controller.

The substrates are positioned on a stainless steel holder, with suitable holes that work as masks for the deposition. The substrate holder can be fixed at different distances above the target and is maintained at the same potential as the anode and the chamber walls. It is possible to insulate the substrate holder electrically in order to apply a voltage bias to control the charged particles that impinge on the substrates. The substrate heating is performed using a metallic base weaved with an electrical resistance (see Fig. A.1(a)). The temperature is measured with a thermocouple inserted into a hole made in one side of the metallic base and controlled by a Shimaden SR52 temperature controller. The temperature controller was connected to a personal computer through the serial port. This way, it was possible to set the temperature and

#### 4. Reactive magnetron sputtering deposition

other controller parameters from the computer and record the substrate temperature during the experiment. In appendix A the procedure used to control and record the temperature values is described.

The setup used to heat and measure the substrate temperature does not make possible to know the actual substrate temperature, because there is an unknown temperature gradient between the substrate surface and the point where the thermocouple is placed. However, if given enough time for the heat transfer fluxes to stabilize, the temperature conditions can be reasonably reproduced in repeated experiments and the effect of temperature upon the films' characteristics may be studied. Nevertheless, if the substrates, the pressure or the sputtering power are changed, for instance, it is not possible to maintain a fixed temperature on the substrate over repeated experiments, since the temperature gradient is very likely to change. Alternative methods to measure the substrate temperature will be discussed in appendix A.

The power source is a Hüttinger PFG 2500 DC generator. This source is able to operate at a maximum voltage of 500 V and to deliver a maximum current of 5 A. It provides three different levels for arc detection and extinction, to prevent damage of the equipment, and an RS-232-C interface for remote control of the unit. The user may set the voltage, the current and the power between 5 % and 100 % of respective range. The RS-232-C serial port was used both to set the source parameters and read the voltage and current values during operation. The setup used to control the power source is described in detail in appendix B.

Pressure inside the chamber is measured using a Balzers TPR 010 Pirani gauge in the pressure range from  $10^5$  Pa to  $10^{-1}$  Pa and using a Balzers IKR 020 Penning gauge in ranges from  $10^{-1}$  Pa to  $10^{-5}$  Pa. The Penning gauge is cleaned periodically to ensure repeatability. If the electrodes of this device are covered by an oxide layer the measurements stray toward lower pressures. There is a second Pirani gauge which measures the pressure at the diffusion pump outlet, and is used to verify that the backing pressure is within the required operating range. The three pressure gauges are connected to a Balzers TPG 300 controller. This instrument is used to calibrate the Pirani readings and to turn on and off the Penning gauge when the pressure gets in or out of the working pressure range of the device.

Given the high influence of the deposition pressure on the produced thin film characteristics, the pressure gauges' mechanisms will be reviewed before proceeding to the presentation of the results. This knowledge is needed since the pressure displayed on the TPG 300 controller is calibrated for nitrogen and thus will not correspond to the pressure inside the chamber when other gases are used. The real pressure has to be determined knowing the composition of the gas mixture inside the chamber and the value read on the pressure controller.

#### 4.5. Pressure gauges

The Pirani gauge is a thermal conductivity device. It is composed of a metal filament with high coefficient of resistance which is heated and immersed in the gas whose pressure is being measured. As the pressure of the gas increases, the temperature of the filament and therefore its electrical resistance tends to decrease. The temperature the filament attains depends on the electrical power received, the heat loss through the surrounding gas, the heat loss through radiation and through the support of the filament. If the electrical power supplied is kept constant, and radiation, convection and conduction (through the filament holder) losses are minimized, the temperature of the filament depends primarily on the loss of energy due to thermal conductivity of the gas. In the viscous range of pressures thermal conductivity of a gas does not depend on the pressure [58, 118]. However, this is no longer valid if the pressure is reduced to the molecular range, which corresponds to a situation where the mean free path of the gas molecules is higher than the recipient dimensions. Since the gas thermal conductivity depends

on the nature of the gas, the pressure values measured by a Pirani gauge have to be corrected for different gas mixtures. This is usually performed using a calibration curve provided by the gauge manufacturer.

The Penning gauge is a cold-cathode ionization gauge. The original form of the device consists of an anode placed between two parallel connected cathodes. The cathodes are metal plates while the anode is usually a loop of metal wire whose plane is parallel to the cathodes. A potential difference of about 2 KV is maintained between the anode and the cathodes and a magnetic field is applied in a direction perpendicular to the cathodes. An electron emitted by the cathode is accelerated towards the anode by the electric field, but generally passes through the anode loop until its path is reversed by the electric field of the second cathode. Due to the applied magnetic field the electron path is very long and therefore, even at low pressures, the ionization probability of the collisions with gas molecules is high during the electron oscillation between the electrodes. The positive ions thus created are captured by the cathodes, producing a current that is measured in the external circuit. The upper pressure limit of the device is set by the glow discharge that starts between the electrodes for pressures above  $10^2$  mbar. If the gauge is operated at the former high pressures the discharge may damage the electrode surface.

There are other types of pressure gauges. One that is also common is the capacitance type pressure sensors. These are composed by a diaphragm whose displacement modulates the device capacitance with respect to a reference back-plate. The values measured by this kind of devices do not depend on the nature of the gas, but pressure range measurements are much lower than the former devices and measurement of low pressures is difficult.

## 4.6. Deposition parameters

Although tin oxide films had been produced previously in our laboratory in the University of Minho [119], the deposition system used in those studies was considerably different [120]. The first stage of this study was then to find out the capability of the sputtering system in the production of SnO<sub>2</sub> layers. Glass slides were chosen as substrates since they are widely available and make easier the characterization procedures that were planned. Every substrate slide was cleaned in alcohol and visually inspected before being enveloped in aluminium foil. The sputtering target is pure tin. This target has the advantage of being much easier to produce than a composite target and makes possible to use the DC sputtering technique, which is less complex than RF systems. This implies, however, that it was necessary to use oxygen as reactive gas, during deposition. Nevertheless, compared with the deposition from SnO<sub>2</sub> targets, this is not an adding constraint, inasmuch as it has been shown previously that in order to produce gas sensitive layers of tin oxide from SnO<sub>2</sub> targets, it may be necessary to introduce oxygen into chamber [3, 121].

The substrate-target distance was adjusted to values that permitted higher film areas with homogeneous thickness. The temperature was set to 300° C, just after changing the samples and closing the chamber, to promote outgassing. Experiments were only performed after a base pressure below  $3 \times 10^{-3}$  Pa or at least two orders of magnitude lower than the deposition pressure, was achieved. About one hour before the deposition, the temperature was set to its final value and when the temperature reached the preset value, oxygen first and then argon were introduced in the system. The pre-sputtering was then performed for the number of minutes predetermined. In the RF chamber it was also performed, in some cases, etching of the substrates before the deposition. To achieve a constant O<sub>2</sub>/Ar partial pressure ratio, a similar ratio was set in the O<sub>2</sub> and Ar flow rates, and the total pressure adjusted to the desired value by varying both fluxes appropriately. In other experiments the O<sub>2</sub> flow rate was fixed at a predefined value and the argon was then adjusted until the desired pressure was attained. If the pumping rate is

#### 4. Reactive magnetron sputtering deposition

Table 4.1.: Range of parameters selected for DC and RF sputtering deposition of tin oxide samples

Parameter	DC sputtering	RF sputtering
Temperature ( $^{\circ}$ C)	60–400	40–400
Source power (W)	—	200–800
Source current (A)	0.08–0.30	—
Pressure ( $\times 10^{-1}$ Pa)	.25–12	4–10
O <sub>2</sub> flow rate (sccm)	3.6–14.8	25–50
Substrate-target distance (mm)	55–76	60–80
Sputtering time (min)	5–120	5–120
Pre-sputtering time (min)	2–27	0–10
Etching power (W)	—	100, 200
Etching time (min)	—	0, 10
Power applied to substrate bias (W)	—	0–50

Table 4.2.: Non-independent parameters controlled during deposition

Parameter	DC sputtering	RF sputtering
Target voltage (V)	200–350	—
Ar flow rate (sccm)	5.4–26	67–160
O <sub>2</sub> partial pressure ( $\times 10^{-1}$ Pa)	.13–.65	4–10

constant, there is a direct dependence of the partial pressures on the gas fluxes and thus these can be used to control the pressures.

In the RF system, the substrate holder was biased in some of the experiments with an RF signal, while in the DC it was always grounded. In the RF power source it was only possible to control the delivered power. In the DC it is possible to set the power, the voltage or the current. It was chosen to maintain voltage at its maximum achievable value and to control the delivered power by setting the maximum current. The working voltage varied between 230 V and 300 V and was higher, for lower sputtering pressures. The current was adjusted in order to achieve the desired power values. The deposition time was set initially at 120 min in the RF sputtering experiments and at 30 min in the DC. After determining the film thickness, the growth rate was calculated and this value used to produce layers with predefined thickness.

The range of each deposition parameter whose influence was studied in the experiments is shown in Table 4.1, both for DC and RF techniques. Table 4.2 shows the values of other parameters controlled during the deposition.

##### 4.6.1. Sputtering atmosphere

There were three main consequences observed in film growth caused by increasing the sputtering pressure and maintaining the oxygen to argon ratio: decrease in the deposition rate, increase of surface roughness and change of the dominant crystal orientation. The experiments were performed at 300 $^{\circ}$  C, with substrate-target distance equal to 65 mm, using a source power of 21 W, a pre-sputtering time of 10 min, O<sub>2</sub>/Ar flux ratio of 0.70 and deposition time of 30 min. Oxygen and argon flow rates were adjusted to obtain pressures between  $2.0 \times 10^{-1}$  Pa and  $7.6 \times 10^{-1}$  Pa in the chamber, while keeping the ratio constant. Table 4.3 summarizes the chosen conditions.

The deposition rate was observed to change from 9.1 nm/min to 28 nm/min, when the

Table 4.3.: Parameters selected to test the influence of sputtering atmosphere on the thin films' characteristics

Parameter	
Substrate-target distance	65 mm
Temperature	300° C
Source power	21 W
Pre-sputtering time	10 min
O <sub>2</sub> flow rate	4.0 sccm–7.2 sccm
O <sub>2</sub> /Ar flux ratio	0.70
Deposition time	30 min
Pressure	$2.0 \times 10^{-1}$ Pa– $7.6 \times 10^{-1}$ Pa

Table 4.4.: Parameters selected to test the influence of substrate temperature on the thin films characteristics

Parameter	
Substrate-target distance	54 mm
Temperature	100° C–400° C
Source power	21 W
Pre-sputtering time	10 min
O <sub>2</sub> flow rate	6.0 sccm
O <sub>2</sub> /Ar flux ratio	1.00
Deposition time	120 min
Pressure	$3.2 \times 10^{-1}$ Pa

Table 4.5.: Parameters selected to test the influence of the oxygen flow rate during deposition on the thin films characteristics

Parameter	
Substrate-target distance	54 mm
Temperature	300° C
Source power	21 W
Pre-sputtering time	10 min
O <sub>2</sub> flow rate	4.0 sccm–6.0 sccm
O <sub>2</sub> /Ar flux ratio	0.50–1.00
Deposition time	30 min
Pressure	$3.2 \times 10^{-1}$ Pa

#### 4. Reactive magnetron sputtering deposition

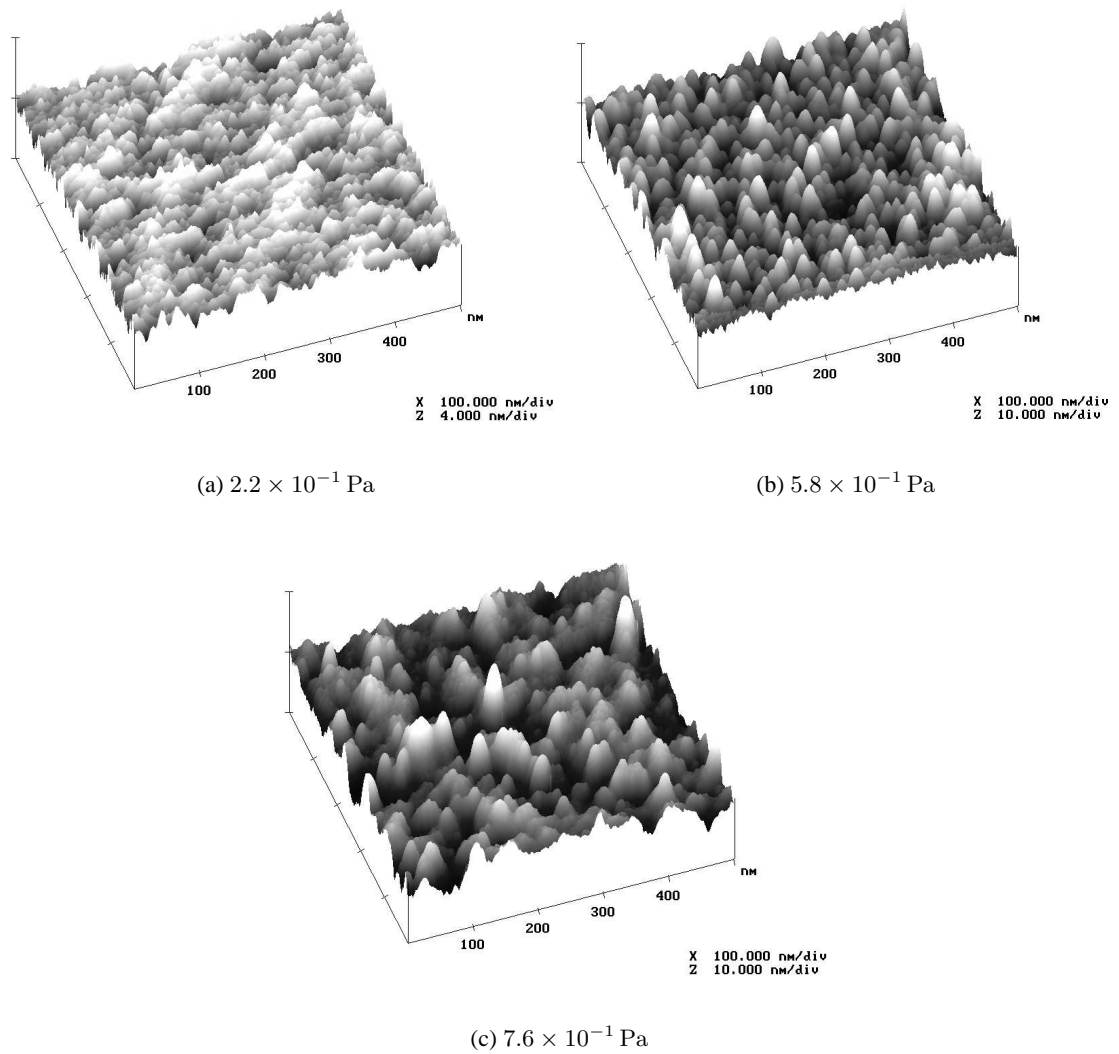


Figure 4.2.: Atomic force microscope surface plots of  $\text{SnO}_2$  samples produced at different deposition pressures

deposition pressure decreases from  $7.6 \times 10^{-1}$  Pa to  $2.2 \times 10^{-1}$  Pa. The surface morphology observed using the atomic force microscope, is shown in Fig. 4.2 for three samples deposited at  $2.2 \times 10^{-1}$  Pa,  $5.8 \times 10^{-1}$  Pa and  $7.6 \times 10^{-1}$  Pa. Sample grown at  $2.2 \times 10^{-1}$  Pa is the one that shows lower roughness, although it is the thickest, about 830 nm thick. The sample with higher roughness, was grown at  $7.6 \times 10^{-1}$  Pa and is just 280 nm thick. It is still necessary to grow films with similar thickness in order to prove the dependence. Nevertheless, given that it was observed that roughness increases with film thickness (see Section 3.4), it is highly unlikely that the dependence will not be confirmed.

Another interesting result may be observed in Fig 4.3 where the evolution of the XRD spectra of five samples produced with varying sputtering pressure is shown. All the peaks detected correspond to the tetragonal  $\text{SnO}_2$  crystal structure. It is observed a clear change in the dominant orientation of the crystallites. In the sample grown at  $2.2 \times 10^{-1}$  Pa, the peak with highest intensity corresponds to direction  $\langle 101 \rangle$ , at  $2.6 \times 10^{-1}$  Pa the highest peak is the  $\langle 211 \rangle$  and above  $5.8 \times 10^{-1}$  Pa the relative intensity of peak  $\langle 110 \rangle$  dominates in the spectra. At  $7.6 \times 10^{-1}$  Pa the observed sample is very thin, which explains the low intensity of the peaks shown. The



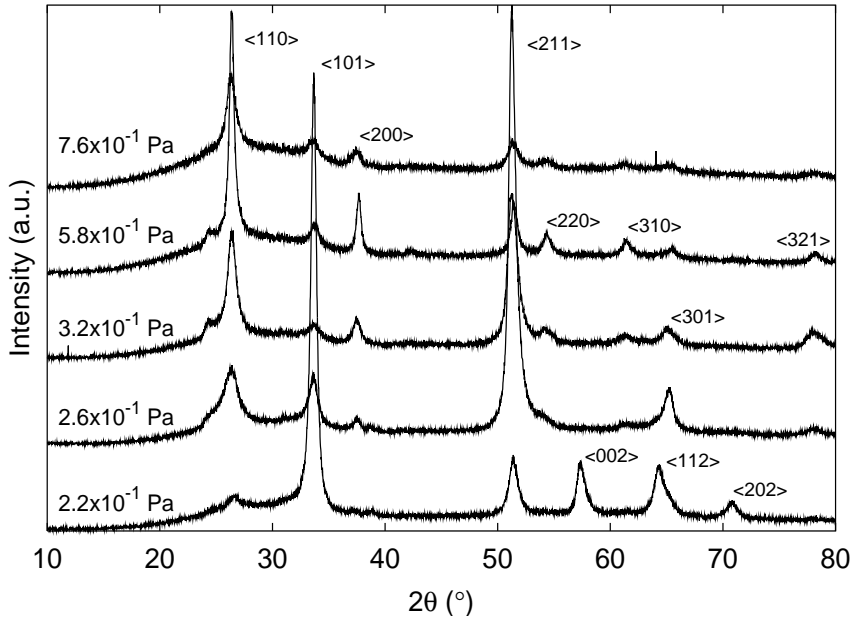


Figure 4.3.: Diffraction spectra of samples produced at different deposition pressure

dependence of the crystal orientation on deposition pressure should also be confirmed using films of similar thickness.

#### 4.6.2. Temperature

Deposition experiments were performed using substrate temperatures between 100°C and 400°C. During these tests substrate-target distance was kept at 54 mm, DC source power at 21 W, oxygen flow rate at 6.0 sccm, O<sub>2</sub>/Ar flux ratio at 1.00 and pressure at  $3.2 \times 10^{-1}$  Pa. The pre-sputtering and deposition times were respectively, 10 min and 120 min. The main effect on the film structure caused by the temperature variation was the increase of the grain structures' size, as observed by atomic force microscopy. This was expected to some extent, since it is known that temperature increase, induces an increase of atoms' mobility promoting thus crystal growth, as explained in Section 4.3.

Fig. 4.4 shows the AFM images of samples produced at 100°C, 300°C and 400°C. In the sample produced at 100°C, surface features have mean sizes lower than 4 nm. Sample produced at 400°C, on the other hand, shows features with mean size above 50 nm. Thickness of these samples was about 1.6 μm and given the surface feature sizes it was not possible to detect structure changes on the scanning electron microscope images.

No clear dependence was found between substrate temperature and deposition rate or preferential orientation of the crystallites. Deposition rate was about  $13 \pm 0.5$  nm/min and crystallite structure showed preferential growth along the <110> direction, in the five samples produced. Fig. 4.5 displays the diffraction spectra of samples produced with different substrate temperatures. Diffraction peaks corresponding to the tetragonal structure of tin dioxide may be observed in each spectrum and only small intensity changes, with substrate temperature variation are detected.

Samples presented residual stresses that led to film delamination a few days after the deposition (see Fig. 4.6). Layers deposited on the thin glass substrates did not delaminate, but acquire a bulge shape due to the stresses. The radius of curvature of the substrate can be used to determine

#### 4. Reactive magnetron sputtering deposition

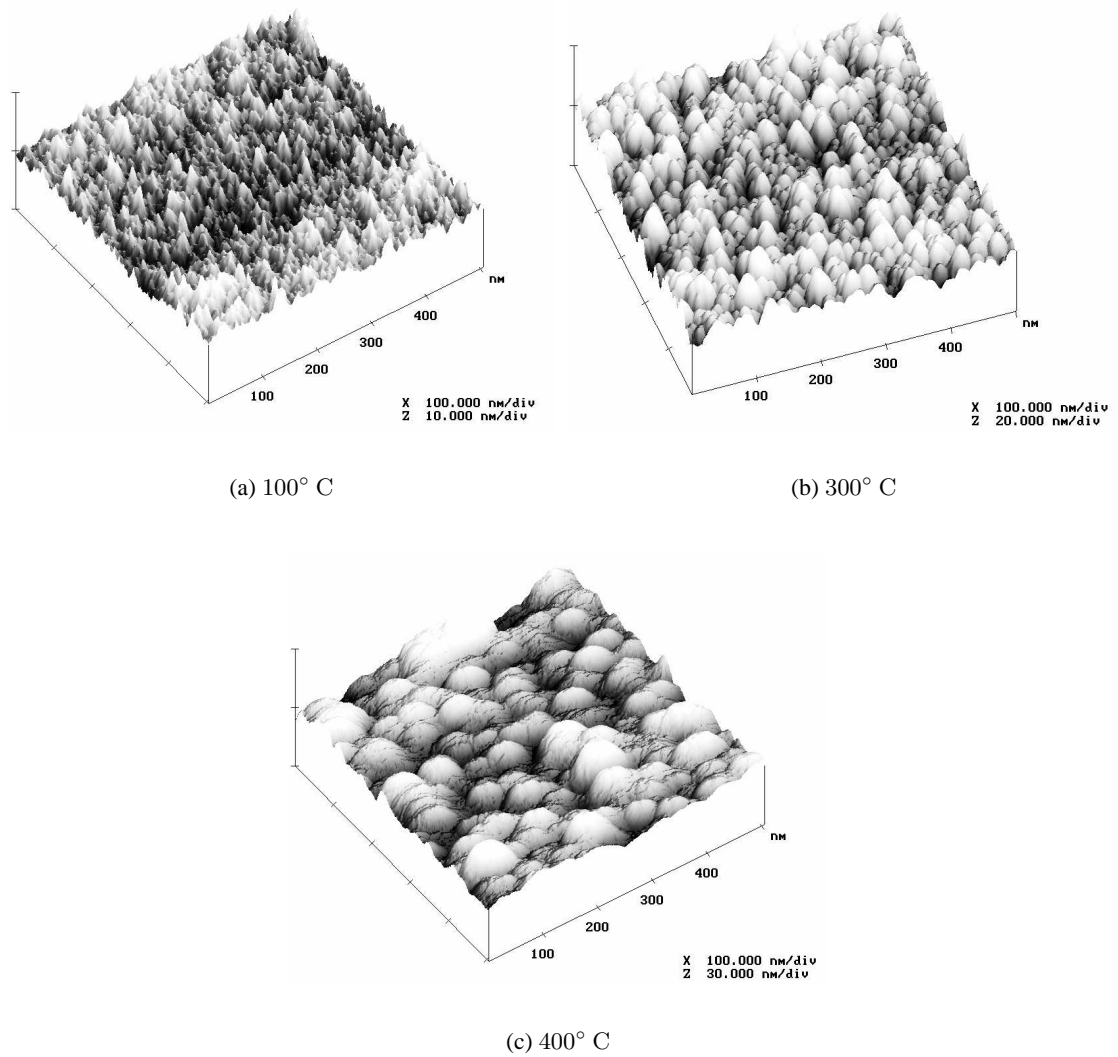


Figure 4.4.: AFM surface plots of samples produced with different substrate temperatures

the in-plane residual stress in the coating [122]. Furthermore, in view of the convex deformation it is possible to conclude that stresses are compressive.

#### 4.6.3. Oxygen partial pressure

Crystalline  $\text{SnO}_2$  layers were obtained using different oxygen partial pressures in the deposition atmosphere but the samples have not yet been analysed in order to determine bulk and surface structure. Nevertheless, it has been observed that for each set of deposition parameters, there is a threshold oxygen partial pressure value below which the tin oxide layer is no longer crystalline.

#### 4.6.4. Applied power

It was verified both in RF and DC sputtering techniques that for increasing sputtering powers, the oxygen partial pressure at which the grown films became amorphous also became higher. In other words, the low limiting oxygen partial pressure that permits to produce polycrystalline samples rises, when the applied sputtering power is increased.

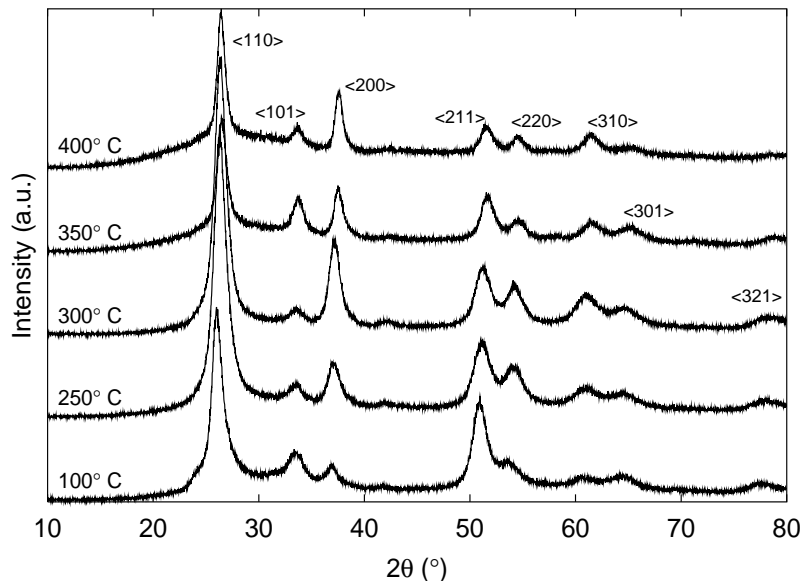


Figure 4.5.: XRD spectra of samples produced with different substrate temperature

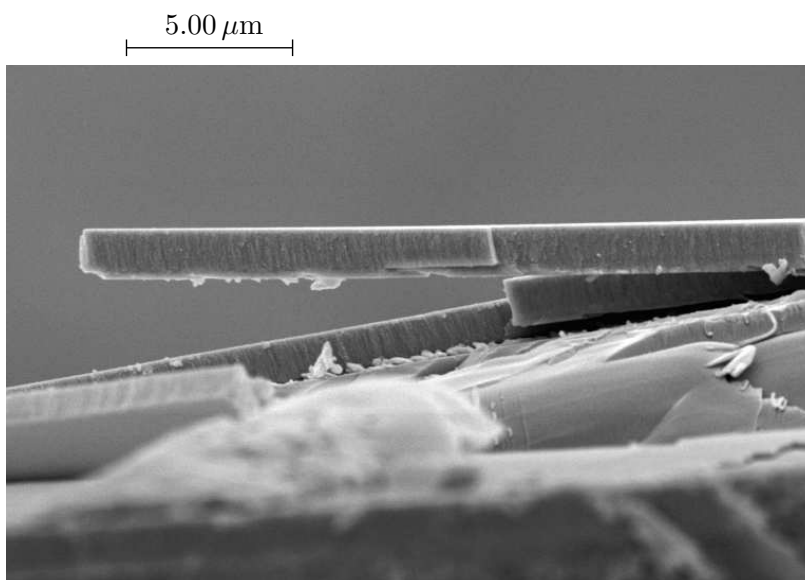


Figure 4.6.: SEM image showing delamination of a  $\text{SnO}_2$  layer

#### 4. Reactive magnetron sputtering deposition

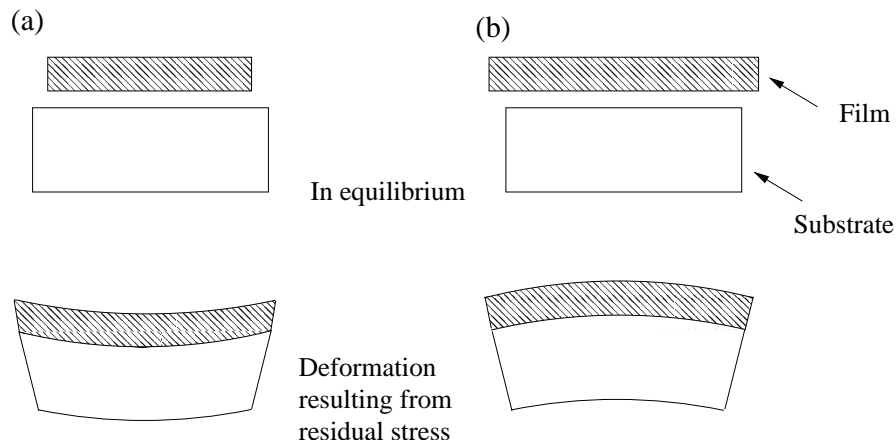


Figure 4.7.: Deformations observed on thin film substrates when there are (a) tensile or (b) compressive residual stresses on the interface.

### 4.7. Repeatability

In spite of the better control of the growth mechanisms that is achieved in thin film techniques when compared with thick film techniques, it is not always possible to guarantee that the processes are reproducible, since, as already mentioned, overlayer growth is a non-equilibrium process. Some of the film characteristics could be easily reproduced when repeating the experiments with the same deposition parameters. Among these characteristics were: sputtering rates, surface roughness, surface morphology and crystal orientation.

### 4.8. Other parameters

Table 4.6.: Parameters used in deposition of samples a14a1, a14a2 and a14a3

Parameter	
Substrate-target distance	80 mm
Temperature	100° C
Source power	200 W
O <sub>2</sub> flow rate	50.0 sccm
O <sub>2</sub> /Ar flux ratio	0.40
Deposition time	240 min
Pressure	$8.0 \times 10^{-1}$ Pa

In case of samples a14a1, a14a2 and a14a3, produced during the same deposition process, different crystalline structures were observed. None of the samples shows a marked crystal orientation, but noticeable differences are exhibited by XRD spectra depicted in Fig. 4.8. Given that the three samples were produced during the same deposition process, the only expected difference was the position relative to the magnetron. Temperature, may also be different given the heating procedure used, but is not likely to affect the crystal structure as observed in this case. These layers were obtained by RF reactive sputtering under the conditions summarized in Table 4.6. Furthermore, substrates were biased during deposition with an RF power supply at 30 W. Until now it was not possible to identify the cause for this occurrence.

Small variations were introduced on the target-distance change, O<sub>2</sub>/Ar flux ratio, pre-

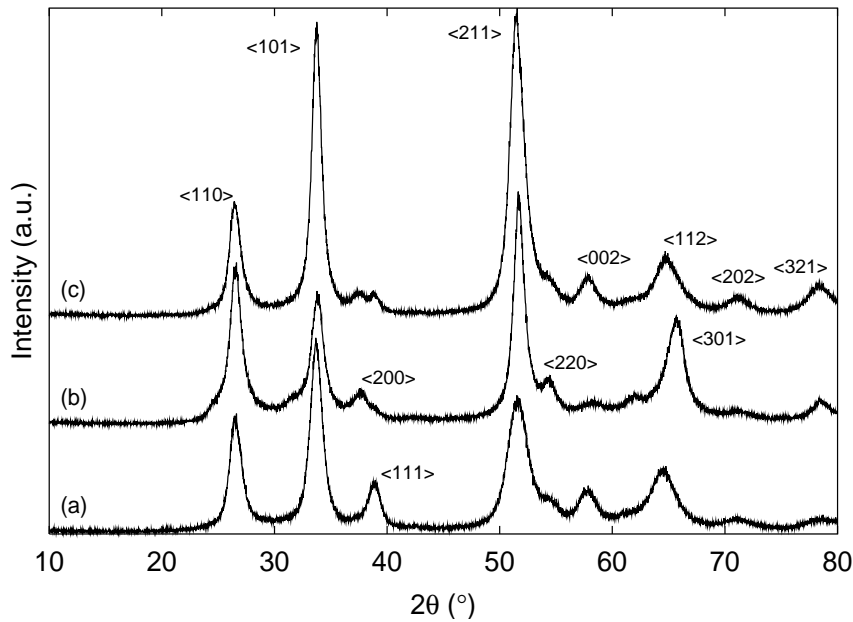


Figure 4.8.: XRD spectra of samples a) a14a1, b) a14a3 and c) a14a2, deposited during the same sputtering process

sputtering time and substrate cleaning to evaluate their influence on the produced layers' structure. However, within the experimented ranges no noticeable changes were observed in the films' characteristics.

Magnetic flux density above the target surface might also affect film characteristics. Experiments were performed using three different magnetron configurations. However no change of the film characteristics could be definitely assigned to this change, since they could also be produced by pressure changes within the measurement error interval.

It was observed that resistivity varied significantly over repeated experiments. In order to explain these variations it is necessary to understand the conduction processes and surface structure changes during heating, in different atmospheric conditions. This needs also a better knowledge of the structure of the grain boundaries and their role in the conduction processes.

#### 4. *Reactive magnetron sputtering deposition*

## 5. A chamber for gas sensor response testing

Once demonstrated the ability to produce polycrystalline SnO<sub>2</sub> layers with different characteristics, and determined the correlation between deposition parameters and the attained characteristics, it was necessary to test the behaviour towards reactive gases. To fulfil this goal a new equipment was built in our laboratory at the University of Minho. The purpose was not only to evaluate gas sensing response, but also to reproduce as much as possible a real environment for a working gas sensor. Therefore several options had to be done as to the variation of the atmosphere composition, the electrical measurements and the samples' heating.

The setup used to test gas sensing behaviour of the films is described in the following sections. Different solutions for the chamber design are evaluated and some improvements are also proposed.

### 5.1. Controlling atmosphere composition

The best way to produce a known mixture of gases is certainly to start from pure gases and then produce the desired mixture. There are several procedures that may be used to produce a predefined mixture of gases. These are usually grouped in two classes: static volumetric methods and dynamic volumetric methods. Static volumetric methods generally use a closed container where different components of the mixture are introduced sequentially. These methods are widely used to build-up a mixture reserve by storage under pressure. Dynamic volumetric methods, on the other hand, consist of the introduction of a given flow rate of a gas *A* into a constant flow rate of a gas *B*. Gases *A* and *B* can either be pure components or mixtures.

Static volumetric methods were rejected from the start inasmuch as during the sensitivity tests the gases undergo transformations which result in atmosphere composition change, if those components are not replaced. Another drawback is met in the elimination of the analysed gas from the chamber to evaluate sensor recovery. To eliminate the analysed gas, it is necessary either to produce vacuum inside the chamber and build a new mixture; feed a new mixture flow during some time into the chamber in order to remove the analysed gas or take the sensor into a new chamber where the atmosphere does not contain the gas under test. The first hypothesis is inconvenient since putting the film under vacuum will change severely the adsorption processes taking place on the surface, and therefore correlation with a real situation would be very difficult. The last is difficult to automate and accomplish, which sets down the second procedure as the most adequate. This method, however, is in the end a dynamic method.

The main dynamic techniques used for the preparation of gas mixtures are: volumetric pumps, sonic orifices, mass flow controllers, diffusion and permeation. Description of each of these techniques is done in International Standard ISO 6145/1-1986. Each method has its own range of applications and requires different equipment to be performed. In this work, the sonic orifices method was used to produce different concentrations of carbon monoxide in a reference atmosphere.

Dry synthetic air is used throughout the experiments as the reference gas for the gas sens-

## 5. A chamber for gas sensor response testing

ing measurements. Dry air was chosen in order to simplify the experimental setup. If water vapour was introduced inside the system, several precautions would have to be taken to avoid condensation, given that this compound condenses at ambient temperature. A strict control of gas temperature and pressure has then to be ensured inside the system in order to use an atmosphere with variable humidity, consequently experimental setups will be more complex. Since humidity is known to increase sensitivity to reducing gases, measured gas response values in dry air will most probably be lower than the ones obtained in real working conditions, where water vapour is almost always present.

Instead of pure carbon monoxide, it was used a mixture of 0.1 % of CO in nitrogen, for two main reasons. The first was to avoid using very low flow rates, that are very difficult to obtain. If the gas introduced in the system is a diluted mixture of CO, the flux used to produce a given concentration of carbon monoxide will be higher than in the case where pure CO was used. The second reason was laboratory safety in case of a leak from the carbon monoxide pipelines.

Depending on the calibration methods used, the units used to express concentration may differ. In most papers on gas sensors, however, concentration of the analysed gas is usually presented in ppm units, expressing the number of particles of a contaminant per total number of particles in a mixture. In sonic orifice technique the calibration of produced gas mixtures may be carried out either by flow rate measurements, comparison methods, tracer methods or direct chemical analyses. Flow rate measurements were chosen for their simplicity and wide applicability.

A small test chamber volume, of 160 cm<sup>3</sup>, was selected to reduce the amount of gases used, speed up introduction and removal of the analysed gas and avoid the need for homogenization of chamber atmosphere, during the experiments.

### 5.1.1. Gas flow in the testing chamber

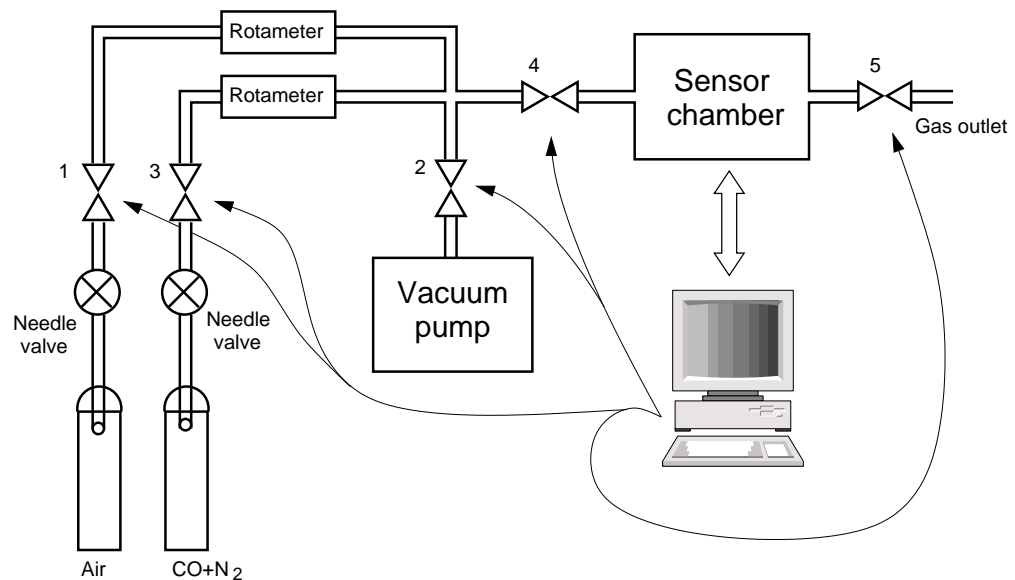


Figure 5.1.: Experimental setup of the system used to test gas sensitivity

The experimental setup used control to the atmosphere in the testing chamber is outlined in Fig. 5.1. In order to guarantee that the atmosphere inside the system is not contaminated, all the gas lines between the outlet valves of the gas containers and the outlet valve of the chamber may be evacuated using a mechanical vacuum pump. This pump is able to reduce the pressure inside



the system down to  $3 \times 10^2$  Pa. Electrically actuated valves, controlled by the parallel port of a personal computer, are positioned at several points of the system. These valves are used to change gas flow, following a procedure that permits the introduction and removal of a known concentration of carbon monoxide inside the testing chamber, during preset time intervals.

Both synthetic air and CO flow rates, are set out by means of two independent straight pattern S-Series Nupro needle valves. These valves have a maximum,  $C_q$ , flow coefficient of 0.004<sup>1</sup> and are operated using a high pressure drop, i.e., with the inlet pressure,  $P_i$ , higher than two times the outlet valve pressure,  $P_o$ . In this flow regime, the flow rate in sccm units through the valve is approximately given by

$$q = 3273C_qP_i\sqrt{\frac{\rho_{air}}{\rho_gT}} \quad (5.1)$$

where  $\rho_{air}$  and  $\rho_g$  are, respectively, the density of air and the density of the gas,  $P_i$  is the inlet pressure in mbar and  $T$  is the absolute upstream temperature. To keep a constant flow through the valve it is necessary to hold constant both the upstream pressure and the temperature.

Since pressure at outlet of the valves is kept only slightly above the ambient pressure, inlet pressure is set at  $2.3 \times 10^5$  Pa (2.3 bar). Using these conditions gas flow rates remain constant in spite of ambient pressure changes.

The pressure in the chamber is checked with a variable capacity Setra 204E sensor. This sensor is able to measure pressure in the range from  $1.0 \times 10^3$  Pa to  $3.0 \times 10^5$  Pa. Gas flow rates are measured with two Brooks 1355 Series rotameters. These can measure air flow rates in the range from 4 sccm to 47 sccm and are calibrated for nitrogen. The rotameters scales are graduated in millimetres. Flow rates,  $q$ , are determined using formula:

$$q \text{ (sccm)} = .313 [h \text{ (mm)}] \quad (5.2)$$

where  $h$  is the position of the float in the scale, in millimetre. Precision of the measurement is about 0.6 sccm. Synthetic air is constrained to flow at a rate of about 37.6 sccm during the experiments. When the mixture containing CO is introduced in the gas flow the overall flow rate through the chamber rises accordingly. This induces a small temperature variation in the tested film, that causes a resistance variation much lower than the one observed for gas sensing responses of practical importance. Since the flow rates cannot be controlled automatically using the existing equipment, this error was accepted in order to permit unattended operation of the experiment.

Concentration of carbon monoxide,  $C_{CO}$ , when the mixture containing this gas flows into the chamber, is calculated using expression:

$$C_{CO} = C'_{CO} \left( \frac{q_{CO}}{q_{CO} + q_{air}} \right) \quad (5.3)$$

where  $C'_{CO}$  is the concentration of carbon monoxide inside the gas cylinder,  $q_{CO}$  is the flow rate of the mixture containing CO and  $q_{air}$  is the flow rate of the synthetic air. Given that air flux is kept constant a straightforward expression may be used to determine carbon monoxide concentration, from the float positions,  $h_{CO}$  and  $h_{air}$ , of the CO and synthetic air rotameters, respectively.

$$C_{CO}(\text{ppm}) = 10^3 \frac{h_{CO}}{h_{air} + h_{CO}} \quad (5.4)$$

<sup>1</sup>The flow coefficient of a valve is a non-dimensional number that accounts for the factors related to the valve structure that affect fluid flow through it.

## 5. A chamber for gas sensor response testing

where both  $h_{\text{CO}}$  and  $h_{\text{air}}$  are measured in millimetres. Given the precision and accuracy of flow rate measurements, carbon monoxide concentration can be varied in a range from 40 ppm to 950 ppm with precision greater than 10%. It is important to note, though, that increasing the flow rate of the mixture containing CO, reduces oxygen concentration in the final gas flowing through the testing chamber. Since oxygen takes part in the sensing mechanism, the flow rate of the CO mixture is never increased above 250 ppm in order to keep oxygen concentration in the chamber above 15%. Higher CO concentration could be achieved without affecting oxygen considerably, if a mixture with higher CO content was used, however, such high concentrations are much above the toxic levels specified for this gas, and thus there is no special interest in its detection.

The elimination of CO from the chamber is carried out by cutting the flux of this gas. In order to speed up this process, the chamber is isolated from the system during some minutes and the gas lines are pumped to vacuum before clean gas starts to flow again into the chamber. During this time, film temperature is likely to rise by a small amount, since heat exchange with the surroundings is decreased. Measured temperature, however holds within the specified values, because the temperature controller keeps the temperature within the specified limits. Furthermore, carbon monoxide concentration is expected to decrease, inasmuch as the molecules react at the film surface forming  $\text{CO}_2$ . These mechanisms explain the changes observed in film resistance during isolation of the chamber (see Fig. 5.5). These values were ignored in the analysis.

### 5.2. Controlling the surface temperature

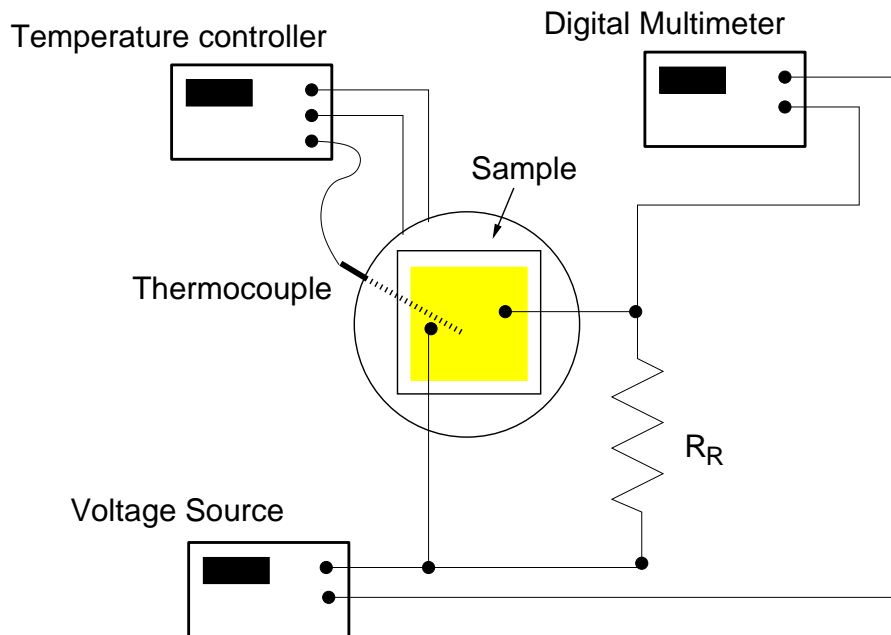


Figure 5.2.: Diagram of the setup used to measure the resistance and heat the samples

Sample heating is carried out using an electrical resistance connected to a Shimaden SR52 temperature controller. Electrical resistance goes through the substrate holder and temperature is measured with a thermocouple as shown in Fig. 5.2. Using this setup it is not possible to know the temperature at the sample surface. However, if gas flow is kept constant and enough time is allowed in order to achieve equilibrium of heat exchanges, experimental conditions can

be reasonably reproduced.

Temperature can be varied between 30° C and 400° C. Its value can be maintained at the specified level by the controller with oscillations lower than 0.3° C.

Commonly, in resistive gas sensors, both the heater and the temperature sensor are placed on the substrate. An arrangement of this sort permits a more accurate surface temperature evaluation but increases sample preparation effort and cost, therefore gas response testing is performed faster if this step is avoided.

### **5.3. Electrical measurements**

Measurement of thin film resistance requires that proper electrical contacts are done on the layer surface. In order to complete this task a number of choices have to be made. In first place it is necessary to decide whether the contacts on the film surface should be permanent or permit separation and rejoining. After this the material and size of the conductor have to be chosen and finally selected the means to effect the connection. Since the film resistance has to be performed at temperatures higher than ambient, it has to be checked that the contacts withstand the working temperatures without considerable change. The contact resistance of the electrical connector should also be low and independent of the flowing current, particularly if thin film resistance is low.

A permanent connection may be obtained by deposition of a metallic layer over the tested layer. Good contacts provide a uniform contact resistance over the contact-film interface and therefore a uniform electric field over the thin film layer. Sometimes several layers have to be deposited in order to achieve the needed characteristics: namely a bottom layer to prevent diffusion into the tested film, a chemically stable top layer, generally using a noble metal, and eventually a medium layer that provides stable adhesion between the top and bottom layers. Ideally, these layered structures should be fabricated under the same production process under vacuum in order to prevent development of oxide layers in the interface by exposure to the atmosphere.

Some experiments were done in order to find which materials were suited to produce electrodes on the tin oxide surface. It was found that silver deposited by thermal evaporation did not adhere to the tin oxide layer. Better results in what concerns to adhesion were obtained, if the deposition was performed by magnetron sputtering, nevertheless, these electrodes revealed to be useless after some tests because silver diffused into the tin oxide films. Chromium, aluminium and molybdenum were also used. None of these materials should be used as the top electrode layer because of oxide development on the surface. From this set molybdenum showed best adhesion to tin oxide surface. It was not verified if there was diffusion into the tin oxide film.

Since the development of good electrode contacts was not one of the goals of this project, these tests were abandoned and pressure contacts were selected to perform the measurements. These contacts provide a fast and simple procedure to measure the resistance of any layer produced in our Laboratory. However, if sensor devices for commercial applications are to be produced, permanent and stable contacts on the sensing film surface will have to be used. In this case, a buffer layer, that avoids diffusion of metal into the sensing layer has to be found and then deposited over this layer a noble metal thin film. If deposition is to be performed using magnetron sputtering, two targets and a means to move the substrate under vacuum are required to perform both steps. In case the noble metal layer does not adhere to the buffer layer it would be necessary to find out an interface layer that with good adhesion to both the bottom buffer layer and the top noble metal contact layer, which would further complicate the process.

In the case of pressure contacts, in addition to electrical stability, it is also necessary to guarantee reduced mechanical wear of the contacts after each use. As to the nature of mechanical

## 5. A chamber for gas sensor response testing

contacts it should be noticed that the surfaces of solids are irregular on a microscopic scale, therefore, when two plane surfaces are placed in contact at a light pressure load, they touch at only a few small spots or asperities. The true area of contact will depend on normal load and the hardness of the materials, however, if area of contact was too high the electric field on the film could hardly be made uniform (see also Section 6.1 for further discussion). In order to have greater control over the electric field on the sensing layer it was then decided to use point contacts, at the expense of obtaining higher resistance values.

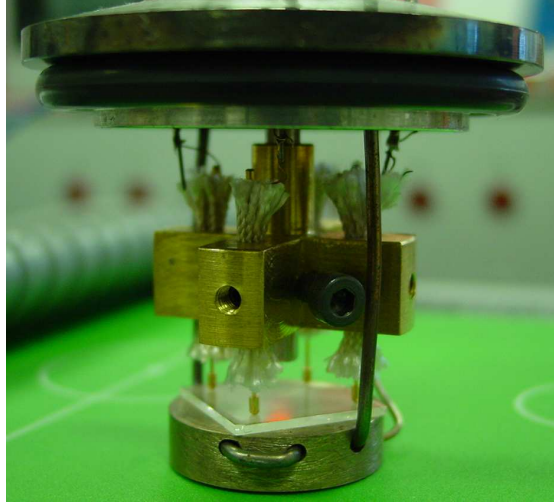


Figure 5.3.: Photograph of the point contact holder

The chosen contacts are gold covered needles terminating in a semi-spherical point. The needles' point is connected to a spring which ensures good contact to the surface. Four of these point contacts were mounted on a brass structure as depicted in Fig. 5.3. Proper insulation between the contacts and the holder is obtained using an insulating sleeve put between the contact needles and the hole where they are fixed. This structure slides along a metallic rod fixed to the top of the testing chamber and is fastened to it by a small screw. The substrate holder is centred in the chamber and is also fixed to the top of it as shown in Fig. 5.3. On the top of the chamber were made six insulated feed-through connections: four to take out electrical signals from the point contacts and two more to provide power to the substrate heater. The connections between the contact needles and the feed-through wires were performed with small section flexible copper wire to permit movement of the contact holder.

Electrical measurements were performed with a HP 34401A digital multimeter using the setup shown in Fig 5.2. This setup was chosen in order to permit variation of the voltage signal applied to the sample. A reference resistance,  $R_R$ , was connected in parallel with the sample. When sample resistance is high, current flowing through the circuit is very low and thus proper lead shielding must be provided in order to reduce electromagnetic noise from other equipment in the laboratory and leakage current errors. Electromagnetic isolation was carried out using coaxial cables to lead all the currents. Reference resistance was placed inside a Faraday box and film chamber provided similar protection for the sample.

Using the setup displayed in Fig. 5.2, a predefined DC voltage,  $V_0$ , is applied to the circuit and the multimeter is used to measure the current flowing through the circuit,  $I$ . Film resistance,  $R_S$ , is then calculated using the following expression:

$$R_S = \frac{(R_{P1} + R_R)(IR_i - V_0) + IR_R R_{P1}}{V_0 - I(R_R + R_i)} \quad (5.5)$$

where  $R_i$  is the internal resistance of the multimeter and  $R_{P_1}$  is the contact resistance of the point probes. Selecting a reference resistance much higher than both  $R_{P_1}$  and  $R_i$ , Eq. 5.5 may be simplified:

$$R_S = \frac{R_R [I(R_i + R_{P_1}) - V_0]}{V_0 - IR_R} \quad (5.6)$$

Observing Eq. 5.6 it is easy to conclude that the internal resistance of the multimeter and the contact resistance of the point probes may only be ignored if the product  $I(R_i + R_{P_1})$  is much lower than  $V_0$ , which corresponds to a situation where  $R_i + R_{P_1} \ll R_S$ , as expected. Other setups where the multimeter was used to measure the voltage across the reference resistance or measure directly the sample's resistance were also tested. Given that the latter setups do not provide better results than the ones obtained with the one shown in Fig 5.2, they will not be described.

The testing chamber was built with four electrical contacts arranged in the vertices of a square with 10.2 mm side. Placement of electrical point probes, makes also possible simultaneous and independent sensitivity tests of two samples side by side. This arrangement makes also possible the use of the van der Pauw method [123] to measure the resistivity of the samples.

## 5.4. Data acquisition system

The multimeter and the temperature controller are connected to a personal computer in order to register measured values during the experiments, as shown in Figs. 5.2 and 5.1. The highest measurement frequency permitted by the developed program is  $1 \text{ s}^{-1}$ . This frequency was selected according with typical response times of metal oxide gas sensors. Lower frequencies can be set by the user in order to decrease the number of recorded data points, before each trial.

Communication with both devices is done using the RS-232-C ports. To permit the connection of several measuring instruments, the computer was equipped with a VScom PCI 800 serial port card from Vision Systems GmbH. The card has 8 ports and admits a maximum baud rate of 115.2 Kbps per port, although such high speeds are not used since the terminal equipment does not support them. This is the case of both the multimeter and the temperature controller, whose maximum transmission baud rate is 9.6 Kbps. This was the baud rate set for all the equipment used.

In addition to recording the measured data the computer is also used to set some of the operation parameters of the equipment. The configuration of the multimeter, for instance, is set remotely to measure either resistance or voltage and the measuring range is adjusted in accordance with the read out values in order to improve accuracy of the data. As to the temperature controller, the parameters that are assigned remotely are the temperature setpoint and the cycle time of the proportional operation (see appendix A for details about these parameters).

## 5.5. Sensitivity

It is widely known [124–126] that there is an almost linear correlation between the logarithm of the film resistance,  $R_S$ , and the logarithm of the concentration of the gas to be detected,  $C_g$ , for limited ranges of the concentration values. This fact suggests that  $R_S$  may be described by expressions of the following form:

$$R_S \approx A \times C_g^{-\alpha} \quad (5.7)$$

where  $A$  and  $\alpha$  are positive constants. Usually these constants are valid only for limited ranges that depend on the kinetic processes involved.

## 5. A chamber for gas sensor response testing

More generally, Clifford and Tuma [127] found that if there is a mixture of several reducing gases in the atmosphere,  $R_S$  may be described by the combination of several terms corresponding to different reactions that remove adsorbed oxygen from the sensor surface.

$$\left(\frac{R_S}{R_0}\right)^{-1/\beta} = \frac{\left(1 + \sum_j K_j \prod_i (C_{ij})^{n_{ij}}\right)}{C_{O_2}} \quad (5.8)$$

In the above expression  $R_0$  represents the resistance in clean air;  $C_{O_2}$  the oxygen concentration in atmosphere;  $C_{ij}$  the reducing gas concentration of compound  $i$  affecting the sensitivity of compound  $j$ ;  $n_{ij}$  is an integer or fractional integer power exponent and  $K_j$  is a constant characteristic of the detected gas. For many terms of the summation there is only one term per gas, such as  $C_{CH_4}$  or  $C_{H_2O}$ . For others there is a product of several like  $C_{H_2O}C_{CO}^2$ .

Results obtained using mixtures of  $O_2$ ,  $CH_4$ ,  $CO$ ,  $H_2O$  and  $H_2$  are consistent with Eq. 5.8. Namely, the following terms were identified:  $K_{CH_4}C_{CH_4}$ ,  $K_{H_2O}C_{H_2O}$ ,  $K_{H_2}C_{H_2}^2$ ,  $K_{CO}C_{H_2O}C_{CO}$  and  $K'_{CO}C_{H_2O}C_{CO}^2$ . Parameter  $\beta$  varies among sensors and depends on sensor temperature. To determine  $\beta$  properly, the sensor response to oxygen has to be measured. The  $K_j$  constants may be termed sensitivity coefficients and are determined from the measured responses. Since this type of response seems to be generally observed in several metal oxide sensors, constants  $K_j$  could be selected to compare the sensitivity of gas sensors, providing a more useful estimate than the usual conductance or resistance ratios appearing in the literature. In addition, these sensitivity coefficients can also provide an absolute measure of the catalytic activity of the sensor's surface. Nevertheless, it is worth to remember that to determine accurately the  $K_j$  coefficients knowledge of the sensing mechanisms is needed.

From Eq. 5.8 it may be inferred that the detection threshold of a device depends not only on the sensitivity to that particular gas, but also on the concentrations of other reducing gases in the atmosphere, which partially mask the response to the gas of interest.

## 5.6. Studying sensor performance

### 5.6.1. Resistance response ratio

As stated before, sensitivity is an estimate of the magnitude of the output response of a sensor. In gas sensor reports this parameter is often replaced by the resistance or conductance ratio which is a dimensionless number. Sensitivity, however, is defined as the rate of change of the output variable with the measurand, which may be determined by the tangent to the transfer function of the sensor and therefore is a dimension dependent quantity. Since this is the most common definition found in reports about sensors, the resistance ratio will not be designated by sensitivity, but will be simply designated resistance ratio. The same applies to the conductance ratio.

The resistance and the conductance ratios may be calculated using one of the following expressions.

$$S = \frac{R_S[C_g]}{R_0} = \frac{G_0}{G_S[C_g]} \quad or \quad (5.9)$$

$$S' = \frac{G_S[C_g] - G_0}{G_0} \quad (5.10)$$

where  $R_0$  is the resistance measured in the reference atmosphere;  $G_0$  is the conductance in the reference atmosphere;  $R_S[C_g]$  is the resistance under concentration,  $C_g$ , of the monitored gas and  $G_S[C_g]$  the inverse of  $R_S[C_g]$ . Reference atmosphere may be either an atmosphere without

the monitored gas or with a predefined concentration of the gas. The most frequent expression used when the sensitivity of a n-type semiconductor to reducing gases are studied is the one corresponding to Eq. 5.9. In this case the reference values are measured in the absence of the stimulating gas. Apparently, the definition is chosen to produce always a number greater than unity. Namely, when the resistance increases with the concentration of the stimulating gas, above equations are inverted, so that the resistance ratio is determined by:  $S = R_0/R_S[C_g]$  or  $S = (R_0 - R_S[C_g])/R_S[C_g]$  [88]. Resistance ratios obtained with Eq. 5.10 are formally equivalent to the ones obtained with Eq. 5.9, since  $S' = S - 1$ , but this has to be accounted for, when comparing with results reported in literature.

This report adopts the most frequent definition used for carbon monoxide sensors. Thus the resistance ratio is calculated using Eq. 5.9, with  $R_0$  defined as the resistance measured when only the synthetic air is flowing through the chamber.

### 5.6.2. Response and recovery times

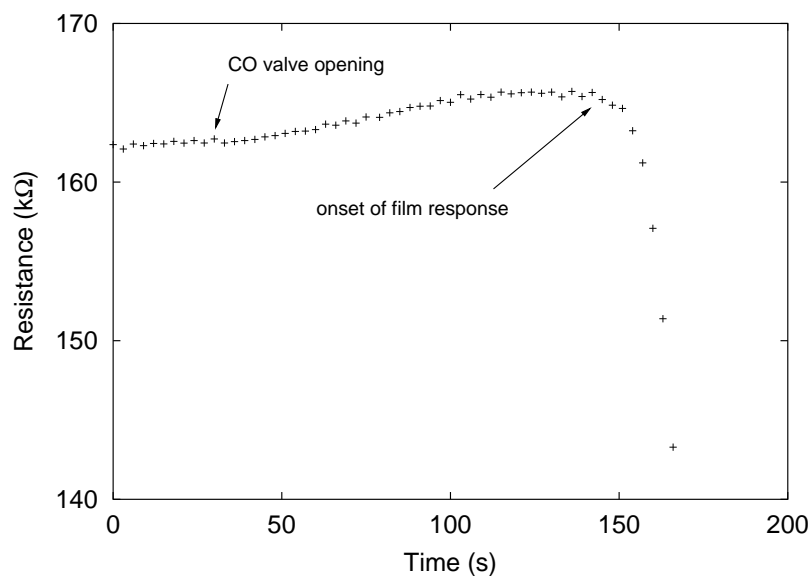


Figure 5.4.: Detail showing the time difference between valve opening and onset of film response

Ideally, response time should be measured against a step wise increase of the monitored gas concentration. However, this cannot be attained perfectly since a nonzero time is needed to transport gas molecules to the film surface. Given the gas fluxes and tube lengths used, it is expected that from the opening of the CO valve to the establishment of a steady mixture in the chamber, it takes more than one minute. Response times measured will always be affected by this deviation (see Fig. 5.4). The same happens to the recovery time, although in this case there is an additional difficulty, which is the removal of carbon monoxide without evacuating the chamber. It was not possible to measure the time needed to eliminate CO completely from the chamber.

Typical response signals of metal oxide gas sensors show a fast initial response that slows down as the final asymptotic value is approached. The response time definition corresponds generally to the time needed to achieve a certain percentage of the final change in the sensor signal. This percentage is usually set at 90 %.

In real situations a fast response time is usually required, but a fast recovery time is not so important. It is important, though, that the sensors may be restored to the standard conditions in

## 5. A chamber for gas sensor response testing

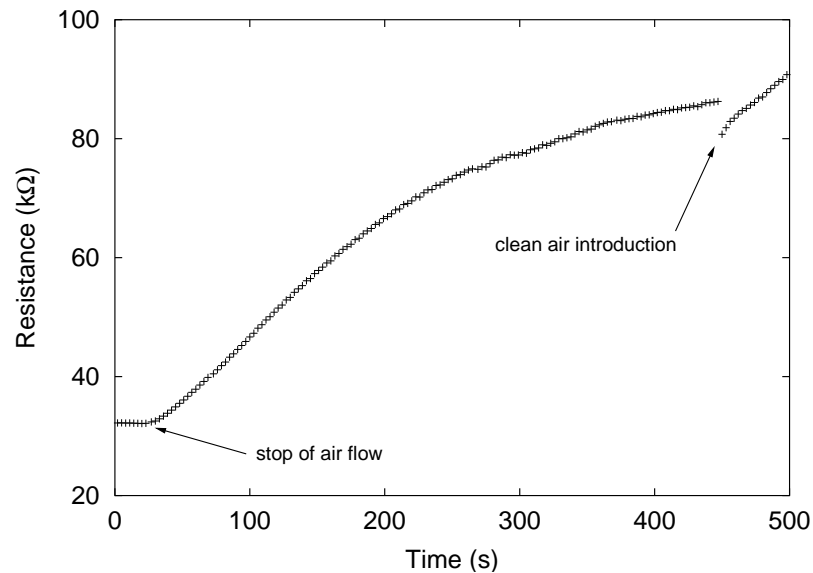


Figure 5.5.: Typical resistance changes observed when the testing chamber is closed with a fixed amount of CO inside

order to be reusable, so this should always be checked in the experiments.

### 5.6.3. Short and long-term stability

Some of the drifts observed in the sensor signal result from unstable ambient parameters or operating conditions of the measurement devices. Other drifts are caused by irreversible transformations in the film. The latter may turn the film useless for gas sensing applications, so they have to be estimated carefully. In order to do this the external sources of error should first be identified and reduced to the minimum level. If they cannot be completely eliminated, accurate characterization should be done and proper corrections applied to the measured values.

Short-term drifts do not cause serious problems, as long as the sensing characteristics are reproduced in consecutive experiments. In order to ensure similar testing conditions from the start, after the chamber is opened, all the system (including the chamber), is pumped to vacuum during 10 minutes. Then clean dry air is introduced in the system and when normal flow conditions are resumed, the sample starts to heat. If heating was performed during vacuum, gas sensing response might not be compared with the real operating conditions, where the sensors are generally operated at atmospheric pressure.

Before introducing carbon monoxide in the chamber, air flow is kept constant for at least one hour for the temperature to stabilize. Stabilization times are also performed whenever the working temperature is varied during the experiment and can be adjusted to reduce the observed drifts.

Since the thermocouple temperature measurement is referenced to the ambient temperature, that varies during the trials, it was speculated that the drifts may in part be due to a drift in the thermocouple reference. To test this hypothesis a more stable reference was provided with an ice bath. Introducing this reference temperature did not show, however, any difference in the measured signal, so this procedure was not continued.

The voltage source and the multimeter are usually turned on before the experiments, in order to prevent that setup time of these instruments introduces additional drifts.



## 6. Tin dioxide response to carbon monoxide

Before presenting the results from the gas sensitivity tests performed in our Laboratory, a brief outline of the current knowledge on sensing mechanisms will be exposed. The description of the sensing mechanisms will be mainly focused on interactions involving carbon monoxide detection, although, other interactions may be referred to illustrate the variety of processes that may take place at metal oxide surfaces during gas detection.

Despite the relatively high number of reports published annually on gas sensing devices (cf. Section 2.3) there is still no generally accepted complete theory explaining sensor operation mechanisms. Several models have been proposed and used to explain the responses observed in particular cases. In the case of resistive gas sensors there is still no model that starting from the materials' characteristics is able to predict the gas sensing behaviour. However there are some general trends quite well established experimentally. These have been verified for different metal oxide resistive sensors and particularly for tin dioxide based materials, either single crystals, thin compact homogeneous films or, thick porous films, such as sintered layers or pellets.

Some of the main models will be briefly described in this chapter. To help retaining the main trends mentioned above, during this description, they are now summarized. Firstly to detect a combustible gas, such as carbon monoxide, oxygen has to be present. When the sensing layer temperature is increased, the sensitivity also increases until a maximum is reached and then usually falls towards zero at higher temperatures. The shape of the sensitivity versus gas concentration curve (the transfer function) is logarithmic over a wide concentration range. The power constant, however, may change over different concentration ranges. A high discrimination is obtained at low concentrations, but is poor at high concentrations. This is in marked contrast with amperometric electrochemical sensors, where the transfer function is approximately linear over the usable range of concentrations [93]. Frequently, resistivity of metal oxide layers exhibits long term drifts, the response is non selective and particularly, is often influenced by water vapour.

### 6.1. The sensor output

Resistive gas sensors' mechanisms belong to the modulating type. Therefore, it is necessary to apply a modulating signal to the sensor, in order to get a useful output. Since the measured property is the resistance, either a current is injected into the material and the voltage drop measured or an electric field is applied and the current measured. In both cases, there is an electric field inside the sensing material and a current flowing through it. Supposing that an electric field is applied using two metallic conductors with different potential, its geometry inside the sample will depend on the geometry of the conductors and on the charge distribution inside the sample. On the other hand, the current flow will depend on the electric field geometry and on the electronic structure of the material.

Before analysing the effect of the layer structure on the signal measurements it is worth to look to the sensor as an electrical element, whose inner structure is unknown. Thus it will

## 6. Tin dioxide response to carbon monoxide

be considered in first place the geometry of the electric field lines at the interface between the electrodes and the sensing material and the way this may affect the information that can be obtained from the measurements. Previously (cf. Section 5.3) some properties of the electric circuit, used to carry the current from the power source to the sensing material and from this to the measuring instrument, were considered. Now, the current flow inside the sample will be discussed.

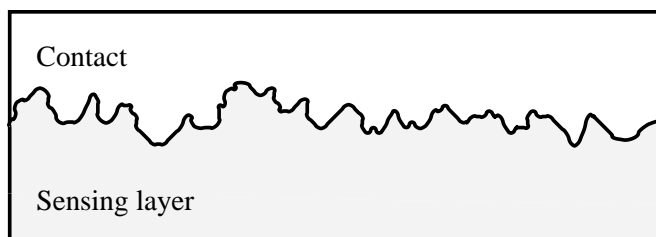


Figure 6.1.: Contact microstructure of a sputtered deposited contact

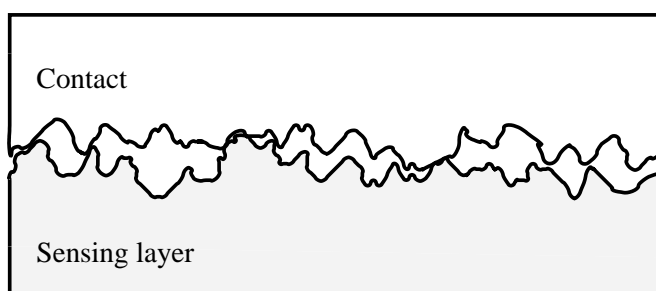


Figure 6.2.: Contact microstructure of a typical mechanical contact

The geometry of the electric field lines may be influenced mainly, by the electrodes' geometry or by contact structure. Microscopically it is possible to have two different kind of contacts structures, there may be a perfect contact between the electrode and the material, such as, the one observed in Fig. 6.1 or a more irregular one such as the one depicted in Fig. 6.2. The first one may be obtained, for instance, when the electrodes are deposited onto the material's surface using a PVD technique. The other one is characteristic of a mechanical contact obtained by pressing a metallic conductor onto the surface. It may readily be perceived that in the case shown in Fig. 6.2 there will be some points where the electric field lines will be very dense. In these points, the current density will be higher, and therefore there will be more heating that may cause structural changes of the surface. In addition, in the transient regime the capacitance generated at the contact interface may have a non-negligible effect on the current.

The case shown in Fig. 6.1 is likely to surpass such problems, but, as already mentioned, depending on the deposition technique and the materials used, structural changes may be induced on the material's surface. Namely there may be diffusion of the electrode material onto the underlying surface.

In both situations it is also necessary to consider the non-linear current-voltage relationship resulting often from a common metal-semiconductor contact. When a metal makes contact with a semiconductor, the Fermi levels of the two materials must be equal at thermal equilibrium and the vacuum level must be continuous. Since the metal work function is generally different from the semiconductor work function, a space-charge layer forms and the energy band bends on the semiconductor surface in order to fulfil the previous conditions. This results in a common situation known as a Schottky barrier. In some cases, this barrier may introduce a significant voltage drop when a current is flowing through it and therefore degrade the device performance.

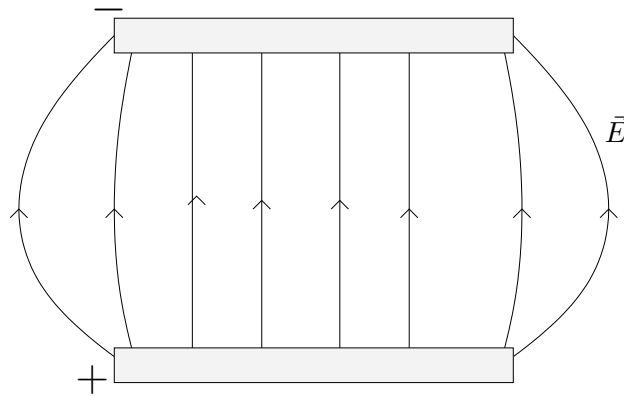


Figure 6.3.: Electric field lines resulting from two long and parallel contacts deposited on a semi-conducting surface

Other interesting situations arise from different geometry of the conductors. Two extreme cases will be considered: infinitely long parallel contacts and point contacts. Although those ideal parallel contacts cannot be obtained in practise, they approximate the behaviour of finite parallel contacts that are sufficiently long to reduce the influence of the extremes to a negligible value. It may again be readily observed that the field lines in the case of point contacts will be very dense near the interface, while in the parallel case these lines will be homogeneously distributed along the interface as shown in Figs. 6.3 and 6.4. This will affect once more the current density flowing in and out of the sample.

Another important consideration is the signal itself. Mainly, one can have a constant field, such as the one provided by a direct current, or a varying signal. In the case of a varying signal, one can also think of a perfect sinusoidal function with a characteristic frequency or a combination of a several sinusoidal functions with different frequencies. The response of the sensor to these kind of signals could be used to produce an electrical analog of the device.

In the case of a constant input signal, if enough time is given to stabilize the charge distributions inside the sample, a constant output could be obtained and this output could be attributed to a characteristic resistance. Furthermore, if this procedure is followed when the layer is immersed in different predetermined gas mixtures, a correlation between the resistance and the gas concentrations may be obtained. This is the usual procedure followed in the case of chemoresistive sensors.

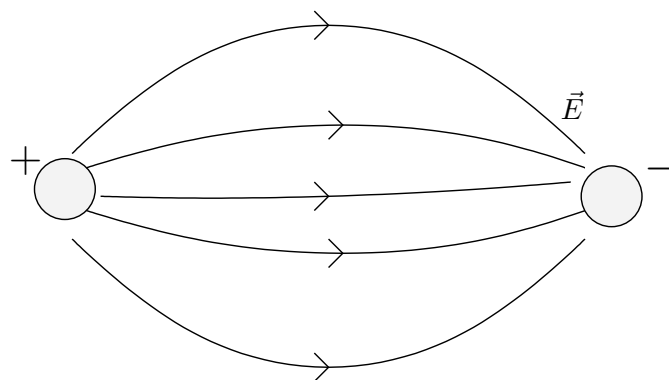


Figure 6.4.: Electric field lines resulting from point contacts made on a semi-conducting surface

## 6.2. The layer structure

To present the effect of the layer structure on the sensitive mechanism the simplest case will be considered, where a constant voltage is applied to the device and the current is measured. The other cases where a variable voltage signal is applied or a current is injected onto the film introduce only small modifications to the analysis and can be considered as improvements to the basic model.

When a potential difference is applied between different points on the sensing material there will be a current flowing between those points. If the material is homogeneous and is deposited on a non-conductive substrate, the current flux will depend on the resistivity, on the distance between the points and on the cross section of the material. If the material is not homogeneous, there may be regions with different resistivity and thus the magnitude of the current will depend on the path taken by the charge carriers.

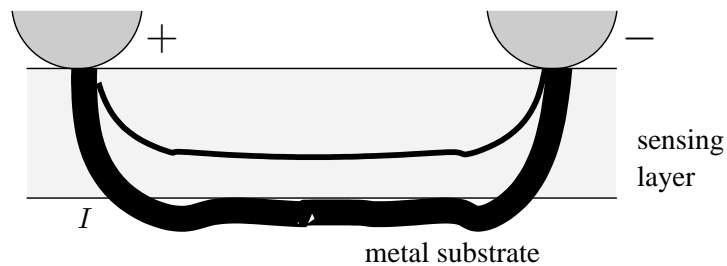


Figure 6.5.: Current paths expected when the sensing layer is deposited on a conducting substrate

The effect of the substrate conductivity is the one that will be addressed in the first place. Suppose that the sensing layer was deposited on a conductor or a semiconductor substrate. In this case the substrate could provide a path for the current flow between the electrodes. If the resistivity of the sensing layer was much higher than the resistivity of the substrate, the electrodes were sufficiently distant and the layer was not too thick, then the current could flow from one electrode to the substrate and from there to the other electrode, as shown in Fig. 6.5.

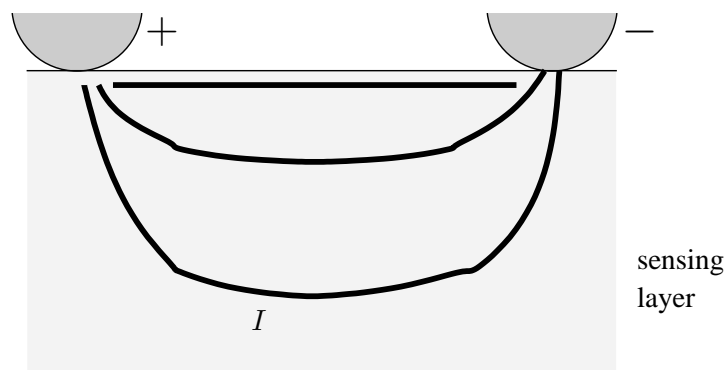


Figure 6.6.: Current paths expected when the sensing layer is deposited on a thick layer

The position of the electrodes is also important. These may be deposited either above or below the sensing layer. Putting them below leaves a larger contact area of the sensing layer with the gas above. However, if the electrodes are made below the sensing layer and the layer is not thin enough, the effect of the surface processes, on the current flowing through the bulk, will be reduced. A similar situation may happen also when the electrodes are above the sensing layer, if the current flows mainly through a region little affected by the surface processes. Different

current paths through a thick layer are shown in Fig. 6.6.

Supposing that the layers are polycrystalline, as the ones produced using magnetron sputtering, it is also necessary to consider the effect of the grain boundaries on the current flow. Phenomena observed at the grain boundaries may be compared with the ones observed at the layer surface. Grain boundaries may be in contact with air, if the grain limits a pore; may be in contact with another material, if the layer has more than one phase in its composition, or may be in contact with another grain. In any case the grain boundaries may provide a barrier to current flow. Assuming a depletion layer is formed on the grain surfaces, such as the one formed on a metal-semiconductor interface, a Schottky barrier is found and the conduction through the barrier will depend on  $eV_S$ :

$$G \propto \exp\left(-\frac{eV_S}{kT}\right) \quad (6.1)$$

If the Schottky barrier formed is controlled by the atmosphere surrounding the layer, the layer may be used in a gas sensing device. Usually these sensing materials are intentionally made highly porous to increase the contact area with the gas. This simultaneously alters significantly the current path through the sample and further complicates the current flow analysis.

Usually the charge carriers are electrons, but as discussed before (see Section 2.2.1) the current might also be carried by ions. Since ions have very low mobility in solid materials, they cannot respond quickly to a potential variation. Nevertheless, ions may considerably influence the electric current, when they accumulate in certain regions of the material and build the so called space charge layers. Since the material has to be electrically neutral, electrons have to go in or out of these regions in order to achieve this condition. The ionic excess is usually caused by crystalline defects, such as, vacancies or doping impurities. It is worth remembering that mobility of point defects increases with temperature, thus if the sensor is operated at high temperature, the electric properties may show long-term variations due to defect mobility.

In porous layers it is also necessary to consider characteristics of the diffusion of the gas particles into the bulk of the material. Designating by  $n$  the density of gas particles in a given volume,  $D$  the diffusion constant and  $z$  the distance from the surface, the flux of the gas particles on the  $z$  direction,  $J_g$ , may be determined from the following equation:

$$J_g = D \frac{dn}{dz} \quad (6.2)$$

which is also known as the Fick's first law of diffusion.

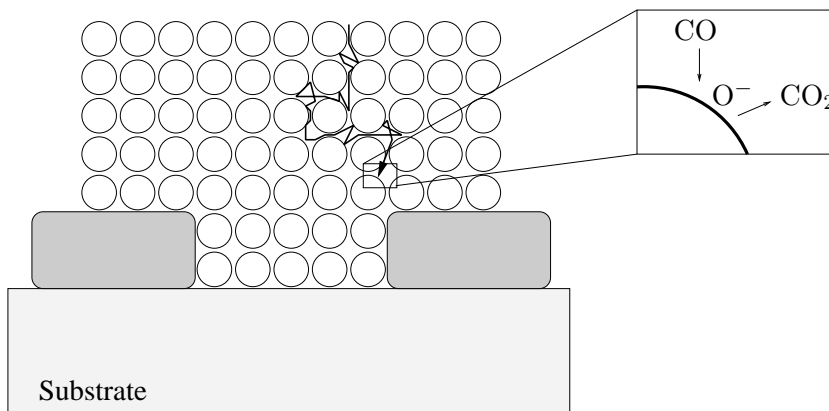


Figure 6.7.: Porous metal oxide layer structure used to support diffusion-reaction model

## 6. Tin dioxide response to carbon monoxide

Based on the diffusion depth of the reactants into the sensing layer, Becker et al. [88] proposed a model to explain different gas sensing behaviour observed in layers with different thickness. They called this model diffusion-reaction model. The fundamental concept behind this model is the supposition that a gas molecule to be detected has to diffuse into the sensing layer to suffer a chemical reaction at some depth  $z$  (see Fig. 6.7). In this way the resistance is changed significantly in those places where the reaction takes place. The model assumes also that the layer is filled by a uniform interconnected net of pores whose width is not much larger than  $0.1 \mu\text{m}$ , so that the diffusion of gaseous particles into the porous body is controlled by the collisions with the pore walls. Under those conditions, the diffusion constant becomes dependent on the pore size. On long diffusion paths, molecules pick up bits of thermal energy in each of their numerous collisions with the pore walls and thus react in the film interior, out of a vibrationally excited state. Considering that the detection reaction is an activated process, films with higher thickness would have higher sensitivity at lower temperatures. The experimental studies carried out by Becker et al. used tin oxide layers with  $300 \text{ nm}$  and  $30 \mu\text{m}$  thickness and atmospheres containing  $\text{CO}$ ,  $\text{CH}_4$ ,  $\text{O}_3$  or  $\text{NO}_2$ .

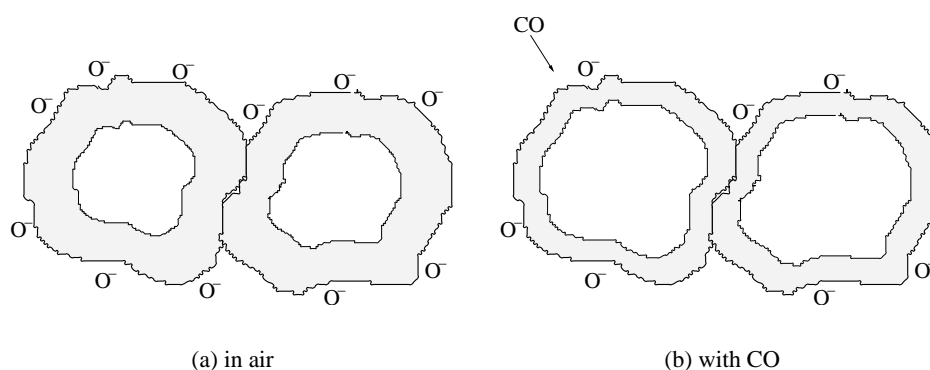


Figure 6.8.: Grain contact model and barrier control scheme

Sakai et al. [128] suggested a similar model and obtained results similar to the ones reported by Becker et al., although the experiments were performed with layers thinner than  $300 \text{ nm}$  and using  $\text{H}_2$ . Sakai also studied the effect of thickness on the sensitivity to  $\text{CO}$ , and reported that it was negligible. The same model was applied later by Matsunaga et al. [129] to describe the gas concentration profile inside a porous film under non-equilibrium situations.

Some interesting effects due to layer structure were also reported by Tang et al. [130]. Namely they sustained that tin dioxide film cracking reduces its resistance. The model proposed to explain this observation, involves the diffusion of water vapour through the cracks. Water can diffuse into the film through the cracks and adsorb there, thus decreasing the resistance. Additionally, it is stated that the removal of water from the cracks is more difficult than removing it from the surface, which results in a longer pre-heating time to stabilize the sensors and speed up degradation.

It is also interesting to note the effect of grain size on gas sensitivity. Xu et al. [131] assumed two different grain joining structures: grain boundary contacts and necks, that may coexist in the same material. In the first case, electrons should move across a potential barrier at each grain boundary, as shown in Fig. 6.8. If there are no necks structures, the gas sensitivity is controlled by the barrier height and is almost independent of the grain size. When grains are connected by neck structures, charge carriers move through a channel formed at each neck, where the resistance is lower than in the depletion region formed close to the surface, as shown in Fig. 6.2. Since the cross-section of each channel is controlled by the space-charge depth,

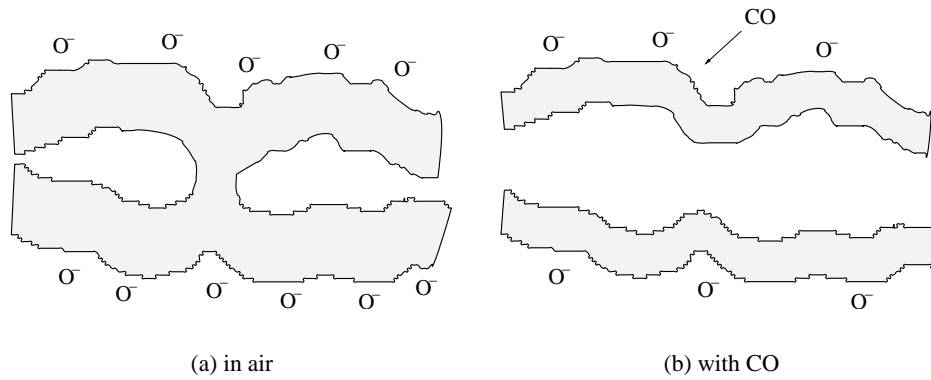


Figure 6.9.: Neck model and space charge layer formation

sensitivity in this case will be highly dependent on the grain size. In the model developed by Xu et al., it was assumed that necks had a diameter  $c. 0.8D_{gr}$ , where  $D_{gr}$  is the mean grain size, and the sensing layer is composed by grains connected mostly by necks and sometimes by grain boundary contacts. Supposing that the space-charge layer had depth  $L$ , there would be three different conduction regimes: grain boundary controlled, neck controlled and grain controlled. Grain boundary controlled develops when the  $2L$  is much lower than  $D_{gr}$ . In this case the contact resistance between grains is much larger than the bulk resistance of the grains and thus the contact resistance variations will control the current flow through the layer. Neck control arises when  $D_{gr}$  is comparable with  $2L$ . In this case, since the space-charge layer resistance is much larger than the bulk resistance of the grain, the neck resistance will control the current flow. Finally, when  $D_{gr}$  is lower than  $2L$  the grain resistance will control the current flow.

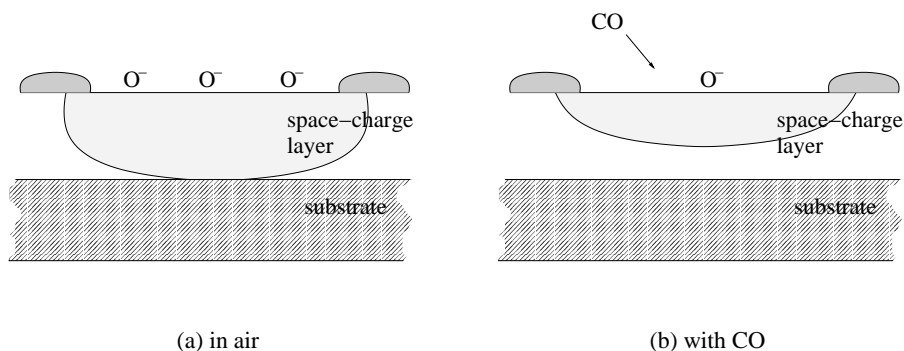


Figure 6.10.: Thickness control on very thin films

If a compact thin film was used, instead of a porous film, a situation similar to the one described above as neck controlled could be obtained, provided that the film thickness,  $d_f$ , was comparable to the depletion layer depth,  $L$ . This case is illustrated in Fig. 6.10.

### 6.3. Surface interactions

In the gas sensing mechanism the most important processes are surface interactions. These may change surface properties and thus affect the measured resistance. As already mentioned, if the current that flows through the sample takes a path far away from the interface between

## 6. Tin dioxide response to carbon monoxide

the sensing layer and the atmosphere, the measured resistance cannot be used to detect gas concentration variations. Therefore in the following discussion it is supposed that the current flowing through the sensing layer is significantly disturbed by surface interactions. This section describes some of the most common interactions taking place on a solid-gas interface and how they are related to some common thermodynamic variables, such as, temperature and pressure.

In case of carbon monoxide detection on tin oxide, the surface of  $\text{SnO}_2$  works as a catalyst to the oxidation reaction of CO. In this mechanism there are several processes that have to be considered: diffusion of the reactants towards the solid surface; adsorption of at least one of the reactants; surface diffusion of the adsorbed reactants; desorption of the reaction products and diffusion of the products into the fluid.

Apart from the catalytic effect of the surface itself, the effect of catalytic particles introduced in the layer structure has to be considered. The transition metals are among the most active metal catalysts, in which the partially filled d-orbitals of valence band electrons exhibit strong localization in space and energy. This allows for strong mixing of metal surface orbitals with the orbitals of a rather large class of adsorbed particles. In order to promote gas sensitivity, however, the oxidation reactions must not take place only on the catalyst surface. One possible way that could increase sensitivity was the formation of an active intermediate layer on the catalyst surface, that after diffusion to the sensitive layer would promote oxidation. These processes will be discussed in Section 6.3.3.

An important distinction will be stated between equilibrium and non-equilibrium processes. Although, the transfer function of gas sensing devices is generally obtained under equilibrium situations, the non-equilibrium processes offer frequently very interesting new possibilities for gas detection, and thus deserve to be studied deeply [132, 133].

### 6.3.1. Adsorption and desorption

In order to affect the current flowing through the sensing layer, gas molecules have to interact with the layer surface. This usually starts through adsorption and desorption processes. These interactions have characteristic lifetimes and energies, that will control adsorption rate, desorption rate and coverage of each atmospheric compound. Unfortunately, none of those characteristics is easy to quantify and, yet, they are needed to evaluate the sensing mechanisms.

On any surface there are usually several compounds adsorbed. Each one has specific activation and binding energies, each one has a specific adsorption and desorption rate, each one has a specific mobility and reaction path on the surface. There will be competition between the different processes taking place, there will be compounds transformed on the surface and some processes that even transform the underlying material. If a given adsorbed species has a long lifetime, it will have higher probability to react either with the surface or with another adsorbed species, provided that one of the species can move easily on the surface, or with an impinging gas compound. On the other hand, species with longer adsorption lifetimes will occupy an adsorption site that otherwise could be available for other species.

In resistive metal oxide gas sensors, the most important adsorbed species is oxygen. This may be adsorbed either in molecular or atomic form, and in neutral or ionic form. Depending on the layer temperature and structure, the dominant species will vary. Since the reaction rates and activation energies of the interaction of these species with other gaseous compounds, namely the reactive gas to be detected by the sensor, depends on the reaction steps considered, those have to be known in order to understand what is happening on the surface when the sensor current is varying.

Vancu et al. [126] proposed a model where it was assumed that only chemisorbed species may influence conduction. Activation energy was assumed lower for  $\text{O}_2^-$  than for  $\text{O}^-$ , and the energy level deeper for  $\text{O}^-$  than for  $\text{O}_2^-$ . Thus  $\text{O}_2^-$  desorbs first and above a given temperature



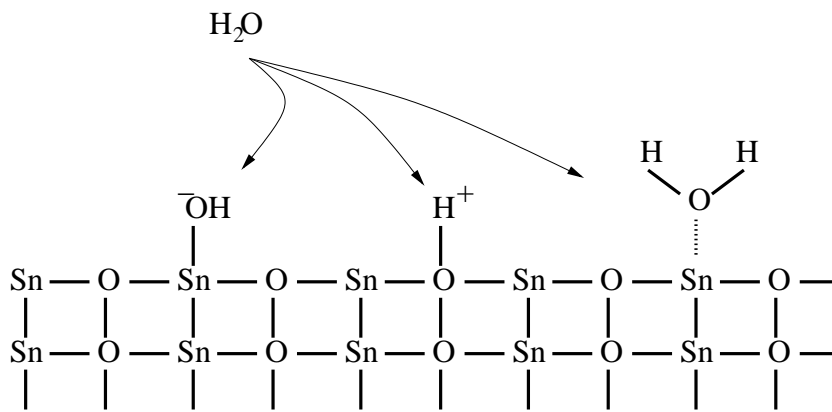


Figure 6.11.: Water adsorption possibilities on a tin dioxide surface

O<sup>-</sup> will dominate. Atomic oxygen may also be adsorbed in unstable doubly charged form. In this case, stabilization is achieved by lattice incorporation. Similarly, water may adsorb as a molecular neutral species (physisorption) or as hydroxyl groups (usually chemisorption), as shown in Fig. 6.11. Resistance changes for water chemisorption have opposite sign relatively to the one produced by oxygen chemisorption. Since water vapour is a common atmospheric component, competition with oxygen would be expected in what concerns adsorption. However, Vancu et al. [126] refer that the adsorption sites for the two processes have different nature and thus, no reciprocal disturbances are expected to occur. However, given that water vapour adsorption may create oxygen vacancies, oxygen adsorption may be enhanced by the presence of water vapour in the atmosphere.

Lets consider now two different cases. One where the resistivity is directly affected by the adsorption of the gaseous species that is to be detected, and the other one where that gaseous species, the stimulating gas, reacts with a different adsorbed species, usually oxygen, that controls the layer resistivity. This second gas is sometimes called sensitizing gas. In the first case, if the coverage is too low there will be no significant resistance change. The same happens if the surface is already covered with another species that screens the surface and blocks adsorption of the stimulating gas. In the second case there will be at least two competing processes: adsorption of the sensitizing species and reaction with the stimulating species. Coverage will then be a function of the adsorption and reaction rates of the sensitizing gas, and of the desorption rate of the reaction product. Furthermore, if the reaction occurs through the Langmuir-Hinshelwood mechanism, it is also necessary to consider the adsorption and diffusion rates of the stimulating species and the adsorption site density for each species.

The potential energy of a molecular gas species varies with its distance from the surface. As the particle approaches the surface its energy falls as it becomes physisorbed into the precursor state for chemisorption. Dissociation into fragments often takes place as the molecule moves into the chemisorbed state, and after an initial increase of energy as the bonds stretch, there is a sharp decrease as the adsorption-substrate bonds strengthen. Even if the molecule is not broken there is likely an initial increase of the potential energy as the substrate atoms adjust in response to the incoming particle. Thus, in all cases, it is expected the existence of a potential barrier separating the physisorbed and the chemisorbed states.

This barrier, though, might be lower than the energy of a distant stationary molecule. In this case, the chemisorption is not an activated process and may be expected to be fast. In other cases, the barrier rises above the energy of a distant molecule. Such chemisorptions are activated and slower than the non-activated kind.

Vancu et al. [126] suggested that in the case of oxygen both the heat of chemisorption and

## 6. Tin dioxide response to carbon monoxide

the chemisorption activation energy increase with increasing coverage, on sintered tin oxide layers. This implies, thus, that both adsorption and desorption processes will become slower. That dependence on the coverage was ascribed to non-uniformity of the surface, to adsorbate-adsorbate repulsion and the progressive formation of space-charge layers.

Adsorption and desorption rates depend on the temperature. Adsorption rate depends also on the number of collisions of the gaseous particles with the surface, and consequently on the pressure. Thus, by varying the partial pressure of the gaseous compounds, or the temperature of the sensing layer, resistivity variations may be induced on the regions near the surface. Desorption will depend only indirectly on the pressure, through the coverage.

### 6.3.2. Reactions

Reactions on a solid surface may proceed through many different microscopic steps. In tin oxide, for instance, interaction with reducing gases can take place either with surface lattice oxygen or with adsorbed oxygen. Those gases containing hydrogen can react after dissociation with surface lattice oxygen. Other gases, like CO, which cannot break strong bonds are more likely to react with adsorbed oxygen. Thus, CO interactions with tin oxide surfaces are usually conditioned by the oxygen partial pressure in the surroundings, but not exclusively.

Oxidation of carbon monoxide on a tin oxide surface may occur through many different reaction paths, depending on the surface composition, structure and temperature and on adsorbed species. Most of the time, the intermediates and complexes formed during reaction are short-living compounds that are not easily identified. However, in order to understand the overall sensing mechanism of carbon monoxide, it is necessary to know what oxygen species are present on the surface and their extent, how does CO adsorb on the surface, which reaction paths are possible and which is the rate of each step, what other elements may interfere in the reaction and if they are present.

When the oxidation reaction rate of carbon monoxide is much higher than the rates of adsorption and desorption of the reactants, the steady state oxygen coverage depends critically on the relative oxygen and CO concentrations in the gas phase. To allow for fast surface reactions the temperature has to be high enough, although not too high, to prevent bulk-surface interactions which can cause long time variations in the sensor parameters.

It is the existence of several reaction paths and several possible reactants that explains, most of the times, the differences observed in different sensor devices. Without the microscopic knowledge, it is almost impossible to evaluate the accuracy of the proposed models.

### 6.3.3. Catalysts and catalysis

Catalysis is a widely developed area and due to its importance in gas sensing mechanisms deserves to be considered separately from common surface reactions. Catalysts are supposed to reduce response time and improve selectivity in gas sensors. However, it is difficult to identify the mechanism responsible for those effects, and the extensive literature on heterogeneous catalysis for product generation, although interesting, is only indirectly useful in the selection of catalysts for gas sensors. The reason for this lies on the aims of both fields of research. In sensors the objectives are selectivity towards a compound and a moderate catalytic activity, while in catalysis one is interested on the selectivity of the reaction products and a high catalytic activity. Thus, in a normal catalysis process there is usually a very pure feed stream and a very pure product is obtained while sensors are supposed to detect a given compound in a possibly contaminated atmosphere, where the components are not completely known.

If small amounts of a catalytic material are deposited on the surface of an n-type semiconductor, the catalyst, if properly chosen, will accelerate oxidation of the reducing agent. Fig. 6.12

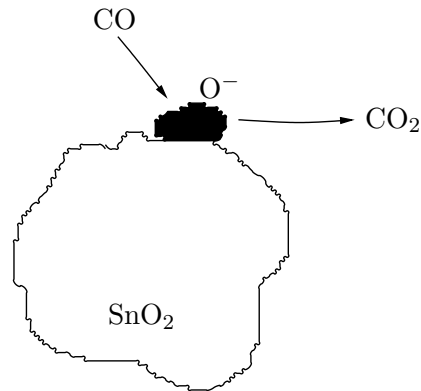


Figure 6.12.: Model of the catalytic oxidation observed on the surface of catalytic particles dispersed on the surface of a gas sensing material

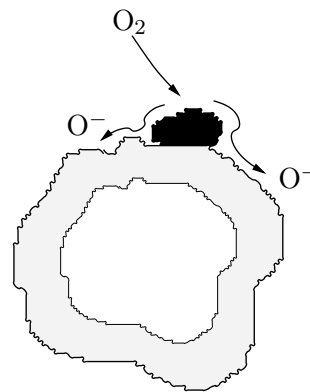


Figure 6.13.: Model of the spillover effect used to explain the mechanism of gas sensing improvement of catalytic particles dispersed on the surface of a gas sensing material

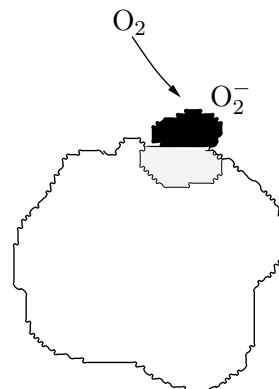


Figure 6.14.: Model of the Fermi energy control effect used to explain the mechanism of gas sensing improvement of catalytic particles dispersed on the surface of a gas sensing material

## 6. Tin dioxide response to carbon monoxide

represents oxidation of the reducing agent on the surface of the catalyst and consecutive desorption of the product into the atmosphere. It is not clear how the reaction occurring at the surface of the catalyst will influence the current flowing through the sensing layer. There are two commonly accepted models: spillover and Fermi energy control [134, 135].

Spillover is well known in heterogeneous catalysis and probably is most active with metal catalysts such as, palladium and platinum. The term spillover refers to the process illustrated in Fig. 6.13. The catalyst dissociates the adsorbed molecule and then the particles “spill over” onto the surface of the underlying material. Fermi energy control is used to designate the process of oxygen adsorption on the catalyst, removing electrons from the catalyst, which subsequently removes electrons from the supporting semiconductor. If surface states associated with deposited catalyst are present in concentrations exceeding  $10^{12} \text{ cm}^{-2}$ , and other surface species can be neglected, the catalyst can control the surface barrier,  $V_S$  [134]. In this model the charged oxygen species adsorbed directly on the semiconductor are neglected when compared to the oxygen species adsorbed on the catalyst. In other words, the catalyst, by Fermi energy control, dominated the depletion of electrons from the semiconductor. If only a few catalyst particles are present on the semiconductor surface, only a small portion of the semiconductor has a surface barrier controlled by the catalyst and the catalyst effect will be inefficient for gas sensing. Fig. 6.15 shows a more desirable situation where the catalyst particles are close enough and uniformly dispersed over the semiconductor surface.

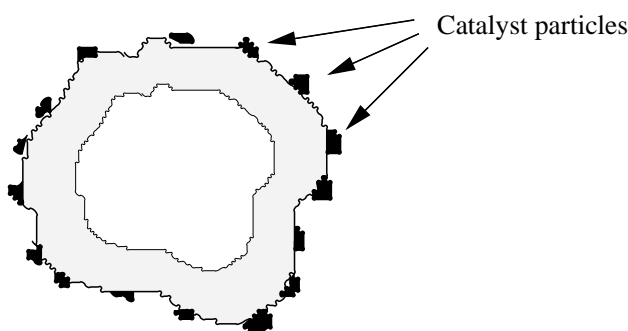


Figure 6.15.: Catalyst particles uniformly dispersed over a semiconductor grain surface

Fermi energy control is supported on the fact that when the electron transfer processes between phases is at equilibrium, the Fermi energy through the system is constant. With a high concentration of adsorbed oxygen on the catalyst surface that lowers the electrochemical potential of electrons, the Fermi energy in the catalyst and in the supporting semiconductor are correspondingly lowered.

The catalyst role in chemical reactions is reduced usually to one or both of the following processes: concentration of the reactants and lowering of the reaction activation energy. Concentration of the reactants may occur through adsorption of the gas phase species, while lowering of the reaction activation energy may be achieved by generation of new and more favourable reaction paths through the interaction with the catalyst.

Related to catalysis is the role of promoters. These may be used to stabilize a valence state or the stoichiometry; increase electron exchange rate or promote the formation of active phases. The mechanisms used to explain the effect of promoters are even less well understood than catalysis. Usually the optimization of the promoters' effect is performed by trial and error.

### 6.3.4. Equilibrium and non-equilibrium

While the transfer function of a gas sensor device is usually obtained under equilibrium situations, response and recovery times are typically non-equilibrium properties. Although equilibrium situations are easier to analyse, they are not very useful if a long time is needed to reach that state. Given the wide range of processes occurring during gas sensing operation, it often takes a long time to reach equilibrium. This is what happens sometimes with resistive gas sensors. Non-equilibrium processes may then be used to avoid this difficulty.

It is worth to consider that thermodynamic equilibrium based formulas are valid only for data obtained in thermodynamic equilibrium experiments. However, in what concerns defects, the time needed to attain thermodynamic equilibrium between the whole bulk of the material and the external medium is relatively short only at temperatures above c.  $0.7T_m$ , where  $T_m$  is the melting point of the material [126]. Given that usually the working temperature is below  $0.7T_m$ , it is not possible to attain equilibrium in the majority of the situations. In spite of this fact, there are some situations where equilibrium formulas may be used, to explain the results. Vancu et al. [126] propose that when the sample is submitted to a thermal treatment attaining temperatures above  $T_m$  and the cooling to the working temperature is fast enough to freeze the high equilibrium state, the total defect concentration may be found by using thermodynamic equilibrium based formulas. However, if the cooling rate was slow and evolution towards a different equilibrium state was possible, no valid information could be obtained in this way.

On the other hand, equilibrium of electrons and holes is established rapidly, so that their concentrations correspond to those at the working temperature. Similarly, due to the fact that the energetic barrier to overcome for adsorption is lower than that for bulk incorporation, the equilibrium state can be established at the surface even when the temperature is not high enough to allow bulk equilibrium.

## 6.4. Microscopic models

In the last decades several microscopic models have been proposed to explain the gas sensing behaviour of tin oxide [93, 136–140]. Most of the work is directed to the understanding of specific observations and since they lack support from microscopic parameters, these may not easily be transposed to every sensing material or atmospheric component.

Most of the accepted theories assume that adsorbed oxygen generates surface states that control the charge carrier density in the regions near the surface. The resistance changes are then explained by the formation of depletion charge layers. At equilibrium, with no electric field applied, the energy bands of an ideal semiconductor would have the same levels from the bulk, up to the surface. However, in the presence of surface states, there will be an excess electric charge at the surface. Since the whole material, bulk and surface has to be neutral, any electric charge on the surface states will be compensated by the formation, just below the surface, of a space charge layer of opposite sign, whose depth will depend on the electronic properties of the semiconductor. Depending on the electric charge on the surface states and on the conductivity type (n or p) of the semiconductor, three different types of space-charge layers may develop below the surface: a depletion layer, an accumulation layer or an inversion layer, as shown in Fig. 6.16.

Since  $\text{SnO}_2$  is a n-type semiconductor and oxygen generates acceptor levels, depletion layers usually appear at the surface of tin oxide in oxygen containing atmospheres. The depletion layer is characterized by two parameters, the depletion layer thickness,  $L$ , and the surface potential or Schottky barrier height,  $V_S$ . Both  $L$  and  $V_S$  depend on the charge stored in the surface states. The microscopic model suggested by McAleer et al. [137] is formulated assuming a dependence

6. Tin dioxide response to carbon monoxide

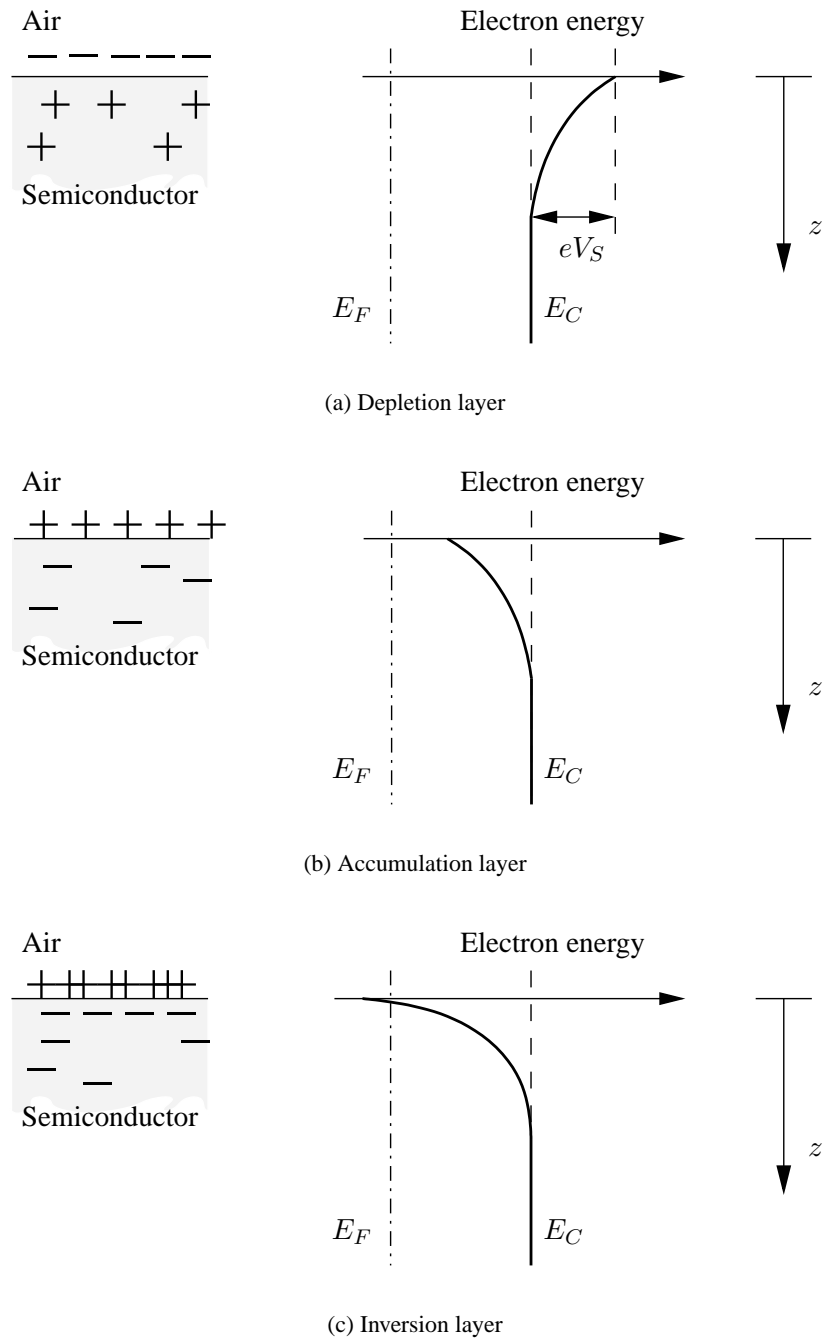


Figure 6.16.: Energy band scheme of the space charge layer that may develop on a n-type semiconductor when charged species adsorb on the surface

of the coverage,  $\theta$ , on the partial pressure of the reducing gas,  $P_R$ , described by the following equation.

$$\theta = \frac{k_1 P_{O_2}^{1/2}}{k_{-1} + k_2 P_R + k_1 P_{O_2}^{1/2}} \quad (6.3)$$

Where  $P_{O_2}$  denotes the partial pressure of oxygen, and  $k_1$ ,  $k_{-1}$  and  $k_2$  the reaction constants of the surface reactions considered.



The surface states are identified with adsorbed oxygen species. The reducing gas, R, reacts with adsorbed oxygen and establishes a steady state coverage of the surface states, which is less than the equilibrium coverage in air. The condition for high sensitivity to the partial pressure of the reducing gas is then:

$$k_{-1} \ll k_2 P_R \ll k_1 P_{O_2}^{1/2} \quad (6.6)$$

## 6.5. Experimental and theoretical work

It is difficult to join efforts from theoretical and experimental investigation, but it is a task that would likely accelerate sensor development and profit from accumulated knowledge from the different groups working in this field.

Theoretical studies usually start from simple problems such as the ones observed in clean surfaces. Although these studies cannot be transposed straightforwardly to the behaviour observed on the usual nanostructured materials, they are fundamental for the understanding of the mechanisms governing the electronic and chemical phenomena occurring at the surfaces. On the other hand, although understanding individual molecular processes is a necessary task, in the end what matters is how they contribute to the final result, and it is the statistical sampling that determines which of these processes are really relevant.

Many heterogeneous catalytic processes, such as the ones occurring on gas sensitive materials, are commonly described as structure sensitive, which means that the reaction turnover rate depends on the morphology of the surface [141]. However, for metal oxides, as well as for insulating materials, the understanding of the surface termination is still very poor [142]. One of the reasons is that electron scattering, spectroscopy techniques and STM are hampered by the insulating nature of the material.

Furthermore, theoretical studies for metal oxides are very demanding because they have to deal with a rather open structure, oxygen with very localized wave functions, large atomic relaxations, big super-cells and, sometimes, as for instance in iron oxide, 3d electrons and magnetism. Under realistic conditions surfaces can be very different from those often studied under UHV conditions. The difference can be dramatic, and the electronic properties and performance may have little resemblance to the low pressure results. This is often referred as the *pressure gap* in more recent publications.

An adequate theory should be valid from the atomistic level, which implies times periods of a few femtoseconds and the formation of small islands (microseconds), up to the formation

## 6. Tin dioxide response to carbon monoxide

of mesoscopic and macroscopic structures (tenths of seconds). It has been common practise to deduce theories separately for each of the length and timescales. On the smallest scales, where electrons and nuclei are meaningful, the effect of quantum mechanics has been taken into account; on the larger scales classical and statistical mechanics (with the quantum effects hidden in statistical parameters) were generally sufficient to explain the experiments. With the beginning of the new millennium, the borders between the theories describing different scales have began to dissolve, and a more unified look into the materials science is beginning to emerge [143]. Chemists, Physicists and Engineers working in this field find it advantageous, or even necessary, to collaborate and find whose connections may and should be made across scales, from big to small, in order to know how big affects small and vice versa.

Over the past decades surface science has assembled an impressive database on the structure of solid surfaces, regarding the chemical composition, the electronic states and the geometric structures. Most of this information, though, pertains to the static equilibrium properties of the surfaces. Questions related to the dynamics of the chemical bond rearrangement on the surfaces, determining, for instance, how these surface structures are actually formed, have been studied to a lesser extent. There are several routes to a detailed microscopic understanding of the dynamics of surface reactions. Among the techniques that can provide detailed insights into chemical dynamics of surfaces may be mentioned quantum dynamic calculations, molecular beam scattering experiments and femtosecond laser experiments [144].

### 6.6. Optimization of tin oxide layers

In chapter 5 were described the characteristics of the chamber developed at the University of Minho to measure the variation of metal oxide layers' resistance on a controlled atmosphere. This chamber was used to test the response of several of the produced tin oxide layers to carbon monoxide. When this project started our goal was to build an equipment that permitted the optimization of metal oxide layers for gas sensors and find some interesting correlations between the layer structure and the sensing characteristics that helped to reveal the sensing mechanisms.

The following results will show that this goal could not be fully achieved. Nevertheless the equipment that was built, although inadequate for the optimization of the layers' response, provides a useful procedure to identify sensitive layers and evaluate their electrical stability under different operating conditions. From the obtained results a number of suggestions of future studies will be formulated.

#### 6.6.1. Sample preparation

Given that the gas sensing tests are performed at relatively high temperatures, if the defect structure of the layer is not in equilibrium, the resistivity will show long term drifts as explained before. In order to stabilize the resistivity after deposition, the effect of a heat treatment was tried on some of the produced samples. Those treatments were performed in air and the highest temperatures achieved were around 500° C. Due to mechanical properties mismatch between the substrate and the deposited layer some of the layers, thicker than 1  $\mu\text{m}$ , did not survive the treatment. The effect of the heat treatment on the crystalline structure was also checked by obtaining XRD spectra before and after the treatment, but no noticeable changes were detected.

The undertaken treatments were unable to stabilize the layers' resistivity. The cause for this failure was attributed to the low temperatures used and the existence of impurities. Given that the SnO<sub>2</sub> melting point is higher than 1600° C [111], the heat treatments should be performed at temperatures near 1200° C in order to guarantee the defect structure equilibrium [126].

Use of glass substrates limited the temperature to which the samples could be submitted and



was a source of impurities, namely sodium that diffused into the tin oxide layer, but permitted to deposit and characterize a high number of samples. A better substrate, in what concerns the gas sensing tests, would be alumina, since it would permit heat treatments of the sample at higher temperatures. Whatever the substrate chosen, though, it is convenient to select a highly pure material in order to prevent the diffusion of foreign elements into the bulk of the deposited layer that may change its electrical properties with time. Given the cost of such high purity materials, these should only be used after the deposition conditions have been thoroughly studied and the characteristics of the layers resulting from the deposition process are well controlled. After this stage, one may then proceed to study the effect of the substrate on the layers' characteristics and the effect of the post deposition treatments.

The question of the electrodes was also addressed. On some of the samples were deposited electrodes of several materials using either magnetron sputtering or thermal evaporation. The electrode materials tested were silver, aluminium and chromium. Silver was interesting because of its very high conductivity and lower cost comparatively to gold or platinum. However, in the produced samples, the silver electrodes prepared, either did not adhere to the underlying layer or diffused onto the sample when heated. Aluminium showed similar problems and chromium did not provide a good metallic contact due to the oxide layer that forms on its surface. To avoid the diffusion of the silver into the tin oxide layer and increase adhesion, it was possible to deposit an interface layer between the tin oxide and the silver layers. This would require the use of two evaporation sources and a rotating substrate. At this stage, in view of the complexity of the problem, the lack of published information on the subject and given that our main goal was the optimization of the sensing layers, it was thought convenient to separate the development of the electrode structure from this study.

### 6.6.2. Limits and yields

The measuring equipment available, does not permit to obtain concluding results when the resistance of the samples is very high. However, layers that show adequate characteristics for gas sensing devices have been produced and it was verified that they show sensitivity to carbon monoxide. Future work should concentrate on the optimization of the substrate, layer thickness and electrode configuration, in order to produce usable devices.

Since the electrical contacts are fixed 10 mm apart, if the samples' thickness is small it is very difficult to determine its response to the atmospheric compounds, due to the increased resistance. Thus, to test the gas sensing response when the film thickness is comparable with the space-charge layer, which corresponds to a situation where a high sensitivity increase is expected, it would be necessary to produce electrodes that were separated by a small distance. Given that the development of the electrodes would take a long time, it would be profitable to join efforts with other groups working in the same area and concentrate our work on thin film production. This has started with the group of the Istituto per la Microelettronica ed i Microsistemi I.M.M.-C.N.R. from Lecce (Italy).

Good results were obtained using films with thickness higher than 500 nm, which permits to evaluate if there is sensitivity, and verify the stability of the resistance. It was observed during the tests that resistance depended significantly on the layer history. Three different causes for resistance change were identified: the atmosphere, the temperature and the layer structure. Furthermore, both the atmosphere and the temperature induce resistance changes not only directly, but also by affecting the layer structure.

In order to distinguish the temperature effect from the atmosphere effect, each layer was submitted to varying temperature profiles, and the resistance variation was recorded at fixed air fluxes. It was verified that the air flux affects the equilibrium temperature reached at the layer surface, but it was not possible to quantify its effect on the resistance given that its magnitude

## 6. Tin dioxide response to carbon monoxide

was similar to the long term drifts observed. Given that the time needed to reach temperature equilibrium was expected to be higher than 60 min and both the temperature response and the gas sensing response were typically below 5 min, it was possible to distinguish gas sensing effects from the effect of the air flux changes.

On the other hand, given that the time needed to reach temperature equilibrium was comparable with the rate of the structural changes' processes, it was often difficult to distinguish if the cause for the long term drifts was due to the temperature changes or to structural changes. If the system had a smaller heat capacity the material would reach temperature equilibrium fastly and thus it would be easier to identify the effect of a varying air flux on the temperature, but in this case it would be more difficult to distinguish the effect of the atmosphere interaction on the surface from the temperature variations induced by the heat exchanges caused by a varying air flux.

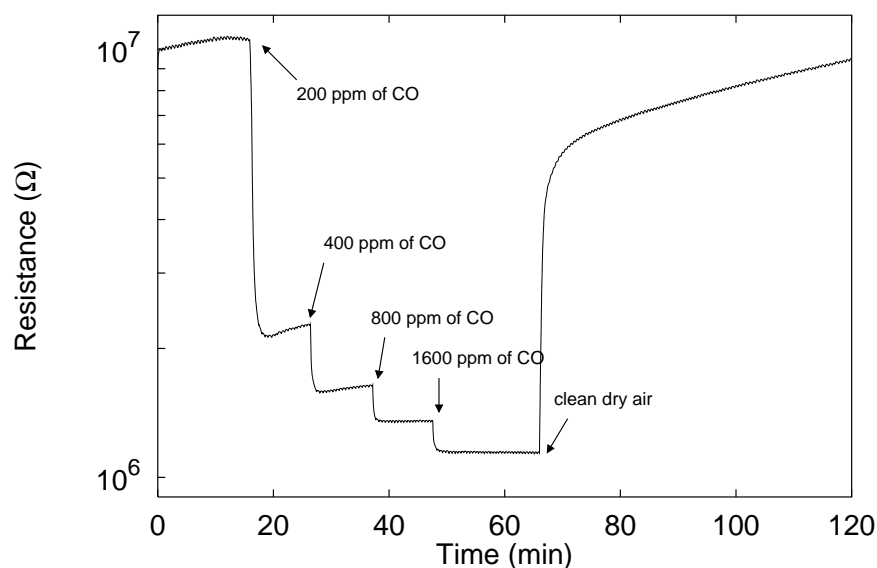


Figure 6.17.: Sample response to concentrations of carbon monoxide between 100 ppm and 1200 ppm

Fig. 6.17 shows the resistance response to carbon monoxide of sample a2e14. This experiment was performed using pure carbon monoxide in order to be able to reach higher concentrations. It is clear the non-linear dependence of the resistance on the concentration, typical of this kind of metal oxide gas sensors.

As shown in the previous chapters it is possible to produce and characterize metal oxide layers with different microstructures and, using the gas sensing test chamber developed at the University of Minho, determine if the layers have sensitivity to a given gaseous substance. Then, in cooperation with other groups, it is possible to work together in the development of a sensing device or in the study of the gas sensing mechanisms, taking our wide knowledge on the thin film production by magnetron sputtering.

## 7. Conclusions

Although the application of metal oxide layers in gas sensing devices have been studied for many years, a complete knowledge of the sensing mechanism is not yet established. The majority of the reports do not present a thorough characterization of the sensing layer structure and are therefore much dependent on the technique used to produce the sensing layer, on the sensor design and on the experimental setup used to measure the sensor signal. Some correlations between the layer characteristics and the gas sensing response are accepted and may be used to guide optimization of a particular production process. However, given that a complete surface characterization is very difficult, that knowledge cannot be used by itself to obtain optimized gas sensing layers. Furthermore, the comparison of gas sensing performance of different devices is frequently hindered by incomplete or setup dependent reporting procedures.

XPS analysis of the produced samples permitted to detect different oxygen species bound to the surface. The tin species, on the other hand, showed binding energies corresponding to typical tin dioxide material. EDX analysis showed that the bulk composition was within the expected  $\text{SnO}_2$  stoichiometry but did not permit to detect small stoichiometric deviations from that value. X-ray diffraction analysis showed polycrystalline layers with typical tetragonal structure and broad peak width, revealing both high strains and small crystallite size. Surface roughness observed in the atomic force microscope, increased with layer thickness. Grain sizes were difficult to determine using the XRD spectra alone, due to the film strains. Thus the microstructure of the samples was studied using both the XRD spectra and the AFM micrographs. Estimated mean grain sizes were within 120 nm and 7 nm. The density of the produced layers ranged from about  $6.9 \text{ g/cm}^3$  to  $3.6 \text{ g/cm}^3$ .

It was observed that the oxygen partial pressure during DC magnetron sputtering deposition is a key factor to obtain polycrystalline tin dioxide layers. When the oxygen partial pressure is varied from 0 to  $1.5 \times 10^{-3}$  mbar using a power close to 20 W, the composition of the layers changes from pure tin to tin dioxide, with an intermediate regime where the layers are amorphous and have low oxygen content. The oxygen partial pressure value above which  $\text{SnO}_2$  layers are produced increases when the applied power is increased. This tendency is attributed to a much higher adsorption rate of the tin atoms on the growing layer, compared with oxygen. When the number of tin atoms arriving at the surface is too high, the layer will be oxygen deficient. Above a certain oxygen partial pressure, the oxygen adsorption will no longer be limited by the number of atoms arriving at the surface, but by lattice incorporation of the oxygen atoms. The oxygen partial pressure threshold value also increases, although with a smaller variation, when the substrate temperature is decreased. In this case the variation may be ascribed to the higher mobility of the atoms with higher temperature, which increases the probability of oxygen incorporation onto the lattice.

Within the pressure range from  $2.0 \times 10^{-3}$  mbar to  $5.0 \times 10^{-2}$  mbar the produced layers were polycrystalline independently of the oxygen to argon ratio used, but provided that the oxygen partial pressure was above the threshold limit. It was noted that above  $1.0 \times 10^{-2}$  mbar the pressure was difficult to control and reproduce, but no cause was yet found for this instability.

Increase of the substrate temperature during deposition was found to increase the mean layer grain structures' sizes. This was expected in part, due to the increased mobility of the adsorbed

## 7. Conclusions

particles promoted by the temperature. The grain sizes, however, do not depend exclusively on the former parameter. The deposition atmosphere affected noticeably the growth structure of the tin oxide layers. When the total deposition pressure was in the range within  $2.2 \times 10^{-3}$  mbar to  $7.6 \times 10^{-3}$  mbar and the oxygen to argon ratio was kept equal to 0.70, it was found a variation of the preferential orientation of the crystalline layers. Namely, at  $2.2 \times 10^{-3}$  mbar, the peak with highest intensity corresponds to direction  $\langle 101 \rangle$ , at  $2.5 \times 10^{-3}$  mbar the highest peak is the  $\langle 211 \rangle$  and above  $5.8 \times 10^{-3}$  mbar the relative intensity of peak  $\langle 110 \rangle$  dominates in the spectra. The cause for this dependence is still being studied.

A major change was also the density of the films that was shown to decrease with total deposition pressure increase. Finally, deposition pressure has a non-negligible influence on the growth rate of the films. The growth rate was found to increase until about  $9.0 \times 10^{-3}$  mbar and then decrease again at least until  $5.0 \times 10^{-2}$  mbar, which was the maximum pressure used. The explanation proposed for the pressure influence, involves the increased scattering of the sputtered tin atoms, that are deviated from the target or arrive with lower energy. This explains the high reduction of the growth rate and the porosity increase.

The setup built in our laboratory to test the gas sensitivity of the produced layers, permits to measure the layer resistance up to 100 M $\Omega$ . The layer temperature may be varied from room temperature up to 400 $^{\circ}$  C. Different gas mixtures can be produced by adjusting the relative flow rates of the analysed gas and the synthetic dry air. Using a mixture of 0.1 % carbon monoxide in nitrogen it is possible to vary the CO concentrations from 40 ppm to 250 ppm. Lower concentrations in the test chamber may be obtained by using a lower concentration mixture of CO.

Some of the produced tin dioxide polycrystalline layers were found to be sensitive to carbon monoxide. The resistance response ratio showed a small increase with surface roughness, but neither a clear correlation with the grain size nor the film thickness was detected. Many layers showed an extremely high resistance and all the layers showed a continuous drift towards higher resistance values. The response to consecutive carbon monoxide pulses showed variations as high as 20 %. The main causes for the instability were attributed to a non-equilibrium defect structure of the grains and to the sodium impurities that diffused from the glass substrates.

### 7.1. Overview of future work

In the course of this work many interesting results were found but many more questions arose. The reason for this additional section lies on those questions that seemed to reveal interesting properties of the studied material or the studied processes. In this description will be kept the same order used in the presentation of the results. It will start with questions concerning the characterization of the layers; then the ones related to the deposition process; the setup used to characterize sensitivity and finally the search for new gas sensing materials. Many questions, in order to be investigated, would require the use of characterization equipment that is not available at the University of Minho. Although these questions will be omitted in this section for brevity, they shall be matter of discussion with other groups that show interest or have the means to follow up their study.

It was observed, for instance, that the produced layers showed significant strains. But are these strains stable in time? What is the effect of the temperature on the strains? If the strains are changed when the sample is submitted to a temperature treatment, there will be effects on the resistance? The study of these questions may start by a detailed analysis of the XRD spectra and the measurement of the radius of curvature of the substrates [122, 145]. These characterization procedures may then be used to obtain some mechanical parameters of the deposited layers and thus evaluate the strain structure and stability. Thermal cycling of the samples may be performed

to study the effect of the temperature and use different substrate materials may help to evaluate the effect of the substrate.

The porosity was estimated by measuring the layer density. This although permitted to find a trend variation of the density with deposition parameters, did not permit to perform precise measurements. It is known that porosity could be evaluated using the refractive index [146]. Can the refractive index provide an accurate method to determine porosity? Is it, at least, more accurate than the mass difference procedure?

In the transmittance spectra was observed a significant variation of the absorption region. How is this related with the bandgap structure of the material? May this analysis help to reveal the defect structure of the oxide layers?

The glass substrates simplified some of the characterization procedures, but were a source of sodium impurities that diffused into the film and were likely to be the main cause for the stresses observed in the films. If the substrates were not transparent it would be impossible to use the transmittance spectra to determine layer thickness. Thus, in the case of non-transparent substrates would be useful to have a fast and non-destructive procedure to measure thickness. Could the diffuse reflectance spectra be used to measure film thickness? How can those measurements be performed?

A dependence of the surface roughness on the film thickness was also observed, but may the dependence be properly quantified? How does film roughness depend on the substrate roughness? Does the roughness variation depend on the substrate temperature during deposition? How does it depend on the other deposition parameters?

In the course of the work, was noted that some parts of the setup or the procedure used to control and determine the deposition parameters could be improved. One was the substrate temperature measurement. A new setup involving the use of a temperature sensor on the surface of the substrate, was formulated. Alternatively, to avoid the use of a sensor on each substrate, there could be a reference substrate, were no film was to be deposited, placed on a thermally symmetric position relative to the real substrate, as described in appendix A. Characterization of the accuracy and precision of a system like this, although very simple, has not been described in the literature known to the author.

The control system installed on the chamber permits to vary the substrate temperature during deposition. If a heater that permitted faster temperature changes was installed inside the deposition chamber, some experiments could be performed with varying temperature during the deposition. In order to be able to reproduce the results, it would also be necessary to have a setup that permitted an accurate control of the temperature, such as the one suggested previously. Thus, this kind of experiments should follow the study of better temperature measuring systems.

Given the flow of gases into and out of the chamber there must be currents, oscillations and pressure gradients inside. This presents some problems both to the stability of the pressure in the deposition region and to the pressure measurement. An accurate study of the gas flow inside the chamber is therefore necessary in order to be able to measure and maintain accurate pressure conditions during deposition, at least over the range that permits to produce good quality layers.

By chance, when the magnetron magnets were changed, it was visible an increase of the crystallite orientation of the produced layers, attributed to the higher magnetic fields. However, given that a similar effect could be produced by the pressure, it was not possible to unequivocally attribute the effect to the magnetic field. The dependence of the crystallite orientation on the magnetic field of the magnetron would also be interesting to investigate.

In the experiments performed with the gas sensor testing chamber was only used carbon monoxide. It would be interesting to use the system to test the gas sensing response to other gases as well. Another interesting experiment would be to put a commercial sensor inside the chamber

## 7. *Conclusions*

and study its performance. This would be very useful to obtain independent measurements of the atmosphere conditions maintained inside the system.

Finally, there is a wide range of experiments that could be performed if other oxides were used or tin oxide was doped with other elements. The system have proved to be able to test sensitivity of tin dioxide to carbon monoxide in air, thus, following the same procedures, any other oxide materials produced in the Thin Film Laboratory at the University of Minho can be tested in the system, either to carbon monoxide or any other available gas.

# Appendix





# A. Temperature control

## A.1. PID Proportional Controllers

Both the temperature control of the substrate during deposition and of the deposited layers during gas sensing tests were performed using two autotuning PID proportional controllers, model Shimaden SR52. Proportional controllers are designed to eliminate the cycling associated with on-off control. A proportional controller decreases the average power being supplied to the heater, as the temperature approaches the set point. This has the effect of slowing down the heater so that it will not overshoot the set point. Instead it will approach the setpoint and maintain a stable temperature. This proportioning action is accomplished in this case by turning on and off the output for short intervals, and thus controlling the average power supplied to the heater.

The time period between two successive turn-ons is known as the *cycle time*. The proportioning action occurs within a *proportional band* around the set point temperature. Outside this band the controller functions as an on-off unit, with the output either fully on (below the band) or fully off (above the band). At the set point (the midpoint of the proportional band), the output on-off ration is 1:1, i.e., the on and off times are equal. If the temperature is further from the set point, but within the proportional band, the on and off times vary in proportion to the temperature difference. If the temperature is below the set point the output will be on longer, and if the temperature is above the set point, the output will be off longer.

A PID controller has in addition an integral function and a derivative function which provide a more accurate and stable temperature control. The integral function is used to adjust for an offset between the steady state temperature and the set point, so that the former agrees with the latter under all operating conditions. The derivative function, on the other hand, compensates for load changes that take place rapidly, reducing overshoot and undershoot under those conditions. Proportional, integral and derivative parameters are adjusted automatically by the controller.

## A.2. Device connections

Temperature is measured using a thermocouple type-K and heat is provided by a resistance connected to a power source that is turned on and off by the temperature controller. Both in the case of the sputtering chamber and the gas testing chamber the thermocouple was fitted to a hole that goes from one side to the geometric centre of the sample holder shown by Figs. A.1(a) and A.1(b). The sample holder is made from a solid metal block to provide high thermal conductivity and enough mass to prevent fast temperature changes. The resistance heater goes through small holes that cross the substrate holder from side to side.

Ideally the temperature should be measured at the layer surface. This could be performed by placing the temperature sensor on the surface. Temperature sensors used in these kind of measurements are usually of the RTD type. These are metallic resistors made of materials that show a high resistivity variation with temperature. The most popular RTD is a platinum sensor which operates over a broad temperature range from about  $-200^{\circ}\text{C}$  to  $600^{\circ}\text{C}$ . A similar device is the thermistor. These may have either positive or negative temperature coefficients and

## A. Temperature control

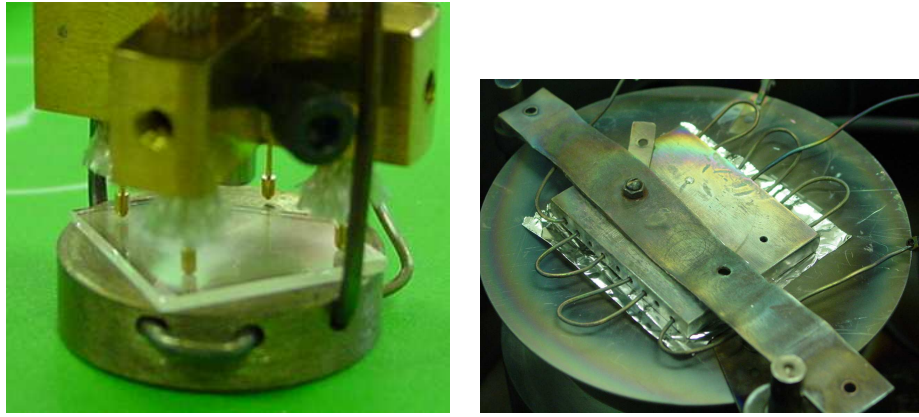


Figure A.1.: Sample holder a) used on the gas sensing chamber and b) on the sputtering chamber

are commonly ceramic semiconductors made of oxides of one of the following metals: nickel, manganese, cobalt, titanium or iron [15].

The latter measuring method would be certainly better than using the setup described before, inasmuch as it would provide the temperature value on the surface of the film. Making temperature measures far from the film implies that there will be an unknown temperature gradient between the temperature sensor and the film surface. If this gradient is kept constant, temperature on the film surface can be considered constant, although unknown. However, neither the effect of temperature variation nor of those parameters that affect the temperature gradient, such as the substrate material, can be accurately evaluated.

In the sputtering chamber, temperature sensors could either be deposited on each substrate or on one of the sample substrates provided that symmetry of the heating geometry was assured. The latter option may provide good temperature data if careful attention is given to heat exchange processes. Moreover, in order for the temperature sensor to be used several times, when the same kind of substrates are used, a protection mask should be placed between the sensor and the target to avoid film growth over the sensor. The mask should be mounted in such a way as to interfere minimally with heat exchanging processes: radiation arriving and leaving the substrate, gas particles impinging on the substrate and thermal conduction through the mask holding structure. Using this procedure, the temperature sensor could only be changed when using different substrates. The effect of the protection mask should nevertheless be determined by comparison with a sensor placed on a film growing substrate to determine measurement accuracy. If possible this temperature measuring procedure should also be compared with non-contact procedures, as thermal infrared detectors.

In the gas sensing chamber a similar procedure could be adopted. When the sensors are produced not for academic studies but for practical applications, the best procedure would be to deposit a temperature sensor on each sensor surface. However, as the main objective of the present work is developing gas sensing materials, it would be again preferable to avoid the procedure necessary to produce the temperature sensor on each substrate. Alternatively, it was possible to use only one sample substrate where the temperature sensor would be located, and positioned side by side with the tested layer. The best characterized temperature sensors are platinum RTDs. However platinum is a well known catalyst for carbon monoxide oxidation and therefore interferes with the gas sensing process [147].

### A.3. Communication interface

Table A.1.: Linux system device files identifying physical serial ports

Filename and path	Port
/dev/ttyS0	1st serial port of PC motherboard (DB-9)
/dev/ttyS1	2nd serial port of PC motherboard (DB-9)
/dev/ttyS2	1st port of serial port card (DB-25)
/dev/ttyS3	2nd port of serial port card (DB-25)
/dev/ttyS4	3rd port of serial port card (DB-25)
/dev/ttyS5	4th port of serial port card (DB-25)
/dev/ttyS6	5th port of serial port card (DB-25)
/dev/ttyS7	6th port of serial port card (DB-25)
/dev/ttyS8	7th port of serial port card (DB-25)
/dev/ttyS9	8th port of serial port card (DB-25)

Temperature controller is remotely set into work through the serial port of a computer, using the RS-232-C interface. The temperature values are acquired using the same procedure. Since the computer has only two serial ports and it was necessary to connect more than two devices to it, the serial port card referred on section 5.4 was installed, adding thus eight more ports to the computer. Both temperature controllers are connected to these additional ports. From the software point of view the serial ports are identified by special device files. The correspondence between the files and physical ports is listed in Table A.1. The device files assigned to ports on serial port expansion are set during the boot process. Special care should be taken when changing the computer configuration since these might change resources assigned to the card.

Table A.2.: Pinout of RS-232-C serial ports on DTEs

9-pin	25-pin	Pin functions
3	2	Transmit Data (TxD)
2	3	Receive Data (RxD)
7	4	Request To Send (RTS)
8	5	Clear To Send (CTS)
6	6	Data Set Ready (DSR)
4	20	Data Terminal Ready (DTR)
1	8	Data Carrier Detect (DCD)
9	22	Ring Indicator (RI)
5	7	Signal ground (GND)

The main difference between the original motherboard ports and the ones provided by the VScom card is the pinout: original ports have 9 pins while the ones provided by the card expansion have 25. If the connections are removed from one port and inserted in another the only change that has to be made in the program is the name of the port. Therefore 25-pin connections may be freely interchanged, provided that the above mentioned modification is performed on the program. The same happens with the two original 9-pin ports of the computer. No matter the number of pins of the physical connection, only 9 pins are actually used in a RS-232-C interface. If a connection is to be changed from a 9-pin port to a 25-pin port, a different cable have to be built, but no other modification besides the one stated above has to be done in the software. Depending on the device and the number of pins of the port, different functions will

## A. Temperature control

be assigned to the pins. In what concerns the devices, there are two main types corresponding to different RS-232-C configurations: Data Terminal Equipment (DTE) and Data Communication Equipment (DCE). All equipment used in these experiments, including the computer, belong to the Data Terminal Equipment type. Table A.2 shows the standard pinout of 9-pin and 25-pin RS-232-C DTEs ports.

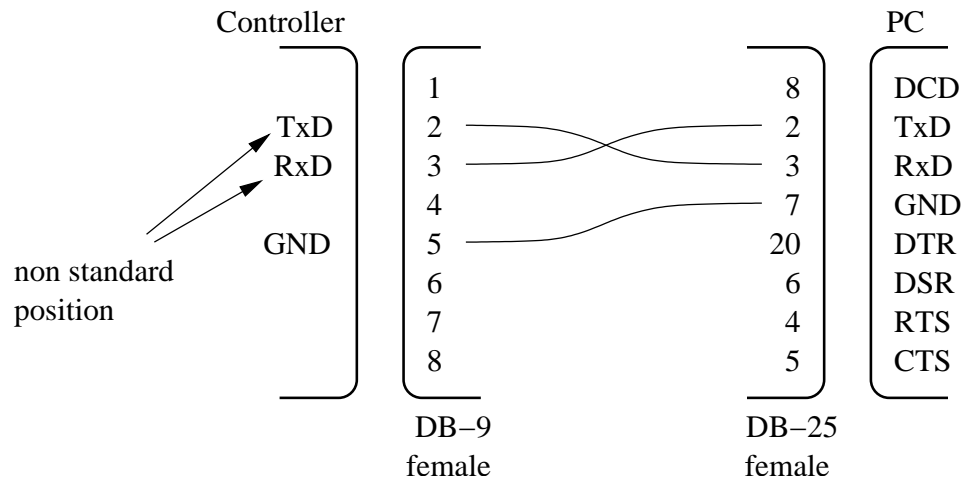


Figure A.2.: Cable wiring between temperature controller port and computer

Of the 9 pin functions only three are sufficient for data transmission and reception: TxD, RxD and signal ground. The others are control signals that may be used to speed up transmission. The temperature controllers use just the main three pins. Pin wiring from the controller port to the computer port is shown in Fig. A.2. Note that pins 2 and 3 are interchanged on the temperature controller and do not correspond to the standard assignment used in DTE as shown in Table A.2<sup>1</sup>. The meaning of the three pins used by the controller are described below.

Table A.3.: Function performed by serial port pins on the temperature controller side

Pin	Function
TxD	transmits data from the controller.
RxD	receives data into the controller.
GND	defines reference voltage.

In spite of the fact that in this case only three pins are used, every function assigned to serial interface pins in the Linux operative system will be briefly described for future reference. Later, if needed, use of each function will be described with more detail. Note however that the corresponding functions performed by the software may be modified by working in the source code of the system, therefore if a different operative system or unusual software is installed in the computer the signal lines may behave differently.

When connecting the serial ports of two devices, GND pins have to be connected always, for the signals to be unequivocally defined. In the case of the computer and the temperature controller, TxD pin in the computer port is connected to RxD pin of the controller, in order to send data from the computer to the device, and RxD pin on the computer is connected to the TxD of the controller, for data to be sent from the controller to the computer. More generally,

<sup>1</sup>This kind of connections is typical of Data Communication Equipment (DCE), such as a modem, and not of DTEs (cf. The Linux Serial Howto [148]). This 9-pin port was not originally built in the controller, but was added in our laboratory. The assignment of the pin functions does not intend to reflect any standard.

Table A.4.: Function performed by serial port pins on a computer running the Linux operative system

Pin	Function
TxD	transmits data from the computer.
RxD	receives data into the computer.
RTS	when set to on, the computer is ready to receive data. Setting to off means the opposite.
CTS	reads the signal state. When on is read, the computer may transmit data and when off it should stop transmission.
DTR	similar to RTS. It <i>is not usually implemented on Linux</i> , therefore should not be used.
DSR	similar to CTS. As DTR, this function <i>is not usually implemented on Linux</i> .
DCD	reads the signal state.
RI	reads the signal state.
GND	defines reference voltage.

these connections are established whenever bidirectional communication is required between serial ports of two DTEs.

Signals transmitted through the TxD–RxD connection wires are series of ones and zeros, while the information required by the user consists of series of digits and letters. Since the computer only understands binary data there must be a correspondence between the digit and letter characters and the binary data. This correspondence is defined by international standards, such as the ASCII character set<sup>2</sup> or the ISO 8859-1 . ASCII is a 7-bits code while ISO 8859-1 is an 8-bit code, which means that each ASCII character corresponds to a binary number with at most 7 digits, while each ISO 8859-1 character corresponds to a number with at most 8 digits. However, the ASCII characters exist in the other character sets and therefore are always represented by the same binary number. As expected, digits and non-accented letters, which belong to the ASCII character set, are represented by the same numbers in every character set.

Table A.5.: Communication data formats permitted by temperature controller

Identifier	Data bits	Parity	Stop bits
7E1	7	even	1
7E2	7	even	2
7n1	7	no	1
7n2	7	no	2
8E1	8	even	1
8E2	8	even	2
8n1	8	no	1
8n2	8	no	2

In order for the information to be correctly transmitted between the controller and the computer, a communication protocol have to be set. This is performed by setting some matching parameters both on the controller and the computer before starting communication.

On the controller side the parameters to be set are: the address, the data format, the communication speed, and the protocol. The address is a number between 0 and 31 used to identify the

<sup>2</sup>Also known as ISO 646

## A. Temperature control

Table A.6.: Communication parameters selected on the temperature controllers for data exchange with the computer

Parameter	Selected value
Address	1
Data format	7E1
Communication speed	9800 bps
Protocol	nomL

device<sup>3</sup>. The communication speed is the inverse of the time taken to transmit each bit and corresponds to the maximum transmission flow rate. The temperature controller admits four different communication speeds: 1200 bps, 2400 bps, 4800 bps or 9600 bps. The protocol might take values `nomL` for the standard protocol of the SR52 controller series or `SrFP` for older devices compatible protocol. As to the data format, it can take eight possible values, that are listed in Table A.5. These values define transmission format of a single character. Although each character is represented by at most a series of 8 bits, whenever a character is transmitted through the serial line more than 8 bits are exchanged between sender and receiver. This is necessary, so that the receiver knows which is the first bit representing the character and which is the last. Thus when a character is transmitted the following sequence of bits are exchanged: first one start bit of value 0, then the data bits representing the character, one optional parity bit and finally one or two stop bits of value 1. Consequently when a 7-bit character is transmitted, a series of 9 to 11 bits are exchanged, depending on the data format. The parity bit is used to check integrity of the data bits exchanged. The parity bit may be set to even, odd or none. With even parity, the parity bit is selected so that the number of bits of value 1 counted among the data bits is even, including the parity bit. If one of the bits gets corrupted, the receiver will detect wrong parity and therefore will mark the received character as an error. Odd parity works in a similar manner. When no parity is selected, the parity bit is not sent. All the referred parameters have to be set on the controller front-panel menu. Parameters used for communication between the temperature controllers and the computer are listed in Table A.6.

---

**Program A.1:** C program used to initialize serial port attached to temperature controller (`openct`)

---

```
#define BAUDRATECT B9600
#define CTDEV "/dev/ttyS3"

int openct(void) {
    int fdct;
    struct termios cttio;

    fdct=open(CTDEV, O_RDWR | O_NOCTTY | O_NONBLOCK);
    if (fdct < 0) {
        perror(CTDEV);
        exit(-1);
    }
    tcgetattr(fdct, &cttio);
    tcflush(fdct, TCIFLUSH);
```

---

<sup>3</sup>It must be set always, because it is part of the communication protocol. When using RS-485 serial connections, this parameter permits to connect up to 32 devices, in series, to a single computer port.

```

cfsetispeed(&cttio, BAUDRATECT);
cfsetospeed(&cttio, BAUDRATECT);

bzero(&cttio, sizeof(cttio));

cttio.c_cflag |= (BAUDRATECT | CS7 | PARENB | CLOCAL | CREAD);
cttio.c_lflag &= ~(ECHO | ICANON);
cttio.c_iflag |= (INPCK | ISTRIP | PARMRK);
cttio.c_oflag &= ~(ONOCR);

tcsetattr(fdct, TCSANOW, &cttio);
sleep(3);

return fdct;
}

```

Data format and communication speed have also to be set on the computer with the same values, otherwise no information can be exchanged between the devices. This operation is performed using the function `openct`. This routine gets no arguments and returns a non-negative integer, called the file descriptor, that uniquely identifies the port attached to the temperature controller. This file descriptor will be used in subsequent `write` and `read` operations to the port.

The function `openct` declares only two variables: the file descriptor `fdct` and the `cttio` structure of type `termios`. Before setting any port parameter it is necessary to get the file descriptor. This is performed using function `open`, which has two arguments. The first should be the path name of the device file used (see Table A.1). The device file corresponding to the serial port connected to the temperature controller is defined by the symbolic constant `CTDEV` outside the function `openct` using a `#define` line

```
#define CTDEV "/dev/ttyS4"
```

In the example given above any occurrence of the symbolic constant `CTDEV` will be replaced by the path name `/dev/ttyS4`, that corresponds to the 3rd port of serial port card (cf. Table A.1).

The second argument of the `open` function sets some flags that will notify the operative system how to handle the communication with the serial port; `O_RDWR`, for instance, requests opening of the file for read and write operations<sup>4</sup>. When the `open` function fails, instead of the file descriptor, it will return `-1` and set the variable `errno` to indicate what went wrong. Therefore, in this case routine  `perror` is called to send a message to the screen telling that something went wrong when opening the device corresponding to `CTDEV`. If port opening succeeds, the `cttio` structure is zeroed and port parameter definition proceeds.

The `termios` structure contains five members that define input parameters, `c_cflag`; output parameters, `c_oflag`; communication parameters, `c_cflag`; local modes that make use of special characters, `c_lflag` and the array of control characters, `c_cc`. The command line

```
cttio.c_cflag |= (B9600 | CS7 | PARENB | CLOCAL | CREAD);
```

assigns to the `c_cflag` member of the `cttio` structure some values that will set the communication speed to 9600 bps (`B9600`), the character size to 7 bits (`CS7`), enables the parity bit (`PARENB`), disables the serial port control lines (`CLOCAL`) and enables data receiver (`CREAD`).

<sup>4</sup>The other possible modes are `O_RDONLY` for read-only operations and `O_WRONLY` for write-only operations.

## A. Temperature control

Table A.7.: Correspondence between communication data formats and flags set by the `termios` structure

Flag	Formats
CS5	5 data bits.
CS6	6 data bits.
CS7	7 data bits.
CS8	8 data bits.
CSTOPB	2 stop bits.
PARENB	enable parity bit.
PARODD	odd parity.
CLOCAL	ignore signals RI and DCD.
CRTSCTS	enable RTS/CTS flow control.

After `cttio` structure is updated with the new values the function `tcsetattr` is invoked to set the parameters associated with the serial port to the ones referred by the structure.

Before any use the functions that control serial port parameters the headers `<termios.h>` and `<unistd.h>` have to be declared using an `#include` statement

```
#include <termios.h>
#include <unistd.h>
```

This declaration is made outside the `openct` routine as shown in program E.3

## A.4. Communication protocol

Table A.8.: Format of data blocks used for communication with the temperature controller

Block unit	Description
@	start character.
00	2-digit device address number.
command	characters that may be used in commands are listed in Table A.9.
:	end character.
00	2-digit BCC check.
\r	ASCII character return.

In the standard protocol, corresponding to value `nomL` indicated in Table A.6, transmission of information to and from the temperature controller is made using data blocks consisting of six different units. Note that the numbers are not transmitted in binary form, but using ASCII digit characters. Every block starts with the code @ followed by the machine number address, which is a 2-digit number. The machine number address have to match the value shown in Table A.6. The following characters make the command transmitted or received by the controller. Table A.9 lists the characters that may be used in commands. A list of available commands and respective formats may be found in the Instruction Manual [149]. After the command, must follow: the end character, ':' ; a 2-digit number, called BCC, that is used to check integrity of the data; and finally a character return, '\r', that ends the data block.

The BCC code is a 2-digit number in hexadecimal format calculated by performing an exclusive OR operation,  $f(a, b) = a \oplus b$ , on the binary character codes following the start character, '@', up to and including the end character, ':', of the transmission block. Thus when the data block '@01D1:4E\r' is transmitted, the BCC value is



$$\begin{aligned}
\text{BCC} &= 0 \oplus 1 \oplus \text{D} \oplus 1 \oplus : \oplus \\
&= (30)_h \oplus (31)_h \oplus (44)_h \oplus (31)_h \oplus (3a)_h \\
&= (0110000)_b \oplus (0110001)_b \oplus (1000100)_b \oplus (0110001)_b \oplus (0111010)_b \\
&= (1001110)_b = (4e)_h
\end{aligned}$$

where the numbers inside  $()_b$  are binary numbers and numbers inside  $()_h$  are hexadecimal numbers. The BCC code is checked by the temperature controller before executing any received command, thus when the BCC received is different from the one computed by the controller an error is generated. In the computer the BCC is computed using routine A.2 (`calcbcc`).

---

**Program A.2:** C program used to compute the BCC check code (`calcbcc`)

---

```

int calcbcc(unsigned char msg[], int msgnum) {
    int tmpbcc=msg[1], posn, bcch, bccl;

    for (posn=2; posn<msgnum; ++posn)
        tmpbcc ^= msg[posn];

    bcch=((posn=(tmpbcc/16))<10) ? posn+'0' : posn+'A'-10;
    bccl=((posn=(tmpbcc-posn*16))<10) ? posn+'0' : posn+'A'-10;

    if (msg[msgnum]=='\0') {
        msg[msgnum]=bcch;
        msg[msgnum+1]=bccl;
        msg[msgnum+2]='\r';
        msg[msgnum+3]='\0';
        return 0;
    }
    else
        return 1;
}

```

---

Routine `calcbcc` has two arguments: the first, `msg` is a string and the second, `msgnum`, is the length of the string received. It returns 0 if the BCC code was computed and 1 otherwise. The string received by the function is the transmission block including the start code '@' and the end command code ':'. The function computes the BCC and appends to the string `msg` the BCC value and the character return, so that when the function finishes the string `msg` is ready to be sent to the controller. The BCC value is not verified in messages received by the computer.

Commands are composed by the command name, which is a two character code, followed by a list of data. There are three different kind of data: numerical data, character data and one letter data. Numerical data have a fixed length of six characters, including the plus (+) or minus (-) sign, that should always precede the digits<sup>5</sup>, and the decimal point, if present. The character data have a fixed length of four characters. If there is a space in the character data it should be replaced by an underscore (\_). Read commands sent to the controller should not be followed by any data. Thus if a command sent to the controller starts with the command name followed by

---

<sup>5</sup>Instead of the numerical codes, + and -, other characters may be used in some special cases. For description of these cases see device Instruction Manual [149]

## A. Temperature control

Table A.9.: Characters used in remote temperature controller commands

Character	Range and meaning of code
{A-Z}	capital letters.
{0-9}	digits.
+	code of numerical data.
-	code of numerical data.
.	decimal point of numerical data.
␣ (space)	code to mark off command from data.
,	code to mark off each data.
;	data omission code (in write commands).
_ (underscore)	used in character data.
?	used for indeterminate data.

a space, the command is taken as a write command. When a write command is received by the controller, it is processed and then either an acknowledgement or an error message is returned.

## A.5. Routines

Several routines were written to setup and acquire data from the temperature controller. Each routine performs a different operation on the controller and care was taken in order to make possible use of the functions in different programs. Up to now five different routines were written: `commode`, `rammode`, `tempcic`, `changesv` and `erroct`.

Routine `commode` sets the temperature controller into communication mode. This is needed in order to be able to change the controller state using write commands. This functions has just one argument, `fdct`, which is the file descriptor. It returns 0 if the function succeeds or the output of routine `erroct` if there was an error.

---

**Program A.3:** C program used to set the temperature controller into communication mode  
(`commode`)

---

```
int commode(int fdct) {
    int erro=0;
    unsigned char *outmsg, inmsg[15];

    outmsg="@01C1:49\r";

    while (erro<=0) {
        write(fdct, outmsg, 9);
        sleep(1);
        erro=read(fdct, &inmsg, 14);
    }

    if (erroct(inmsg)==1)
        return 1;
    else if (inmsg[7]!='C') {

        outmsg="@01C1 _COM:77\r";

        erro=0;
        while (erro<=0) {
            write(fdct, outmsg, 14);
            sleep(1);
            erro=read(fdct, &inmsg, 14);
        }
        return erroct(inmsg);
    }
    else
        return 0;
}
```

---

Routine `rammode` puts the controller in RAM mode, which means that every write operation will be written in the volatile memory of the device instead of using the EEPROM. This procedure prolongs the lifetime of the EEPROM memory, inasmuch as the writing cycles into this memory are finite. Similarly to routine `commode`, this receives solely the file descriptor `fdct` as an argument, and returns 0 in case of success and the output of routine `erroct` if there was an error.

---

**Program A.4:** C program used to set the temperature controller into RAM mode (`rammode`)

---

```

int rammode(int fdct) {
    int erro=0;
    unsigned char *outmsg, inmsg[15];

    outmsg="@01C2:4A\r";

    while (erro<=0) {
        write(fdct, outmsg, 9);
        sleep(1);
        erro=read(fdct, &inmsg, 14);
    }

    if (erroct(inmsg)==1)
        return 1;
    else if (inmsg[8]!='A') {

        outmsg="@01C2 _RAM:6B\r";

        erro=0;
        while (erro<=0) {
            write(fdct, outmsg, 14);
            sleep(1);
            erro=read(fdct, &inmsg, 14);
        }
        return erroct(inmsg);
    }
    else
        return 0;
}

```

---

Routine `tempcic` changes the cycle time of proportional operation to 3 s. This procedure is used to reduce oscillations near the set point temperature. This parameter can take values between 1 s and 120 s. The routine takes the file descriptor `fdct` as an argument and returns 0 in case of success and 1 in case of error.

---

**Program A.5:** C program used to set the temperature controller into RAM mode (`tempcic`)

---

```

int tempcic(int fdct) {
    int erro=0;
    unsigned char *outmsg, inmsg[29];

    outmsg="@0103 ,+00003;:68\r";

    while (erro<=0) {
        write(fdct, outmsg, 18);
        sleep(1);
        erro=read(fdct, &inmsg, 28);
    }
}

```

```

}

if (errnoct(inmsg)==1)
    return 1;
else
    return 0;
}

```

---

Routine `changesv` is used to change the temperature set point. It receives the file descriptor `fdct` and the temperature value `sv`, and returns 0 in case of success and 1 in case of error. The temperature value is given in degree Celsius. Note that the number sent to the controller has one decimal place. Below is quoted the line where the message block, used to set the temperature, is defined. The temperature value is stored in variable `sv` and its format is defined by the string `%+06.1f`.

```
    sprintf(outmsg, "@01D2 %+06.1f;:", sv);
```

The format depends on the type of input and measuring range selected. In this case, the controller was set to thermocouple input and measuring range from 0.0° C to 800.0° C (code `6_k2`). This setting should not be altered unless the measuring sensor is changed.

---

**Program A.6:** C program used to change the set point temperature (`changesv`)

---

```

int changesv(int fdct, float sv) {
    unsigned char outmsg[20], inmsg[30];
    int msgnum;
    float aux=10;

    sprintf(outmsg, "@01D2 %+06.1f;:", sv);
    msgnum=strlen(outmsg);
    calcbcc(outmsg, msgnum);

    write(fdct, outmsg, 17);
    sleep(1);

    while (read(fdct, &inmsg, 29)==0)
        ;
    if (inmsg[3]=='E' && inmsg[4]=='R')
        inmsg[11]='\0';
    else {
        inmsg[29]='\0';
        sscanf(inmsg, "%s%6f", outmsg, &aux);
        aux=abs((int) (aux-sv));
    }

    if (errnoct(inmsg)==0 && aux<1)
        return 0;
    else
        return 1;
}

```

Routine `erroct` is used to check the error messages sent by the controller and convert them to user readable messages that are sent to the screen. The function receives the message sent by the controller and verifies if it is an error message. Error messages sent from the controller, are identified by the character sequence ER followed by an underscore and a 2-digit number. This routine returns 1 if the message received is an error message and 0 otherwise.

---

**Program A.7:** C program used to detect error messages from the temperature controller  
(`erroct`)

---

```
int erroct(unsigned char msg[]) {
    unsigned int erro=((msg[6]-'0')*10+msg[7]-'0');

    if (msg[3]=='E' && msg[4]=='R') {
        switch (erro) {
            case 1:
                printf("Hardware error (pg. 39 do Instr. Manual)\n");
                break;
            case 6:
                printf("Command error (pg. 39 do Instr. Manual)\n");
                break;
            case 7:
                printf("Text format error (pg. 39 do Instr. Manual)\n");
                break;
            case 8:
                printf("Data format error (pg. 39 do Instr. Manual)\n");
                break;
            case 9:
                printf("Data error (pg. 39 do Instr. Manual)\n");
                break;
            case 11:
                printf("Write mode error (pg. 39 do Instr. Manual)\n");
                break;
            case 12:
                printf("Specifications option error (pg. 39 do Instr.\n
Manual)\n");
                break;
            default:
                printf("Outro erro\n");
                break;
        }
        return 1;
    }
    else
        return 0;
}
```

---

## A.6. User interface

Program `s_aquece.c` was written, using the functions described in Section A.5, to set temperature before film deposition. This program reads the temperature from file `fich-filme` stored in directory `$HOME/tmp`. The input file should have the substrate temperature set point in degree Celsius on the first line of file `fich-filme`. This value is read by program `s_aquece.c` and stored in variable `temperatura` in line

```
fscanf(fpi, "%f\n", &temperatura);
```

After setting the temperature the program exits, but leaves the controller in communication mode, which prevents manual change of set point on the device.

---

**Program A.8:** C program used to set the substrate temperature before film deposition (`s_aquece.c`)

---

```
#include <sys/types.h>
#include <sys/stat.h>
#include <fcntl.h>
#include <termios.h>
#include <unistd.h>
#include <stdio.h>
#include <errno.h>
#include <string.h>
#include <stdlib.h>

#define BAUDRATE B9600
#define CTDEV "/dev/ttyS3"

int calcbcc(unsigned char msg[], int msgnum);
int openct();
int commode(int fdio);
int rammode(int fdio);
int tempcic(int fdio);
int changesv(int fdio, float svtemp);
int erroct(unsigned char msg[]);

main ()
{
    FILE *fpi;
    int fdct;
    float stemp, temperatura;
    char *fichtmp;

    fichtmp=getenv("HOME");
    strcat(fichtmp, "/tmp/fich-filme");
    fpi=fopen(fichtmp, "r");
    fscanf(fpi, "%f\n", &temperatura);
    fclose(fpi);

    fdct=openct();
```

## A. Temperature control

```
    if (commode(fdct)==1) {
        printf("Nao foi ativado o Communication Mode!\n");
        exit(1);
    }
    if (rammode(fdct)==1) {
        printf("Nao foi ativado o RAM Mode!\n");
        exit(1);
    }
    if (tempcic(fdct)==1) {
        printf("Nao foi alterado o PCS!\n");
        exit(1);
    }
    stemp=temperatura;
    if (changesv(fdct, stemp)==1) {
        printf("Nao foi alterado o SV!\n");
        exit(1);
    }

    close(fdct);

return 0;
}

int calcbcc(unsigned char msg[], int msgnum) {
... see program A.2 on page 99 ...}

int commode(int fdct) {
... see program A.3 on page 101 ...}

int rammode(int fdct) {
... see program A.4 on page 102 ...}

int tempcic(int fdct) {
... see program A.5 on page 102 ...}

int erroct(unsigned char msg[]) {
... see program A.7 on page 104 ...}

int openct(void) {
... see program A.1 on page 96 ...}

int changesv(int fdct, float sv) {
... see program A.6 on page 103 ...}
```

---

The Bash script A.9 was written in order to ease the task of producing the input file of program `s_aquece.c`. To use this script, a user just has to run the command `sputtering-heat` in the Bash command prompt and then insert the temperature value when asked by the program. The script does some format check to the entered value to prevent errors. Namely the temperature must be set between 10° C and 400° C. Higher temperatures could damage the





## A. Temperature control

```
mkdir -p "$HOME/tmp"  
echo "$temperatura" > $HOME/tmp/fich-filme  
nohup s_aquece.exe &  
exit 0
```

---

To cool the substrate it is possible to do it directly on the controller or use script A.10. To change the temperature set point using the controller front panel it is necessary to set previously the operation mode to local. The script `sputtering-cool` starts by verifying if program `s_aquece.exe` is still running and then runs program `s_arrefece.exe`, which is the compiled version of program A.11. However, if program `s_aquece.exe` is still running it stops this program before running `s_arrefece.exe`.

---

**Program A.10:** Bash script used to stop substrate heating (`sputtering-cool`)

---

```
#!/bin/bash  
# Bash version 2.04.11 or higher  
programa=`ps -u $USER | grep -e 's_aquece.exe' | grep -v -e 'grep'`  
numero=`expr "$programa" : '[^0-9]*\([0-9]*\)``  
if expr "$numero" \> 1 > /dev/null  
then  
    kill "$numero"  
    sleep 9  
fi  
nohup s_arrefece.exe &  
exit 0
```

---

Program `s_arrefece.c` uses a new routine called `locmode`. The structure of this routine is very similar to routine `commode` on page 101. To write routine `locmode`, the following lines of `commode`:

```
else if (inmsg[7]!='C') {  
    ...  
    outmsg="@01C1 _COM:77\r";  
    ...}
```

were replaced by:

```
else if (inmsg[7]!='M') {  
    ...  
    outmsg="@01C1 _LOC:76\r"; ...}
```

Routine `locmode` is used to change the controller operation mode to local.

---

**Program A.11:** C program used to stop substrate temperature heating (`s_arrefece.c`)

---

```
#include <sys/types.h>  
#include <sys/stat.h>  
#include <fcntl.h>  
#include <termios.h>  
#include <unistd.h>  
#include <stdio.h>  
#include <errno.h>
```

```

#include <string.h>
#include <stdlib.h>

#define BAUDRATE B9600
#define CTDEV "/dev/ttyS3"

int calcbcc(unsigned char msg[], int msgnum);
int openct();
int locmode(int fdio);
int rammode(int fdio);
int changesv(int fdio, float temperatura);
int erroct(unsigned char msg[]);

main ()
{
    int fdct;
    float stemp=10;

    fdct=openct();

    if (rammode(fdct)==1)
        printf("Nao foi ativado o RAM Mode!\n");
    if (changesv(fdct, stemp)==1)
        printf("A resistencia ficou ligada!!!\n");
    if (locmode(fdct)==1)
        printf("O controlador ficou em modo remoto!\n");

    close(fdct);

return 0;
}

int calcbcc(unsigned char msg[], int msgnum) {
... see program A.2 on page 99 ...}

int locmode(int fdct) {
    int erro=0;
    unsigned char *outmsg, inmsg[15];

    outmsg="@01C1:49\r";

    while (erro<=0) {
        write(fdct, outmsg, 9);
        sleep(1);
        erro=read(fdct, &inmsg, 14);
    }

    if (erroct(inmsg)==1)
        return 1;
    else if (inmsg[7]!='M') {

```

## A. Temperature control

```
    outmsg="@01C1 _LOC:76\r";

    erro=0;
    while (erro<=0) {
        write(fdct, outmsg, 14);
        sleep(1);
        erro=read(fdct, &inmsg, 14);
    }
    return erroct(inmsg);
}
else
    return 0;
}

int rammode(int fdct) {
... see program A.4 on page 102 ...}

int erroct(unsigned char msg[]) {
... see program A.7 on page 104 ...}

int openct(void) {
... see program A.1 on page 96 ...}

int changesv(int fdct, float sv) {
... see program A.6 on page 103 ...}

```

---

## B. Power source control

Remote power source control was conceived in order to permit continuous monitoring of the current and voltage applied to the magnetron and also change of deposition parameters (during deposition), at preset time instants. This work is inserted in a larger project intended to automate control and data acquisition of all the deposition parameters. In order to complete this objective it is still needed an interface to communicate with the pressure controller and the mass flow meters' controller. The power supply, nevertheless, is already equipped with a remote RS-232-C interface that permits to set and read almost all the device functions. In the following sections will be described the communication interface with the power supply and a program that is used to control both the DC power supply and the substrate temperature during film deposition.

### B.1. Communication interface

The RS-232-C port of the DC power supply is connected to the third port of the serial port card (see Table A.1). Cable wiring between the computer and the power supply is shown in Fig. B.1. As in the case of the temperature controller, only the three main pins of the serial port are used: Tx/D, Rx/D and GND. On the power source side the communication parameters are fixed to 9600 bps communication speed and data format to one start bit, eight data bits and one stop bit. On the computer side these parameters are set by routine B.1.

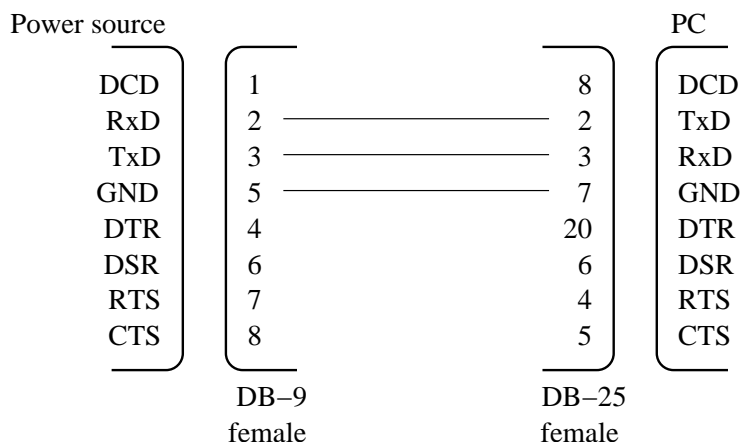


Figure B.1.: Cable wiring between DC power supply serial port and computer

Routine `opendc` has no arguments and returns the file descriptor corresponding to the serial port attached to the power source. See Table A.7 for a description of the meaning of the flags set by the `termios` functions.

---

**Program B.1:** C program used to initialise serial port attached to DC power source (`opendc`)

---

```
#define BAUDRATEDC B9600
```

## B. Power source control

```
#define DCDEV "/dev/ttyS4"

int opendc(void) {
    int fddc;
    struct termios dctio;

    fddc=open(DCDEV, O_RDWR | O_NOCTTY | O_NONBLOCK);
    if (fddc < 0) {
        perror(DCDEV);
        exit(-1);
    }
    tcgetattr(fddc, &dctio);
    tcflush(fddc, TCIFLUSH);

    bzero(&dctio, sizeof(dctio));

    dctio.c_cflag |= (BAUDRATEDC | CS8 | CLOCAL | CREAD);

    tcsetattr(fddc, TCSANOW, &dctio);
    sleep(3);

    return fddc;
}
```

---

## B.2. Communication protocol

Table B.1.: Format of data blocks used for communication with the DC power source

Block character	Description
1st char.	address code.
2st char.	function code.
3st char.	numerical data high byte.
4st char.	numerical data low byte.
5st char.	check sum value.

Transmission blocks into and out of the DC power supply are composed always of five characters. Since the transmitted characters are not restricted to letters and numbers, but may be any 8-bit character, they will be mentioned throughout this section by their hexadecimal codes, independently of the actual character they represent in a particular character set. Note that in C language a hexadecimal number is prefixed by 0x.

The first character is the address code which in this case is set to 0. The second is the function code. To the binary form of the function code may be added a wait bit which is used to mark a read function. A list of some function codes is presented in Table B.2. The third and fourth characters are used to transmit data values and the fifth character is a check sum value.

When a read function is sent to the power supply a wait bit must be added to the second character. Since the function values are all lower than 0x80 the highest bit of the character would be always 0 if the wait bit was not added to the function value. Thus, when a read

Table B.2.: Character code values of some of the functions performed by the DC power source

Value	Function
0x41	read or write power set point in watt.
0x42	read or write voltage set point in volt.
0x43	read or write current set point in centiampere.
0x4E	read or write control mode.
0x4F	read or write power status.
0x51	read actual power value.
0x52	read actual voltage value.
0x53	read actual current value.

function is sent to the controller, the function value is added to number 0x80, which sets the highest bit of the character to 1. Actually, the addition is performed in the program using a bitwise inclusive OR operation between the function value and 0x80, but it could also be performed using integer addition. The following line illustrates the procedure used to add the wait bit to the function code, which in this case is the one corresponding to the control mode, 4e.

```
outmsg[1]=0x4e | WBIT;
```

The numerical data values are transmitted as 16-bit numbers. The third character carries the eight higher bits of the number and the fourth character carries the eight lower bits. Thus, to transmit to the power source the value 2445, which in binary form is represented by 0000 1001 1000 1101, the third character would be  $((int) 2445/256)=0x09$  and the fourth would be  $2445\%256=0x8D$ , where  $((int) x)$  is the integer part of number  $x$  and  $x\%y$  is the remainder of the integer division of  $x$  by  $y$ .

The check sum is used to check integrity of the transmitted block. It is calculated by performing an exclusive OR operation,  $f(a, b) = a \oplus b$ , on the binary character codes of the first four characters. Whenever a message block is received by the power source it verifies the check sum. If the received check sum does not correspond to the calculated check sum, the device responds with a message block, whose second character has value 0x15. This value is used to denote an error. In the computer the check sum is computed using routine B.2 (exorop).

---

**Program B.2:** C program used to compute the check sum in the power source message block (exorop)

---

```
int exorop(unsigned char msg[]) {
    int posn;

    msg[4]=msg[0];
    for (posn=1; posn<4; ++posn)
        msg[4] ^= msg[posn];

    return 0;
}
```

---

Routine `exorop` has one argument, `msg`, and returns always the value 0. The argument `msg` is then used to pass the message block to the function, that computes and appends the check sum to the received variable. When the function ends the message is ready to be sent.

### B.3. Routines

Several routines were written to setup and acquire data from the DC power supply. Each routine performs a different operation on the controller and care was taken in order to make possible use of the functions in different programs. Up to now seven different routines were written: `opmode`, `rsmode`, `onoffonte`, `changesp`, `lesp`, `leval` and `errodc`.

Routine `opmode` sets the power source into one of the four possible operation modes: local, realtime, remote or RS232. Each mode is identified by a numerical value: 2 corresponds to realtime and 4 to RS232. When the unit is in the RS232 mode, the only function that may be changed on the front panel is the operation mode. However, the operation mode can only be changed when the unit is in state "OFF". Thus, in the RS232 mode, the power source can only be switched to state "OFF" using the serial port or the power off button. RS232 mode have to be used because the unit have to be in this mode to respond to some of the functions sent through the serial port.

---

**Program B.3:** C program used to enquire or set operation mode of the DC magnetron power source (`opmode`)

---

```
#define DCUNIT 0
#define WBIT 0x80
#define REALTIME 2
#define RS232 4

int opmode(int fddc, unsigned int controlo) {
    unsigned char outmsg[5], inmsg[5];

    outmsg[0]=DCUNIT;

    if (controlo==RS232) {
        outmsg[1]=0x4e | WBIT;
        outmsg[2]=0;
        outmsg[3]=0;
        exorop(outmsg);
        write(fddc,outmsg,5);
        sleep(1);

        while(read(fddc,&inmsg,5)==0)
            ;

        if (inmsg[3]<RS232) {
            printf("Colocar a fonte em modo RS232!!!\n\
Power source must be in RS232 mode\n");
            return -1;}
        return errodc(inmsg);
    }
    else if (controlo==REALTIME) {
        outmsg[1]=0x4e;
        outmsg[2]=0;
        outmsg[3]=controlo;
        exorop(outmsg);
```



```

write(fddc,outmsg,5);
sleep(1);

while(read(fddc,&inmsg,5)==0)
    ;

return errodc(inmsg);
}
else {
printf("O controlo tem de ser Realtime[2]\
ou RS232[4]\n");
return -1;
}
}

```

---

Routine `rsmode` is used to set the power source into RS232 mode. It is very similar to `opmode`.

---

**Program B.4:** C program used to set DC power source to RS232 operation mode (`rsmode`)

---

```

#define DCUNIT 0
#define WBIT 0x80
#define RS232 4

int rsmode(int fddc, unsigned int controlo) {
    unsigned char outmsg[5], inmsg[5];

    outmsg[0]=DCUNIT;

    if (controlo==RS232) {
        outmsg[1]=0x4e | WBIT;
        outmsg[2]=0;
        outmsg[3]=0;
        exorop(outmsg);
        write(fddc,outmsg,5);
        usleep(100000);

        while(read(fddc,&inmsg,5)==0)
            ;

        if (inmsg[3]<RS232)
            return -1;
        return errodc(inmsg);
    }
    else
        return -1;
}

```

---

## B. Power source control

Routine `onoffonte` is used to switch the source to the “ON” or “OFF” state. The “ON” state corresponds to the situation when the power unit is applying an electric field to the magnetron. The “ON” state is identified by number 2 and “OFF” by 0.

---

**Program B.5:** C program used to switch the DC power source to “ON” or “OFF” state (`onoffonte`)

---

```
int onoffonte(int fddc, unsigned int controlo) {
    unsigned char outmsg[5], inmsg[5];

    outmsg[0]=DCUNIT;
    outmsg[1]=0x4f;
    outmsg[2]=0;
    outmsg[3]=controlo;

    if (outmsg[3]==0 || outmsg[3]==2) {
        exorop(outmsg);
        write(fddc, outmsg, 5);
        usleep(300000);

        while(read(fddc, &inmsg, 5)==0)
            ;

        return errodc(inmsg);
    }
    else {
        printf("Para desligar usar '0' e para ligar '2'\n");
        return -1;
    }
}
```

---

Routine `changesp` is used to read and change the set point values of the power, voltage and current of the unit. It may only operate on one value at a time.

---

**Program B.6:** C program used to enquire and change the set point values of the power, voltage and current of the DC power source (`changesp`)

---

```
int changesp(int fddc, float valor, unsigned int unidade) {
    unsigned char outmsg[5], inmsg[5];
    int valorig;

    outmsg[0]=DCUNIT;
    outmsg[1]=(0x40+(unsigned int) unidade) | WBIT;
    outmsg[2]=0;
    outmsg[3]=0;
    exorop(outmsg);

    write(fddc, outmsg, 5);
    usleep(300000);

    while (read(fddc, &inmsg, 5)==0)
```

```

;

if (errodc(inmsg) < 0)
    return -1;
else
    valorig=inmsg[2]*256+inmsg[3];

outmsg[0]=DCUNIT;
outmsg[1]=0x40+((unsigned int) unidade);
outmsg[2]=((unsigned int) valor)/256;
outmsg[3]=((unsigned int) valor)%256;
exorop(outmsg);

write(fddc, outmsg, 5);
usleep(300000);

while (read(fddc, &inmsg, 5)==0)
    ;
if (errodc(inmsg) < 0)
    return -1;
else
    return valorig;
}

```

---

Routine `lesp` is use to read the set point values of the power, voltage and current.

---

**Program B.7:** C program used to read the set point values of the power, voltage and current applied by the source (`lesp`)

---

```

int lesp(int fddc, unsigned int unidade) {
    unsigned char outmsg[5], inmsg[5];

    outmsg[0]=DCUNIT;
    outmsg[1]=(0x40+(unsigned int) unidade) | WBIT;
    outmsg[2]=0;
    outmsg[3]=0;
    exorop(outmsg);

    write(fddc, outmsg, 5);
    usleep(100000);

    while (read(fddc, &inmsg, 5)==0)
        ;

    if (errodc(inmsg) < 0)
        return -1;
    else
        return inmsg[2]*256+inmsg[3];
}

```

---

## B. Power source control

Routine `leval` is used to read the actual values of the power, voltage and current of the unit.

---

**Program B.8:** C program used to read the actual values of the power, voltage and current of the DC power source (`leval`)

---

```
float leval(int fddc, unsigned int unidade) {
    unsigned char outmsg[5], inmsg[5];

    outmsg[0]=DCUNIT;
    outmsg[1]=(0x50+(unsigned int) unidade) | WBIT;
    outmsg[2]=0;
    outmsg[3]=0;
    exorop(outmsg);

    write(fddc, outmsg, 5);
    usleep(100000);

    while (read(fddc, &inmsg, 5)==0)
        ;
    if (errodc(inmsg) < 0)
        return -1;
    else
        return inmsg[2]*256+inmsg[3];
}
```

---

Routine `errodc` is used to check if the reply from the power supply unit contains the error code.

---

**Program B.9:** C program used to check if the reply from the power supply unit contains the error code (`errodc`)

---

```
int errodc(unsigned char msg[]) {
    if (msg[1]==0x15) {
        printf("Erro de transmissão\n");
        return -1;}
    else
        return 0;
}
```

---

## B.4. User interface and data acquisition

Using the functions described in Section B.3 program `fonte.c` was written to control and register power supplied by the DC unit and the substrate temperature. This program was designed to permit variation of the substrate temperature during deposition, if needed. The program includes two functions not yet described: `instante` and `celsius`.

Function `instante` is used to get the current time. The time is made available to the main program through the argument variable `inst` which is a string. Given the stability of the computer internal clock, the time measuring accuracy should keep constant even during very

long tests. Since function `instante` is run some time before the measurement is triggered, a deviation is expected between the value saved in the variable `inst` and the measuring instant. However, this deviation should be much smaller than the time measuring precision, which was set to one second.

---

**Program B.10:** C program used to get the current time (`instante`)

---

```
void instante(char inst[]) {
    time_t tp;
    struct tm agora;
    if ((tp=time(NULL))!=-1)
        printf("time: nao foi possivel saber a data!\n");
    else
        agora=*localtime(&tp);

    strftime(inst, THORA, "%H:%M:%S", &agora);
}
```

---

Function `celsius` receives the message block sent by the temperature controller, `inmsg`, and returns the temperature measured by the thermocouple.

---

**Program B.11:** C program used to take the temperature value from the message block sent by the controller (`celsius`)

---

```
float celsius(unsigned char inmsg[]) {
    float pv, sv;
    unsigned char header[6];

    sscanf(inmsg, "%s%f%f", header, &pv, &sv);
    return pv;
}
```

---

Program `fonte.c` reads parameters from file `fich-produc` stored in directory `$HOME/tmp`. A sample input file is shown in Fig. B.2. The values read from the input file are stored in variables listed in Table B.3. Variable `fich` holds the complete path name of the output data file; `notas` is a string that holds a sequence of at most 80 characters ending with a #, used to store notes; `segu` is the time interval in seconds between two consecutive read commands; `valorsp` is an array with three elements used to store the set point values of power, voltage and current;

Table B.3.: Some variables used in program `fonte.c`

Variable	Description
<code>fich</code>	output file path name.
<code>notas</code>	notes with a maximum of 80 characters and ending with #.
<code>segu</code>	sampling time interval in seconds.
<code>valorsp[0]</code>	power set point in watt.
<code>valorsp[1]</code>	voltage set point in volt.
<code>valorsp[2]</code>	current set point in centiampere.
<code>sputt</code>	power "ON" time in minutes.

## B. Power source control

and `sputt` is the time during which the DC power source is in the “ON” state. This time can be either the pre-sputtering time, if the shutter is closed, or the deposition time, when the shutter is open.

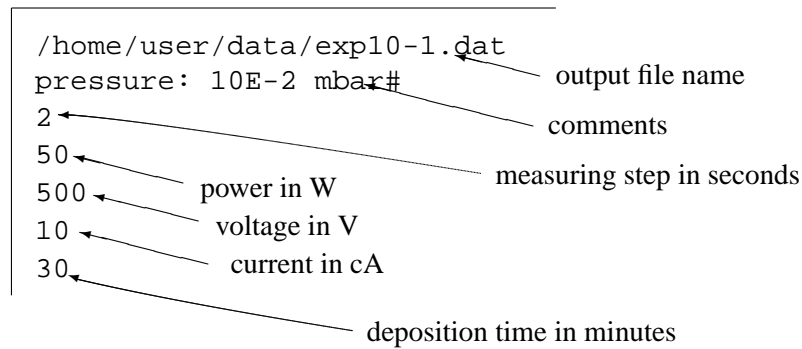


Figure B.2.: Example of input file `fich-produc` of program `fonte.c`

---

**Program B.12:** C program used to control DC power source and substrate temperature during film deposition (`fonte.c`)

---

```
#include <sys/types.h>
#include <sys/stat.h>
#include <fcntl.h>
#include <termios.h>
#include <unistd.h>
#include <stdio.h>
#include <errno.h>
#include <string.h>
#include <stdlib.h>
#include <time.h>

#define BAUDRATEDC B9600
#define BAUDRATECT B9600
#define DCDEV "/dev/ttyS4"
#define CTDEV "/dev/ttyS3"
#define DCUNIT 0
#define WBIT 0x80
#define POWER 1
#define VOLTAGE 2
#define CURRENT 3
#define ON 2
#define OFF 0
#define REALTIME 2
#define RS232 4
#define TDATA 80
#define THORA 9

char inst[THORA];

void instante(char inst[]);
```

```

int exorop(unsigned char dcmsg[]);
int opendc();
int opmode(int fdio, unsigned int controlo);
int onoffonte(int fdio, unsigned int controlo);
int changesp(int fdio, float valor, unsigned int unidade);
float leval(int fdio, unsigned int unidade);
int errodc(unsigned char dcmsg[]);
int calcbcc(unsigned char msg[], int msgnum);
int openct();
float celsius(int fdio);
int erroct(unsigned char msg[]);

main ()
{
    FILE *fpi, *fpo;
    int fddc, fdct, n, nn, hh, mm, ss, dif;
    long int tini;
    unsigned char inmsg[5];
    unsigned int segu, sputt;
    float valorsp[3], valoract[3], temperatura;
    char *data=(char *)malloc(TDATA), fich[60], notas[80];
    char *fichtmp=(char *)malloc(60), msg[9];
    time_t tp;
    struct tm agora;

    if ((tp=time(NULL))== -1)
        printf("time: não foi possível saber a data!\n");
    else
        agora=*localtime(&tp);

    strftime(data, TDATA, "Data: %d/%m/%Y Início: %H:%M:%S\n", &agora);
    fichtmp=getenv("HOME");
    strcat(fichtmp, "/tmp/fich-produc");
    fpi=fopen(fichtmp, "r");
    fscanf(fpi, "%s\n%[^#]#%u\n%f\n%f\n%f\n%u\n", fich, notas, &segu, \
&valorsp[0], &valorsp[1], &valorsp[2], &sputt);
    fclose(fpi);
    valorsp[0]=valorsp[0]/10;
    sputt=sputt*60;

    fpo=fopen(fich, "a");
    fprintf(fpo, "%s#%s\n\n", data, notas);

    fdct=openct();

    fddc=opendc();

    if (opmode(fddc,RS232) < 0)
        exit(-1);
}

```

## B. Power source control

```
for(n=0; n<3; ++n)
    if (changesp(fddc,valorsp[n],(unsigned int)(n+1)) < 0) {
        switch (n) {
            case 0:
                strcpy(msg,"potência");
                break;
            case 1:
                strcpy(msg,"tensão");
                break;
            case 2:
                strcpy(msg,"corrente");
                break;
        }
        printf("Não foi alterado o SP da %s!\n", msg);
        exit(-1);
    }

if (onoffonte(fddc,ON) < 0) {
    printf("A fonte não foi ligada!\n");
    exit(-1);
}

/* Fonte Ligada */
dif=0;
instante(inst);
sscanf(inst, "%d:%d:%d", &hh, &mm, &ss);
tini=hh*3600+mm*60+ss;
n=1;

while ((unsigned int)dif < (sputt-segu)) {
    for (nn=0; nn<3; ++nn)
        valoract[nn]=level(fddc,(unsigned int)(nn+1));
    temperatura=celsius(fdct);
    fprintf(fpo, "%6d\t%s\t%5.0f\t%5.0f\t%5.2f\t%5.1f\n", n, inst,\
            valoract[0]*10, valoract[1], valoract[2]/100, temperatura);
    fflush(fpo);
    tcflush(fdct,TCIOFLUSH);
    tcflush(fddc,TCIOFLUSH);

    usleep(segu*1000000-400000);
    instante(inst);
    sscanf(inst, "%d:%d:%d", &hh, &mm, &ss);
    dif=hh*3600+mm*60+ss-tini;
    ++n;
}

dif=(int)sputt-dif;
if (dif >= 0) {
```



```

segu=(unsigned int)dif;
if (dif == 0)
    usleep(segu*1000000-500000);
instante(inst);
for (nn=0; nn<3; ++nn)
    valoract[nn]=leval(fddc,(unsigned int)(nn+1));
temperatura=celsius(fdct);
fprintf(fpo, "%6d\t%s\t%5.0f\t%5.0f\t%5.2f\t%5.1f\n", n, inst,\
        valoract[0]*10, valoract[1], valoract[2]/100, temperatura);
}
if (onoffonte(fddc,OFF) < 0) {
    printf("A fonte não foi desligada!\n");
    exit(-1);
}

fclose(fpo);
close(fddc);
close(fdct);

return 0;
}

void instante(char inst[]) {
... see program B.10 on page 119 ...}

int exorop(unsigned char msg[]) {
... see program B.2 on page 113 ...}

int errodc(unsigned char msg[]) {
... see program B.9 on page 118 ...}

int opendc(void) {
... see program B.1 on page 111 ...}

int opmode(int fddc, unsigned int controlo) {
... see program B.3 on page 114 ...}

int onoffonte(int fddc, unsigned int controlo) {
... see program B.5 on page 116 ...}

int changesp(int fddc, float valor, unsigned int unidade) {
... see program B.6 on page 116 ...}

float leval(int fddc, unsigned int unidade) {
... see program B.8 on page 118 ...}

int calcbcc(unsigned char msg[], int msgnum) {
... see program A.2 on page 99 ...}

int openct(void) {

```

## B. Power source control

```
... see program A.1 on page 96 ...}

int erroct(unsigned char msg[]) {
... see program A.7 on page 104 ...}

float celsius(int fdio) {
... see program B.11 on page 119 ...}
```

---

The Bash script B.13 was written in order to ease the task of producing the input file of program `fonte.c`. To use this script, a user have to run the command `sputtering-on` at the Bash command prompt and then insert the parameters asked by the program. The script does some format check to the data to prevent errors and presents default values inside square brackets. If no input value is given the default value will be assumed. The text read by the user may be either in English or in Portuguese.

---

**Program B.13:** Bash script used to write input file of program `fonte.c` (`sputtering-on`)

---

```
#!/bin/bash
# Bash version 2.04.11 or higher
echo ... verificando o estado da fonte DC.
echo ... verifying power source status.
mkdir -p "$HOME/tmp"
if spfonte.exe; then valor=0;
else valor=-1;
fi
if expr "$valor" \< 0 > /dev/null
then
    echo Colocar a fonte em modo RS232!!!
    echo Power source must be in RS232 mode!!!
    exit -1
fi

directoria="$HOME/tmp"
valor=`grep -e 'W' "$directoria"/fonte-sp`
potencia=`expr "$valor" : '[^0-9]*\([0-9]*\) '`
potencia=`expr "$potencia" \* 10`
valor=`grep -e 'V' "$directoria"/fonte-sp`
tensao=`expr "$valor" : '[^0-9]*\([0-9]*\) '`
valor=`grep -e 'cA' "$directoria"/fonte-sp`
corrente=`expr "$valor" : '[^0-9]*\([0-9]*\) '`

lingua=1
directoria="tmp"
modo=1
amostra="abc"
comentarios="abc"
segundos=0
tempo=0
read -e -p "Choose language:\`
```

```

Português (1) English (2)? " lingua
if expr "$lingua" != 1 > /dev/null
then
    confirmacao='n'
    read -e -p "Directory where the files will be\
saved [$directoria]? " valor
    if expr "$valor" != "" > /dev/null
    then
        directoria="$valor"
    fi
    until ls "$HOME/$directoria" > /dev/null
    do
echo "Directory $directoria does not exist!"
        read -e -p "Directory where the files will\
be saved? " directoria
    done
    directoria="$HOME/$directoria"
    while expr "$confirmacao" != y > /dev/null
    do
read -e -p "Film deposition (1) or\
Pre-sputtering (2) [$modo]? " valor
        if expr "$valor" != "" > /dev/null
        then
            modo="$valor"
        fi
    while expr "$modo" \> 2 > /dev/null
    do
        read -e -p "Film deposition (1) or\
Pre-sputtering (2)? " modo
    done
    read -e -p "Experiment reference\
[$amostra]?" valor
        if expr "$valor" != "" > /dev/null
        then
            amostra="$valor"
        fi
    ensaio=1
    if ls "$directoria/$amostra"-[0-9]*.dat\
> /dev/null 2>&1
    then
        until ls "$directoria/$amostra-$ensaio.dat"\
> /dev/null 2>&1
        do
            ensaio=`expr "$ensaio" + 1`
        done
        while ls "$directoria/$amostra-$ensaio.dat"\
> /dev/null 2>&1
        do
            ensaio=`expr "$ensaio" + 1`

```

## B. Power source control

```
done
fi
ficheiro=`echo -n "$amostra-$ensaio"`
ensaio=1
if expr "$modo" = 1 > /dev/null
then
    ficheiro=`echo -n "$ficheiro.dat"`
else
    while ls "$directoria/$ficheiro.pre$ensaio"\
    > /dev/null 2>&1
    do
        ensaio=`expr "$ensaio" + 1`
    done
    ficheiro=`echo -n "$ficheiro.pre$ensaio"`
fi
echo "Comments (max. 80 characters) "
read -e -p "[$comentarios]? " valor
    if expr "$valor" != "" > /dev/null
    then
        comentarios="$valor"
    fi
read -e -p "Sampling frequency (between 1 and\
60 s) [$segundos]: " valor
    if expr "$valor" != "" > /dev/null
    then
        segundos="$valor"
    fi
while expr \( "$segundos" \< 1 \) \|\ \
\(\ "$segundos" \> 60 \) > /dev/null
do
    read -e -p "Sampling frequency (between 1\
and 60 s): " segundos
done
read -e -p "Power (10 to 2500 W)\
[$potencia]: " valor
while expr \( \(\ "$valor" \< 10 \) \|\ \
\(\ "$valor" \> 2500 \) \) \& \
\(\ length "$valor" != 0 \)\
> /dev/null
do
    read -e -p "Power (10 to 2500 W)\
[$potencia]: " valor
done
if expr "$valor" != "" > /dev/null
then
    potencia="$valor"
fi
read -e -p "Voltage (10 to 500 V)\
[$tensao]: " valor
```

```

while expr \( \( "$valor" \< 10 \) \| \
    \( "$valor" \> 500 \) \) \& \
    \( length "$valor" != 0 \)\
> /dev/null
do
    read -e -p "Voltage (10 to 500 V)\
[$tensao]: " valor
done
if expr "$valor" != "" > /dev/null
then
    tensao="$valor"
fi
read -e -p "Current (5 to 500 cA)\
[$corrente]: " valor
while expr \( \( "$valor" \< 5 \) \| \
    \( "$valor" \> 500 \) \) \& \
    \( length "$valor" != 0 \)\
> /dev/null
do
    read -e -p "Current (5 to 500 cA)\
[$corrente]: " valor
done
if expr "$valor" != "" > /dev/null
then
    corrente="$valor"
fi
read -e -p "Deposition time (in minutes)\
[$tempo]: " valor
    if expr "$valor" != "" > /dev/null
    then
        tempo="$valor"
    fi
while expr "$tempo" \< 1 > /dev/null
do
    echo "The deposition time must be greater\
than 1!"
    read -e -p "Deposition time (in minutes): "\
tempo
done
echo
echo "File: $ficheiro"
echo "Comments: $comentarios"
echo "Sampling Frequency: $segundos s"
echo "Power: $potencia W"
echo "Voltage: $tensao V"
echo "Current: $corrente cA"
echo "Deposition Time: $tempo min"
read -e -p "Start experiment (y/n)? " confirmacao
done

```

## B. Power source control

```
else
    confirmacao='n'
    read -e -p "Directoria onde ficam gravados os\
ficheiros [$directoria]? " valor
    if expr "$valor" != "" > /dev/null
    then
        directoria="$valor"
    fi
    until ls "$HOME/$directoria" > /dev/null 2>&1
    do
        echo "A directoria $directoria não existe!"
        read -e -p "Directoria onde ficam gravados os\
ficheiros? " directoria
    done
    directoria="$HOME/$directoria"
    while expr "$confirmacao" != s > /dev/null
    do
read -e -p "Deposição (1) ou pré-sputtering\
(2) [$modo]? " valor
        if expr "$valor" != "" > /dev/null
        then
            modo="$valor"
        fi
    while expr "$modo" \> 2 > /dev/null
    do
        read -e -p "Deposição (1) ou\
pré-sputtering (2)? " modo
    done
    read -e -p "Referência do ensaio [$amostra]?" valor
        if expr "$valor" != "" > /dev/null
        then
            amostra="$valor"
        fi
    ensaio=1
    if ls "$directoria/$amostra"-[0-9]*.dat\
> /dev/null 2>&1
    then
        until ls "$directoria/$amostra-$ensaio.dat"\
> /dev/null 2>&1
        do
            ensaio=`expr "$ensaio" + 1`
        done
        while ls "$directoria/$amostra-$ensaio.dat"\
> /dev/null 2>&1
        do
            ensaio=`expr "$ensaio" + 1`
        done
    fi
    ficheiro=`echo -n "$amostra-$ensaio"`
```

```

ensaio=1
if expr "$modo" = 1 > /dev/null
then
    ficheiro='echo -n "$ficheiro.dat"'
else
    while ls "$directoria/$ficheiro.pre$ensaio" \
    > /dev/null 2>&1
    do
        ensaio='expr "$ensaio" + 1'
    done
    ficheiro='echo -n "$ficheiro.pre$ensaio"'
fi
echo "Comentários (max. 80 caracteres)"
    read -e -p "[Comentarios]? " valor
    if expr "$valor" != "" > /dev/null
    then
        comentarios="$valor"
    fi
read -e -p "Intervalo de amostragem (entre 1\
e 60 s) [$segundos]: " valor
    if expr "$valor" != "" > /dev/null
    then
        segundos="$valor"
    fi
while expr \( "$segundos" \< 1 \) \| \( \
"$segundos" \> 60 \) > /dev/null
do
    read -e -p "Intervalo de amostragem (entre\
1 e 60 s): " segundos
done
read -e -p "Potência (10 a 2500 W) [$potencia]: "\
valor
while expr \( \( "$valor" \< 10 \) \| \( "$valor"\
\> 2500 \) \) \& \( length "$valor" != 0 \) > /dev/null
do
    read -e -p "Potência (10 a 2500 W)\
[$potencia]: " valor
done
if expr "$valor" != "" > /dev/null
then
    potencia="$valor"
fi
read -e -p "Tensão (10 a 500 V) [$tensao]: " valor
while expr \( \( "$valor" \< 10 \) \| \( "$valor"\
\> 500 \) \) \& \( length "$valor" != 0 \) > /dev/null
do
    read -e -p "Tensão (10 a 500 V)\
[$tensao]: " valor
done

```

## B. Power source control

```
if expr "$valor" != "" > /dev/null
then
    tensao="$valor"
fi
read -e -p "Corrente (5 a 500 cA) [$corrente]: " valor
while expr \( \( "$valor" \< 5 \) \| \( "$valor" \>\
500 \) \) \& \( length "$valor" != 0 \) > /dev/null
do
    read -e -p "Corrente (5 a 500 cA)\
[$corrente]: " valor
done
if expr "$valor" != "" > /dev/null
then
    corrente="$valor"
fi
read -e -p "Tempo de deposição (em minutos)\
[$tempo]? " valor
    if expr "$valor" != "" > /dev/null
    then
        tempo="$valor"
    fi
while expr "$tempo" \< 1 > /dev/null
do
    echo "O tempo de deposição tem de\
ser maior do que 1!"
    read -e -p "Tempo de deposição\
(em minutos): " tempo
done
echo
echo "Ficheiro: $ficheiro"
echo "Comentários: $comentarios"
echo "Intervalo de amostragem: $segundos s"
echo "Potência: $potencia W"
echo "Tensão: $tensao V"
echo "Corrente: $corrente cA"
echo "Tempo de deposição: $tempo min"
read -e -p "Tudo certo (s/n)? " confirmacao
done
fi

mkdir -p "$HOME/tmp"
echo "$directoria/$ficheiro" > "$HOME/tmp/fich-produc"
echo "$comentarios#" >> "$HOME/tmp/fich-produc"
echo "$segundos" >> "$HOME/tmp/fich-produc"
echo "$potencia" >> "$HOME/tmp/fich-produc"
echo "$tensao" >> "$HOME/tmp/fich-produc"
echo "$corrente" >> "$HOME/tmp/fich-produc"
echo "$tempo" >> "$HOME/tmp/fich-produc"
```



```
nohup fonte.exe &
exit 0
```

---

The default values for the power, voltage and current source set points are the ones in effect on the device. They are read using program `spfonte.c` listed below. The compiled version of `spfonte.c` was called `spfonte.exe`.

---

**Program B.14:** C program used to control DC power source and substrate temperature during film deposition (`spfonte.c`)

---

```
#include <sys/types.h>
#include <sys/stat.h>
#include <fcntl.h>
#include <termios.h>
#include <unistd.h>
#include <stdio.h>
#include <errno.h>
#include <string.h>
#include <stdlib.h>

#define BAUDRATE B9600
#define DCDEV "/dev/ttyS4"
#define DCUNIT 0
#define WBIT 0x80
#define POWER 1
#define VOLTAGE 2
#define CURRENT 3
#define RS232 4

int exorop(unsigned char dcmsg[]);
int opendc();
int lesp(int fdio, unsigned int unidade);
int errodc(unsigned char dcmsg[]);
int rsmode(int fdio, unsigned int controlo);

main ()
{
    FILE *fpo;
    int fddc, n, valorig[3];
    char *fichtmp=(char *)malloc(60), msg[9];

    fichtmp=getenv("HOME");
    strcat(fichtmp, "/tmp/fonte-sp");
    fpo=fopen(fichtmp, "w");

    fddc=opendc();

    if (rsmode(fddc,RS232) < 0)
        exit(-1);
```

## B. Power source control

```
for(n=1; n<4; ++n)
    if ((valorig[n-1]=lesp(fddc,(unsigned int)(n))) < 0) {
        switch (n) {
            case 1:
                strcpy(msg,"potência");
                break;
            case 2:
                strcpy(msg,"tensão");
                break;
            case 3:
                strcpy(msg,"corrente");
                break;
        }
        printf("Não foi alterado o SP da %s!\n", msg);
        exit(-1);
    }

    fprintf(fpo,"%6dW\n%6dV\n%6dcA\n",\
        valorig[0],valorig[1],valorig[2]);

    fclose(fpo);
    close(fddc);

return 0;
}

int exorop(unsigned char msg[]) {
... see program B.2 on page 113 ...}

int errodc(unsigned char msg[]) {
... see program B.9 on page 118 ...}

int opendc(void) {
... see program B.1 on page 111 ...}

int lesp(int fddc, unsigned int unidade) {
... see program B.7 on page 117 ...}

int rsmode(int fddc, unsigned int controlo) {
... see program B.4 on page 115 ...}

```

---

## C. Electric valves control

In the gas sensor testing chamber were used five Joucomatic electrically actuated valves of series 115. Position of the valves in the system is shown in Fig. 5.1. Valves 1 and 4 are normally open and the other three are normally closed when in off state. The response time is reported by the manufacturer to be lower than 15 ms with a maximum differential pressure of 6 bar between inlet and outlet. In order to control these valves remotely an electronic setup was mounted on the laboratory that permits to turn on and off the power supply of each valve using the parallel port signals of the computer. Henceforth this electronic setup will be called valve controller.

The valve controller can be used to control the valves either manually or remotely. The front panel of the controller have nine on-off switches, as shown in Fig. C.1(a). The rear panel has the nine connections shown in Fig. C.1(b). One connection on the rear panel is used to supply power to the controller, seven are used to supply power to electric valves and the last one is used to connect the controller to the parallel port of the computer. On the front panel the rightmost switch is used to switch the controller from the manual to the remote controlling mode. When the mode switch is in the remote position the other front panel switches do nothing. In manual position the seven switches on the left may be used to supply power to the valves connected on the rear panel. The next sections of this appendix describe the parallel port configuration and how it can be used to control the electric valves.



Figure C.1.: Valve controller (a) front panel and (b) rear panels

## C.1. The parallel port

There are five common types of parallel ports: SPP, PS/2, EPP, ECP and multi-mode. The SPP port emulates the original IBM PC port's design. It has eight outputs, five inputs and four bidirectional lines. The newer versions are compatible with the original design, but add new abilities, mainly for increased transmission rate. Since there was no need to read from the port, the SPP type was assumed.

The parallel port uses a variety of computer's resources. Every port uses a range of addresses, though the number and location of the addresses varies. Many ports have an IRQ level assigned, and ECPs may have a DMA channel assigned. The resources assigned to a port cannot conflict with those used by other system components, including other parallel ports. The parallel port that comes with a computer have an assigned address and possibly an IRQ level and a DMA channel. It is possible to change these assignments, but should be done with care to avoid conflict with existing ports and other resources.

Table C.1.: Pin assignments on SPP parallel ports

Pin	Functions
2–9	Output data bits. Pin 2 corresponds to the least significant bit and 9 to the most significant bit.
1, 14, 16, 17	Bidirectional control lines.
10–13, 15	Input control lines.
18–25	signal ground.

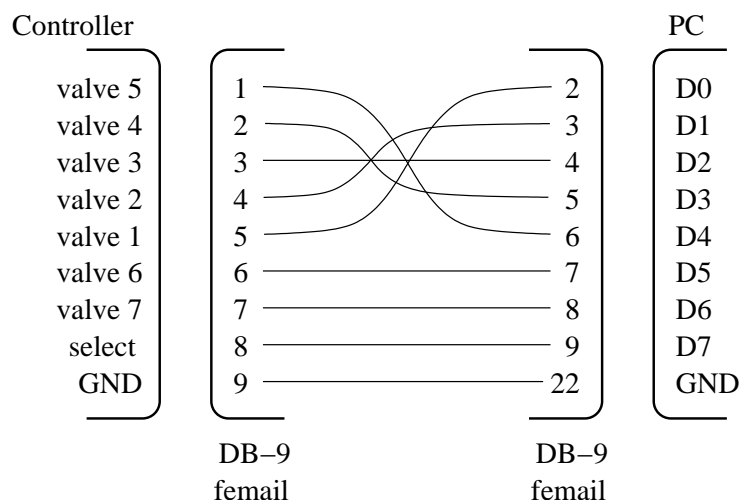


Figure C.2.: Cable wiring between the valve controller and the computer parallel port

The parallel port connector is usually a female 25-pin port. For the SPP type parallel port the pin assignments are shown in Table C.1. The connection between the computer and the valve controller uses only the output data and signal ground pins as shown in Fig. C.2. As in the case of the serial ports, the parallel ports are identified from the software point of view, by special device files. The computer used in the experimental setup has only one port accessible through the device file `/dev/parport0`.

During the boot process of the computer, the output bit signals of the parallel may change. This may interfere with the valve state, even if the mode switch is in the manual position. Therefore when the computer is turned on the valve controller power should always be off, to prevent

unwanted valve turn on. When the boot process finishes, the output bit signals are usually set to off. If this is not the case a routine have to be run just after the boot process to put these pins in off state, thus preventing unintentional valve turn on, when the valve controller is turned on.

## C.2. Commands and routines

In the Linux operative system running on the used computer the parallel port pin signals are controlled using a special device driver called `ppdev`. If a kernel version lower than 2.4 is used, a patch have to be applied. All the newer versions include the `ppdev` driver, but may be disabled by default. The laboratory computer is running kernel version 2.4.3-12 and has the `ppdev` driver enabled. If the driver is not enabled the functions will produce an error when run.

Routines `openpp` and `ppinit` are used respectively to get the file descriptor and initialise the parallel port. Routine `openpp` has no arguments and returns the file descriptor for the parallel port if the open command succeeds.

---

**Program C.1:** C program used to get the file descriptor for the parallel port (`openpp`)

---

```
#define PPDEV "/dev/parport0"

int openpp(void) {
    int ppfd;

    ppfd=open(PPDEV, O_WRONLY);
    if (ppfd==-1) {
        perror ("open");
        exit(-1);
    }
    return ppfd;
}
```

---

Routine `ppinit` receives the file descriptor by argument and returns always 0. In case of failure the routine causes the program to exit. It uses `ioctl` function to request port access exclusivity.

---

**Program C.2:** C program used to initialise the parallel port (`ppinit`)

---

```
int ppinit(int fdpp) {

    if (ioctl(fdpp, PPEXCL)) {
        perror("PPEXCL");
        close(fdpp);
        exit(-1);
    }
    if (ioctl(fdpp, PPCLAIM)) {
        perror("PPCLAIM");
        close(fdpp);
        exit(-1);
    }
}
```

### C. Electric valves control

```
return 0;
}
```

Remote valve control is performed using the output data bits of the parallel port. These bits are set using command

```
ioctl(fdpp, PPWDATA, vcont);
```

where `vcont` is a pointer to the character array `*vcont`, that is sent through the port data lines and `fdpp` is the file descriptor identifying the parallel port. Thus if character code 0111 1111 is sent through the data lines: pin 9 signal will be set to 0 and the other output data bits (see Table C.1) will be set to 1. The pin data signals will maintain their state until another `ioctl` call is made. Pins 2 through 8 are used to turn on power supply to ports 1 through 7 (see Fig. C.1(b)) when their signal is 0. Pin 9 is used to turn on or off remote valve control, so that, signals of pins 2 through 8 only take effect if pin 9 has value 1. An example of how the valves' state is set using the value stored in `*vcont` is shown in Table. C.2.

Table C.2.: Example of correspondence between valve setting and the value of variable `*vcont`

Valves <sup>a</sup>							*vcont	
7	6	5	4	3	2	1	hex	binary
-	-	-	-	-	-	-	0xFF1111	1111
-	-	-	-	-	-	-	0x5C0101	1100
-	+	-	-	-	+	+	0xDC1101	1100

<sup>a</sup>+ valve switched on; - valve switched off

The following definitions may be declared in the beginning of the program to help changing the electric valves' state. Constants `REMOFF` and `REMON` turn pin 9, respectively, into state 0 or 1, and all the other pins to state 1.

```
#define VALV1 0xFE
#define VALV2 0xFD
#define VALV3 0xFB
#define VALV4 0xF7
#define VALV5 0xEF
#define VALV6 0xDF
#define VALV7 0xBF
#define REMOFF 0x7F
#define REMON 0xFF
```

After initialising the parallel port, the variable `*vcont` is set to `0xFF` to enable remote setting of the valves and guarantee that all the valves are switched off at the start of the procedure.

```
*vcont = REMON;
ioctl(fdpp, PPWDATA, vcont);
```

Then, to turn on valve 4 the following commands may be given

```
*vcont &= VALV4;
ioctl(fdpp, PPWDATA, vcont);
```

and to turn off valve 4 is used

```
*vcont |= VALV4;
ioctl(fdpp, PPWDATA, vcont);
```

## D. Multimeter data acquisition

Remote multimeter control and data acquisition is performed using the device serial port. The following sections describe the serial port connections, the communication protocol and language used to program the multimeter operation.

### D.1. Communication interface

The RS-232-C port of the multimeter is connected to the first serial port of the computer (see Table A.1). The multimeter is configured as a DTE device, but unlike the temperature controller and the magnetron power source, it uses some of the serial port control flow lines in communication, namely the DTR and DSR pins. As already stated before (see Section A.3) these pin functions are not usually implemented in Linux. However, since the function of DTR is similar to RTS and DSR is similar to CTS, the communication is possible if the connections are made as shown in Fig. D.1 and hardware control flow is set on the computer. Thus, DTR pin on the multimeter is connected to CTS pin on the computer and DSR on the multimeter port is connected to RTS on the computer.

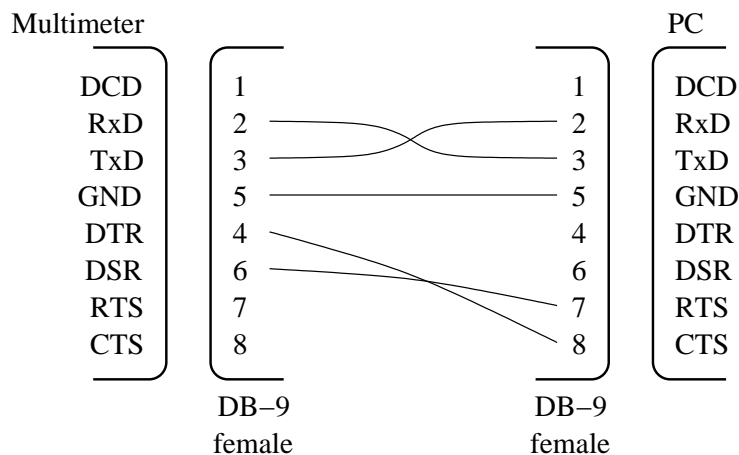


Figure D.1.: Cable wiring between multimeter serial port and computer

On the multimeter, the DTR line have to be TRUE before the multimeter accepts data from the computer. After setting DTR to FALSE the multimeter will accept up to 10 characters. The multimeter sets the DTR line to FALSE when its input buffer is full or when the multimeter wants to send data over the interface, e.g., when it has processed a query command and wants to send the response. In addition, the multimeter monitors the DSR line to determine when the controller is ready to accept data. The transmission from the multimeter is suspended if the DSR line is FALSE and will resume when the DSR line goes TRUE.

On the computer RTS line have to be TRUE before the computer accepts data from the multimeter. Before sending data over the serial port the computer will check the CTS line, and will stop flow if it is set to FALSE.

Table D.1.: Communication parameters selected on the multimeter for data exchange with the computer

Parameter	Selected value
Interface	RS-232
Communication speed	9600 BAUD
Parity and data bits	NONE: 8 BITS
Stop bits	2
Language	SCPI

In order to enable communication through the multimeter serial port some parameters have to be set on the device. In first place it is necessary to set the interface to RS-232<sup>1</sup>, under command `INTERFACE` and menu choice `I/O MENU`. The communication flow rate may be selected from the following: 300, 600, 1200, 2400, 4800 or 9600 bps. It was set to 9600 BAUD, under command `BAUD RATE` and menu choice `I/O MENU`. There are three possible character data formats: no parity and 8 data bits; even parity and 7 data bits; and odd parity and 7 data bits (See section A.3 for details about the meaning of the parity). It was set to no parity and 8 data bits, under command `PARITY` and menu choice `I/O MENU`. When the interface is set to RS-232 the only language accepted by the multimeter is SCPI. This will be the language used to program the device remotely.

On the computer the parameters are set by routine `openh`. This routine has no arguments and returns the file descriptor corresponding to the serial port attached to the power source. See Table A.7 for a description of the meaning of the flags set by the `termios` functions used in routine `openh`. It may be verified that the parameters set by the computer match those selected on the multimeter.

---

**Program D.1:** C program used to initialise the serial port attached to the multimeter (`openh`)

---

```
#define BAUDRATEHP B9600
#define HPDEV "/dev/ttyS0"

int openhp(void) {
    int fdhp;
    struct termios hptio;

    fdhp=open(HPDEV, O_RDWR | O_NOCTTY | O_NONBLOCK);
    if (fdhp < 0) {
        perror(HPDEV);
        exit(-1);
    }
    tcgetattr(fdhp, &hptio);
    tcflush(fdhp, TCIFLUSH);
    cfsetispeed(&hptio, BAUDRATEHP);
    cfsetospeed(&hptio, BAUDRATEHP);

    bzero(&hptio, sizeof(hptio));

    hptio.c_cflag=(BAUDRATEHP | CRTSCTS | PARENB | CSTOPB\
```

---

<sup>1</sup>The default choice for the device is HP-IB/488.



```

| CS7 | CLOCAL | CREAD);
hptio.c_lflag &= ~(ICANON | ECHO);
hptio.c_iflag=(INPCK | ISTRIP | INLCR | PARMRK);
hptio.c_oflag &= ~OPOST;

tcsetattr(fdhp, TCSANOW, &hptio);
sleep(3);

return fdhp;
}

```

---

## D.2. Communication language

Remote programming of the multimeter is performed using SCPI language. SCPI commands are based on a hierarchical structure. In this system, associated commands are grouped together under a common node or root. A colon (:) separates a command keyword from a lower level keyword. Most of the commands have an abbreviated form. Only the abbreviated form of the commands will be used in the programs. Although it is possible to use simultaneously upper and lower case letters in command writing, only upper case letters will be used.

A command string sent to the multimeter must terminate with a newline character (\n). Common commands begin with an asterisk (\*). Some commands need parameters. These are separated from the command keyword by a space character. There are four different parameter formats: numeric, discrete, boolean or string. Numeric parameters should be decimal numbers and may be written using scientific notation. Special values like MIN, MAX or DEF may be accepted. If only specific numerical values are accepted by the command, the multimeter will automatically round the received value. Discrete parameters are used to program settings that have a limited number of values. Boolean parameters may be OFF or 0 to state a FALSE value, and ON or 1 to state TRUE. Finally, string parameters can contain any set of ASCII characters. A string parameter must begin and end with a single (') or double quote character ("). A quote may be included in the string by typing it twice without any character in between.

Three routines were written to send specific commands to the multimeter: `selrange`, `medevolt` and `mederes`.

Routine `selrange` is used to set the measuring range of the multimeter either to the 10 V range or to the 100 V range. To decide in which range to put the multimeter the routine reads one voltage value. Whenever the range is changed, this routine writes in the output file of the program a message stating the new range. The routine receives the multimeter port file descriptor and the output file pointer and returns always 0.

---

### Program D.2: C program used to select measuring range of the multimeter (`selrange`)

---

```

int selrange(int fdhp, FILE *fpo) {
    char escala[18];
    float volt;

    write(fdhp, ":VOLT:DC:RANG 100\n", 18);
    usleep(30000);
    write(fdhp, ":READ?\n", 7);
    usleep(500000);
}

```

#### D. Multimeter data acquisition

```
while (read(fdhp, &escala, 18)==0)
    ;

sscanf(escala, "%f", &volt);
if (volt<9.2) {
    write(fdhp, ":VOLT:DC:RANG 10\n", 17);
    fprintf(fpo, "# Range: 10 V\n");
}
else
    fprintf(fpo, "# Range: 100 V\n");

usleep(30000);
return 0;
}
```

---

Routine `medevolt` is used to put the multimeter in the voltage measurement mode, and also sets the multimeter internal resistance to a value greater than  $10\text{ G}\Omega$ , in the  $10\text{ V}$  measuring range. In the  $100\text{ V}$  range the internal multimeter resistance is always  $10\text{ M}\Omega$ . Therefore if the layer resistance is close or higher than  $10\text{ M}\Omega$ , the multimeter internal resistance have a significant effect on the measured values.

This routine receives the multimeter file descriptor and returns always 0. Before exiting the routine checks if the multimeter is measuring from the front or rear panel terminals. If the multimeter is reading from the front panel terminals it beeps and shows in the front panel the message “TERMINAIS”, to alert the user to toggle the input terminal switch. The routine continues when it verifies that the multimeter is reading from the rear terminals.

---

**Program D.3:** C program used to put the multimeter in voltage measurement mode (`medevolt`)

---

```
int medevolt(int fdhp) {
    unsigned char medi[6];

    write(fdhp, ":SYST:REM\n", 10);
    sleep(1);
    write(fdhp, "*CLS;*RST\n", 10);
    sleep(1);
    /*Ranges: 0.01,1,10,100*/
    write(fdhp, ":CONF:VOLT:DC 100\n", 18);
    sleep(1);
    write(fdhp, ":INP:IMP:AUTO ON\n", 17);
    sleep(1);
    write(fdhp, ":ROUT:TERM?\n", 12);
    usleep(3000);
    while (read(fdhp, &medi, 6)==0)
        ;

    while (medi[0]!='R') {
        write(fdhp, ":DISP:TEXT 'TERMINAIS'\n", 23);
        sleep(1);
        write(fdhp, ":SYST:BEEP\n", 11);
    }
}
```

```

    sleep(1);
    write(fdhp, ":ROUT:TERM?\n",12);
    sleep(1);
    while (read(fdhp, &medi, 6)==0)
        ;
}
write(fdhp, ":DISP:TEXT:CLE\n",15);

return 0;
}

```

---

Routine `mederes` is used to put the multimeter in resistance measurement mode. It receives the multimeter file descriptor and returns always 0.

---

**Program D.4:** C program used to put the multimeter in resistance measurement mode  
(`mederes`)

---

```

int mederes(int fdhp) {

    write(fdhp, ":SYST:REM\n", 10);
    sleep(1);
    write(fdhp, "*CLS;*RST\n", 10);
    sleep(1);
    write(fdhp, ":CONF:RES\n", 10);
    sleep(1);

    return 0;
}

```

---

#### *D. Multimeter data acquisition*

## E. Gas sensor testing procedure

Gas sensor testing experiments take usually several hours. During each trial, layer temperature and resistance is measured and registered by the computer at predefined regular intervals. Atmosphere inside the chamber is also controlled by the computer. The time and changes performed are recorded in the output file, along with the temperature and resistance values. Since the program that controls the experiment reads the parameters from a file with a strict format, a Bash script was written to help in this task. This program also helps the user to check if the system is ready to start measurement. The following sections describe the Bash scripts used to start and stop the gas sensor tests and the program that controls the experiments.

### E.1. User interface

Bash script used to start the gas sensor testing procedure is called `sensor-on`. This script starts by asking the parameters needed to write the input file of program `sensor.exe` and then details the procedure that the user has to follow to prepare the equipment for the test. After choosing the language, the user may select one of two different procedures. One is called `Fast procedure` and the other is called `Slow procedure`. The latter should be used when the chamber was opened to place inside a new layer. The `Fast procedure` may be used if the `Slow procedure` was used before, ended normally and the chamber was not opened afterwards. After performing the actions mentioned in the script program `sensor.exe` is started.

---

**Program E.1:** Bash script used to set parameters of film testing procedure (`sensor-on`)

---

```
#!/bin/bash
# Bash version 2.04.11 or higher
lingua=1
directoria="tmp"
amostra="abc"
comentarios="abc"
segundos=3
temperatura=300
numdeg=1
tempmin=0
tempest=3
tempres=15
temprec=25
resposta=2
pulsos=3
procedi=0
read -e -p "Choose language: Português (1) English\
(2)? " lingua
```

## E. Gas sensor testing procedure

```
if expr "$lingua" != 1 > /dev/null
then
    echo "Choose the procedure:"
    echo "1) Fast procedure (the chamber has been\
kept in clean air)"
    echo "2) Slow procedure (the chamber was opened\
to insert a new layer)"
    while expr \( "$procedi" != 1 \) \& \( \
"$procedi" != 2 \) > /dev/null
    do
        read -e -p "Choice? " procedi
    done
    confirmacao='n'
    read -e -p "Directory where the files will be saved\
[$directoria]? " valor
    if expr "$valor" != "" > /dev/null
    then
        directoria="$valor"
    fi
    until ls "$HOME/$directoria" > /dev/null
    do
        read -e -p "Directory where the files will be\
saved? " directoria
    done
    directoria="$HOME/$directoria"
    while expr "$confirmacao" != y > /dev/null
    do
        read -e -p "Sample Reference [$amostra]? " valor
        if expr "$valor" != "" > /dev/null
        then
            amostra="$valor"
        fi
        ensaio=1
        if ls "$directoria/$amostra"-[0-9]*.dat\
> /dev/null 2>&1
        then
            until ls "$directoria/$amostra-$ensaio.dat"\
> /dev/null 2>&1
            do
                ensaio=`expr "$ensaio" + 1`
            done
            while ls "$directoria/$amostra-$ensaio.dat"\
> /dev/null 2>&1
            do
                ensaio=`expr "$ensaio" + 1`
            done
        fi
        echo "Comments (max. 80 characters)"
        read -e -p "[$comentarios] " valor
```

```

if expr "$valor" != "" > /dev/null
then
    comentarios="$valor"
fi
read -e -p "Sampling frequency (between 1 and\
 60 s) [$segundos]: " valor
if expr "$valor" != "" > /dev/null
then
    segundos="$valor"
fi
while expr \( "$segundos" \< 1 \) \| \(\
"$segundos" \> 60 \) > /dev/null
do
    read -e -p "Sampling frequency (between\
 1 and 60 s): " segundos
done
read -e -p "Maximum Temperature (between\
 100 and 400 C) [$temperatura]: " valor
if expr "$valor" != "" > /dev/null
then
    temperatura="$valor"
fi
while expr \( "$temperatura" \< 10 \) \| \(\
"$temperatura" \> 400 \) > /dev/null
do
    read -e -p "Maximum Temperature (between\
 100 and 400 C): " temperatura
done
read -e -p "Number of Temperature Steps\
 (min. 1) [$numdeg]: " valor
if expr "$valor" != "" > /dev/null
then
    numdeg="$valor"
fi
while expr "$numdeg" \< 1 > /dev/null
do
    read -e -p "Number of Temperature Steps\
 (min. 1): " numdeg
done
if expr "$numdeg" = 1 > /dev/null
then
    tempmin="$temperatura"
else
    read -e -p "Minimum Temperature (between\
 100 C and Tmax) [$tempmin]: " valor
    if expr "$valor" != "" > /dev/null
    then
        tempmin="$valor"
    fi

```

### E. Gas sensor testing procedure

```
while expr \( "$tempmin" \< 100 \) \|| \(\
"$tempmin" \>= "$temperatura" \) > /dev/null
do
read -e -p "Minimum Temperature (between\
100 C and Tmax): " tempmin
done
fi
read -e -p "Stabilization Time (in hours)\
[$tempest]: " valor
if expr "$valor" != "" > /dev/null
then
tempest="$valor"
fi
while expr \( "$tempest" \< 1 \) \|| \(\
"$tempest" \> 9 \) > /dev/null
do
read -e -p "Stabilization Time (in\
hours): " tempest
done
read -e -p "Response Time (in minutes)\
[$tempres]: " valor
if expr "$valor" != "" > /dev/null
then
tempres="$valor"
fi
while expr \( "$tempres" \< 1 \) \|| \(\
"$tempres" \> 60 \) > /dev/null
do
read -e -p "Response Time (in minutes):\
" tempres
done
read -e -p "Recovery Time (in minutes)\
[$temprec]: " valor
if expr "$valor" != "" > /dev/null
then
temprec="$valor"
fi
while expr \( "$temprec" \< 1 \) \|| \(\
"$temprec" \> 180 \) > /dev/null
do
read -e -p "Recovery Time (in minutes):\
" temprec
done
read -e -p "Measures resistance (1) or\
voltage (2) [$resposta]? " valor
if expr "$valor" != "" > /dev/null
then
resposta="$valor"
fi
```



```

while expr \( "$resposta" \< 1 \) \| \(\
"$resposta" \> 2 \) > /dev/null
do
    echo "Invalid option!"
    read -e -p "Measures resistance (1) or\
voltage (2)? " resposta
done
if expr "$resposta" = 1 > /dev/null
then
    mede="resistance"
else
    mede="voltage"
fi
read -e -p "Number of CO tests per temperature\
step (min. 1) [$pulsos]: " valor
if expr "$valor" != "" > /dev/null
then
    pulsos="$valor"
fi
while expr "$pulsos" \< 1 > /dev/null
do
    read -e -p "Number of CO tests per\
temperature step (min. 1): " pulsos
done

echo
echo "File: $amostra-$ensaio.dat"
echo "Comments: $comentarios"
echo "Sampling frequency: $segundos s"
echo "Maximum temperature: $temperatura C"
echo "Minimum temperature: $tempmin C"
echo "Number of temperature steps: $numdeg"
echo "Stabilization time: $stempest h"
echo "Response time: $tempres min"
echo "Recovery time: $temprec min"
echo "Measures $mede"
echo "Number of CO pulses: $pulsos"
read -e -p "Proceed (y/n)? " confirmacao
done

case $procedi in
    1) echo -----\
-----\
        echo Now follow each procedure and press the\
digits inside the brackets.
        echo -----\
-----\
        read -s -p "Verify that the chamber pressure is\
above 1200 mbar [1] " -d 1

```

## E. Gas sensor testing procedure

```
    echo
    read -s -p "Switch valve controller to MAN\
position [2] " -d 2
    echo
    echo "Switch on valve 5 and adjust air needle valve"
    read -s -p "til the flowmeter reaches the 120 mm\
position [3] " -d 3
    echo
    echo "Switch on valve 3 and adjust CO needle valve"
    read -s -p "til the flowmeter reaches the 40 mm\
position [4] " -d 4
    echo
    read -s -p "Switch off valve 3 and wait 30 seconds\
[5] " -d 5
    echo
    read -s -p "Switch off valve 5 [6] " -d 6
    echo
    read -s -p "Switch valve controller to REM position\
[7] " -d 7
    echo;;
    2) echo -----\
-----\
    echo Now follow each procedure and press the\
digits inside the brackets.
    echo -----\
-----\
    read -s -p "Verify that CO and air bottles are\
closed [1] " -d 1
    echo
    read -s -p "Open valve connecting vacuum pump\
to system [2] " -d 2
    echo
    read -s -p "Switch valve controller to MAN position\
[3] " -d 3
    echo
    echo "Switch on valve 2 and wait for the pressure\
to reach 60 mbar"
    read -s -p "Open air needle valve if necessary\
[4] " -d 4
    echo
    read -s -p "Switch off valve 2 (and close needle\
valve) [5] " -d 5
    echo
    read -s -p "Open air and CO bottles [6] " -d 6
    echo
    read -s -p "Switch on valve 5 and wait for the\
pressure to rise to 1200 mbar) [7] " -d 7
    echo
    echo "Open completely exit valve and adjust air\
```

```

needle"
  read -s -p "valve til the flowmeter reaches the\
120 mm position [8] " -d 8
  echo
  echo "Switch on valve 3 and adjust CO needle valve"
  read -s -p "til the flowmeter reaches the 40 mm\
position [9] " -d 9
  echo
  read -s -p "Switch off valve 3 and wait 30\
seconds [10] " -d 0
  echo
  read -s -p "Switch off valve 5 [11] " -d 1
  echo
  read -s -p "Switch valve controller to REM\
position [12] " -d 2
  echo;;
esac
else
  echo "Escolher o procedimento:"
  echo "1) Procedimento rápido (a câmara foi\
mantida com ar sintético)"
  echo "2) Procedimento lento (a câmara foi\
aberta para colocar nova amostra)"
  while expr \( "$procedi" != 1 \) \& \( \
"$procedi" != 2 \) > /dev/null
  do
    read -e -p "Opção? " procedi
  done
  confirmacao='n'
  read -e -p "Directoria onde ficam gravados os\
ficheiros [$directoria]? " valor
  if expr "$valor" != "" > /dev/null
  then
directoria="$valor"
  fi
  until ls "$HOME/$directoria" > /dev/null
  do
    read -e -p "Directoria onde ficam gravados\
os ficheiros? " directoria
  done
  directoria="$HOME/$directoria"
  while expr "$confirmacao" != s > /dev/null
  do
read -e -p "Nome da amostra [$amostra]? " valor
if expr "$valor" != "" > /dev/null
then
  amostra="$valor"
fi
ensaio=1

```

## E. Gas sensor testing procedure

```
if ls "$directoria/$amostra"-[0-9]*.dat\  
> /dev/null 2>&1  
then  
    until ls "$directoria/$amostra-$ensaio.dat"\  
> /dev/null 2>&1  
    do  
ensaio=`expr "$ensaio" + 1`  
    done  
    while ls "$directoria/$amostra-$ensaio.dat"\  
> /dev/null 2>&1  
    do  
ensaio=`expr "$ensaio" + 1`  
    done  
fi  
echo "Comentários (max. 80 caracteres)"  
read -e -p "[$comentarios] " valor  
if expr "$valor" != "" > /dev/null  
then  
    comentarios="$valor"  
fi  
read -e -p "Intervalo de amostragem (entre 1\  
e 60 s) [$segundos]: " valor  
if expr "$valor" != "" > /dev/null  
then  
    segundos="$valor"  
fi  
while expr \( "$segundos" \"$segundos" \> 60 \) > /dev/null  
do  
    read -e -p "Intervalo de amostragem (entre\  
1 e 60 s): " segundos  
done  
read -e -p "Temperatura máxima (entre 100 e\  
400 C) [$temperatura]: " valor  
if expr "$valor" != "" > /dev/null  
then  
    temperatura="$valor"  
fi  
while expr \( "$temperatura" \"$temperatura" \> 400 \) > /dev/null  
do  
    read -e -p "Temperatura máxima (entre 100\  
e 400 C): " temperatura  
done  
read -e -p "Número de degraus (min. 1)\  
[$numdeg]: " valor  
if expr "$valor" != "" > /dev/null  
then  
    numdeg="$valor"
```

```

fi
while expr "$numdeg" \< 1 > /dev/null
do
    read -e -p "Número de degraus (min. 1):\
    " numdeg
done
if expr "$numdeg" = 1 > /dev/null
then
    tempmin="$temperatura"
else
    read -e -p "Temperatura mínima (entre\
    100 C e Tmax) [$tempmin]: " valor
    if expr "$valor" != "" > /dev/null
    then
tempmin="$valor"
        fi
        while expr \( "$tempmin" \< 100 \) \|\ (\
"$tempmin" \>= "$temperatura" \) > /dev/null
        do
read -e -p "Temperatura mínima (entre\
    100 C e Tmax): " tempmin
        done
    fi
read -e -p "Tempo de estabilização (em horas)\
[$tempest]: " valor
if expr "$valor" != "" > /dev/null
then
    tempest="$valor"
fi
while expr \( "$tempest" \< 1 \) \|\ (\
"$tempest" \> 9 \) > /dev/null
do
    read -e -p "Tempo de estabilização\
    (em horas): " tempest
done
read -e -p "Tempo de resposta (em minutos)\
[$tempres]: " valor
if expr "$valor" != "" > /dev/null
then
    tempres="$valor"
fi
while expr \( "$tempres" \< 1 \) \|\ (\
"$tempres" \> 60 \) > /dev/null
do
    read -e -p "Tempo de resposta\
    (em minutos): " tempres
done
read -e -p "Tempo de recuperação (em\
    minutos) [$temprec]: " valor

```

## E. Gas sensor testing procedure

```
if expr "$valor" != "" > /dev/null
then
    temprec="$valor"
fi
while expr \( "$temprec" \< 1 \) \| \(\
"$temprec" \> 180 \) > /dev/null
do
    read -e -p "Tempo de recuperação\
(em minutos): " temprec
done
read -e -p "Mede 1-resistência ou 2-tensão\
[$resposta]? " valor
if expr "$valor" != "" > /dev/null
then
    resposta="$valor"
fi
while expr \( "$resposta" \< 1 \) \| \(\
"$resposta" \> 2 \) > /dev/null
do
    echo "Resposta invalida!"
    read -e -p "Mede 1-resistência ou\
2-tensão? " resposta
done
if expr "$resposta" = 1 > /dev/null
then
    mede="resistencia"
else
    mede="tensao"
fi
read -e -p "Número de pulsos de CO (min. 1)\
[$pulsos]: " valor
if expr "$valor" != "" > /dev/null
then
    pulsos="$valor"
fi
while expr "$pulsos" \< 0 > /dev/null
do
    read -e -p "Número de pulsos de CO\
(min. 1): " pulsos
done
echo
echo "Ficheiro: $amostra-$ensaio.dat"
echo "Comentários: $comentarios"
echo "Intervalo de amostragem: $segundos s"
echo "Temperatura máxima: $temperatura C"
echo "Temperatura mínima: $tempmin C"
echo "Número de degraus: $numdeg"
echo "Tempo de estabilização: $tempest h"
echo "Tempo de resposta: $tempres min"
```

```

echo "Tempo de recuperação: $temprec min"
echo "Mede $mede"
echo "Número de pulsos: $pulsos"
read -e -p "Tudo certo (s/n)? " confirmacao
done

case $procedi in
  1) echo -----\
-----
      echo Executar cada um dos procedimentos e de\
seguida premir os dígitos indicados.
      echo -----\
-----
      read -s -p "Verificar se a pressão na câmara\
está acima dos 1200 mbar [1] " -d 1
      echo
      read -s -p "Colocar o controlador das válvulas\
na posição MAN [2] " -d 2
      echo
      echo "Ligar a válvula 5 e ajustar a válvula"
      read -s -p "de agulha do ar até o fluxímetro\
indicar 120 mm [3] " -d 3
      echo
      echo "Ligar válvula 3 e ajustar a válvula de agulha"
      read -s -p "do CO até o fluxímetro indicar 40 mm\
[4] " -d 4
      echo
      read -s -p "Desligar válvula 3 e esperar 30\
segundos [5] " -d 5
      echo
      read -s -p "Desligar válvula 5 [6] " -d 6
      echo
      read -s -p "Colocar o controlador das válvulas\
na posição REM [7] " -d 7
      echo;;
  2) echo -----\
-----
      echo Executar cada um dos procedimentos e de\
seguida premir os dígitos indicados.
      echo -----\
-----
      read -s -p "Verificar se as garrafas de ar e CO\
estão fechadas [1] " -d 1
      echo
      read -s -p "Abrir a válvula que liga a bomba de\
vácuo ao sistema [2] " -d 2
      echo
      read -s -p "Colocar o controlador das válvulas\
na posição MAN [3] " -d 3

```

## E. Gas sensor testing procedure

```
    echo
    echo "Ligar válvula 2 e esperar que a pressão\
atinja 60 mbar"
    read -s -p "Se necessário abrir a válvula de\
agulha do ar [4] " -d 4
    echo
    read -s -p "Desligar válvula 2 (e fechar a\
válvula de agulha) [5] " -d 5
    echo
    read -s -p "Abrir as garrafas de ar e CO [6] " -d 6
    echo
    read -s -p "Ligar válvula 5 e esperar que a\
pressão suba aos 1200 mbar [7] " -d 7
    echo
    echo "Abrir totalmente a válvula de saída e\
ajustar a válvula"
    read -s -p "de agulha do ar até o fluxímetro\
indicar 120 mm [8] " -d 8
    echo
    echo "Ligar válvula 3 e ajustar a válvula de agulha"
    read -s -p "do CO até o fluxímetro indicar 40 mm\
[9] " -d 9
    echo
    read -s -p "Desligar válvula 3 e esperar 30\
segundos [10] " -d 0
    echo
    read -s -p "Desligar válvula 5 [11] " -d 1
    echo
    read -s -p "Colocar o controlador das válvulas na\
posição REM [12] " -d 2
    echo;;
esac
fi

mkdir -p "$HOME/tmp"
echo "$directoria/$amostra-$ensaio.dat"\
> $HOME/tmp/fich-res
echo "$comentarios#" >> $HOME/tmp/fich-res
echo "$segundos" >> $HOME/tmp/fich-res
echo "$temperatura" >> $HOME/tmp/fich-res
echo "$tempmin" >> $HOME/tmp/fich-res
echo "$numdeg" >> $HOME/tmp/fich-res
echo "$tempest" >> $HOME/tmp/fich-res
echo "$tempres" >> $HOME/tmp/fich-res
echo "$temprec" >> $HOME/tmp/fich-res
echo "$resposta" >> $HOME/tmp/fich-res
echo "$pulsos" >> $HOME/tmp/fich-res

nohup sensor.exe &
```



```
exit 0
```

---

Another script was written to help the users of the gas sensor testing chamber to stop an experiment or change the samples. Three different procedures may be selected: 1) Interrupt an experiment, 2) Change a sample or 3) Halt the experiments for some days. The first one is used to stop a running experiment. If program `sensor.exe` is running, it is stopped and then program `sensor-off.exe` is started. The second is used to describe the procedure needed to take out a sample and place a new one inside the chamber. The third describes the procedure recommended to leave the experimental setup safely stopped for some days.

---

**Program E.2:** Bash script used to stop a gas sensing test or take a sample out of the chamber  
(`sensor-off`)

---

```
#!/bin/bash
# Bash version 2.04.11 or higher
programa=`ps -u $USER | grep -e 'sensor.exe' |\
grep -v -e 'grep'`
numero=`expr "$programa" : '[^0-9]*\([0-9]*\)\'`
lingua=1
read -e -p "Choose language: Português (1)\
English (2)? " lingua
if expr "$lingua" != 1 > /dev/null
then
    echo "Choose the procedure:"
    echo "1) Interrupt an experiment"
    echo "2) Change a sample"
    echo "3) Halt the experiments for some days"
    while expr \( "$procedi" != 1 \) \& \( "$procedi" \
!= 2 \) \& \( "$procedi" != 3 \) > /dev/null
    do
read -e -p "Choice? " procedi
    done
    case $procedi in
    1) if kill "$numero" 2> /dev/null
    then
echo Wait 15 minutes for the heater cooling!
sleep 300
sensor-off.exe && echo "Cooling ended."
        else
echo "There was no program running or\
it did not stop."
echo "Please call the maintainer if\
something is wrong."
        fi;;
    2) echo -----\
-----\
        echo Follow each procedure and press the digits\
inside the brackets.
        echo -----\
-----\

```

## E. Gas sensor testing procedure

```
-----  
    echo "Verify that sample temperature is below 40° C"  
    read -s -p "and pressure in the chamber above\  
1010 mbar [1] " -d 1  
    echo  
    echo "Verify that valve connecting vacuum pump\  
to system is open"  
    read -s -p "and all the electric valves are off\  
[2] " -d 2  
    echo  
    read -s -p "Switch valve controller to MAN\  
position [3] " -d 3  
    echo  
    read -s -p "Switch on valve 1 [4] " -d 4  
    echo  
    read -s -p "Open the chamber and change the\  
sample [5] " -d 5  
    echo  
    echo "Verify that the needle contacts are\  
pressing on the film"  
    read -s -p "and close the chamber [6] " -d 6  
    echo  
    echo "Switch on valve 2 and wait for"  
    read -s -p "the pressure to reach 60 mbar [7] " -d 7  
    echo  
    read -s -p "Switch off valves 2 and 1 [8] " -d 8  
    echo  
    read -s -p "Switch valve controller to REM\  
position [9] " -d 9  
    echo  
    echo "The chamber is ready for the experiments"  
    echo -----\  
-----; ;  
    3) echo -----\  
-----  
    echo Follow each procedure and press the digits\  
inside the brackets.  
    echo -----\  
-----  
    read -s -p "Close de air and CO bottles [1] " -d 1  
    echo  
    read -s -p "Close exit valve [2] " -d 2  
    echo  
    read -s -p "Switch valve controller to MAN\  
position [3] " -d 3  
    echo  
    read -s -p "Switch on valve 2 and open air\  
needle valve [4] " -d 4  
    echo
```

```

    read -s -p "Switch on valve 3 and open CO\
needle valve [5] " -d 5
    echo
    read -s -p "Wait for both flowmeters to reach\
0 mm [6] " -d 6
    echo
    read -s -p "Switch off valve 3 and 2 [7] " -d 7
    echo
    read -s -p "Switch valve controller to REM\
position [8] " -d 8
    echo
    read -s -p "Close air and CO needle valves\
[9] " -d 9
    echo
    read -s -p "Close valve connecting vacuum pump\
to system [10] " -d 0
    echo
    read -s -p "Switch off valve controller [11] " -d 1
    echo
    echo -----\
-----;
    esac
else
    echo "Escolher o procedimento:"
    echo "1) Interromper uma experiência"
    echo "2) Substituir uma amostra"
    echo "3) Parar as experiência por alguns dias"
    while expr \( "$procedi" != 1 \) \& \( \
"$procedi" != 2 \) \& \( "$procedi" != 3 \) > /dev/null
    do
        read -e -p "Opção? " procedi
    done
    case $procedi in
    1) if kill "$numero" 2> /dev/null
    then
        echo Esperar 15 minutos para que a amostra\
arrefeça!
        sleep 300
        sensor-off.exe && echo "O arrefecimento\
terminou."
    else
        echo "O programa das experiências não estava\
a correr ou não foi terminado."
    echo "Se existir algum problema fale com o\
responsável pela experiência."
    fi;;
    2) echo -----\
-----
        echo Executar cada um dos procedimentos e de\

```

## E. Gas sensor testing procedure

```
seguida premir os dígitos indicados.
echo -----\
-----
echo "Verificar se a temperatura da amostra é\
inferior a 40° C"
read -s -p "e a pressão na câmara acima de\
1010 mbar [1] " -d 1
echo
echo "Verificar se a válvula que liga a bomba de\
vácuo ao sistema está aberta"
read -s -p "e as válvulas eléctricas estão\
desligadas [2] " -d 2
echo
read -s -p "Colocar o controlador das válvulas\
na posição MAN [3] " -d 3
echo
read -s -p "Ligar válvula 1 [4] " -d 4
echo
read -s -p "Abrir a câmara e substituir a\
amostra [5] " -d 5
echo
echo "Verificar se os contactos eléctricos\
estão sobre o filme"
read -s -p "e depois fechar a câmara [6] " -d 6
echo
echo "Ligar válvula 2 e esperar que"
read -s -p "a pressão na câmara atinja 60 mbar\
[7] " -d 7
echo
read -s -p "Desligar as válvulas 2 and 1 [8] " -d 8
echo
read -s -p "Colocar o controlador das válvulas\
na posição REM [9] " -d 9
echo
echo "A câmara está pronta para as experiências."
echo -----\
-----;;
3) echo -----\
-----

echo Executar cada um dos procedimentos e de\
seguida premir os dígitos indicados.
echo -----\
-----

read -s -p "Fechar as garrafas de ar e de CO\
[1] " -d 1
echo
read -s -p "Fechar a válvula de saída [2] " -d 2
echo
read -s -p "Colocar o controlador das válvulas\
```

```

na posição MAN [3] " -d 3
    echo
    read -s -p "Ligar válvula 2 e abrir a válvula\
de agulha do ar [4] " -d 4
    echo
    read -s -p "Ligar válvula 3 e abrir a válvula\
de agulha do CO [5] " -d 5
    echo
    read -s -p "Esperar que ambos os fluxímetros\
indiquem 0 mm [6] " -d 6
    echo
    read -s -p "Desligar válvulas 3 e 2 [7] " -d 7
    echo
    read -s -p "Colocar o controlador das válvulas\
na posição REM [8] " -d 8
    echo
    read -s -p "Fechar as válvulas de agulha do ar\
e do CO [9] " -d 9
    echo
    read -s -p "Fechar a válvula que liga a bomba de\
vácuo ao sistema [10] " -d 0
    echo
    read -s -p "Desligar o controlador das válvulas\
[11] " -d 1
    echo
    echo -----\
----- ;
    esac
fi
exit 0

```

---

## E.2. The program

Program `sensor.c` contains the source code of program `sensor.exe`. This program is used to control the valves during gas sensing tests and register the measured temperature and resistance values. It reads sequentially the parameters from file `fich-res` stored in directory `$HOME/tmp`.

---

**Program E.3:** C program used to control the equipment and acquire the data during gas sensing tests (`sensor.c`)

---

```

#version 1.9 (01/01/2002)

#include <sys/types.h>
#include <sys/stat.h>
#include <sys/ioctl.h>
#include <fcntl.h>
#include <termios.h>
#include <unistd.h>

```

## E. Gas sensor testing procedure

```
#include <stdio.h>
#include <errno.h>
#include <string.h>
#include <stdlib.h>
#include <time.h>
#include <linux/ppdev.h>

#define BAUDRATEHP B9600
#define BAUDRATECT B9600
#define HPDEV "/dev/ttyS0"
#define CTDEV "/dev/ttyS2"
#define PPDEV "/dev/parport0"
#define TDATA 80
#define THORA 9
#define TCO 240
#define TVAC 600
#define TAR 300
#define VALV1 0xfe
#define VALV2 0xfd
#define VALV3 0xfb
#define VALV4 0xf7
#define VALV5 0xef
#define VALV6 0xdf
#define VALV7 0xbf
#define REMOFF 0x7f
#define REMON 0xff

char inst[THORA];
void instante(char inst[]);
int calcbcc(unsigned char msg[], int msgnum);
int openhp(void);
int openct(void);
int openpp(void);
int mederes(int fdio);
int medevolt(int fdio);
int selrange(int fdio, FILE *fpo);
int ctinit(int fdio);
int ppinit(int fdio);
int commode(int fdio);
int rammode(int fdio);
int tempcic(int fdio);
int changesv(int fdio, float svtemp);
int levalor(int fdhp, int fdct, FILE *fpo, unsigned int resol);
float celsius(unsigned char inmsg[]);
int erroct(unsigned char msg[]);

main ()
{
    FILE *fpi, *fpo, *fpl;
```

```

int fdhp, fdct, fdpp, n, mciclo=1, sobdesc=-1;
unsigned int segu, nn, numdeg, tempoest, tempores, temporec;
unsigned int nnn, pulsos, mede, resol;
unsigned char *vcont=(unsigned char *)malloc(2);
float stemp, tempmax, tempmin, degdif;
char *data=(char *)malloc(TDATA), fich[60], notas[80];
char *fichtmp=(char *)malloc(60);
time_t tp;
struct tm agora;

if ((tp=time(NULL))== -1)
    printf("time: nao foi possivel saber a data!\n");
else
    agora=*localtime(&tp);

strftime(data, TDATA, "Data: %d/%m/%Y Inicio: %H:%M:%S\n", &agora);
fichtmp=getenv("HOME");
strcat(fichtmp, "/tmp/fich-res");
fpi=fopen(fichtmp, "r");
fscanf(fpi, "%s\n%[^#]#%u\n%f\n%f\n%u\n%u\n%u\n%u\n%u\n%u", fich,\
notas, &segu, &tempmax, &tempmin, &numdeg, &tempoest, &tempores,\
&temporec, &mede, &pulsos);
fclose(fpi);

fpo=fopen(fich, "a");
fichtmp=getenv("HOME");
strcat(fichtmp, "/tmp/sensor.erros");
fpl=fopen(fichtmp, "w");
fprintf(fpo, "%s#%s\n\n", data, notas);

fdhp=openhp();
fdct=openct();
fdpp=openpp();

/*Inicializa multimetro*/
if (mede==1)
    mederes(fdhp);
else {
    medevolt(fdhp);
    selrange(fdhp, fpo);
}

/*Inicializa controlador das valvulas*/
*vcont = REMON;
ppinit(fdpp);

/*Inicializa controlador de temperatura*/
stemp=tempmax;
ctinit(fdct);

```

## E. Gas sensor testing procedure

```
if (numdeg > 1)
    degdif=(tempmax-tempmin)/(numdeg-1);
else
    degdif=0.00;
tempoest=tempoest*60*60;
tempores=tempores*60;
temporec=temporec*60;

for (n=0; n < (numdeg*2-1); ++n) {
    changesv(fdct, stemp);

    resol=10;
    /*Limpa camara durante 10 minutos*/
    /*Desliga valvula 5; liga valvula 1*/
    *vcont |= ~VALV5;
    *vcont &= VALV1;
    ioctl(fdpp, PPWDATA, vcont);
    sleep(1);
    /*Liga valvula 2*/
    *vcont &= VALV2;
    ioctl(fdpp, PPWDATA, vcont);
    for (nn=0; nn<TVAC; nn+=resol)
        levalor(fdhp,fdct,fpo,resol);

    /*Desliga valvula 2*/
    *vcont |= ~VALV2;
    ioctl(fdpp, PPWDATA, vcont);
    sleep(1);
    /*Desliga valvula 1*/
    *vcont |= ~VALV1;
    ioctl(fdpp, PPWDATA, vcont);
    sleep(1);
    /*Fim da limpeza*/

    for (nn=0; nn<TAR; nn+=resol)
        levalor(fdhp,fdct,fpo,resol);
    /*Liga valvula 5*/
    *vcont &= VALV5;
    ioctl(fdpp, PPWDATA, vcont);
    for (nn=0; nn<tempoest; nn+=resol)
        levalor(fdhp,fdct,fpo,resol);

    for (nnn=0; nnn<pulsos; ++nnn) {
        /*Liga valvula 3*/
        *vcont &= VALV3;
        ioctl(fdpp, PPWDATA, vcont);
        instante(inst);
        fprintf(fpo, "\n# Liga CO as: %s\n\n", inst);
    }
}
```



```

    resol=segu;
    for (nn=0; nn<tempores; nn+=resol) {
levalor(fdhp,fdct,fpo,resol);
    }
    /*Liga valvulas 1 e 4; desliga valvulas 3 e 5*/
    *vcont |= (~VALV3 | ~VALV5);
    *vcont &= (VALV1 & VALV4);
    ioctl(fdpp, PPWDATA, vcont);
    sleep(1);
    /*Se necessario alterar aqui parametros do CT*/
    /*Liga valvula 2*/
    *vcont &= VALV2;
    ioctl(fdpp, PPWDATA, vcont);

    resol=3;
    for (nn=0; nn<TCO; nn+=resol) {
levalor(fdhp,fdct,fpo,resol);
    }

    /*Desliga valvula 2*/
    *vcont |= ~VALV2;
    ioctl(fdpp, PPWDATA, vcont);
    sleep(1);
    /*Desliga valvula 1*/
    *vcont |= ~VALV1;
    ioctl(fdpp, PPWDATA, vcont);

    for (nn=0; nn<180; nn+=resol) {
levalor(fdhp,fdct,fpo,resol);
    }

    /*Liga valvula 5; desliga valvula 4*/
    *vcont |= ~VALV4;
    *vcont &= VALV5;
    ioctl(fdpp, PPWDATA, vcont);
    instante(inst);
    fprintf(fpo, "\n# Desliga CO as: %s\n\n", inst);

    resol=segu;
    for (nn=0; nn<temporec; nn+=resol) {
if ((nn+resol) > temporec)
    resol=temporec-nn;
levalor(fdhp,fdct,fpo,resol);
    }
    }
    mciclo++;
    stemp=stemp+sobdesc*degdif;
    if (mciclo==numdeg)

```

## E. Gas sensor testing procedure

```
        sobdesc=1;
    }

    /*Desliga aquecedor*/
    stemp=10;
    changesv(fdct, stemp);

    sleep(600);
    *vcont = REMON;
    ioctl(fdpp, PPWDATA, vcont);
    fclose(fpl);
    fclose(fpo);
    close(fdhp);
    close(fdct);
    close(fdpp);

return 0;
}

void instante(char inst[]) {
... see program B.10 on page 119 ...}

int calcbcc(unsigned char msg[], int msgnum) {
... see program A.2 on page 99 ...}

int medevolt(int fdhp) {
... see program D.3 on page 140 ...}

int selrange(int fdhp, FILE *fpo) {
... see program D.2 on page 139 ...}

int mederes(int fdhp) {
... see program D.4 on page 141 ...}

int ctinit(int fdct) {

    if (commode(fdct)==1) {
        printf("Nao foi ativado o Communication Mode!\n");
        exit(-1);
    }
    if (rammode(fdct)==1) {
        printf("Nao foi ativado o RAM Mode!\n");
        exit(-1);
    }
    if (tempcic(fdct)==1) {
        printf("Nao foi alterado o PCS!\n");
        exit(-1);
    }

    return 0;
}
```

```

}

int ppinit(int fdpp) {
... see program C.2 on page 135 ...}

int comcode(int fdct) {
... see program A.3 on page 101 ...}

int ramcode(int fdct) {
... see program A.4 on page 102 ...}

int tempcic(int fdct) {
... see program A.5 on page 102 ...}

int levalor(int fdhp, int fdct, FILE *fpo, unsigned int resol) {
... see program E.4 on page 165 ...}

float celsius(unsigned char inmsg[]) {
... see program B.11 on page 119 ...}

int erroct(unsigned char msg[]) {
... see program A.7 on page 104 ...}

int openhp(void) {
... see program D.1 on page 138 ...}

int openct(void) {
... see program A.1 on page 96 ...}

int openpp(void) {
... see program C.1 on page 135 ...}

int changesv(int fdct, float sv) {
... see program A.6 on page 103 ...}

```

---

In order to be able to read the temperature and resistance values at close instants, a new routine `levalor` was written. This routine triggers multimeter measurements and reads the values from the multimeter and from the temperature controller. It also writes the time, temperature and resistance (or voltage) values to the output file and then exits returning always 0.

---

**Program E.4:** C program used to read the values from the multimeter and the temperature controller (`levalor`)

---

```

int levalor(int fdhp, int fdct, FILE *fpo, unsigned int resol) {
    char sinal[18];
    unsigned int segu;
    unsigned char inmsg[24];
    float temperatura, oor;

    instante(inst);

```

## E. Gas sensor testing procedure

```
write(fdhp, ":READ?\n", 7);
write(fdct, "@01D1:4E\r", 9);
sleep(resol);

while (read(fdhp, &sinal, 18)==0)
    ;
while (read(fdct, &inmsg, 23)==0)
    ;

/* Verifica o valor da tensao */
while (sscanf(sinal,"%f",&oor)>1e+6) {
    selrange(fdhp,fpo);
    instante(inst);
    write(fdhp, ":READ?\n", 7);
    write(fdct, "@01D1:4E\r", 9);
    sleep(1);
    while (read(fdhp, &sinal, 18)==0)
        ;
    while (read(fdct, &inmsg, 23)==0)
        ;
}

temperatura=celsius(inmsg);
fprintf(fpo, "%s\t%.15s\t%.5.1f\n", inst, sinal, temperatura);
fflush(fpo);
tcflush(fdhp,TCIOFLUSH);
tcflush(fdct,TCIOFLUSH);

return 0;
}
```

---

Program `sensor-off.c` is used to cool the sample and switch off the electric valves when a gas sensing test is stopped by the user, before the procedure is finished. It is run when the first procedure option of script `sensor-off` is selected.

---

**Program E.5:** C program used to turn off the heater and the electric valves when a gas sensor test is interrupted (`sensor-off.c`)

---

```
#include <sys/types.h>
#include <sys/stat.h>
#include <sys/ioctl.h>
#include <fcntl.h>
#include <termios.h>
#include <unistd.h>
#include <stdio.h>
#include <errno.h>
#include <string.h>
#include <stdlib.h>
#include <linux/ppdev.h>
```

```

#define BAUDRATECT B9600
#define CTDEV "/dev/ttyS4"
#define PPDEV "/dev/parport0"
#define VALV5 0xef
#define REMON 0xff
#define REMOFF 0x7f

int calcbcc(unsigned char msg[], int msgnum);
int openct();
int openpp(void);
int commode(int fdio);
int rammode(int fdio);
int ppinit(int fdio);
int changesv(int fdio, float temperatura);
int erroct(unsigned char msg[]);

main ()
{
    int fdct, fdpp;
    float stemp=10;
    unsigned char *vcont=(unsigned char *)malloc(2);

    fdpp=openpp();
    *vcont = ON;
    ppinit(fdpp);
    /*Liga valvula 5*/
    *vcont &= VALV5;
    ioctl(fdpp, PPWDATA, vcont);

    fdct=openct();

    if (commode(fdct)==1)
        printf("Nao foi ativado o Communication Mode!\n");
    if (rammode(fdct)==1)
        printf("Nao foi ativado o RAM Mode!\n");
    if (changesv(fdct, stemp)==1)
        printf("A resistencia ficou ligada!!!\n");

    close(fdct);

    sleep(600);
    *vcont = OFF;
    ioctl(fdpp, PPWDATA, vcont);
    close(fdpp);

    return 0;
}

int calcbcc(unsigned char msg[], int msgnum) {
... see program A.2 on page 99 ...}

```

## *E. Gas sensor testing procedure*

```
int commode(int fdct) {  
... see program A.3 on page 101 ...}  
  
int rammode(int fdct) {  
... see program A.4 on page 102 ...}  
  
int erroct(unsigned char msg[]) {  
... see program A.7 on page 104 ...}  
  
int ppinit(int fdpp) {  
... see program C.2 on page 135 ...}  
  
int openpp(void) {  
... see program C.1 on page 135 ...}  
  
int openct(void) {  
... see program A.1 on page 96 ...}  
  
int changesv(int fdct, float sv) {  
... see program A.6 on page 103 ...}
```

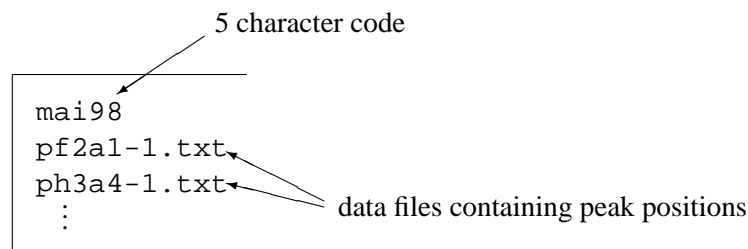
---

## F. Optical parameters computation

The program used to compute optical parameters was named `espessuras`. It was entirely written in Fortran 77 mainly because the author was familiarised with this language and needed to develop rapidly a tool that helped in the analysis of the growing number of transmittance spectra of produced films. Therefore most of the decision related to the program structure reflect restriction imposed by this programming language and some lack of skill of the programmer. The latest version of this language, Fortran 90, provides much more features than its predecessor and therefore should be considered on future improvements of the program. Since Fortran 77 is compatible with the new standard, some of the routines may be used in the future versions.

### F.1. The input files

The program starts by reading the file `ficheiros.esp`, which is a text file containing in the first line, a five character code that describes the set of data<sup>1</sup>. The following lines are the names of the data files containing the peak positions of each spectrum. These filenames have to start with a `p`, followed by a code containing 5, 6 or 7 characters identifying the data and ending with a `.txt` extension. To go ahead with the calculations, filenames starting with a `v` and containing the valley positions, must exist for each listed file. These should be identified by the same character code of the corresponding peak files and also end with a `.txt` extension. An example of the input file of program `espessuras` is shown in Fig. F.1. This file has to be put in a directory called `tmp` under the user home directory, `$HOME`.



The diagram shows a text file with the following content:

```
mai98
pf2a1-1.txt
ph3a4-1.txt
:
```

Annotations:

- An arrow points from the text "5 character code" to the first line "mai98".
- Two arrows point from the text "data files containing peak positions" to the second and third lines "pf2a1-1.txt" and "ph3a4-1.txt".

Figure F.1.: Example of input file `ficheiros.esp` of program `espessuras`

As in the case of programs described before, Bash script F.1 was written in order to help producing the input file with the format and in the location required by the `espessuras` program. An English version of this script was not yet produced. The variables used are easily identified and do not require any further description. This script, after writing the input file on disk, runs the program `espessuras.exe` which is the compiled version of `espessuras.f`.

<sup>1</sup>This code was thought to hold the month and year identifying the set of calculations. In order to change its size, the format specifier, `A5`, in line

```
10  FORMAT ('# Resultado do calculo da espessura'/
+         '# Data: ',A5)
```

has to be modified.

---

**Program F.1:** Bash script used to produce the input file of program *espessuras* (calc-esp)

---

```
#!/bin/bash
confirmacao='n'
directoria="/tmp"
until ls "$directoria" > /dev/null
do
    mkdir "$directoria"
done
echo -e "Calcula as espessuras a partir dos extremos\
relativos dos expectros\nde transmissão. Correr este\
script _na directoria_ onde estão os\nficheiros!"
while expr "$confirmacao" != s > /dev/null
do
    echo -n "Grupo de ficheiros (mmmAA)? "
    read -e ficheiro
    echo $ficheiro >$directoria/ficheiros.esp
    mais='s'
    while expr "$mais" = s > /dev/null
    do
        echo -n "Nome do ficheiro (pfilename.txt)? "
        read -e ficheiro
        ls -l $ficheiro >>$directoria/ficheiros.esp
        echo -n "Mais ficheiros (s/n)? "
        read -e mais
    done
    echo
    cat $directoria/ficheiros.esp
    echo -n "Tudo certo (s/n)? "
    read -e confirmacao
done
espessuras.exe &
exit 0
```

---

## F.2. The program

Program *espessuras* (F.2) declares seven constants of type `INTEGER`, described in Table F.1: `inv`, `inp`, `fich`, `out`, `calc`, `nfich` and `nmax`. The first five are the `UNIT` number specifiers of, respectively, the valley data original file, the peak data original file, the program input file, the output results file and the output auxiliary file. Constant `nfich` defines the maximum number of peak files that may be analysed each time the program is run and has to match the number of elements of array `filein`. If `nfich` was to be modified, the number of elements of array `filein`, should also be modified in line

```
CHARACTER*13 filein(99)
```

because some loop constructs rely on constant `nfich` to stop before the last `filein` array element. The maximum number of peak files that may be analysed in a single program run is



the number attributed to `nfich` in the `PARAMETER` declaration subtracted, by one<sup>2</sup>. Constant `nmax` must match the number of elements of arrays `xv`, `xp`, `yv` and `yp`. Just like constant `nfich`, it has to be changed if the number of elements of the arrays `xv`, `xp`, `yv` and `yp` were to be modified. This constant defines the maximum number of peaks or valleys that the program can read from the original data files.

Table F.1.: Constants defined in the main program unit of `espestras.f`

Variable	Description
<code>inv</code>	UNIT number specifier of the peak data original file.
<code>inp</code>	UNIT number specifier of the valley data original file.
<code>fich</code>	UNIT number specifier of the program input file.
<code>out</code>	UNIT number specifier of the output results file.
<code>calc</code>	UNIT number specifier of the output auxiliary file.
<code>nfich</code>	maximum number of analysed peak files added to one
<code>nmax</code>	maximum number of peaks (or valleys) per spectrum

It may also be observed in program F.2 that there are seven `INTEGER` variables: `n`, `j`, `k`, `nf`, `err`, `vv` and `pp`; four `REAL` variables: `xv`, `xp`, `yv` and `yp`; and eight `CHARACTER` variables: `filein`, `finaux11`, `finaux12`, `finaux13`, `foutaux10`, `foutaux11`, `foutaux12` and `foutaux13`. Some are auxiliary variables whose meaning is easily identified in the program structure, that is the case of `n`, `j`, `k`, `err`, `finaux11`, `finaux12`, `finaux13`, `foutaux10`, `foutaux11`, `foutaux12` and `foutaux13`. Then there is the `filein` array, whose first element holds the five character code that identifies the set of data values analysed, and the elements with subscripts from 2 to `nf` hold the peak file names to be analysed. The variable `nf` is then the highest subscript value of `filein` array that holds a peak file name to be analysed. The arrays `xp` and `yp` hold respectively the wavelength values in nanometre and the transmittance in percentage. The corresponding values for valleys are `xv` and `yv`. Finally `pp` and `vv` hold, respectively, the number of peaks read by the program and the number of valleys.

Table F.2.: Most important variables used in the main program unit

Variable	Description
<code>filein(1)</code>	five character code that identifies the set of data values to be analysed
<code>filein(i)</code>	with <code>i</code> between 2 and <code>nf</code> holds the name of a peak file to be analysed
<code>nf</code>	number of filenames stored in array <code>filein</code> added to one
<code>xp</code>	wavelength of peaks in nanometre
<code>yp</code>	transmittance of peaks in percentage
<code>xv</code>	wavelength of valleys in nanometre
<code>yv</code>	transmittance of valleys in percentage
<code>pp</code>	number of peak values stored in arrays <code>xp</code> and <code>yp</code>
<code>vv</code>	number of valleys stored in arrays <code>xv</code> and <code>yv</code>

The main program calls only two routines: `INVERTE` and `AESPEC`, whose action is explained below. The other routines described are called by the subroutines and not by the main program.

<sup>2</sup>The first element of array `filein` is used to hold the five character code that describes the set of data (see also Table F.2).

**Program F.2:** Fortran program used to analyse the interference fringe values observed in the optical transmittance spectra (espessuras.f)

```

    INTEGER      n, j, k, inp, inv, out, calc, fich, nfich, nf, err,
+              vv, pp, nmax
    REAL         xv(50), xp(50), yp(50), yv(50)
    CHARACTER*13 filein(99)
    CHARACTER    finaux11*11, finaux12*12, finaux13*13,
+              foutaux10*10, foutaux11*11, foutaux12*12,
+              foutaux13*13
    PARAMETER    (inv=1, inp=2, fich=3, out=4, calc=5, nfich=99,
+              nmax=50)

10  FORMAT ('# Resultado do calculo da espessura'/
+         '# Data: ',A5)
11  FORMAT ('Nao foi encontrado o ficheiro v',A)

    OPEN (fich, FILE="/tmp/ficheiros.esp", STATUS='OLD')
    READ (fich,'(A)',ERR=20,END=20) (filein(j), j=1, nfich)
20  CLOSE (fich)
    nf=j-1

    DO 90 k=2,nf

        err=-1
        IF (filein(k)(12:12).EQ.' ') THEN
            finaux11=filein(k)(1:11)
            foutaux10=finaux11(2:7)//'.esp'
            foutaux11=finaux11(2:7)//'.calc'
            OPEN (inp, FILE=finaux11, STATUS='OLD')
            finaux11='v'//filein(k)(2:11)
            OPEN (inv, FILE=finaux11, ERR=80, IOSTAT=err, STATUS='OLD')
            OPEN (out, FILE=foutaux10, STATUS='NEW')
            OPEN (calc, FILE=foutaux11, STATUS='NEW')
        ELSEIF (filein(k)(13:13).EQ.' ') THEN
            finaux12=filein(k)(1:12)
            foutaux11=finaux12(2:8)//'.esp'
            foutaux12=finaux12(2:8)//'.calc'
            OPEN (inp, FILE=finaux12, STATUS='OLD')
            finaux12='v'//filein(k)(2:12)
            OPEN (inv, FILE=finaux12, ERR=80, IOSTAT=err, STATUS='OLD')
            OPEN (out, FILE=foutaux11, STATUS='NEW')
            OPEN (calc, FILE=foutaux12, STATUS='NEW')
        ELSE
            finaux13=filein(k)
            foutaux12=finaux13(2:9)//'.esp'
            foutaux13=finaux13(2:9)//'.calc'
            OPEN (inp, FILE=finaux13, STATUS='OLD')
            finaux13='v'//filein(k)(2:13)
            OPEN (inv, FILE=finaux13, ERR=80, IOSTAT=err, STATUS='OLD')

```

```

        OPEN (out, FILE=foutaux12, STATUS='NEW')
        OPEN (calc, FILE=foutaux13, STATUS='NEW')
ENDIF

WRITE (out,10) filein(1)

n=1
READ (inp,'(/)')
33  READ (inp,*,ERR=36,END=36) j, xp(n), yp(n)
    n=n+1
    IF (n.LT.(nmax+1)) GO TO 33
36  CONTINUE
    j=n-1

    CALL INVERTE(xp,j)
    CALL INVERTE(yp,j)
    pp=j

n=1
READ (inv,'(/)')
43  READ (inv,*,ERR=46,END=46) j, xv(n), yv(n)
    n=n+1
    IF (n.LT.(nmax+1)) GO TO 43
46  CONTINUE
    j=n-1

    CALL INVERTE(xv,j)
    CALL INVERTE(yv,j)
    vv=j

CALL AESPEC(pp,xp,yp,vv,xv,yv)

80  IF (err.GT.0) THEN
        PRINT 11, filein(k)(2:)
    ENDIF
    CLOSE (inp, ERR=90)
    CLOSE (inv, ERR=90)
    CLOSE (out, ERR=90)
    CLOSE (calc, ERR=90)

90  CONTINUE

100 END

SUBROUTINE INVERTE(x, n)
[ ... see program F.3 on page 174 ... ]

SUBROUTINE AESPEC(np,px,py,nv,vx,vy)
[ ... see program F.4 on page 176 ... ]

```

## F. Optical parameters computation

```
SUBROUTINE ESCOLHE(px,py,vx,vy,l,p,v,w)
[ ... see program F.5 on page 179 ... ]
```

```
SUBROUTINE CTSLIT(n,pv,l,p,v)
[ ... see program F.6 on page 190 ... ]
```

```
SUBROUTINE EXTRAP(n,pv,xx,y)
[ ... see program F.7 on page 191 ... ]
```

```
SUBROUTINE ESPESS(l,p,v,d,dd,w,np)
[ ... see program F.8 on page 192 ... ]
```

---

Routine `INVERTE(x,n)` inverts a vector `x` with `n` elements. It is used to invert the peak and valley arrays (see program F.2).

---

### Program F.3: Fortran routine used to invert a vector array (`INVERTE`)

---

```
SUBROUTINE INVERTE(x, n)

INTEGER n, j
REAL x(n), aux

DO 10 j=1,n/2
    aux=x(n-j+1)
    x(n-j+1)=x(j)
    x(j)=aux
10 CONTINUE

END
```

---

Routine `AESPEC(np,px,py,nv,vx,vy)` receives the values of peaks and valleys, determines optical parameters and stores the calculated values in the output files. The function arguments are `np` the number of peaks, `px` the peaks' wavelengths, `py` the peaks' transmittance, `nv` the number of valleys, `vx` the valleys' wavelengths and `vy` the valleys' transmittance. Both the peaks and the valleys have to be stored in ascending order of wavelength in the arrays.

Table F.3.: Arguments of routine `AESPEC`

Variable	Description
<code>np</code>	number of peaks.
<code>nv</code>	number of valleys.
<code>px</code>	peak wavelengths in nanometre and in ascending order.
<code>py</code>	peak transmittance in percentage.
<code>vx</code>	valley wavelengths in nanometre and in ascending order.
<code>vy</code>	valley transmittance in percentage.

Two new constants are introduced in the routine: `lmin` and `lmax`. Constants `lmin` and `lmax` define, respectively, the minimum and maximum wavelengths that will be used in the

calculation, i.e., peaks and valleys with wavelength outside this interval will be rejected. This should roughly correspond to the interval where absorption is weak (see Section 3.4). Constants `out` and `calc` although not common to all the subroutines, are defined where needed with the same values used in the main program unit (see Table F.1).

Table F.4.: Constants introduced in routine AESPEC

Variable	Description
<code>lmin</code>	wavelength minimum value in nanometre.
<code>lmax</code>	wavelength maximum value in nanometre.

In this routine three new arrays are introduced: `l`, `p` and `v`. Variable `l` holds all the wavelengths in ascending order; `p` holds the transmittance values of the peaks and `v` holds the transmittance values of the valleys. The final thickness will be saved in variable `d` and the standard deviation of this value in `dd`. The other are auxiliary variables. Among the auxiliary variables the array `w` plays a special role and needs a detailed description, given below.

Table F.5.: Main variables introduced in routine AESPEC

Variable	Description
<code>l</code>	wavelength of peaks and valleys in ascending order.
<code>p</code>	value of the peak envelope curve at the wavelengths specified by <code>l</code> , expressed in the form required by Eq. 3.6 on page 35.
<code>v</code>	value of the valley envelope curve at the wavelengths specified by <code>l</code> , expressed in the form required by Eq. 3.7 on page 35.
<code>d</code>	layer thickness in nanometre.
<code>dd</code>	standard deviation of thickness value.

The array `w` is used to store information that may help to evaluate the usefulness of the final values. Before the calculus, some data is used to decide whether there are enough values to proceed. If there are not enough values, the program will write a brief message to the out file describing why the calculus was not performed and will proceed to the next spectrum that is to be analysed. The variables `w(5)`, `w(6)` and `w(7)` need to have a value different from 1, for the calculations to advance. After the calculus these variables will have a different meaning.

In the end of the routine, variable `w(1)` holds the number of points used in the thickness calculation, `w(2)` holds the subscript of array `l` where the first usable point is stored and `w(3)` holds the subscript corresponding to the last usable point. Variable `w(4)` is used to keep the lower subscript of array `v` where the experimental transmittance values are stored. Thus, if `w(4)=1` the experimental transmittance values of the valleys are stored in the `v` elements with odd subscript, and consequently experimental peak transmittance values are stored in the `p` array elements with even subscript. On the other hand, `w(4)=2` specifies that the experimental transmittance values of the valleys are stored in the `v` elements with even subscript and the peak transmittance values in the `p` elements with odd subscript. Variable `w(5)` assumes value 1 if the difference between the interference fringe order of consecutive fringes exceeds constant `mdif0` (see Table F.8) and value 0 otherwise<sup>3</sup>. Variables `w(6)` and `w(7)` hold respectively the minimum and maximum difference of the interference fringe order of two consecutive fringes. Variable `w(8)` holds the number of points eliminated because of a missing value. Variable `w(9)` takes the value 0 if the sequence of peak transmittance is monotonous. Otherwise it will

<sup>3</sup>Interference fringe order of each point is stored in the auxiliary output file and can be checked afterwards if needed.

## F. Optical parameters computation

count the oscillations. Finally,  $w(10)$  holds the number of points with interference fringe order in agreement with the final thickness value.

Table F.6.: The auxiliary array  $w$

Variable	Description
$w(1)$	Number of points used in the thickness calculation.
$w(2)$	Subscript of array $l$ holding first usable point.
$w(3)$	Equal to $w(2) + w(1) - 1$ .
$w(4)$	Lowest subscript corresponding to experimental transmittance of valleys. May have value 1 or 2.
$w(5)$	Has value 1 when there is at least one peak or value missing in the sequence. In this case the optical parameters are not determined and the program proceeds analysing the next spectrum. The value of this variable must be 0 in order to advance with the calculations. On subroutine <code>ESPESS</code> this variable may assume value 1 if the difference between the interference fringe order of consecutive fringes exceeds constant <code>mdif0</code> (see program F.8).
$w(6)$	Has value 1 when there are less than four points to perform the calculus. In this case the optical parameters are not determined and the program proceeds analysing the next spectrum. The value of this variable must be 0 in order to advance with the calculations. On subroutine <code>ESPESS</code> this variable holds the minimum difference of the interference fringe order of two consecutive fringes.
$w(7)$	Holds the maximum difference of the interference fringe order of two consecutive fringes.
$w(8)$	Number of points eliminated because of a missing value.
$w(9)$	Takes the value 0 if the sequence of peak transmittance is monotonous. Otherwise it will count the oscillations.
$w(10)$	Number of points with interference fringe order in agreement with the final thickness value.

The routine `AESPEC` calls four other routines: `ESCOLHE`, `CTSLIT`, `EXTRAP` and `ESPESS`.

**Program F.4:** Fortran routine used to store the calculated values in the output files (`AESPEC`)

```

SUBROUTINE AESPEC(np,px,py,nv,vx,vy)

  INTEGER n, j, k, np, nv, out, calc, an, bn, w(10)
  REAL px(np), py(np), vx(nv), vy(nv), l(np+nv), p(np+nv),
+     v(np+nv), d, dd, lmin, lmax
  PARAMETER (out=4, calc=5, lmin=350., lmax=2.7E3)

C   Chooses values between lmin and lmax
  j=1
10  IF (px(j).LT.lmin) THEN
      j=j+1
      GOTO 10

```

```

ENDIF

k=j-1
30  IF ((px(j).LE.lmax).AND.(j.LE.np)) THEN
      px(j-k)=px(j)
      py(j-k)=py(j)
      j=j+1
      GOTO 30
ENDIF
an=j-1-k
DO 40 n=an+1,np
      px(n)=0.0
      py(n)=0.0
40  CONTINUE

j=1
50  IF (vx(j).LT.lmin) THEN
      j=j+1
      GOTO 50
ENDIF

k=j-1
70  IF ((vx(j).LE.lmax).AND.(j.LE.nv)) THEN
      vx(j-k)=vx(j)
      vy(j-k)=vy(j)
      j=j+1
      GOTO 70
ENDIF
bn=j-1-k
DO 80 n=bn+1,nv
      vx(n)=0.0
      vy(n)=0.0
80  CONTINUE
w(1)=an
w(2)=bn

IF (px(1).LT.vx(1)) THEN
      w(4)=2
ELSE
      w(4)=1
ENDIF

DO 200 j=5,10
      w(j)=0
200 CONTINUE
DO 210 j=1,np+nv
      l(j)=0.0
      p(j)=0.0
      v(j)=0.0

```

## F. Optical parameters computation

```
210 CONTINUE
CALL ESCOLHE(px,py,vx,vy,l,p,v,w)

k=w(4)+(-1)**(w(4)+1)
WRITE (calc, '(''# PICOS (sem correccao)')')
WRITE (calc, '(F9.1,F9.1)') (l(j),p(j)*100.,j=k,w(1),2)
WRITE (calc, '(//'# VALES (sem correccao)')')
WRITE (calc, '(F9.1,F9.1)') (l(j),v(j)*100.,j=w(4),w(1),2)

IF (w(5).EQ.1) THEN
    WRITE (out, '(''# Os picos/vales nao sao alternados')')
    GOTO 1000
ENDIF

IF (w(6).EQ.1) THEN
    WRITE (out, '(''# Nao existem picos/vales suficientes')')
    GOTO 1000
ENDIF

IF (w(7).EQ.1) THEN
    WRITE (out, '(''# O espectro nao apresenta picos/vales')')
    GOTO 1000
ENDIF

IF (w(8).GT.0) THEN
    WRITE (out, '(''# Foram eliminados',I2,
+         ' picos/vales')') w(8)
ENDIF

IF (w(9).GT.0) THEN
    WRITE (out, '(''# Os picos oscilaram',I2,' vezes')') w(9)
ENDIF

CALL CTSLIT(w(1),w(4),l,p,v)
WRITE (calc, '(''# CTSLIT')')
WRITE (calc, '(F9.1)') (l(j),j=1,w(1))

k=w(4)+(-1)**(w(4)+1)
CALL EXTRAP(w(1),k,l,p)
CALL EXTRAP(w(1),w(4),l,v)

CALL ESPESS(l,p,v,d,dd,w,w(1))

IF (w(5).EQ.1) THEN
    WRITE (out, '(''# Os numeros de ordem sao absurdos')')
ENDIF

WRITE (calc, '(''# PICOS (com correccao)')')
WRITE (calc, '(F9.1,F9.1)') (l(j),p(j)*100.,j=1,w(1))
```



```

WRITE (calc, '(//'# VALES (com correccao)')')
WRITE (calc, '(F9.1,F9.1)') (l(j),v(j)*100.,j=1,w(1))

WRITE (out, '( '# d= ',F6.0,' ' +- ',F4.0,' ' nm ( ',
+      4I3.2,I2,SP,2I4.2,' ' )')') d,dd,w(1),w(10),w(8),
+      w(9),w(5),w(6),w(7)

1000 END

```

Routine ESCOLHE(px,py,vx,vy,l,p,v,w) receives arrays px, py, vx, vy and w and returns l, p, v and w. It introduces three new constants: amin, bmin and homog. Constant homog holds the minimum percentage value difference between a peak (valley) and its consecutive valley (peak) transmittance. When thickness inhomogeneity is high the peak and valley transmittance values are very close and fringes are not well defined, thus the spectrum is rejected. Constant amin holds the minimum ratio between the transmittance value of peaks (valleys) with low wavelength and the peak (valley) with higher transmittance. This parameter is used to reject the points with low transmittance and low wavelength values, corresponding to the region of high absorption. In the high wavelength region, it is sometimes observed a decrease of the transmittance. The constant bmin is used to reject points with transmittance below its value multiplied by the highest peak (valley) transmittance.

Table F.7.: Constants introduced in routine ESCOLHE

Variable	Description
homog	Minimum percentage difference between a peak (valley) and its consecutive valley (peak) transmittance.
amin	Minimum ratio between the transmittance of peaks (valleys) with low wavelength and the peak (valley) with higher transmittance.
bmin	Minimum ratio between the transmittance of peaks (valleys) with high wavelength and the peak (valley) with higher transmittance.

Routine ESCOLHE detects some problems in the data but the final values should be validated by the user, especially in the case where fringe points are missing in the input data files. After several tests it was found that the best way to select the points was to look into the calculated interference fringe order. It is suggested not to use this routine in future versions.

---

**Program F.5:** Fortran routine that chooses points to use in the optical parameter calculation (ESCOLHE)

---

```

SUBROUTINE ESCOLHE(px,py,vx,vy,l,p,v,w)

INTEGER n, j, k, np(2), nv(2), out, an, bn, w(10)
REAL px(*), py(*), vx(*), vy(*), l(*), p(*),
+      v(*), aux1, aux2, amin, bmin, homog
PARAMETER (out=4, amin=0.80, bmin=0.98, homog=3.0)

np(1)=1
nv(1)=1
np(2)=w(1)

```

## F. Optical parameters computation

```

      nv(2)=w(2)
      WRITE (out, '( '# Constantes: ' ',2F5.2,F4.1)') amin,
+      bmin, homog

C      Checks if the there is some point missing in the sequence
C      Variables used:
C      j,k - auxiliary variables
C      n - number of sets without consecutive points
C      p(odd), v(odd) - lower subscript of set
C      p(even), v(even) - upper subscript of set
      n=1
      k=1
      j=1
      p(n)=1
      v(n)=1
      IF (w(4).EQ.1) THEN
5      IF (k.LT.nv(2)) THEN
          IF (px(j).LT.vx(k+1)) THEN
              IF (vx(k+1).LT.px(j+1)) THEN
                  j=j+1
              ELSE
                  IF (px(j+1).LT.200.) THEN
                      k=nv(2)-1
                  ELSE
                      p(n+1)=REAL(j)
                      v(n+1)=REAL(k)
                      j=j+1
                      n=n+2
                      p(n)=REAL(j)
                      v(n)=REAL(k+1)
                      IF ((vx(k+1).GE.px(j+1)).AND.
+                      ((j+1).LE.np(2))) THEN
                          j=j+1
                          p(n)=REAL(j)
                          IF ((vx(k+1).GE.px(j+1)).AND.
+                          ((j+1).LE.np(2))) THEN
                              w(5)=1
                              k=nv(2)-1
                          ENDIF
                      ENDIF
                      j=j+1
                  ENDIF
              ENDIF
          ELSE
              p(n+1)=REAL(j-1)
              v(n+1)=REAL(k)
              n=n+2
              p(n)=REAL(j)
              v(n)=REAL(k+1)

```

```

        ENDIF
        k=k+1
        GOTO 5
    ELSE
        IF (px(j).GT.200.) THEN
            p(n+1)=REAL(j)
        ELSE
            p(n+1)=REAL(j-1)
        ENDIF
        v(n+1)=REAL(k)
    ENDIF
ELSE
15  IF (k.LT.np(2)) THEN
        IF (vx(j).LT.px(k+1)) THEN
            IF (px(k+1).LT.vx(j+1)) THEN
                j=j+1
            ELSE
                IF (vx(j+1).LT.200.) THEN
                    k=np(2)-1
                ELSE
                    v(n+1)=REAL(j)
                    p(n+1)=REAL(k)
                    n=n+2
                    j=j+1
                    v(n)=REAL(j)
                    p(n)=REAL(k+1)
                    IF ((px(k+1).GE.vx(j+1)).AND.
+                      ((j+1).LE.nv(2))) THEN
                        j=j+1
                        v(n)=REAL(j)
                    IF ((px(k+1).GE.vx(j+1)).AND.
+                      ((j+1).LE.nv(2))) THEN
                        w(5)=1
                        k=np(2)-1
                    ENDIF
                ENDIF
                j=j+1
            ENDIF
        ENDIF
    ELSE
        v(n+1)=REAL(j-1)
        p(n+1)=REAL(k)
        n=n+2
        v(n)=REAL(j)
        p(n)=REAL(k+1)
    ENDIF
    k=k+1
    GOTO 15
ELSE

```

## F. Optical parameters computation

```

        IF (vx(j).GT.200.) THEN
            v(n+1)=REAL(j)
        ELSE
            v(n+1)=REAL(j-1)
        ENDIF
        p(n+1)=REAL(k)
    ENDIF
ENDIF
ENDIF

C    Chooses the bigger set
    n=2
    aux2=0.0
20  IF ((v(n).GE.1).OR.(p(n).GE.1)) THEN
        aux1=v(n)+p(n)-v(n-1)-p(n-1)+2
        IF (aux1.GT.aux2) THEN
            np(1)=INT(p(n-1))
            np(2)=INT(p(n))
            nv(1)=INT(v(n-1))
            nv(2)=INT(v(n))
            aux2=aux1
        ENDIF
        n=n+2
        GOTO 20
    ENDIF

WRITE (out,'(4I3)') w(4),np(2),nv(2)

C    Checks if there are enough points
    k=np(2)-np(1)
    j=nv(2)-nv(1)
    IF ((k.LT.2).OR.(j.LT.2)) THEN
        w(5)=1
    ENDIF
    IF (w(5).EQ.1) GOTO 1000

C    Puts the chosen values on vector arrays: px, py
    k=np(1)-1
    DO 21 n=np(1),np(2)
        px(n-k)=px(n)
        py(n-k)=py(n)
21  CONTINUE
    np(1)=1
    np(2)=np(2)-k
    w(8)=w(1)-np(2)

WRITE (out,'(3I3)') k,w(1),w(8)
DO 22 n=np(2)+1,w(1)
    px(n)=0.0
    py(n)=0.0

```

```

22  CONTINUE

C    Puts the chosen values on vector arrays: vx, vy
    k=nv(1)-1
    DO 25 n=nv(1),nv(2)
        vx(n-k)=vx(n)
        vy(n-k)=vy(n)
25  CONTINUE
    nv(1)=1
    nv(2)=nv(2)-k
    w(8)=w(8)+w(2)-nv(2)

    WRITE (out,'(3I3)') k,w(2),w(8)
    DO 26 n=nv(2)+1,w(2)
        vx(n)=0.0
        vy(n)=0.0
26  CONTINUE

    IF (px(1).LT.vx(1)) THEN
        w(4)=2
    ELSE
        w(4)=1
    ENDIF

C    Checks if difference between two consecutive points is higher
C    than homog, starting by the ones with lower subscript
    IF (w(4).EQ.1) THEN
110  IF ((np(1).LE.np(2)).AND.(nv(1).LE.nv(2))) THEN
        IF (nv(1).EQ.np(1)) THEN
            j=np(1)
            aux1=py(j)-vy(j)
            IF (aux1.LT.homog) THEN
                j=j+1
                nv(1)=j
                GOTO 110
            ENDIF
        ELSE
            j=np(1)
            aux1=py(j)-vy(j+1)
            IF (aux1.LT.homog) THEN
                j=j+1
                np(1)=j
                GOTO 110
            ENDIF
        ENDIF
    ELSE
        w(7)=1
        GOTO 1000
    ENDIF

```

## F. Optical parameters computation

```

ELSE
120   IF ((np(1).LE.np(2)).AND.(nv(1).LE.nv(2))) THEN
      IF (nv(1).EQ.np(1)) THEN
        j=nv(1)
        aux1=py(j)-vy(j)
        IF (aux1.LT.homog) THEN
          j=j+1
          np(1)=j
          GOTO 120
        ENDIF
      ELSE
        j=nv(1)
        aux1=py(j+1)-vy(j)
        IF (aux1.LT.homog) THEN
          j=j+1
          nv(1)=j
          GOTO 120
        ENDIF
      ENDIF
    ELSE
      w(7)=1
      GOTO 1000
    ENDIF
  ENDIF

C   Checks if difference between two consecutive points is higher
C   than homog, starting by the ones with higher subscript
  IF (w(4).EQ.1) THEN
130   IF (nv(2).EQ.np(2)) THEN
        j=np(2)
        aux1=py(j)-vy(j)
        IF (aux1.LT.homog) THEN
          j=j-1
          np(2)=j
          GOTO 130
        ENDIF
      ELSE
        j=nv(2)
        aux1=py(j-1)-vy(j)
        IF (aux1.LT.homog) THEN
          j=j-1
          nv(2)=j
          GOTO 130
        ENDIF
      ENDIF
    ELSE
140   IF (nv(2).EQ.np(2)) THEN
        j=np(2)
        aux1=py(j)-vy(j)

```

```

        IF (aux1.LT.homog) THEN
            j=j-1
            nv(2)=j
            GOTO 140
        ENDIF
    ELSE
        j=np(2)
        aux1=py(j)-vy(j-1)
        IF (aux1.LT.homog) THEN
            j=j-1
            np(2)=j
            GOTO 140
        ENDIF
    ENDIF
ENDIF
ENDIF
C      Checks if there are enough points
n=np(2)-np(1)
k=nv(2)-nv(1)
IF ((n.LT.1).OR.(k.LT.1)) THEN
    w(6)=1
    GOTO 1000
ENDIF
C      Finds out subscript of peak with maximum transmittance
an=1
aux1=py(an)
DO 28 n=2,np(2)
    IF (py(n).GT.aux1) THEN
        an=n
        aux1=py(an)
    ENDIF
28 CONTINUE
C      Finds out subscript of valley with maximum transmittance
bn=1
aux1=vy(bn)
DO 29 n=2,nv(2)
    IF (vy(n).GT.aux1) THEN
        bn=n
        aux1=vy(bn)
    ENDIF
29 CONTINUE
C      Rejects valleys and peaks of lower subscript with transmittance
C      below amin*vy(bn) and amin*py(an), respectively
IF (w(4).EQ.1) THEN
    n=np(1)
30    IF (py(n).LT.(amin*py(an))) THEN

```

F. Optical parameters computation

```

        n=n+1
        np(1)=n
        nv(1)=n
        GOTO 30
    ENDIF
    n=nv(1)
35    IF (vy(n).LT.(amin*vy(bn))) THEN
        n=n+1
        nv(1)=n
        np(1)=n-1
        GOTO 35
    ENDIF
ELSE
    n=nv(1)
40    IF (vy(n).LT.(amin*vy(bn))) THEN
        n=n+1
        np(1)=n
        nv(1)=n
        GOTO 40
    ENDIF
    n=np(1)
45    IF (py(n).LT.(amin*py(an))) THEN
        n=n+1
        nv(1)=n-1
        np(1)=n
        GOTO 45
    ENDIF
ENDIF
ENDIF

C    Rejects valleys and peaks of upper subscript with transmittance
C    below bmin*vy(bn) and bmin*py(an), respectively
    IF (w(4).EQ.1) THEN
        IF (nv(2).GT.np(2)) THEN
            n=np(2)
50        IF (py(n).LT.(bmin*py(an))) THEN
            n=n-1
            np(2)=n
            nv(2)=n+1
            GOTO 50
        ENDIF
        n=nv(2)
55        IF (vy(n).LT.(bmin*vy(bn))) THEN
            n=n-1
            nv(2)=n
            np(2)=n
            GOTO 55
        ENDIF
    ELSE
        n=nv(2)

```



```

60      IF (vy(n).LT.(bmin*vy(bn))) THEN
          n=n-1
          np(2)=n
          nv(2)=n
          GOTO 60
        ENDIF
        n=np(2)
65      IF (py(n).LT.(bmin*py(an))) THEN
          n=n-1
          nv(2)=n+1
          np(2)=n
          GOTO 65
        ENDIF
      ENDIF
    ELSE
      IF (nv(2).EQ.np(2)) THEN
        n=np(2)
70      IF (py(n).LT.(bmin*py(an))) THEN
          n=n-1
          np(2)=n
          nv(2)=n
          GOTO 70
        ENDIF
        n=nv(2)
75      IF (vy(n).LT.(bmin*vy(bn))) THEN
          n=n-1
          nv(2)=n
          np(2)=n+1
          GOTO 75
        ENDIF
      ELSE
        n=nv(2)
80      IF (vy(n).LT.(bmin*vy(bn))) THEN
          n=n-1
          np(2)=n+1
          nv(2)=n
          GOTO 80
        ENDIF
        n=np(2)
85      IF (py(n).LT.(bmin*py(an))) THEN
          n=n-1
          nv(2)=n
          np(2)=n
          GOTO 85
        ENDIF
      ENDIF
    ENDIF
  ENDIF

```

C Checks if there are enough points

## F. Optical parameters computation

```

      n=np(2)-np(1)
      k=nv(2)-nv(1)
      IF ((n.LT.1).OR.(k.LT.1)) THEN
        w(6)=1
        GOTO 1000
      ENDIF

C      Divides by 100 the transmittance values and builds
C      the arrays l, p, v
      IF (w(4).EQ.1) THEN
        IF (nv(1).EQ.np(1)) THEN
          n=1
          DO 150 j=np(1),np(2)
            l(n)=vx(j)
            v(n)=vy(j)/100.
            n=n+1
            l(n)=px(j)
            p(n)=py(j)/100.
            n=n+1
150          CONTINUE
          w(2)=1
          IF (nv(2).GT.np(2)) THEN
            l(n)=vx(nv(2))
            v(n)=vy(nv(2))/100.
            w(1)=n
            w(3)=n
          ELSE
            n=n-1
            w(1)=n
            w(3)=n
          ENDIF
        ELSE
          n=1
          DO 160 j=nv(1),nv(2)
            l(n)=px(j-1)
            p(n)=py(j-1)/100.
            n=n+1
            l(n)=vx(j)
            v(n)=vy(j)/100.
            n=n+1
160          CONTINUE
          w(2)=1
          w(4)=2
          IF (nv(2).EQ.np(2)) THEN
            l(n)=px(np(2))
            p(n)=py(np(2))/100.
            w(1)=n
            w(3)=n
          ELSE

```

```

        n=n-1
        w(1)=n
        w(3)=n
    ENDIF
ENDIF
ELSE
    IF (nv(1).EQ.np(1)) THEN
        n=1
        DO 170 j=nv(1),nv(2)
            l(n)=px(j)
            p(n)=py(j)/100.
            n=n+1
            l(n)=vx(j)
            v(n)=vy(j)/100.
            n=n+1
170    CONTINUE
        w(2)=1
        IF (nv(2).LT.np(2)) THEN
            l(n)=px(np(2))
            p(n)=py(np(2))/100.
            w(1)=n
            w(3)=n
        ELSE
            n=n-1
            w(1)=n
            w(3)=n
        ENDIF
    ELSE
        n=1
        DO 180 j=np(1),np(2)
            l(n)=vx(j-1)
            v(n)=vy(j-1)/100.
            n=n+1
            l(n)=px(j)
            p(n)=py(j)/100.
            n=n+1
180    CONTINUE
        w(2)=1
        w(4)=1
        IF (nv(2).EQ.np(2)) THEN
            l(n)=vx(nv(2))
            v(n)=vy(nv(2))/100.
            w(1)=n
            w(3)=n
        ELSE
            n=n-1
            w(1)=n
            w(3)=n
        ENDIF
    
```

## F. Optical parameters computation

```
        ENDIF
    ENDIF

C    Checks if sequence of peaks is monotonous
    IF (w(4).EQ.1) THEN
        aux1=p(2)-p(4)
        DO 200 j=4,w(3)-2,2
            aux2=p(j+2)-p(j)
            aux1=aux1*aux2
            IF (aux1.LT.0) THEN
                w(9)=w(9)+1
            ENDIF
            aux1=aux2
200    CONTINUE
        ELSE
            aux1=p(1)-p(3)
            DO 210 j=3,w(3)-2,2
                aux2=p(j+2)-p(j)
                aux1=aux1*aux2
                IF (aux1.LT.0) THEN
                    w(9)=w(9)+1
                ENDIF
                aux1=aux2
210    CONTINUE
        ENDIF
        IF (w(9).GT.0) THEN
            w(9)=w(9)-1
        ENDIF

1000 END
```

---

Routine CTSLIT( $n, pv, l, p, v$ ) receives the arrays  $l, p$  and  $v$ , and variables  $n$  and  $pv$  and returns the new transmittance values in arrays  $p$  and  $v$ . Variable  $n$  holds the number of elements in the array, and  $pv$  the  $w(4)$  value (see Table F.6). This routine introduces a new constant  $lslit$  that holds the slit width in nanometre.

---

**Program F.6:** Fortran routine that corrects transmittance values for finite slit width of the spectrophotometer (CTSLIT)

---

```
    SUBROUTINE CTSLIT(n,pv,l,p,v)

    INTEGER n, j, k, pv
    REAL l(n), p(n), v(n), aux1, lslit
    PARAMETER (lslit=5)

    DO 10 j=2,n-1
        aux1=l(j+1)-l(j-1)
        p(j)=p(j)+(p(j)*lslit/aux1)**2
        v(j)=v(j)-(v(j)*lslit/aux1)**2
10    CONTINUE
```

```

IF (pv.EQ.1) THEN
  v(1)=v(1)-(v(1)*lslit*0.5/(l(2)-l(1)))**2
  k=MOD(n,2)
  IF (k.EQ.0) THEN
    p(n)=p(n)+(p(n)*lslit*0.5/(l(n)-l(n-1)))**2
  ELSE
    v(n)=v(n)-(v(n)*lslit*0.5/(l(n)-l(n-1)))**2
  ENDIF
ELSE
  p(1)=p(1)+(p(1)*lslit*0.5/(l(2)-l(1)))**2
  k=MOD(n,2)
  IF (k.EQ.0) THEN
    v(n)=v(n)-(v(n)*lslit*0.5/(l(n)-l(n-1)))**2
  ELSE
    p(n)=p(n)+(p(n)*lslit*0.5/(l(n)-l(n-1)))**2
  ENDIF
ENDIF
END

```

---

Routine EXTRAP(*n*,*pv*,*xx*,*y*) receives in array *xx* the wavelength values and in the array *y* the transmittance values. Variable *n* holds the number of wavelength values in array *xx* and *pv* holds the lowest subscript with non-zero transmittance. It returns in the array *y* the experimental values that were received and the extrapolated values computed by the routine.

---

**Program F.7:** Fortran routine used to determine values of the peak and valley envelope functions (EXTRAP)

---

```

SUBROUTINE EXTRAP(n,pv,xx,y)

  INTEGER n, j, pv
  REAL xx(n), y(n)

  DO 10 j=pv+1,n-1,2
    y(j)=(xx(j)-xx(j-1))*(y(j+1)-y(j-1))/(xx(j+1)-xx(j-1))+y(j-1)
10  CONTINUE

  WRITE (5,('( '# EXTRAP 1' '/)')
  WRITE (5,(F9.1)') xx(1)
  j=MOD(n,2)
  WRITE (5,(2I3)') j,n
  IF (pv.EQ.2) THEN
    y(1)=(xx(1)-xx(2))*(y(4)-y(2))/(xx(4)-xx(2))+y(2)
    IF (j.EQ.1) THEN
      y(n)=(xx(n)-xx(n-1))*(y(n-3)-y(n-1))/(xx(n-3)-xx(n-1))+y(n-1)
    ENDIF
  ELSE IF (j.EQ.0) THEN
    y(n)=(xx(n)-xx(n-1))*(y(n-3)-y(n-1))/(xx(n-3)-xx(n-1))+y(n-1)
    WRITE (5,('( '# EXTRAP 2' '/)')

```

F. Optical parameters computation

```

WRITE (5, '(F9.1)') xx(1)
ENDIF

END

```

Routine `ESPES`( $l, p, v, d, dd, w, np$ ) does the final calculations. It receives the arrays  $l, p, v$  and  $w$ , along with the integer  $np$  which holds the number points where the optical parameters will be calculated. The routine returns  $d$  and  $dd$  which hold, respectively, the mean and the standard deviation of the thickness value. This routine introduces two constants:  $s$ , which holds the refraction index of the glass substrates, and `mdifo` which holds an integer value used to evaluate deviation of the results from the model equations (see also Table F.6). The value of `mdifo` is the maximum difference between the interference fringe order calculated with the mean thickness value and the thickness obtained with Eq. 3.16 on page 36. This value must match the length of array  $an$ , so that the lowest subscript of  $an$  is  $-mdifo$  and the highest is  $mdifo$ .

Table F.8.: Constants introduced in routine `ESPES`

Variable	Description
$s$	Refraction index of the glass substrates.
<code>mdifo</code>	Maximum difference permitted between the interference fringe order calculated with the mean thickness value and the thickness obtained with Eq. 3.16

Some of the variables used in the routine are described in Table F.9. Variable `num` holds the refractive index values calculated using Eq. 3.5 on page 34. These values are then used to determine the thickness using Eq. 3.16. These thickness values are stored in array `dum`. Variable  $m(1)$  holds the lowest interference fringe order of experimental fringes, which should correspond to the point (peak or valley) with higher wavelength. Variable  $m(np)$ , holds the subscript of the point with lower wavelength, which should correspond to the highest interference fringe order usable. The other elements of array  $m$  hold the experimental interference fringe order determined using the `num` and `dum` values in Eq. 3.17 on page 37. Finally `ddois` holds the thickness values calculated using again Eq. 3.17, but with the corrected interference fringe order.

Table F.9.: Main variables used in routine `ESPES`

Variable	Description
<code>num</code>	Refractive index values calculated with Eq. 3.5.
<code>dum</code>	Thickness values calculated with Eq. 3.16 using the <code>num</code> values.
$m(1)$	Highest interference fringe order of experimental fringes.
$m(np)$	Subscript of usable point with lower wavelength.
$m(i)$	With $i$ between 1 and $np$ holds the interference fringe calculated using Eq. 3.17 and rounded to the nearest integer in the case of peaks or half-integer in the case of valleys.
<code>ddois</code>	Thickness values calculated using Eq. 3.17 and the corrected values of the fringe order.

---

**Program F.8:** Fortran routine used to calculate optical parameters (`ESPES`)

---

```

SUBROUTINE ESPESS(l,p,v,d,dd,w,np)

INTEGER n, j, k, out, calc, w(*), np, an(-10:10), mdifo
REAL l(*), p(*), v(*), s, dum(np), num(np), ddois(np),
+   m(np), d, dd, aux
PARAMETER (out=4, calc=5, s=1.53, mdifo=10)

WRITE (out, '( '# Indice de refracao do vidro: ',F5.3)') s
WRITE (calc, '(//'# Indice de refracao')')

DO 10 j=1,w(1)
  aux=2*s*(p(j)-v(j))/(p(j)*v(j)+(s**2+1)/2
  num(j)=SQRT(aux+SQRT(aux**2-s**2))
  WRITE (calc, '(F9.1,F9.3)') l(j),num(j)
10 CONTINUE

WRITE (calc,
+   '(//'# Numero de ordem das franjas e dl')')

DO 20 j=2,w(1)-1
  dum(j)=l(j-1)*l(j+1)/(2*(l(j+1)*num(j-1)-l(j-1)*num(j+1)))
  WRITE (calc, '( '# ',F6.0)') dum(j)
  aux=2*num(j)*dum(j)/l(j)
  k=1+(-1)**(j+w(4)+1)
  n=1+(-1)**(j+w(4))
  m(j)=INT(aux+0.25*k)+0.2500*n
  WRITE (calc, '(F9.1,F6.1)') l(j),m(j)
20 CONTINUE

m(np)=2

C   Calculates interference fringe order deviation frequencies
DO 30 j=-10,10
  an(j)=0
30 CONTINUE
an(0)=1
k=m(np)
DO 40 n=k+1,np-1
  aux=m(n)-(m(k)-0.5*(n-k))
  IF (aux.GE.0) THEN
    j=INT(aux+0.2)
  ELSE
    j=INT(aux-0.2)
  ENDIF
  IF (ABS(j).GT.mdifo) THEN
    w(5)=1
  ELSE
    an(j)=an(j)+1
  ENDIF

```

## F. Optical parameters computation

```

40    CONTINUE

      WRITE (calc,
+      '(/'/'/'# Numero de pontos versus dif. no. de ordem'')')
C    Finds the most frequent interference fringe order
      j=-10
      w(10)=an(j)
      WRITE (calc,'(''# '' ,I3)') an(j)
      DO 50 n=-9,10
        IF (an(n).GT.w(10)) THEN
          j=n
          w(10)=an(j)
        ENDIF
        WRITE (calc,'(''# '' ,I3)') an(n)
50    CONTINUE

      k=m(np)
      m(1)=m(k)+j

C    Determines the minimum and maximum deviation of interference
C    fringe order
      w(6)=11
      DO 60 n=-10,10
        IF (an(n).GT.0) THEN
          IF (w(6).EQ.11) THEN
            w(6)=n
          ELSE
            w(7)=n
          ENDIF
        ENDIF
60    CONTINUE

C    Computes d and dd
      d=0.0
      dd=0.0

      WRITE (calc,'(/'/'/'# Espessuras'')')

      DO 100 j=m(np),np-1
        ddois(j)=(m(1)-0.5*(j-2))*l(j)*0.5/num(j)
        d=d+ddois(j)

        WRITE (calc,'(F6.0)') ddois(j)

        dd=dd+ddois(j)**2
100   CONTINUE
      n=np-m(np)
      dd=SQRT((n*dd-d*d)/(n*(n-1)))

```



d=d/n

1000 END

---



## G. Sample labelling

Identification of the samples was performed using a string code composed of letters and digits. The string starts with a letter which corresponds to a series of depositions. Following the first letter, there is one or two digits identifying each deposition trial. Different samples produced during the same experiment, are identified each with the letter ‘a’ followed by one or two digits. Thus the sample labelled ‘f8a4’ is the sample ‘a4’, produced during the deposition experiment ‘f8’. The following table shows the deposition parameters corresponding to the samples mentioned in the text.

Table G.1.: Deposition parameters of some samples and corresponding label codes

	a2	a14	e5	e11	e16	e99	f8	g11	h3	l9
Electrical signal mode	RF	RF	DC	DC	DC	DC	DC	DC	DC	DC
Temperature (°C)	200	100	—	211	202	208	400	400	300	100
Substrate-target distance (mm)	60	80	61	63	63	62	56	55	67	65
Source power (W)	400	200	20	20	30	30	22	22	22	20
Pressure ( $\times 10^{-1}$ Pa)	6	8	6.9	6.5	3.0	3.3	2.5	2.3	1.5	25
O <sub>2</sub> flow rate (sccm)	25	50	7.0	7.0	6.3	6.1	6.0	6.0	4.0	4.5
Deposition time (min)	120	240	30	30	30	245	30	120	30	50

*G. Sample labelling*

# Bibliography

- [1] Zhihong Jin, Huan-Jun Zhou, Zhang Li Jin, Robert F. Savinell, and Chung-Chiun Liu. Application of nano-crystalline porous tin oxide thin film for CO sensing. *Sensors and Actuators B [Chemical]*, 52:188–194, 1998.
- [2] D. S. Vlachos, C. A. Papadopoulos, and J. N. Avaritsiotis. Dependence of sensitivity of SnO<sub>x</sub> thin-film gas sensors on vacancy defects. *J. Appl. Phys.*, 80(10):6050–6054, 1996.
- [3] G. Micocci, A. Serra, P. Siciliano, A. Tepore, and Z. Ali-Adib. CO sensing characteristics of reactively sputtered SnO<sub>2</sub> thin films prepared under different oxygen partial pressure values. *Vacuum*, 47(10):1175–1177, 1996.
- [4] A. Cricenti, R. Generosi, M. A. Scarselli, P. Perfetti, P. Siciliano, A. Serra, A. Tepore, C. Coluzza, J. Almeida, and G. Margaritondo. Morphological, chemical and electrical characterization of Pt–SnO<sub>2</sub> thin film grown on rough and mechanically polished Al<sub>2</sub>O<sub>3</sub> substrates. *J. Phys. D: Appl. Phys.*, 29:2235–2239, 1996.
- [5] R. Botter, T. Aste, and D. Beruto. Influence of microstructures on the functional properties of tin oxide-based gas sensors. *Sensors and Actuators B [Chemical]*, 22:27–35, 1994.
- [6] G. Blaustein, M. S. Castro, and C. M. Aldao. Influence of frozen distributions of oxygen vacancies on tin oxide conductance. *Sensors and Actuators B [Chemical]*, 55:33–37, 1999.
- [7] Geraint Williams and Gary S. V. Coles. The gas-sensing potential of nanocrystalline tin dioxide produced by a laser ablation technique. *MRS Bulletin*, 24(6):25–29, 1999.
- [8] B. Ruhland, TH. Becker, and G. Müller. Gas-kinetic interactions of nitrous oxides with SnO<sub>2</sub> surfaces. *Sensors and Actuators B [Chemical]*, 50:85–94, 1998.
- [9] H. A. Schultens and D. Schild. *Biophysical properties of olfactory receptor neurones*, chapter 2, pages 13–23. In Gardner and Bartlett [150], 1992. NATO ASI Series. Series E: Applied sciences - Vol. 212.
- [10] Paul R. Wheeler, H. George Burkitt, and Victor G. Daniels, editors. *Functional histology: a text and colour atlas*. Churchill Livingstone, second edition, 1987.
- [11] Robert M. Berne and Matthew N. Levy, editors. *Principles of physiology*. Wolfe Publications, 1990.
- [12] J. W. Gardner and P. N. Bartlett. *Pattern recognition in odour sensing*, chapter 11, pages 161–179. In Gardner and Bartlett [150], 1992. NATO ASI Series. Series E: Applied sciences - Vol. 212.
- [13] G. H. Dodd, P. N. Bartlett, and J. W. Gardner. *Odours – The stimulus for an electronic nose*, chapter 1, pages 1–11. In Gardner and Bartlett [150], 1992. NATO ASI Series. Series E: Applied sciences - Vol. 212.

## Bibliography

- [14] Richard B. Brown and Edward T. Zellers. *Environmental Monitoring*, chapter 20. Volume 1 of Göpel et al. [16], 1989.
- [15] Jacob Fraden. *Handbook of modern sensors: Physics, designs and applications*. AIP Press, second edition, 1997.
- [16] W. Göpel, J. Hesse, and J. N. Zemel, editors. *Fundamentals and general aspects*, volume 1 of *Sensors: A comprehensive survey*. VCH, 1989.
- [17] W. Göpel, J. Hesse, and J. N. Zemel, editors. *Thermal sensors*, volume 4 of *Sensors: A comprehensive survey*. VCH, 1990.
- [18] W. Göpel, J. Hesse, and J. N. Zemel, editors. *Chemical and Biochemical sensors. Part I*, volume 2 of *Sensors: A comprehensive survey*. VCH, 1991.
- [19] W. Göpel, J. Hesse, and J. N. Zemel, editors. *Chemical and Biochemical sensors. Part II*, volume 3 of *Sensors: A comprehensive survey*. VCH, 1992.
- [20] M. Tabib-Azar. *Sensor Parameters*, chapter 2. Volume 1 of Göpel et al. [16], 1989.
- [21] Dermot Diamond, editor. *Principles of chemical and biological sensors*, volume 150 of *Chemical Analysis*. John Wiley & Sons, Inc., 1998.
- [22] Emery Lightner Moore and Ramon Perez de Paula. *Optical fibers and integrated optics*, chapter 8. Volume 2 of Göpel et al. [18], 1991.
- [23] Jörg Arndt. *Ceramics and oxides*, chapter 9. Volume 1 of Göpel et al. [16], 1989.
- [24] V. Raineri, V. Privitera, W. Vandervorst, L. Hellemans, and J. Snauwaert. Carrier distribution in silicon devices by atomic force microscopy on etched surfaces. *Appl. Phys. Lett.*, 64(3):354–356, jan 1994.
- [25] J. Arbiol, P. Gorostiza, A. Cirera, A. Cornet, and J. R. Morante. In situ analysis of the conductance of SnO<sub>2</sub> crystalline nanoparticles in the presence of oxidizing or reducing atmosphere by scanning tunneling microscopy. *Sensors and Actuators B [Chemical]*, 2001. submitted.
- [26] Shuji Hasegawa and François Grey. Electronic transport at semiconductor surfaces — from point-contact transistor to micro-four-point probes. *Surf. Sci.*, 500:84–104, 2002.
- [27] Hans Lüth. *Surface and interfaces of solid materials*. Springer-Verlag, third edition, 1995.
- [28] Maurice H. Francombe and John L. Vossen, editors. *Thin Films for Emerging Applications*, volume 16 of *Physics of Thin Films*. Academic Press, 1992.
- [29] R. A. Stradling and P. C. Klipstein, editors. *Growth and characterisation of semiconductors*. Adam Hilger, 1990.
- [30] W. H. Brattain and J. Bardeen. *Bell Syst. Tech. J.*, 32:1, 1953.
- [31] G. Heiland. Zum einfluss von adsorbiertem sauerstoff auf die elektrische leitfähigkeit von zinkoxydkristallen. *Z. Phys.*, 138:459–464, 1954. H03.
- [32] T. Seiyama, A. Kato, K. Fukushi, and M. Nagatini. *Anal. Chem.*, 34:1502–1503, 1962.

- [33] A. Hoel, J. Ederth, J. Kopniczky, P. Heszler, L. B. Kish, E. Olsson, and C. G. Granqvist. Conduction invasion noise in nanoparticle WO<sub>3</sub>/Au thin-film devices for gas sensing application. *Smart Mater. Struct.*, 11:640–644, 2002.
- [34] L. Lozzi, L. Ottaviano, M. Passacantando, S. Santucci, and C. Cantalini. The influence of air and vacuum thermal treatments on the NO<sub>2</sub> gas sensitivity of WO<sub>3</sub> thin films prepared by thermal evaporation. *Thin Solid Films*, 391:224–228, 2001.
- [35] J. L. Solis, S. Saukko, L. Kish, C. G. Granqvist, and V. Lantto. Semiconductor gas sensors based on nanostructured tungsten oxide. *Thin Solid Films*, 391:255–260, 2001.
- [36] R. Pohle, M. Fleischer, and H. Meixner. In situ infrared emission spectroscopic study of the adsorption of H<sub>2</sub>O and hydrogen-containing gases on Ga<sub>2</sub>O<sub>3</sub> gas sensors. *Sensors and Actuators B [Chemical]*, 68:151–156, 2000.
- [37] T. Schwebel, M. Fleischer, and H. Meixner. CO-sensor for domestic use based on high temperature stable Ga<sub>2</sub>O<sub>3</sub> thin films. In *Proceedings of the 1997 International Conference on Solid-State Sensors and Actuators*, volume 1, pages 547–550, 1997. published in Sens. Actuators B.
- [38] M. Fleischer and H. Meixner. Sensing reducing gases at high temperatures using long-term stable Ga<sub>2</sub>O<sub>3</sub> thin films. *Sensors and Actuators B [Chemical]*, 6:257–261, 1992.
- [39] H. Steffes, C. Imawan, F. Solzbacher, and E. Obermeier. Fabrication parameters and NO<sub>2</sub> sensitivity of reactively RF-sputtered In<sub>2</sub>O<sub>3</sub> thin films. *Sensors and Actuators B [Chemical]*, 68:249–253, 2000.
- [40] M. Ivanovskaya, P. Bogdanov, G. Faglia, and G. Sberveglieri. The features of thin film and ceramic sensors at the detection of CO and NO<sub>2</sub>. *Sensors and Actuators B [Chemical]*, 68:344–350, 2000.
- [41] Seung-Ryeol Kim, Hyung-Ki Hong, Chul Han Kwon, Dong Hyun Yun, Kyuchung Lee, and Yung Kwon Sung. Ozone sensing properties of In<sub>2</sub>O<sub>3</sub>-based semiconductor thick films. *Sensors and Actuators B [Chemical]*, 66:59–62, 2000.
- [42] I. Hayakawa, Y. Iwamoto, K. Kikuta, and S. Hirano. Gas sensing properties of platinum dispersed-TiO<sub>2</sub> thin film derived from precursor. *Sensors and Actuators B [Chemical]*, 62:55–60, 2000.
- [43] Katarzyna Zakrzewska, Marta Radecka, and Mieczyslaw Rekas. Effect of Nb, Cr, Sn additions on gas sensing properties of TiO<sub>2</sub> thin films. *Thin Solid Films*, 310:161–166, 1997.
- [44] R. M. Geatches, A. V. Chadwick, and J. D. Wright. Single-crystal metal oxide gas sensors. *Sensors and Actuators B [Chemical]*, 4:467–472, 1991.
- [45] N. Jayadev Dayan, S. R. Sainkar, R. N. Karekar, and R. C. Aiyer. Formulation and characterization of ZnO:Sb thick-film gas sensors. *Thin Solid Films*, 325:254–258, 1998.
- [46] Kazuhiro Hara and Noriyuki Nishida. H<sub>2</sub> sensors using Fe<sub>2</sub>O<sub>3</sub>-based thin film. *Sensors and Actuators B [Chemical]*, 20:181–186, 1994.
- [47] S. Capone, G. Leo, R. Rella, P. Siciliano, L. Vasanelli, M. Alvisi, L. Mirengi, and A. Rizzo. Physical characterization of hafnium oxide thin films and their application as gas sensing devices. *J. Vac. Sci. Technol. A*, 16(6):3564–3568, 1998.

## Bibliography

- [48] G. Micocci, A. Serra, A. Tepore, S. Capone, R. Rella, and P. Siciliano. Properties of vanadium oxide thin films for ethanol sensor. *J. Vac. Sci. Technol. A*, 15(1):34–38, 1997.
- [49] Oliver Schilling and K. Colbow. A mechanism for sensing reducing gases with vanadium pentoxide films. *Sensors and Actuators B [Chemical]*, 21:151–157, 1994.
- [50] B. K. Miremadi, R. C. Singh, Z. Chen, S. Roy Morrison, and K. Colbow. Chromium oxide gas sensors for the detection of hydrogen, oxygen and nitrogen oxide. *Sensors and Actuators B [Chemical]*, 21:1–4, 1994.
- [51] Y. F. Dong, W. L. Wang, and K. J. Liao. Ethanol-sensing characteristics of pure and Pt-activated CdIn<sub>2</sub>O<sub>4</sub> films prepared by r.f. reactive sputtering. *Sensors and Actuators B [Chemical]*, 67:254–257, 2000.
- [52] C. Tragut. The influence of the surface transfer reaction on the response characteristics of resistive oxygen sensors. *Sensors and Actuators B [Chemical]*, 7:742–746, 1992.
- [53] J. L. Zhang, Y. D. Lu, B. R. Li, and J. L. Zeng. The preparation and electrical conduction of Li<sub>2</sub>SnO<sub>3</sub> thick film humidity sensitive material. In *Proceedings. 43rd Electronic Components and Technology Conference*, pages 1095–1098, 1993.
- [54] Simon M. Sze. *Semiconductor Devices: Physics and Technology*. John Wiley & Sons, 1985.
- [55] V. N. Mishra and R. P. Agarwal. Effect of electrode material on sensor response. *Sensors and Actuators B [Chemical]*, 22:121–125, 1994.
- [56] Neil W. Ashcroft and N. David Mermin. *Solid State Physics*. Saunders, 1976.
- [57] W. Göpel and K.-D. Schierbaum. *Specific molecular interactions and detection principles*, chapter 4. Volume 2 of Göpel et al. [18], 1991.
- [58] P. W. Atkins. *Physical Chemistry*. Oxford University Press, fourth edition, 1990.
- [59] Andrew Zangwill. *Physics at surfaces*. Cambridge University Press, 1988.
- [60] Kyung Hyun Cha, Hee Chan Park, and Kwang Ho Kim. Effect of palladium doping and film thickness on the H<sub>2</sub>-gas sensing characteristics of SnO<sub>2</sub>. *Sensors and Actuators B [Chemical]*, 21:91–96, 1994.
- [61] Marta Radecka, Katarzyna Zakrzewska, and Mieczyslaw Rekas. SnO<sub>2</sub>–TiO<sub>2</sub> solid solutions for gas sensors. *Sensors and Actuators B [Chemical]*, 47:194–204, 1998.
- [62] H.-P. Hübner and S. Drost. Tin oxide gas sensors: an analytical comparison of gas-sensitive and non-gas-sensitive thin films. *Sensors and Actuators B [Chemical]*, 4:463–466, 1991.
- [63] A. Cricenti, R. Generosi, M. A. Scarselli, P. Perfetti, P. Siciliano, A. Serra, A. Tepore, J. Almeida, C. Coluzza, and G. Margaritondo. Pt:SnO<sub>2</sub> thin films for gas sensor characterized by atomic force microscopy and x-ray photoemission spectromicroscopy. *J. Vac. Sci. Technol. B*, 14(2):1527–1530, Mar/Apr 1996.
- [64] Fan Lu, Songying Chen, and Shaoyi Peng. Effects of different adsorbed species on ultra-fine CO sensors. *Sensors and Actuators B [Chemical]*, 50:220–226, 1998.



- [65] Tohru Nomura, Yuki Fujimori, Maki Kitora, Yoshinobu Matsuura, and Isao Aso. Battery operated semiconductor CO sensor using pulse heating method. *Sensors and Actuators B [Chemical]*, 52:90–95, 1998.
- [66] Shinji Kanefusa, Masayoshi Nitta, and Miyoshi Haradome. H<sub>2</sub>S gas detection by ZrO<sub>2</sub>-doped SnO<sub>2</sub>. *IEEE Transactions on Electron Devices*, ED-35(1):65–69, 1988.
- [67] Jun Tamaki, Tomoki Maekawa, Norio Miura, and Nobotu Yamazoe. CuO–SnO<sub>2</sub> element for highly sensitive and selective detection of H<sub>2</sub>S. *Sensors and Actuators B [Chemical]*, 9:197–203, 1992.
- [68] R. B. Vasiliev, M. N. Romyantseva, N. V. Yakovlev, and A. M. Gaskov. CuO/SnO<sub>2</sub> thin film heterostructures as chemical sensors to H<sub>2</sub>S. *Sensors and Actuators B [Chemical]*, 50:186–193, 1998.
- [69] V. V. Malyshev and A. V. Pislyakov. SnO<sub>2</sub>-based thick-film-resistive sensor for H<sub>2</sub>S detection in the concentration range of 1–10 mg m<sup>-3</sup>. *Sensors and Actuators B [Chemical]*, 47:181–188, 1998.
- [70] F. J. Gutiérrez, L. Arés, J. I. Robla, M. C. Horrillo, I. Sayago, J. M. Getino, and J. A. de Agapito. NO<sub>x</sub> tin dioxide sensors activities, as function of doped materials and temperature. *Sensors and Actuators B [Chemical]*, 15–16:354–356, 1993.
- [71] Geraint Williams and Gary S. V. Coles. NO<sub>x</sub> response of tin dioxide based gas sensors. *Sensors and Actuators B [Chemical]*, 15–16:349–353, 1993.
- [72] U. Hofer, H. Böttner, E. Wagner, and C. D. Kohl. Highly sensitive NO<sub>2</sub> sensor device featuring a JFET-like transducer mechanism. *Sensors and Actuators B [Chemical]*, 47:213–217, 1998.
- [73] T. Ratcheva, I. Stambolova, and K. Konstantinov. PH<sub>3</sub> detection by SnO<sub>2</sub>–ZrO<sub>2</sub> thin films. *Sensors and Actuators B [Chemical]*, 21:199–204, 1994.
- [74] Dong Hyun Yun, Chul Han Kwon, Hyung-Ki Hong, Seung-Ryeol Kim, Kyuchung Lee, Ho Geun Song, and Ji Eon Kim. Highly sensitive and selective ammonia gas sensor. In *Proceedings of the 1997 International Conference on Solid-State Sensors and Actuators*, volume 2, pages 959–962, 1997.
- [75] R. P. Gupta, Z. Gergintschew, D. Schipanski, and P. D. Vyas. YBCO-FET room temperature ammonia sensor. *Sensors and Actuators B [Chemical]*, 63:35–41, 2000.
- [76] A. Teeramongkonrasmee and M. Sriyudthsak. Methanol and ammonia sensing characteristics of sol–gel derived thin film gas sensor. *Sensors and Actuators B [Chemical]*, 66:256–259, 2000.
- [77] R. Huck, U. Böttger, D. Kohl, and G. Heiland. Spillover effects in the detection of H<sub>2</sub> and CH<sub>4</sub> by sputtered SnO<sub>2</sub> films with Pd and PdO deposits. *Sens. Actuators*, 17:355–359, 1989.
- [78] Soon-Don Choi and Duk-Dong Lee. CH<sub>4</sub> sensing characteristics of K-, Ca-, Mg-impregnated SnO<sub>2</sub> sensors. *Sensors and Actuators B [Chemical]*, 77:335–338, 2001.
- [79] A. Cirera, A. Cabot, A. Cornet, and J. R. Morante. CO–CH<sub>4</sub> selectivity enhancement by in situ Pd-catalysed microwave SnO<sub>2</sub> nanoparticles for gas detectors using active filter. *Sensors and Actuators B [Chemical]*, 78:151–160, 2001.

## Bibliography

- [80] Y. K. Fang and J. J. Lee. A tin oxide thin film sensor with high ethanol sensitivity. *Thin Solid Films*, 169:51–56, 1989.
- [81] M. Labeau, B. Gautheron, G. Delabouglise, J. Peña, V. Ragel, A. Varela, J. Román, J. Martinez, J. M. González-Calbet, and M. Vallet-Regi. Synthesis, structure and gas sensitivity properties of pure and doped SnO<sub>2</sub>. *Sensors and Actuators B [Chemical]*, 15–16:379–383, 1993.
- [82] B. Gautheron, M. Labeau, G. Delabouglise, and U. Schmatz. Undoped and Pd-doped SnO<sub>2</sub> thin films for gas sensors. *Sensors and Actuators B [Chemical]*, 15–16:357–362, 1993.
- [83] Jyh-Jier Ho, Y. K. Fang, K. H. Wu, W. T. Hsieh, C. H. Chen, G. S. Chen, M. S. Ju, Jing-Jenn Lin, and S. B. Hwang. High sensitivity ethanol gas sensor integrated with a solid-state heater and thermal isolation improvement structure for legal drink-drive limit detecting. *Sensors and Actuators B [Chemical]*, 50:227–233, 1998.
- [84] Tadashi Takada. A new method for gas identification using a single semiconductor sensor. *Sensors and Actuators B [Chemical]*, 52:45–52, 1998.
- [85] Wan-Young Chung, Chang-Hyun Shim, Soon-Don Choi, and Duk-Dong Lee. Tin oxide microsensor for LPG monitoring. *Sensors and Actuators B [Chemical]*, 20:139–143, 1994.
- [86] A. R. Phani. X-ray photoelectron spectroscopy studies on Pd doped SnO<sub>2</sub> liquid petroleum gas sensor. *Appl. Phys. Lett.*, 71(16):2358–2360, October 1997.
- [87] V. A. Chaudhary, I. S. Mulla, and K. Vijayamohan. Impedance studies of an LPG sensor using surface ruthenated tin oxide. *Sensors and Actuators B [Chemical]*, 55:127–133, 1999.
- [88] Th. Becker, S. Ahlers, Chr. Bosch-v.Braunmühl, G. Müller, and O. Kiesewetter. Gas sensing properties of thin- and thick-film tin-oxide materials. *Sensors and Actuators B [Chemical]*, 77:55–61, 2001.
- [89] Kan-Sen Chou, Tzy-Kuang Lee, and Feng-Jiin Liu. Sensing mechanism of a porous ceramic as humidity sensor. *Sensors and Actuators B [Chemical]*, 56:106–111, 1999.
- [90] P. Schmidt-Zhang, K.-P. Sandow, F. Adolf, W. Göpel, and U. Guth. A novel thick film sensor for simultaneous O<sub>2</sub> and NO monitoring in exhaust gases. *Sensors and Actuators B [Chemical]*, 70:25–29, 2000.
- [91] Colin Baird. *Environmental Chemistry*. W. H. Freeman and Company, second edition, 1998.
- [92] Praxair material safety data sheet, October 1997. Form no.: P-4576-F.
- [93] N. Bârsan, J. R. Stetter, Jr. M. Findlay, and W. Göpel. High-performance gas sensing of CO: comparative tests for semiconducting (SnO<sub>2</sub>-based) and for amperometric gas sensors. *Anal. Chem.*, 71(13):2512–2517, 1999.
- [94] F. C. Stedile, B. A. S. de Barros, Jr., C. V. Barros Leite, F. L. Freire, Jr., I. J. R. Baumvol, and W. H. Schreiner. Characterization of tin oxide thin films deposited by reactive sputtering. *Thin Solid Films*, 170:285–291, 1989.

- [95] J. Mizsei. Activating technology of SnO<sub>2</sub> layers by metal particles from ultrathin metal films. *Sensors and Actuators B [Chemical]*, 15–16:328–333, 1993.
- [96] G. B. Barbi and J. Santos Blanco. Structure of tin oxide layers and operating temperature as factors determining the sensitivity performances to NO<sub>x</sub>. *Sensors and Actuators B [Chemical]*, 15–16:372–378, 1993.
- [97] Ulrich Hofer, Gerd Kühner, Werner Schweizer, Gerd Sulz, and Klaus Steiner. CO and CO<sub>2</sub> thin-film SnO<sub>2</sub> gas sensors on Si substrates. *Sensors and Actuators B [Chemical]*, 22:115–119, 1994.
- [98] R. M. Voshchilova, D. P. Dimitrov, N. I. Dolotov, A. R. Kuz'min, A. V. Makhin, V. A. Moshnikov, and Yu. M. Tairov. Forming the structure of gas-sensitive layers of tin dioxide produced by reactive magnetron sputtering. *Semiconductors*, 29(11):1036–1039, November 1995.
- [99] M. Di Giulio, G. Micocci, A. Serra, A. Tepore, R. Rella, and P. Siciliano. Characteristics of reactively sputtered Pt–SnO<sub>2</sub> thin films for CO gas sensors. *J. Vac. Sci. Technol. A*, 14(4):2215–2219, 1996.
- [100] C. S. Rastomjee, R. S. Dale, R. J. Schaffer, F. H. Jones, R. G. Egdell G. C. Georgiadis, M. J. Lee, T. J. Tate, and L. L. Cao. An investigation of doping of SnO<sub>2</sub> by ion implantation and application of ion-implanted films as gas sensors. *Thin Solid Films*, 279:98–105, 1996.
- [101] P. Serrini, V. Briois, M. C. Horrillo, A. Traverse, and L. Manes. Chemical composition and crystalline structure of SnO<sub>2</sub> thin films used as gas sensors. *Thin Solid Films*, 304:113–122, 1997.
- [102] J. Gutiérrez, J. Getino, M. C. Horrillo, L. Arés, J. I. Robla, C. García, and I. Sayago. Electrical characterization of a thin film tin oxide sensor array for VOCs detection. *Thin Solid Films*, 317:429–431, 1998.
- [103] A. Galdikas, A. Mironas, D. Senulienė, and A. Šetkus. Gas sensitivity studies by optical spectroscopy below absorption edge in tin oxide thin film sensors. *Thin Solid Films*, 323:275–284, 1998.
- [104] F. Cirilli, S. Kačiulis, G. Mattogno, A. Galdikas, A. Mironas, D. Senulienė, and A. Šetkus. Influence of Cu overlayer on the properties of SnO<sub>2</sub>-based gas sensors. *Thin Solid Films*, 315:310–315, 1998.
- [105] Jose P. Santos and Juan A. de Agapito. The interaction of oxygen with nanocrystalline SnO<sub>2</sub> thin films in the framework of the electron theory of adsorption. *Thin Solid Films*, 338:276–280, 1999.
- [106] M. Ruske, G. Bräuer, J. Pistner, U. Pfäfflin, and J. Szczyrbowski. Properties of SnO<sub>2</sub> films prepared by DC and MF reactive sputtering. *Thin Solid Films*, 351:146–150, 1999.
- [107] Vladimir V. Kissine, Sergei A. Voroshilov, and Victor V. Sysoev. A comparative study of SnO<sub>2</sub> and SnO<sub>2</sub>:Cu thin films for gas sensor applications. *Thin Solid Films*, 348:304–311, 1999.
- [108] V. V. Kissine, V. V. Sysoev, S. A. Voroshilov, and V. V. Simakov. Effect of oxygen adsorption on the conductivity of thin SnO<sub>2</sub> films. *Semiconductors*, 34(3):308–311, 2000.

## Bibliography

- [109] N. Ikeo. *Handbook of X-ray photoelectron spectroscopy*. JEOL, 1991.
- [110] B. D. Cullity. *Elements of X-ray diffraction*. Addison-Wesley, second edition, 1978.
- [111] Grigorii Valentinovich Samsonov, editor. *The oxide handbook*. IFI/Plenum, New York, second edition, 1982.
- [112] Mitsuharu Konuma. *Film deposition by plasma techniques*, volume 10 of *Atoms and Plasmas*. Springer-Verlag, 1992.
- [113] R. Swanepoel. Determination of the thickness and optical constants of amorphous silicon. *J. Phys. E: Sci. Instrum.*, 16:1214–22, 1983.
- [114] R. Swanepoel. Determination of surface roughness and optical constants of inhomogeneous amorphous silicon films. *J. Phys. E: Sci. Instrum.*, 17:896–903, 1984.
- [115] T. Lindström, J. Isidorsson, and G. A. Niklasson. Surface smoothing and roughening in sputtered SnO<sub>2</sub> films. *Thin Solid Films*, 401:165–170, 2001.
- [116] John A. Thornton and Alan S. Penfold. *Cylindrical magnetron sputtering*, chapter II-2, pages 75–113. Academic Press, 1978.
- [117] Brian N. Chapman. *Glow discharge processes*. John Wiley & Sons, 1980.
- [118] Alexander Roth. *Vacuum technology*. Elsevier Science, second edition, 1983.
- [119] M. M. D. Ramos, J. B. Almeida, M. I. C. Ferreira, and M. P. dos Santos. Thin film deposition by magnetron sputtering and determination of some physical parameters. *Thin Solid Films*, 176:219–226, 1989.
- [120] J. B. Almeida, M. I. C. Ferreira, M. P. dos Santos, and M. Ramos. Construction and performance of a magnetron sputtering apparatus. *Nuc. Instrum. Methods Phys. Res. B*, 18:651, 1987.
- [121] Vladimir V. Kissine, Sergei A. Voroshilov, and Victor V. Sysoev. Oxygen flow effect on gas sensitivity properties of tin oxide film prepared by r.f. sputtering. *Sensors and Actuators B [Chemical]*, 55:55–59, 1999.
- [122] V. Teixeira, M. Andritschky, W. Fischer, H. P. Buchkremer, and D. Stöver. Analysis of residual stresses in thermal barrier coatings. *J. Mater. Process. Technol.*, 92–93:209–216, 1999.
- [123] L. J. van der Pauw. A method of measuring specific resistivity and hall effect of discs of arbitrary shape. *Philips Res. Repts*, 13:1–9, 1958.
- [124] N. Bârsan, R. Grigorovici, R. Ionescu, Manuela Motronea, and Ana Vancu. Mechanism of gas detection in polycrystalline thick film SnO<sub>2</sub> sensors. *Thin Solid Films*, 171:53–63, 1989.
- [125] J. Watson. A note on the electrical characterization of solid-state gas sensors. *Sensors and Actuators B [Chemical]*, 8:173–177, 1992.
- [126] Ana Vancu, Radu Ionescu, and Nicolae Bârsan. *Chemoresistive gas sensors*, chapter 6, pages 437–491. Sensors Series. Institute of Physics Publishing, 1992.

- [127] P. K. Clifford and D. T. Tuma. Characteristics of semiconductor gas sensors: I. Steady state gas response. *Sens. Actuators*, 3:233–254, 1982/83.
- [128] Go Sakai, Nam Seok Baik, Norio Miura, and Noboru Yamazoe. Gas sensing properties of tin oxide thin films fabricated from hydrothermally treated nanoparticles. Dependence of CO and H<sub>2</sub> response on film thickness. *Sensors and Actuators B [Chemical]*, 77:116–121, 2001.
- [129] Naoki Matsunaga, Go Sakai, Kengo Shimano, and Noboru Yamazoe. Diffusion equation-based study of thin film semiconductor gas sensor-response transient. *Sensors and Actuators B [Chemical]*, 83:216–221, 2002.
- [130] Zhenan Tang, Philip C. H. Chan, Rajnish K. Sharma, Guizhen Yan, I-Ming Hsing, and Johnny K. O. Sin. Investigation and control of microcracks in tin oxide gas sensing thin-films. *Sensors and Actuators B [Chemical]*, 79:39–47, 2001.
- [131] Chaonan Xu, Jun Tamaki, Norio Miura, and Noboru Yamazoe. Grain size effects on gas sensitivity of porous SnO<sub>2</sub>-based elements. *Sensors and Actuators B [Chemical]*, 3:147–155, 1991.
- [132] Wolfgang Göpel. Chemical imaging I. Concepts and visions for electronic and bioelectronic noses. *Sensors and Actuators B [Chemical]*, 52:125–142, 1998.
- [133] Udo Weimar and Wolfgang Göpel. Chemical imaging II. Trends in practical multiparameter sensor systems. *Sensors and Actuators B [Chemical]*, 52:143–161, 1998.
- [134] S. Roy Morrison. Selectivity in semiconductor gas sensors. *Sens. Actuators*, 12:425–440, 1987.
- [135] N. Yamazoe, Y. Kurokawa, and T. Seiyama. Effects of additives on semiconductor gas sensors. *Sens. Actuators*, 4:283–289, 1983.
- [136] Jay N. Zemel. Theoretical description of gas-film interactions on SnO<sub>x</sub>. *Thin Solid Films*, 163:189–202, 1988.
- [137] Jerome F. McAleer, Patrick T. Moseley, John O. W. Norris, and David E. Williams. Tin dioxide gas sensors. *J. Chem. Soc., Faraday Trans. 1*, 83:1323–1346, 1987.
- [138] K. D. Schierbaum, U. Weimar, and W. Göpel. Comparison of ceramic, thick-film and thin-film chemical sensors based upon SnO<sub>2</sub>. *Sensors and Actuators B [Chemical]*, 7:709–716, 1992. SN172.
- [139] H. Geistlinger. The influence of chemisorption on the defect equilibrium of metal oxide thin films. *J. Appl. Phys.*, 80(3):1370–1380, 1996.
- [140] V. V. Kissine, V. V. Sysoev, and S. A. Voroshilov. Conductivity of SnO<sub>2</sub> thin films in the presence of surface adsorbed species. *Sensors and Actuators B [Chemical]*, 79:163–170, 2001.
- [141] D. P. Woodruff. Solved and unsolved problems in surface structure determination. *Surf. Sci.*, 500:147–171, 2002.
- [142] Catherine Stampfl, M. Veronica Ganduglia-Pirovano, Karsten Reuter, and Matthias Scheffler. Catalysis and corrosion: the theoretical surface-science context. *Surf. Sci.*, 500:368–394, 2002.

## Bibliography

- [143] Frank Starrost and Emily A. Carter. Modeling the full monty: baring the nature of surfaces across time and space. *Surf. Sci.*, 500:323–346, 2002.
- [144] M. Bonn, A. W. Kleyn, and G. J. Kroes. Real time chemical dynamics at surfaces. *Surf. Sci.*, 500:475–499, 2002.
- [145] Pengtao Gao, L. J. Meng, M. P. dos Santos, V. Teixeira, and M. Andritschky. Influence of sputtering power and the substrate–target distance on the properties of ZrO<sub>2</sub> films prepared by RF reactive sputtering. *Thin Solid Films*, 377–378:557–561, 2000.
- [146] Pengtao Gao, L. J. Meng, M. P. dos Santos, V. Teixeira, and M. Andritschky. Characterization of ZrO<sub>2</sub> films prepared by rf reactive sputtering at different O<sub>2</sub> concentrations in the sputtering gases. *Vacuum*, 56:143–148, 2000.
- [147] J. Kappler, A. Tomescu, N. Bârsan, and U. Weimar. CO consumption of Pd doped SnO<sub>2</sub> based sensors. *Thin Solid Films*, 391:186–191, 2001.
- [148] David S. Lawyer. *The Linux Serial Howto*, May 1999.
- [149] Shimaden Co., Ltd. *SR52 Series Digital Controller — Communication Interface — Instruction Manual*, second edition.
- [150] Julian W. Gardner and Philip N. Bartlett, editors. *Sensors and sensory systems for an electronic nose*. Kluwer Academic Publishers, 1992. NATO ASI Series. Series E: Applied sciences - Vol. 212.

# List of Figures

1.1. Picture showing the position of the olfactory epithelium and air flow during normal breathing . . . . .	2
1.2. Detail of the olfactory epithelium showing the receptor cells' structure . . . . .	2
2.1. Typical structure of a sensor system . . . . .	6
2.2. Picture of a Bosch lambda sensor used in the automotive industry to control the combustion atmosphere inside the motor cylinders. This is one of the most common catalytic type sensors. . . . .	12
2.3. Evolution of the number of papers published from 1990 to 2001 on gas sensors (at the time this search was performed there was no information concerning the year 1996) . . . . .	19
2.4. Types of point defects on a simple crystal lattice . . . . .	21
3.1. XPS spectra of samples a) a14a22, b) e11a1 and c) e99a3 . . . . .	27
3.2. Detail of the XPS Sn 3d <sub>5/2</sub> peak of sample e99a3 . . . . .	28
3.3. Detail of O 1s peak of XPS spectra of samples a) a14a22 and b) e11a1, before and after a light ion bombardment . . . . .	29
3.4. Diagram of a tetragonal SnO <sub>2</sub> unit cell . . . . .	31
3.5. XRD spectra of three polycrystalline SnO <sub>2</sub> samples with different thickness . . . . .	31
3.6. Scanning electron microscope images of a) the surface and b) a cut of sample a14a2 . . . . .	32
3.7. AFM surface plots of samples a) f8a4 and b) h3a4 . . . . .	33
3.8. Photograph showing samples with different colour, corresponding to films with different composition and structure . . . . .	33
3.9. Transmission spectra of SnO <sub>2</sub> layers with different thickness . . . . .	34
3.10. Transmission spectra taken along different directions of one of the thick samples . . . . .	37
3.11. Transmission spectra of samples e11a24 and 19a2. Only the spectrum A of sample e11a24 was successfully used in the determination of the sample's thickness. . . . .	39
4.1. DC sputtering chamber system . . . . .	45
4.2. Atomic force microscope surface plots of SnO <sub>2</sub> samples produced at different deposition pressures . . . . .	50
4.3. Diffraction spectra of samples produced at different deposition pressure . . . . .	51
4.4. AFM surface plots of samples produced with different substrate temperatures . . . . .	52
4.5. XRD spectra of samples produced with different substrate temperature . . . . .	53
4.6. SEM image showing delamination of a SnO <sub>2</sub> layer . . . . .	53
4.7. Deformations observed on thin film substrates when there are (a) tensile or (b) compressive residual stresses on the interface. . . . .	54
4.8. XRD spectra of samples a) a14a1, b) a14a3 and c) a14a2, deposited during the same sputtering process . . . . .	55

## List of Figures

5.1. Experimental setup of the system used to test gas sensitivity . . . . .	58
5.2. Diagram of the setup used to measure the resistance . . . . .	60
5.3. Photograph of the point contact holder . . . . .	62
5.4. Detail showing the time difference between valve opening and onset of film response . . . . .	65
5.5. Typical resistance changes observed when the testing chamber is closed with a fixed amount of CO inside . . . . .	66
6.1. Contact microstructure of a sputtered deposited contact . . . . .	68
6.2. Contact microstructure of a typical mechanical contact . . . . .	68
6.3. Electric field lines resulting from two long and parallel contacts deposited on a semiconducting surface . . . . .	69
6.4. Electric field lines resulting from point contacts made on a semiconducting surface . . . . .	69
6.5. Current paths expected when the sensing layer is deposited on a conducting substrate . . . . .	70
6.6. Current paths expected when the sensing layer is deposited on a thick layer . . . . .	70
6.7. Porous metal oxide layer structure . . . . .	71
6.8. Grain contact model and barrier control scheme . . . . .	72
6.9. Neck model and space charge layer formation . . . . .	73
6.10. Thickness control on very thin films . . . . .	73
6.11. Water adsorption possibilities on a tin dioxide surface . . . . .	75
6.12. Model of the catalytic oxidation . . . . .	77
6.13. Model of the spillover effect . . . . .	77
6.14. Model of the Fermi energy control effect . . . . .	77
6.15. Catalyst particles uniformly dispersed over a semiconductor grain surface . . . . .	78
6.16. Energy band scheme of the space charge layer that may develop on a n-type semiconductor when charged species adsorb on the surface . . . . .	80
6.17. Sample response to concentrations of carbon monoxide between 100 ppm and 1200 ppm . . . . .	84
A.1. Sample holder a) used on the gas sensing chamber and b) on the sputtering chamber . . . . .	92
A.2. Cable wiring between temperature controller port and computer . . . . .	94
B.1. Cable wiring between DC power supply serial port and computer . . . . .	111
B.2. Example of input file <code>fich-produc</code> of program <code>fonte.c</code> . . . . .	120
C.1. Valve controller (a) front panel and (b) rear panels . . . . .	133
C.2. Cable wiring between the valve controller and the computer parallel port . . . . .	134
D.1. Cable wiring between multimeter serial port and computer . . . . .	137
F.1. Example of input file <code>ficheiros.esp</code> of program <code>espessuras</code> . . . . .	169



# List of Tables

2.1. Classification scheme based on the sensor' input stimulus . . . . .	6
3.1. Thickness values obtained for samples e11a24 and l9a2 using SEM images and transmittance spectra. . . . .	39
4.1. Range of parameters selected for DC and RF sputtering deposition of tin oxide samples . . . . .	48
4.2. Non-independent parameters controlled during deposition . . . . .	48
4.3. Parameters selected to test the influence of sputtering atmosphere on the thin films' characteristics . . . . .	49
4.4. Parameters selected to test the influence of substrate temperature on the thin films characteristics . . . . .	49
4.5. Parameters selected to test the influence of the oxygen flow rate during deposition on the thin films characteristics . . . . .	49
4.6. Parameters used in deposition of samples a14a1, a14a2 and a14a3 . . . . .	54
A.1. Linux system device files identifying physical serial ports . . . . .	93
A.2. Pinout of RS-232-C serial ports on DTEs . . . . .	93
A.3. Function performed by serial port pins on the temperature controller side . . . . .	94
A.4. Function performed by serial port pins on a computer running the Linux operative system . . . . .	95
A.5. Communication data formats permitted by temperature controller . . . . .	95
A.6. Communication parameters selected on the temperature controllers for data exchange with the computer . . . . .	96
A.7. Correspondence between communication data formats and flags set by the <code>termios</code> structure . . . . .	98
A.8. Format of data blocks used for communication with the temperature controller . . . . .	98
A.9. Characters used in remote temperature controller commands . . . . .	100
B.1. Format of data blocks used for communication with the DC power source . . . . .	112
B.2. Character code values of some of the functions performed by the DC power source	113
B.3. Some variables used in program <code>fonte.c</code> . . . . .	119
C.1. Pin assignments on SPP parallel ports . . . . .	134
C.2. Example of correspondence between valve setting and the value of variable <code>*vcont</code> . . . . .	136
D.1. Communication parameters selected on the multimeter for data exchange with the computer . . . . .	138
F.1. Constants defined in the main program unit of <code>espessuras.f</code> . . . . .	171
F.2. Most important variables used in the main program unit . . . . .	171

*List of Tables*

F.3.	Arguments of routine AESPEC . . . . .	174
F.4.	Constants introduced in routine AESPEC . . . . .	175
F.5.	Main variables introduced in routine AESPEC . . . . .	175
F.6.	The auxiliary array w . . . . .	176
F.7.	Constants introduced in routine ESCOLHE . . . . .	179
F.8.	Constants introduced in routine ESPRESS . . . . .	192
F.9.	Main variables used in routine ESPRESS . . . . .	192
G.1.	Deposition parameters of some samples and corresponding label codes . . . . .	197

# List of Routines

A.1.	C program used to initialize serial port attached to temperature controller ( <code>openct</code> )	96
A.2.	C program used to compute the BCC check code ( <code>calcbcc</code> )	99
A.3.	C program used to set the temperature controller into communication mode ( <code>commode</code> )	101
A.4.	C program used to set the temperature controller into RAM mode ( <code>rammode</code> )	102
A.5.	C program used to set the temperature controller into RAM mode ( <code>tempcic</code> )	102
A.6.	C program used to change the set point temperature ( <code>changesv</code> )	103
A.7.	C program used to detect error messages from the temperature controller ( <code>erroct</code> )	104
A.8.	C program used to set the substrate temperature before film deposition ( <code>s_aquece.c</code> )	105
A.9.	Bash script used to write input file of program <code>s_aquece.c</code> ( <code>sputtering-heat</code> )	107
A.10.	Bash script used to stop substrate heating ( <code>sputtering-cool</code> )	108
A.11.	C program used to stop substrate temperature heating ( <code>s_arrefece.c</code> )	108
B.1.	C program used to initialise serial port attached to DC power source ( <code>opendc</code> )	111
B.2.	C program used to compute the check sum in the power source message block ( <code>exorop</code> )	113
B.3.	C program used to enquire or set operation mode of the DC magnetron power source ( <code>opmode</code> )	114
B.4.	C program used to set DC power source to RS232 operation mode ( <code>rsmode</code> )	115
B.5.	C program used to switch the DC power source to “ON” or “OFF” state ( <code>onofonte</code> )	116
B.6.	C program used to enquire and change the set point values of the power, voltage and current of the DC power source ( <code>changesp</code> )	116
B.7.	C program used to read the set point values of the power, voltage and current applied by the source ( <code>lesp</code> )	117
B.8.	C program used to read the actual values of the power, voltage and current of the DC power source ( <code>leval</code> )	118
B.9.	C program used to check if the reply from the power supply unit contains the error code ( <code>errodc</code> )	118
B.10.	C program used to get the current time ( <code>instante</code> )	119
B.11.	C program used to take the temperature value from the message block sent by the controller ( <code>celsius</code> )	119
B.12.	C program used to control DC power source and substrate temperature during film deposition ( <code>fonte.c</code> )	120
B.13.	Bash script used to write input file of program <code>fonte.c</code> ( <code>sputtering-on</code> )	124
B.14.	C program used to control DC power source and substrate temperature during film deposition ( <code>spfonte.c</code> )	131
C.1.	C program used to get the file descriptor for the parallel port ( <code>openpp</code> )	135
C.2.	C program used to initialise the parallel port ( <code>ppinit</code> )	135
D.1.	C program used to initialise the serial port attached to the multimeter ( <code>openhp</code> )	138
D.2.	C program used to select measuring range of the multimeter ( <code>selrange</code> )	139
D.3.	C program used to put the multimeter in voltage measurement mode ( <code>medevolt</code> )	140
D.4.	C program used to put the multimeter in resistance measurement mode ( <code>mederes</code> )	141

## List of Routines

E.1.	Bash script used to set parameters of film testing procedure ( <code>sensor-on</code> ) . .	143
E.2.	Bash script used to stop a gas sensing test or take a sample out of the chamber ( <code>sensor-off</code> ) . . . . .	155
E.3.	C program used to control the equipment and acquire the data during gas sensing tests ( <code>sensor.c</code> ) . . . . .	159
E.4.	C program used to read the values from the multimeter and the temperature controller ( <code>levalor</code> ) . . . . .	165
E.5.	C program used to turn off the heater and the electric valves when a gas sensor test is interrupted ( <code>sensor-off.c</code> ) . . . . .	166
F.1.	Bash script used to produce the input file of program <code>espessuras</code> ( <code>calc-esp</code> )	170
F.2.	Fortran program used to analyse the interference fringe values observed in the optical transmittance spectra ( <code>espessuras.f</code> ) . . . . .	172
F.3.	Fortran routine used to invert a vector array ( <code>INVERTE</code> ) . . . . .	174
F.4.	Fortran routine used to store the calculated values in the output files ( <code>AESPEC</code> )	176
F.5.	Fortran routine that chooses points to use in the optical parameter calculation ( <code>ESCOLHE</code> ) . . . . .	179
F.6.	Fortran routine that corrects transmittance values for finite slit width of the spectrophotometer ( <code>CTSLIT</code> ) . . . . .	190
F.7.	Fortran routine used to determine values of the peak and valley envelope functions ( <code>EXTRAP</code> ) . . . . .	191
F.8.	Fortran routine used to calculate optical parameters ( <code>ESPRESS</code> ) . . . . .	192

# Glossary

## Abbreviations

<b>AES</b>	Auger Electron Spectroscopy.
<b>AFM</b>	Atomic Force Microscopy.
<b>ASCII</b>	American Standard Code for Information Interchange.
<b>BAW</b>	Bulk Acoustic Wave.
<b>CEMUP</b>	University of Porto Materials Centre.
<b>CTS</b>	Clear To Send.
<b>CVD</b>	Chemical Vapour Deposition.
<b>DC</b>	Direct Current.
<b>DCE</b>	Data Communication Equipment.
<b>DMA</b>	Direct Memory Access.
<b>DTR</b>	Data Terminal Ready.
<b>ECP</b>	Extended Capabilities Port.
<b>EDS</b>	Energy Dispersive Spectroscopy.
<b>EDX</b>	Energy Dispersive X-ray analysis.
<b>EELS</b>	Electron Energy Loss Spectroscopy.
<b>EEPROM</b>	Electrical Erasable Programmable Read Only Memory.
<b>EPP</b>	Enhanced Parallel Port.
<b>ESD</b>	Electron Stimulated Desorption.
<b>EXAFS</b>	Extended X-ray Absorption Fine Structure.
<b>FD</b>	Field Desorption.
<b>FWHM</b>	Full Width at Half Maximum.
<b>HREELS</b>	High Resolution EELS.
<b>IEE</b>	The Institution of Electrical Engineers.
<b>IID</b>	Ion Impact Desorption.

## GLOSSARY

<b>IRQ</b>	Interrupt ReQuest.
<b>ISO</b>	International Organization for Standardization.
<b>JCPDS</b>	Joint Committee on Powder Diffraction Standards.
<b>JFET</b>	Junction Field Effect Transistor.
<b>LED</b>	Light Emitting Diode.
<b>LEED</b>	Low Energy Electron Diffraction.
<b>LEIS</b>	Low-Energy Ion Scattering.
<b>LPG</b>	Liquid Petroleum Gases.
<b>MOSFET</b>	Metal-Oxide-Semiconductor Field Effect Transistor.
<b>PD</b>	PhotoDesorption.
<b>PDF</b>	Powder Diffraction File.
<b>PID</b>	Proportional Integral Derivative.
<b>PL</b>	PhotoLuminescence.
<b>PVD</b>	Physical Vapour Deposition.
<b>RBS</b>	Rutherford BackScattering.
<b>RF</b>	Radio Frequency.
<b>RGTO</b>	Rheotaxial Growth and Thermal Oxidation.
<b>RTD</b>	Resistance Temperature Detector.
<b>RTS</b>	Request To Send.
<b>RxD</b>	Receive Data.
<b>SAW</b>	Surface Acoustic Wave.
<b>SCPI</b>	Standard Commands for Programmable Instruments.
<b>SEM</b>	Scanning Electron Microscopy.
<b>SIMS</b>	Secondary Ion Mass Spectroscopy.
<b>SPP</b>	Standard Parallel Port.
<b>STM</b>	Scanning Tunnelling Microscopy.
<b>TEM</b>	Transmission Electron Microscopy.
<b>TxD</b>	Transmit Data.
<b>UHV</b>	Ultra High Vacuum.
<b>UPS</b>	Ultraviolet Photoelectron Spectroscopy.

<b>WDS</b>	Wavelength Dispersive Spectroscopy.
<b>WDX</b>	Wavelength Dispersive X-ray analysis.
<b>XPS</b>	X-ray Photoelectron Spectroscopy.
<b>XRD</b>	X-Ray Diffraction.

### Roman Symbols

$B$	FWHM of XRD peak after correction for the instrument broadening.
$C_g$	gas concentration.
$C_{ij}$	concentration of compound $i$ ( $j$ represents the gas compound whose sensitivity is affected by $i$ ).
$C_{O_2}$	oxygen concentration in atmosphere.
$C_q$	flow coefficient of a valve.
$d$	plane spacing in crystals.
$D$	diffusion constant.
$d_f$	film thickness.
$\bar{d}_f$	mean film thickness.
$\Delta d_f$	maximum deviation from mean thickness.
$D_{gr}$	average crystallite diameter.
$G_0$	film conductance in air.
$G_S[C_g]$	conductance under a $C_g$ concentration of the monitored gas.
$h$	float position in rotameter scale.
$I$	electric current.
$J_g$	flux of gas particles from the surface.
$k$	Boltzmann constant.
$K_j$	sensitivity coefficient of reducing gas $j$ .
$M_E$	atomic mass of element E.
$m$	interference fringe order.
$N$	number of particles.
$n$	number of particles per unit volume (density).
$n_f$	film refractive index.
$n_{ij}$	power coefficient affecting influence of concentration $C_{ij}$ on the sensor resistance change.

## GLOSSARY

$n_s$	refractive index of film substrate.
$P$	pressure.
$q$	flow rate.
$R_0$	resistance in clean air.
$R_i$	multimeter internal resistance.
$R_R$	reference resistance.
$R_S$	sample resistance.
$R_S[C_g]$	resistance under a $C_g$ concentration of the monitored gas.
$s$	sputtering yield.
$S$	Resistance or conductance ratio.
$T$	temperature.
$T_M$	peaks of the transmittance spectra.
$T_m$	valleys of the transmittance spectra.
$T_{Md}$	envelope of interference fringe maxima.
$T_{md}$	envelope of interference fringe minima.
$T_{MW}$	peaks of the transmittance spectra corrected for slit width.
$T_{mW}$	valleys of the transmittance spectra corrected for slit width.
$T'_M$	Experimental values of $T_{Md}$ .
$T'_m$	Experimental values of $T_{md}$ .
$V$	volume.
$V_0$	source voltage.
$W$	spectrophotometer slit width.
$x$	absorbance.

## Greek Symbols

$\alpha_s$	absorption coefficient of film substrate.
$\delta(t)$	ideal impulse function.
$\lambda$	wavelength.
$\rho_X$	X-ray density.
$\theta$	surface coverage.
$\theta_B$	Bragg diffraction angle.